

Aeolian Sediment Transport at the Hondsbossche Dunes

The influence on beach and dune development

M. Wittebrood



TU Delft



hoogheemraadschap
Hollands
Noorderkwartier

Aeolian Sediment Transport at the Hondsbossche Dunes

The influence on beach and dune development

by

Marloes Wittebrood

to obtain the degree of

Master of Science
in Civil Engineering

at the Delft University of Technology,
to be defended publicly on Friday June 2nd, 2017 at 11:00 AM.

Thesis committee: Prof. dr. ir. S.G.J. Aarninkhof, TU Delft
Dr. ir. S. de Vries, TU Delft
Ir. P. M. G. J. Goessen, Hoogheemraadschap Hollands Noorderkwartier
Ir. W. P. Bodde, Witteveen+Bos
Dr. ir. B. C. van Prooijen, TU Delft

An electronic version of this thesis is available at <http://repository.tudelft.nl/>.



hoogheemraadschap
Hollands
Noorderkwartier

Acknowledgements

This MSc thesis completes my Master's degree of my study Hydraulic Engineering at the Delft University of Technology and is part of the specialization Coastal Engineering. The research is a collaboration between the Water Authority Hoogheemraadschap Hollands Noorderkwartier in Heerhugowaard and TU Delft.

I grew up in the Northwest part of the Netherlands and was protected behind the Hondsbossche & Pettermer sea defence. I have good memories of the moments that I visited the beaches of Petten or Camperduin with family and friends. During my study I developed an interest in the large-scale applications of sand for coastal safety purposes, here in the Netherlands but also abroad. When I was looking for a master thesis topic, the execution of the Hondsbossche project came along perfectly. In the spring of 2016 I was enthusiastic to start my research in this new topic for me into aeolian sediment transport and dune development. I am grateful to Petra and Sierd that you gave me the opportunity to work on this research in collaboration between Hoogheemraadschap Hollands Noorderkwartier and TU Delft.

I would like to warmly thank all my committee members: Stefan Aarninkhof, Sierd de Vries, Petra Goessen, Willem Bodde, and Bram van Prooijen for your input and guidance. Petra, thank you for your supervision, your critical guiding was helping me a lot and your enthusiasm is motivational. Thank you for including me in the coastal management world, to conferences and the dunes during sunny and stormy days. Sierd, thank you for your help, and guiding me in the right direction at the right time. You helped me to keep on being positive, I really appreciated your spontaneous walk-in moments. Furthermore, thank you Bas for helping me to set-up the AeoliS model and always replied soon and extensively to my questions.

Working for 2 days a week in Heerhugowaard I would also like to thank those at HHNK at the coastal department. Vincent many thanks to teach me new computer skills and having enjoyable conversations during lunch. Also, Kees, Jan-Willem and Hans thank you for showing me your very interesting work along the coast. Thank you to the people involved in the EcoShape consortium and other researchers that I met for sharing your expertise and enthusiasm for research into this aeolian sediment transport.

At the other 3 days of the week I was working with Christel, Anais, and Bart at the TU Delft. I really enjoyed our time together and the supportive suggestions for my research and job applications. All the ladies of 'Burgerlijke Kuikens' and 'Vesper', I had a great time with you during and after studies and I really appreciate your support the last year. Special thanks to Rinske who helped me for critical writing and suggestions till the last moment. Bianca, as high school friends we started together this study journey in Delft 8 years ago and how special that we finish this journey together in one week difference. Simone, thank you for making me laugh throughout this research with silly jokes about our passions asphalt and sediment. And thanks to you and your mum for an English review of parts of my work. Kim, the differences can almost not be larger: Groningen-Delft, Alpha-Beta, but I appreciate your support from distance throughout this process and your friendship in 26 years.

Last but not least I would like to thank my parents for their invaluable support through this time. I felt very welcome every week that I stayed the night at home in Heerhugowaard and I appreciate your mental and physical support by giving me advice when needed and providing me with food supply for in Delft and joined me to the Hondsbossche Dunes during sunny and in specially stormy days. Lovely sister, thank you for encouraging me throughout this time and Big Bro Bob, I think it is you that deserves most of my credits, because you showed me how fascinating an engineering study and student life in Delft could be.

Marloes Wittebrood, May 2017

Abstract

In 2014-2015 the coastal stretch between Petten and Camperduin was strengthened by using 35 million m³ of sand. At the seaward side of the Hondsbossche & Pettemer sea defence (HPZ) a beach and dune system was built which is called the 'Hondsbossche Dunes'. The old sea dike has disappeared behind the new dunes and is not longer an active part of the primary flood defence system. Since 2015 the Hondsbossche Dunes (HD) protect the hinterland against flooding during storm events and simultaneously it creates a large opportunity for the development of new nature and recreation areas. Along the Hondsbossche Dunes five different dune profile types have been constructed to stimulate morphological dynamics of the system. The profile types vary in dune width, dune height and the seaward slope of the dune front, depending on the required sediment volumes needed at a specific alongshore location to reduce the coastal risk. Profile type 2 and 3 exist in the North and in the South of the Hondsbossche Dunes. A beach and foreshore is constructed in front of the dunes to increase the sediment volume that is contained by the system.

The Hondsbossche Dunes have the advantage of being a dynamic system which is highly adaptive to changes in climatic forcing. This climatic forcing redistribute the marine sand from the foreshore towards the dunes. The new flood defence system became a dynamic system, which requires analysing and modelling of the effect of sediment transport on the dune development. Current research into the new system has mainly focussed on analysing and modelling the effect of marine sediment transport on the morphological development of the foreshore and beach, however the aeolian sediment residing in the dunes provides a direct buffer against storm erosion. To this day, the predicted influence of aeolian sediment transport on dune development for this system is only based on previous research and expertise obtained from studies for the Dutch coast and reference projects. For this reason, the quantification and understanding how aeolian and marine sediments are transported towards the dunes is required in order to realize an effective approach for management and maintenance of the HD system regarding to the expected sea level rise and land subsidence.

Research objective and methodology

The main objective of this thesis is to explore the effect of aeolian sediment transport on the morphological development of the beach and dunes at the Hondsbossche Dunes, thereby concluding on the differences in response within the five different dune profile types. A conceptual framework of the parameters that characterize the system is introduced which distinguishes three components: (1) climatic forcing, (2) sediment supply and (3) dune types. Insight into these three components is obtained by a twofold approach: a data-analysis at the JARKUS transects for the first 19 months after construction and the application of the wind-sediment transport model Aeolis at a two-dimensional scale. The aim of the data-analysis is to derive spatial and temporal volume changes of the beach and dunes in order to analyse the morphological development of the system since construction. Moreover, it is aimed to find spatial and temporal variations in aeolian sediment supply and how these relate with measured dune volume change. The aim of the model application is to study the influence of alongshore variations in sediment supply on the dune growth rates. The project area is divided into five sub domains and modelled as individual systems in order to simulate alongshore variability in median grain size. The performance of the model is analysed by comparing the measured and modelled erosion and deposition patterns. Besides, the model results are validated for the measured dune growth rates.

Results

The results obtained from the data-analysis show that an alongshore variations in beach and dune development is strongly present, for which the morphological changes were most pronounced in the seven months after construction. High beach volume losses were observed along the Hondsbossche Dunes with an average value 29 m³/m/y in the period May 2015 - December 2016. This predominantly occurred due to the initial adaptation of the system to the climatic forcing and more and higher south-western waves in the storm season between November 2015 and September 2016. This is seen in a strong erosion along the Southern shoulder. The volumetric losses were transported in alongshore direction leading to accretion of the beaches

Northwards and Southwards of the Hondsbossche Dunes. The volumetric losses of the beach are associated with a shoreline retreat of on average 37 m/y and a steepening of the beach slope. The accretion of the beaches in the North and in the South are associated with a shoreline extension up to 9 m/y and the development of milder beach slopes. Besides, volumetric losses were transported in cross-shore direction resulting in an average dune growth of 28 m³/m/y. Alongshore variation in dune growth are significant with a minimum up of 14 m³/m/y at profile type 1 in the North to 45-48 m³/m/y at profile type 2 and 3 in the South. Dune growth is also pronounced between March 2016 - September 2016. This is the result of an increase in sediment availability due to an increase in beach volume, respectively beach width alongshore.

The dune volumes changes are correlated to beach width, beach slope and median grain size, but a unique relation could not be defined. Often higher dune growth rates are reached when the beach width is larger and the beach slope milder. However, a spatial variation in dune growth is observed for equivalent beach width or slope. This is caused by an alongshore variation in local conditions that blocks the aeolian sediment transport paths towards the dunes. The local factors that show their influence are: the location with respect to the dominant wind direction, beach width, beach slope, median grain size and dune geometry.

The AeoliS model is able to reproduce large scale spatial patterns of erosion and deposition under influence of varying climatic conditions. Deposition in the intertidal zone as an effect of marine forcing is not simulated, since this is not included in the model yet. The model shows to predict alongshore variations in dune growth as a result of spatial variations in sediment availability regarding to topography and grain size characteristics. The model overestimates the measurements with a factor varying from 1.2 to 3. The negligence of an update in the topography might cause the model to overestimate the measured dune growth rates more at locations where large temporal variations in beach topography were measured (subdomain 2- Northern shoulder) than at locations where small temporal variations are measured (subdomain 3- middle part). This results in a large sediment availability in time while the measurements show a relatively large decrease in beach width and therefore a reduction in sediment availability. The overestimation is highest in the first period as a result of high and onshore directed wind forcing and a large sediment availability. High wind speed increases the capacity of the wind to transport sediment, whereas the large sediment availability is likely to be a result of the negligence of soil moisture and marine sediment transport in the model. The overestimation is less pronounced in the last period in which low and offshore wind is measured which reduces the pick-up of sediment into aeolian transport towards the dunes.

Conclusion

It can be concluded that the five man-made profile types show an appreciable different response to the aeolian sediment transport towards the dunes. Dune growth of a profile type is likely to be determined by: (1) a temporal variability in local processes that determines the aeolian sediment supply towards the dunes and (2) the dune geometry that determines the capacity of the profile type to capture the sediments. The capacity of aeolian sediment transport to build dunes is experienced to be higher if the beach slope and beach width suffer from low spatial and temporal variations as a result of marine forcing. Besides, fine grains at the beach promotes the pick-up and transport of sediment. From the model study it is suggested that the soil moisture content has influenced the aeolian sediment availability for transport towards the dunes, in particular in the first period this is relevant in which often large wet surfaces were observed. Dune growth is higher if the dune consist of a lower foredune with a mild slope, equivalent to profile type 3 and a large supply of sediments towards the dunes. A large supply is stimulated during high and onshore directed winds and a favourable location with respect to the dominant wind direction. This is seen by the large dune growth at profile type 2 and 3 along the Southern shoulder.

For a better understanding of the morphological processes that dominates the dune growth, scientific recommendations are given regarding to the data-analysis and the numerical model. It recommended to analyse in more depth the sediment exchange between the foreshore and the beach and the influence of subsidence on the measured dune volume changes. A sensitivity analysis of the model input parameters contributes to the understanding of model parameters on the results. Moreover, recommendations are given for the coastal management of the system. A lower foredune with a mild slope is advised for fast recovery of the dunes when a sever storm has passed.

Contents

Acknowledgement	iii
Abstract	vi
Symbols	xi
Abbreviations	xiii
1 Introduction	1
1.1 Introduction of the research topic	1
1.2 Background on the Hondsbossche & Pettermer Sea Defence	2
1.2.1 History of Construction	2
1.2.2 A New Design: Hondsbossche Dunes	2
1.3 Problem Description	6
1.4 Conceptual Framework	7
1.5 Research Objective and Questions	7
1.6 Research Approach	8
1.7 Thesis Outline	9
2 Literature Review	11
2.1 Coastal Dune Formation	11
2.1.1 Aeolian Sediment Transport	11
2.2 Aeolian Sediment Transport Equation	13
2.2.1 Wind Driven Sediment Transport	13
2.2.2 Application to Coastal Areas	13
2.3 Aeolian Transport Model- AeLiS	14
2.3.1 Introduction to AeLiS	15
2.3.2 Model Description	15
2.3.3 Application to the Hondsbossche Dunes	16
3 Methods	17
3.1 Method: Data analysis	17
3.1.1 Data	17
3.1.2 Zonation of the Cross-shore Profile	19
3.1.3 Definition of the Cross-shore Transects	20
3.1.4 Volumes Changes of the Zones	20
3.1.5 Beach Slope	22
3.1.6 Beach Width	22
3.1.7 Relation Aeolian Sediment Availability and Dune Volume Change	23
3.2 Method: Modelling	23
3.2.1 Model Schematization	24
3.2.2 Measured and Modelled Sedimentation and Erosion Patterns	28
3.2.3 Quantification of Modelled Dune Volume Change	28
3.2.4 Verification of the Modelled Dune Volume Change	29
4 Results	31
4.1 Results: Data Analysis	31
4.1.1 Measured Erosion and Deposition over the Project Domain	31
4.1.2 Volume Change of the Surf Zone and the Intertidal Zone	32
4.1.3 Volume Change of the Dry Beach Zone	34
4.1.4 Volume Change of the Dunes	38
4.1.5 Dry Beach Slope	42

4.1.6	Dry Beach Width	44
4.1.7	Relation Aeolian Sediment Availability and Dune Volume Change	48
4.1.8	Differences between Profile Types	51
4.2	Results: Modelling	53
4.2.1	Measured and Modelled Sedimentation and Erosion Patterns	53
4.2.2	Measured and Predicted Dune Volume Changes	70
5	Discussion	79
5.1	Spatio-Temporal Variations in Dune Growth	79
5.1.1	Results of Dune Development	79
5.1.2	Interpretation of the Assumptions	81
5.1.3	Importance of Marine Sediment Supply	82
5.2	Modelling Dune Growth	82
5.2.1	Model Schematization	82
5.2.2	Model Results	83
6	Conclusions & Recommendations	85
6.1	Conclusions.	85
6.1.1	Morphological Development since Construction	85
6.1.2	Governing Processes and Parameters	86
6.1.3	Modelling Alongshore Variation in Dune Growth	87
6.1.4	Conclusion on Main Research Question	87
6.2	Recommendations	89
6.2.1	Scientific Recommendations.	89
6.2.2	Management Recommendations	89
	Bibliography	95
A	Background Design	97
A.1	New Approach to Failure Probabilities	97
A.2	History of Construction	97
A.3	Design Requirements and Methodology	98
A.4	Design of the Dunes.	98
A.4.1	Project boundaries.	98
A.4.2	Dune Profile Types	98
A.4.3	Overview of the Profile Characteristics.	99
A.4.4	Design Drawings.	101
A.4.5	Expected Aeolian Transport and Morphological Development.	103
A.4.6	Monitoring EcoShape	103
B	Aeolian Transport Model- DUBEVEG	105
B.1	Introduction to the model.	105
B.2	Model Description	105
B.2.1	Spatial and temporal scales	106
B.3	Application to Hondsbossche Dunes	106
C	Data Availability	107
C.1	Bathymetry	107
C.2	Topography.	108
C.2.1	Comparison Two Airborne LiDAR Datasets	108
C.2.2	Locations Dune Valley	108
C.2.3	Grain Size Measurements	109
D	Climatic Conditions	111
D.1	Wind	111
D.2	Waves.	113
D.3	Tidal Levels	114

E	Definition of Cross-shore Transects	117
E.1	Location of cross-shore transects	117
E.1.1	Discarded transects transects	117
E.2	Connection HD system - Natural dunes Petten (North)	120
F	Derivation of Beach and Dune Volumes	123
F.1	Dune volume per Profile Type.	123
F.2	Beach volume per Profile Type	124
G	Model Input	127
G.1	Topography Hondsbossche Dunes	127
G.2	Sieving Curves	130
G.3	Model configuration files	131
G.3.1	Subdomain 1.	131
G.3.2	Subdomain 2.	132
G.3.3	Subdomain 3.	133
G.3.4	Subdomain 4.	134
G.3.5	Subdomain 5.	135
H	Additional results - Data analysis	137
H.1	Natural dune growth north	137
H.2	Morphological Change of Dune Valley	137
H.3	Beach Slope.	139
H.3.1	Cross-shore profiles	139
H.3.2	Mean Beach Slope	139
H.4	Beach Width	144
H.4.1	MHW Position and Dune foot Position.	144
H.4.2	Correlations	148
H.5	Results per profile type	148
I	Erosion and Sedimentation Plots	151
I.1	Full Domain	151
J	Additional Results - AeoliS Model	157
J.1	Periodic Dune Volume Changes.	157

Symbols

Symbol	Description
α	Factor to convert from wind velocity to drag velocity [-]
ΔV_{dunes}	Dune growth rates [$m^3/m/y$]
θ_{cor}	Correction angle between north an shore normal [°]
$\theta_{z,i}$	Angle wind direction [°]
ρ	Air density [kg/m^3]
ρ_a	Air density at 20 °C [kg/m^3]
ρ_s	Density of sand grains [kg/m^3]
τ	Shear stress [N/m^2]
A	Empirical coefficient based on the Shields function [-]
A_g	Surface of 10 by 10 meter grid cell [m^2]
C_b	Empirical coefficient related to sediment size distribution [-]
C_k	Empirical coefficient [-]
D	Reference grain diameter [μm]
D_{50}	Median grain size [μm]
d	Grain diameter relative to reference grain diameter D of 250 [μm]
d_n	Nominal grain diameter of sand [μm]
dt	Time between two wind measurements [s]
dy	Alongshore distance of grid cell [m]
F_c	Critical fetch [m]
g	Gravitational acceleration [m/s^2]
i	Measurement number [-]
k	Bed height [m]
k'	Surface roughness height [m]
p	Porosity [-]
q	Aeolian sediment transport rate [$kg/s/m$]
$q_{sat,i}$	Saturated sediment transport rate for measurement i [$kg/s/m$]
$q_{x,i}$	Saturated sediment transport capacity in shore-normal direction for measurement i [$kg/s/m$]
$q_{x,tot}$	Total sediment transport capacity in onshore direction i [m^3/m]
t_0	Time at beginning [d]
t_{end}	Total amount of days [d]
u_*	Drag velocity [m/s]
u_t	Velocity threshold at the measured height k' above the surface [m/s]
u_{t*}	Drag velocity threshold [m/s]
u_z	Wind velocity at elevation z [m/s]
$u_{z,cor}$	Correction wind velocity between north and shore normal [m/s]
z	Specific height [m]

Abbreviations

HHNK	Hoogheemraadschap Hollands Noorderkwartier (Water Authority)
HPZ	Hondsbossche & Pettemer zeewering or Hondsbossche & Pettemer seadefence
HD	Hondsbossche Duinen or Hondsbossche Dunes
RSP	Rijksstrandpaal - Dutch reference system for annual coastline measurements
2DH	Two-Dimensional in a horizontal plane
2DV	Two-Dimensional in a vertical plane
AeoLiS	Aeolian sediment transport with Limited Supply
KNMI	Koninklijk Nederlands Meteorologisch Instituut
MSL	Mean Sea Level
NAP	Normaal Amsterdams Peil or Amsterdam Ordnance Datum
RTK-GPS	Real-Time Kinematic Global Positioning System
DUBEVEG	DUne, BEach, VEgetation
LiDAR	Light Detection and Ranging
JARKUS	Jaarlijkse kustmeting or Annual coastline measurements

Introduction

1.1. Introduction of the research topic

About 75% of the Dutch coastline is made up of sandy beaches and dunes [Muller, 2011] which function as the primary flood defence system and protect the low-lying hinterland against flooding. Traditionally, dunes were stabilized and/or reinforced when a certain safety level was not met [de Vries et al., 2012]. Since the 1990s beach and shoreface nourishments have been executed to mitigate erosion of the Dutch coastline [Luijendijk et al., 2017]. The increased understanding of the contribution of natural coastal processes to redistribute the sand in the coastal system and the demand to limit the environmental and ecological impact, has resulted in an upscale of the size and new applications of the nourishment strategy along the Dutch coast. In 2011, a concentrated mega-scale nourishment called the Sand Engine ('Zandmotor' in Dutch) was implemented with the intention to feed sand to adjacent coastal stretches by alongshore diffusion [de Schipper et al., 2016]. Recently, in 2015, on the sea dike foreshore of the Hondsbossche & Pettemer sea defence ('Hondsbossche & Pettemerzeewering in Dutch', hereinafter referred to as HPZ) a beach and dune system was built with the aim to increase the local coastal safety and not for maintenance of the adjacent coastal stretches. The new system, called the Hondsbossche Dunes ('Hondsbossche Duinen in Dutch', hereinafter referred to as HD) is located between Petten and Camperduin in the Northwest of the Netherlands, as shown in the upper image of Figure 1.1.



Figure 1.1: Overview of the study area. **Upper figure:** the location of the Hondsbossche & Pettemer sea defence along the Dutch Coast, adapted from [Google, 2016]. **Lower left figure:** Situation prior construction, taken from Camperduin. The Hondsbossche & Pettemer sea defence is depicted. Adapted from [Oudeluis, 2012]. **Lower right figure:** Situation immediately post construction, taken from Camperduin. The Hondsbossche Dunes is depicted seaward of the Hondsbossche & Pettemer sea defence and has increased locally the coastal safety. Adapted from [Informatiecentrum Kust, 2012].

During the construction period in 2015, almost 35 million m³ of sand, 1.5 times the volume supplied to the Sand Engine [Hoonhout, 2017], was supplied to this section by two different techniques: through beach and through foreshore nourishment. This was about 85 percent of the total volume of 40 million m³ of sand: the new coastal zone required 26 million m³ sand for reinforcement and 14 million m³ sand to compensate for expected losses due to settlement, marine and aeolian processes in the construction and maintenance period [Kroon et al., 2015]. Land equipment has been used to reshape the nourished sand into a coastal landscape of beach and dunes. The lower left and right image in Figure 1.1 gives an impression of the coastal area prior and immediately post construction.

Since April 2015 the HD has been in use as a new coastal area and replaces the HPZ as the primary flood defence system. It protects the low-lying hinterland against flooding during storm events. Simultaneously, it creates a large opportunity for development of new nature and recreation areas. The contractors are responsible for the maintenance of this system to meet the required safety standards set by the Water Act for the coming twenty years. The Water Authority Hoogheemraadschap Hollands Noorderkwartier (hereinafter referred to as HHNK), and the public departments of 'Rijkswaterstaat' within the Dutch Ministry of Infrastructure and the Environment remain ultimately responsible for the safety of this dynamic system and will take over the maintenance from the contractors in 2036.

This research analysed the morphological behaviour of the beach and dunes of the newly developed coastal area in order to optimise future maintenance of the beach and dunes.

1.2. Background on the Hondsbossche & Pettermer Sea Defence

1.2.1. History of Construction

The HPZ is a five-kilometre-long sea defence of which the latest version was realised in 1981. The sea defence connected the high dunes of Camperduin with the lower dunes of Petten. For almost 600 years this six-kilometre-long coastal section was under heavy attack from storm surges. Different types of defences were constructed to protect the low-lying hinterland against flooding. Since 1981 the dike has stood at a height of 12 meters above NAP and has groynes in front to reduce wave impact. The HPZ is one coastal defence, although the Pettermer part of the sea defence consists of a shorter section of 1.5 kilometres in the North with a steeper slope. The HPZ formed a fixed outcrop, see the left lower image of Figure 1.1, and has influenced the behaviour of the adjacent coastal stretches.

1.2.2. A New Design: Hondsbossche Dunes

Motivation

Every six years and in the future every 12 years, the primary defences along the Dutch coast are assessed to guarantee the safety of the low-lying hinterland. This is regulated by the Dutch Water Act under the responsibility of the Dutch Ministry of Infrastructure and the Environment. The HPZ should protect the low-lying hinterland against storm surge flooding with a return period of 1/10.000 years, which was the legal safety standard for the entire Holland coast¹. The second round of tests carried out in 2001-2006 showed that the HPZ did not pass the safety assessment in 2005. The assessment for this coastal area was divided into four parts: the Hondsbossche sea defence (4.7 kilometres), the Pettermer sea defence (1.5 kilometres), the connection dike-dune North in Petten and the connection dike-dune South in Camperduin. The criteria for both sea defences were: dike crest height, revetment of the outer dike slope, stability of the dike embankment and stability of the foreshore. The connections were assessed for the required sand volume to counteract the impact of a normative storm [Joosten, R., 2005].

The Hondsbossche sea defence was rejected for inadequate strength of the revetment of the lower outer slope along a stretch of 0.6 kilometres. The dike crest height was rejected under strong hydraulic conditions along the entire Hondsbossche sea defence and one kilometre of the Pettermer sea defence due to the low erosion resistance of the dike crest and the revetment on the inner dike slope against overtopping [Joosten, R., 2005]. Therefore, the seaward slope of the Hondsbossche sea defence was covered with basalt over a length of approximately four kilometres and sheet piles were drilled into the Pettermer sea defence with a height of 0.7

¹Since January 2017 the Water Act has included a new approach to failure probabilities of the primary sea defences and the secondary dike systems [Ministerie van Infrastructuur en Milieu, 2016]. The probability of flooding safety for the new design of the Hondsbossche Dunes has therefore changed from 1/10.000 to 1/3.000 years [Ministerie van Infrastructuur en Milieu, 2016]. In Appendix A the new approach is discussed

meter above the dike crest and over a length of one kilometre to reduce the impact of wave overtopping. It was stated that the overtopping discharge at the Pettermer sea defence was still too large to fulfil the erosive criteria for the revetment. The Northern connection failed the safety assessment under strong hydraulic conditions, while extra nourishments took place in 2004 and 2005 because the sand volume in the cross-shore profile was too low to counteract erosion of the dunes and dike under normative storm conditions [Joosten, R., 2005]. The rejected HPZ became part of a larger reinforcement project, the 'weak links', in which a total of ten locations were recommended for adaptations in order to comply with the Water Act.

The design

In October 2013 the design phase of the coastal area between Petten and Camperduin was finalized. Although increasing the safety of the current system was still the main design requirement, it was desirable to create an appealing coastal area [Smit et al., 2015]. The responsible Water Authority HHNK worked together with their stakeholders on the design criteria of this coastal area. Different design solutions have been reviewed by using the social cost-benefit analysis. The final design appears to be a softer alternative rather than making the current sea defence even stronger. The old sea dike has disappeared behind the new dunes and is no longer an active part of the primary flood defence system.

Figure 1.2 shows the aerial overview of the entire project domain. The length of the total project area is about 11 kilometres, indicated as the area between RSP² 17.08 and RSP 28.32, of which the HD system covers a length of approximately seven kilometres, indicated as the area between RSP 20.25 and RSP 27.00. The most seaward position of the mean high water line of the HD system (NAP +0.8 m contour) protrudes 340 m from the position of the HPZ dike crest height. The beach consists of grains varying in size and shells content alongshore. Along the HD system five different dune profile types have been constructed to stimulate morphological dynamics of the system. The profile types vary in dune width, dune height and the seaward slope of the dune front, depending on the required sediment volumes at an alongshore location to reduce the coastal risk. The red cross-shore lines in Figure 1.2 identify the alongshore locations of the five man-made dune profile types. Furthermore, variation in the amount and the pattern of the local features is constructed. Two examples of these features are the low-lying deposition areas and vegetation which should stimulate the local variation in sedimentation and erosion patterns. The major characteristics for each dune profile type are given. More details about the design of this project can be found in Appendix A.

²RSP mean RijksStrandPaal and is the Rijkswaterstaat reference system used for annual coastline surveys.

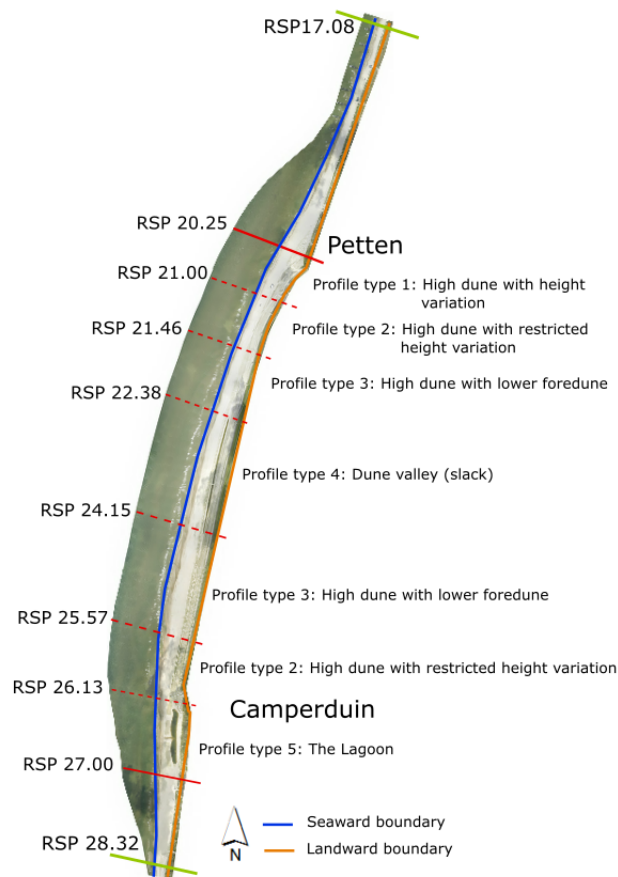


Figure 1.2: Aerial picture of the project domain of the Hondsbossche Dunes. The seaward and the landward boundary of the study area are indicated by the blue and respectively orange line. The alongshore location of the five different man-made dune profiles is indicated by red cross-sectional lines and RSP² coordinates (Rijkswaterstaat reference system).

Profile type 1- High dune with variations in height

This profile type is located at the Northern end of the HD system, as can be seen in Figure 1.2. The highest part of this dune section is at +26.20 m NAP with an initial dune slope of 1:1.7 m forming the panorama dunes of this area, see Figure 1.3a for a cross-sectional schematization. At both sides of the panorama dune, lower dunes are constructed of which the geometry is equal to profile type 2.

Profile type 2- High dune with restricted variations in height

Profile type 2 has been constructed at two sections along the HD system, as can be seen in Figure 1.2. The dune crest of profile type 2 has a height of approximately +12.5 m NAP with an initial dune slope of 1:2.1 m, see Figure 1.3b for a cross-sectional schematization. At the dune crest no low-lying deposition areas were constructed, only areas without vegetation have been constructed.

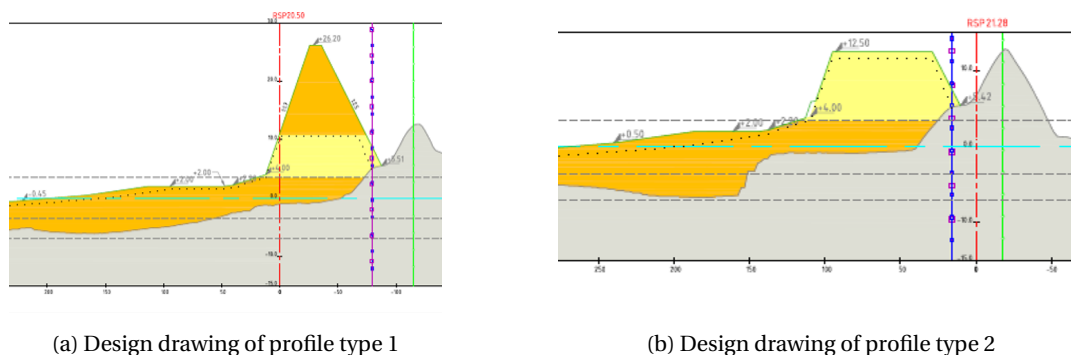


Figure 1.3: Schematization of dune profile type 1 (left) and 2 (right) coloured in yellow and orange, adapted from: [Leenders and Smit, 2016]. Profile type 1 is schematized as a high dune with a steep slope while profile type 2 is a low dune with a milder slope. At the right of both figures the HPZ is depicted in gray.

Profile type 3- High dune with lower foredune

Profile type 3 has also been constructed at two sections along the HD-system, see Figure 1.2. The profile type consists of a lower foredune with a height of approximately +5.50 m NAP and with an initial dune slope of 1:4 m. This lower foredune stands in front of a higher landward dune which has a height of approximately +10 m NAP and with an initial dune slope of 1:1.8 m, see Figure 1.4a for a cross-sectional schematization. At the dune crest low-lying deposition areas have been constructed varying in depth.

Profile type 4- Dune valley

Profile type 4 is located in the middle section of the HD system, see Figure 1.2. The profile type consists of two rows of dunes divided by a wet valley (or dune slack). The crest of the seaward foredune varies around a height of +6 m NAP with an initial seaward dune slope of 1:3 m and an initial landward dune slope towards the valley of 1:1.1 m. At the dune crest small open areas have been constructed and at the landward slope a curling pattern of vegetation. The crest of the landward dune has a height of approximately +11 m NAP. The dune slope toward the valley consists of a milder and steeper part. It has an initial dune slope of approximately 1:1.6 m up to a level of +7 m NAP and a slope of 1:1.3 m until the crest, see Figure 1.4b for a cross-sectional schematization. At the landward dune crest, variation in vegetation patterns and low-lying deposition areas have been constructed to create initial variations in morphology.

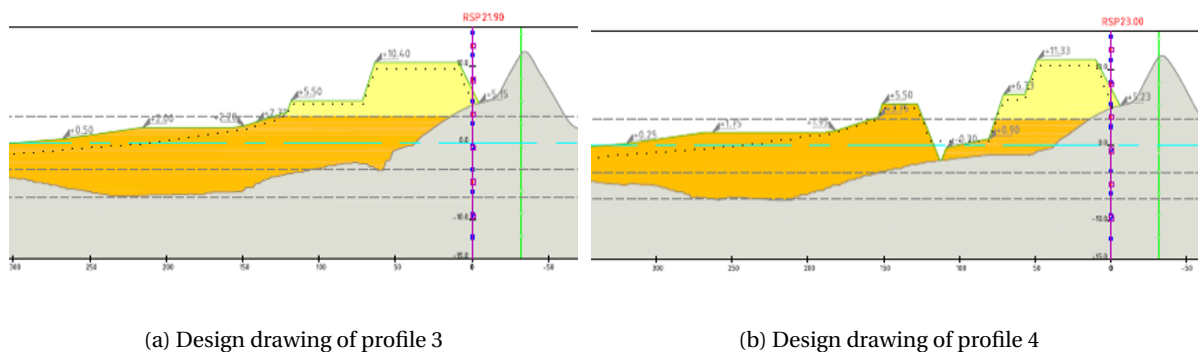


Figure 1.4: Schematization of dune profile type 3 (left) and 4 (right) in yellow and orange, adapted from: [Leenders and Smit, 2016]. Profile type 3 is schematized as a high dune with a lower dune in front that has a mild slope. Profile type 4 is schematized as two dune rows with in between a wet valley, the seaward dune is low and has a relatively mild slope. At the right of both figures the HPZ is depicted in gray.

Profile type 5- The lagoon

Profile type 5 is located at the Southern end of the HD system, see Figure 1.2. The low and small dunes have a crest height of approximately +5 m NAP and an initial dune slope of 1:2 m. The dune row separates the beach from the lagoon, see Figure 1.5 for a cross-sectional schematization. Only the seaward slope and dune crest is covered by vegetation.

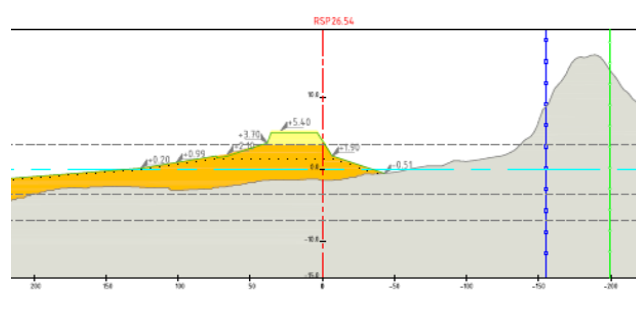


Figure 1.5: Schematization of dune profile type 5 in yellow and orange, adapted from: [Leenders and Smit, 2016]. Profile type 5 is schematized as a low dune with a relatively steep dune front slope. At the right of profile type 5 is depicted the lagoon and the natural dunes at Camperduin in gray.

1.3. Problem Description

The development of the new coastal area, between Camperduin and Petten, has changed the primary flood defence system for this section from a static into a dynamic system. The new flood defence system consists of a dune row with five different profile types that stimulate the morphological dynamics of this system. A beach and foreshore is constructed in front of the dunes to increase the sediment volume that is contained by the system. Unlike a fixed sea dike such as the HPZ, the man-made dunes (HD) have the advantage of being a dynamic system which is highly adaptive to changes in climatic forcing. This climatic forcing redistributes the marine sand from the foreshore towards the dunes. Hence the new flood defence system between Camperduin and Petten became a dynamic system, which requires analysing and modelling of the effect of sediment transport on the dune development.

Current research into the new system has mainly focussed on analysing and modelling the effect of marine sediment transport on the morphological development of the foreshore and beach, however the aeolian sediment residing in the dunes provides a direct buffer against storm erosion. To this day, the predicted influence of aeolian sediment transport on dune development for this system is only based on previous research and expertise obtained from studies for the Dutch coast and reference projects. For this reason, the quantification and understanding how aeolian and marine sediments are transported towards the dunes is required in order to realize an effective approach for management and maintenance of the HD system regarding to the expected sea level rise and land subsidence.

1.4. Conceptual Framework

Figure 1.6 shows the conceptual framework of processes which are anticipated to influence the morphological development of the new dunes. The processes that influence the system are divided into three components. The first component is the 'Climatic forcing' and considers wind, wave and tidal conditions which form the driving forces to the system. The second component is 'Sediment supply'. This category considers the influence of sediment exchange in cross-shore direction between the foreshore and the constructed beach and dune system under the climatic forcing conditions. This also includes physical parameters of the beach that governs sediment availability for dune growth: the beach slope and the beach width. Furthermore, alongshore variation in sediment characteristics influence the sediment supply towards the dunes. The third component is 'Dune types' and considers the influence of the five initial different constructed dune profiles on the alongshore variations in morphological development.

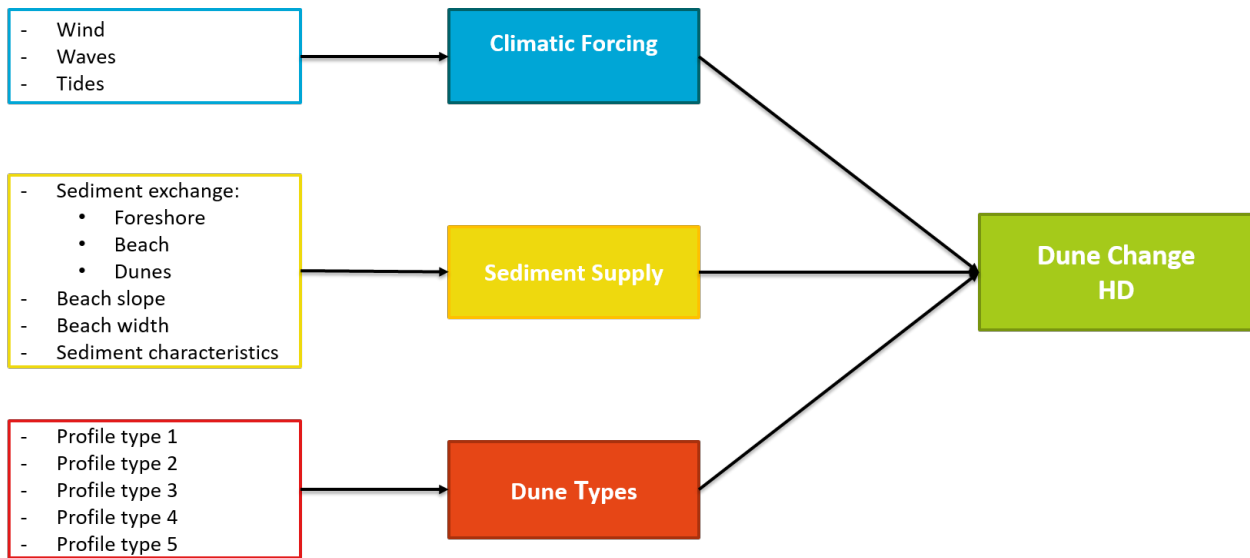


Figure 1.6: Conceptual framework of the dune change at the Hondbossche Dunes. The system is influenced by three major aspects: Climatic Forcing, Sediment Supply (aeolian and marine supply) and Dune Types (5 different profile types).

1.5. Research Objective and Questions

The objective of this study is to explore the effect of aeolian sediment transport on the morphological development of the beach and dunes of the HD system. Specifically, the research attempts to gain insight into the response of the different dune profile types. Although this study will be based on one particular case at the HD, the insights aim to provide a guide for dune maintenance of the Water Authority elsewhere along the coast and for other large-scale sandy strategies.

The following research question has been formulated for the Hondbossche Dunes to meet the objective and are addressed in the concluding chapter of this thesis:

How do different man-made dune geometries respond to the aeolian sediment transport towards the dunes?

The sub-research questions related to this main research question are:

1. What is the observed morphological development of the dry beach and dunes since construction?
2. What are the processes and parameters that influence the morphological development of the dry beach and dunes?
3. To what extent are existing models able to reproduce and predict the measured alongshore variations in dune growth?

1.6. Research Approach

This section outlines the steps that were taken to achieve the research objectives. The research includes a literature review, data analysis and numerical modelling which is schematized in Figure 1.7. Firstly, the existing literature on aeolian sediment transport and dune development is investigated in order to obtain insight into the relevant physical parameters and processes influencing aeolian sediment transport.

Secondly, the current available data of the HD system is evaluated to analyse how the system has developed since construction and to investigate which parameters are relevant and what are the driving processes.

Thirdly, two types of models are compared which have been developed for research into aeolian sediment transport and dune development in coastal areas. The first model is AeoliS, which has been developed at the Coastal Engineering department of Delft University of Technology. The second model is DUBEVEG, which has been developed at the Soil Physics and Land Management department of Wageningen University together with Imares. Relevant physical parameters and processes which have been included in these models and the model description are considered. Emphasis is put on the application of both models to simulate aeolian sediment transport for the HD system.

Consequently, the model AeoliS, used for modelling the Sand Motor, is modified based on topography, relevant climatic conditions and sediment characteristics for the HD system. The modelled sediment transport rates are compared to measured dune growth rates. Emphasis is put on understanding the influence of alongshore variations in aeolian sediment supply on aeolian sediment transport rates towards the dunes. In addition, the limitations of the model to reproduce and predict aeolian sediment transport and dune growth along the HD system are discussed.

The results originated from the data analysis and the numerical modelling has led to an understanding of the parameters and processes that influence aeolian sediment transport and dune growth at the HD system.

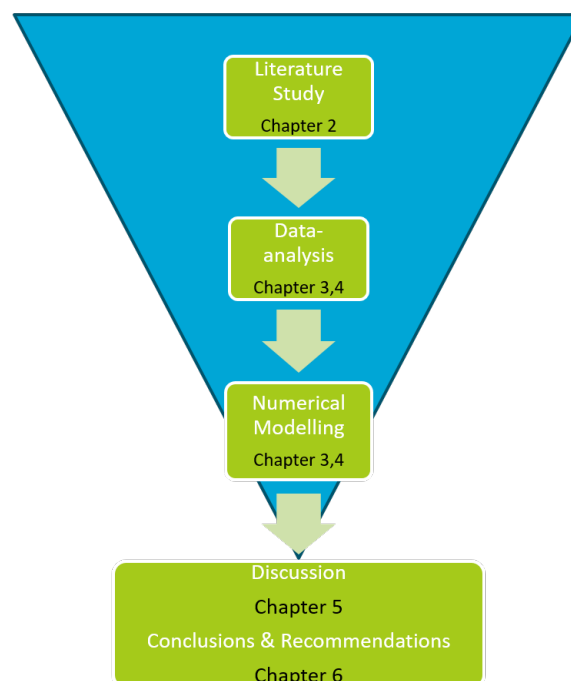


Figure 1.7: Steps in the research process

1.7. Thesis Outline

Chapter 2 presents a broad theoretical background on aeolian sediment transport. After introducing the physical processes involved in aeolian sediment transport and dune development, an introduction to the model AeLiS is given. Chapter 3 presents the methodology used for respectively the data analysis and the model study of the HD system. Chapter 4 presents the results of the data analysis into the morphological development of the system and the application of the AeLiS model to reproduce and predict aeolian sediment transport along the HD system. Chapter 5 provides a discussion about the results obtained in this research and Chapter 6 summarises the main findings and presents the recommendations for further research on aeolian sediment transport at the HD system and for management and maintenance of the HD system.

2

Literature Review

The aim of this chapter is to give a theoretical background on aeolian sediment transport in coastal areas and a description of the numerical model AeoliS that has been used in this study. This chapter starts with the theoretical background behind coastal dune formation and aeolian sediment transport. Then, the aeolian transport formulation that is used in this research will be discussed. Finally, the wind sediment transport model AeoliS is described.

2.1. Coastal Dune Formation

Research into the formation of dunes by wind started with the work of Bagnold: 'The Physics of Wind Blown Sand and Desert Dunes' [Bagnold, 1954]. Bagnold was first commander of the British army during the second World and served in the Libyan desert. Bagnold identified the main factors influencing the aeolian sediment transport rates in desert environments [de Vries et al., 2012] where different types of dunes can develop. Coastal dunes form only where there is a source of sediments, an onshore wind fast enough to move the sands, and a location at least far enough from the wave activity for depositions of sand. Vegetation will enhance deposition of grains in transit and anchor local depositions [Nordstrom et al., 1970]. In contrast to the dry desert dunes, coastal dunes arise from interactions between ecological and physical processes [Durán and Moore, 2013]. Eventually, it depends on the local wind climate in combination with the local topography how the dunes will develop.

Dune formation is the result of the interaction between sediments characteristics and different shear flow caused by the wind. In some areas vegetation might be a significant factor and interactions with topographical obstacles could also result in dune development. As the dune grows in height, the airflow is modified by interactions between the form of the dune and the air flow, see Figure 2.1. This results in modification of the boundary layer flow and will cause streamline convergence towards the crest. The air flow will increase the speed and the shear stress at the windward slope due to air compression. On the lee side, flow expansion, separation and streamline divergence occurs [Lancaster, 1970]. This creates secondary flow circulations (eddies) in the lee side of the dune. Further downwind, the moving air is reattached to the ground surface. The interactions between flow and dune shape changes as wind varies in direction, resulting in different type of dune patterns.

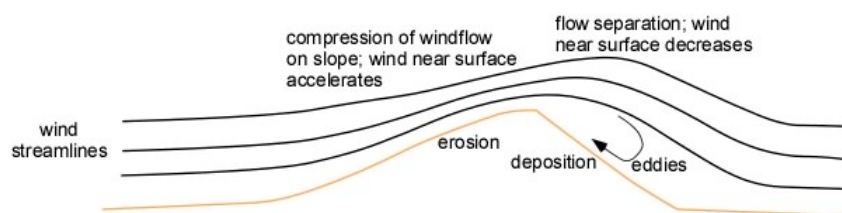


Figure 2.1: Theoretical description of wind flow over a dune, adapted from: [College, 2003]

2.1.1. Aeolian Sediment Transport

The wind transport the sediments from the sources towards the dunes. This is what is called aeolian sediment transport. The movement of sediments by wind results from momentum transfer from the air to the sediments. Aeolian sediment transport can be divided into three phases:

1. Initiation of sediment motion (erosion)
2. Transport of sediments
3. Deposition of sediments

In the majority of studies into aeolian sediment transport an empirical formula for the transport rate is derived from a logarithmic wind profile using the shear velocity u_* to the 3rd power. After a review of the general theory of air flow and sediment motion, the sediment transport equations will be examined in more detail.

Wind Flow over a Surface

Air flow over a surface will induce a surface shear stress to the surface as a result of a net downward flow of momentum. The shear stress τ is the force the wind exerts on a surface:

$$\tau = \rho u_*^2 \quad (2.1)$$

where:

$$\begin{aligned} \rho &= \text{the air density [kg/m}^3\text{]} \quad (\text{approximately } 1.22 \text{ kg/m}^3) \\ u_* &= \text{the drag velocity [m/s]} \end{aligned}$$

By assuming Prandtl's rough surface law (also called the law of wall) to describe turbulent air flow, Bagnold (1937) defines measured wind velocity at any height as:

$$u_z = 5.75 u_*' \log_{10} \frac{z}{k'} + u_t \quad (2.2)$$

where k' [m] is a measure for surface roughness height (often in the order of 0.01 m for normal dune sand), z [m] represents the specified height, u_*' is the velocity gradient of the flow and u_t [m/s] is the threshold velocity at the measured height k' above the surface. This equation predicts shear velocity based on wind velocity measurements.

Initiation of Sediment Motion

When wind is blowing over a moveable bed of sand particles, individual grains will start to move when the shear stress exceeds a threshold value. The fluid forces of lift and drag enhances the grains into motion upwards and parallel to the wind direction. For a sand grain resting on the bed, the lift force arises due to an uneven velocity distribution over the particle [Nordstrom et al., 1970], causing an upward directed pressure gradient and thus a lift force upward. The drag force results from the force of the air against the exposed areas of the grain. It is a function of the wind velocity and the surface roughness. The inertial forces, gravity force and inter particle cohesion, reduce the initiation of motion. The latter force is influenced by a number of factors related to the physical properties of the bed, for example surface moisture or shell content [Muller, 2011]. Combining the forces acting on a single grain will result in ratio of the effectiveness wind shear stress and the resisting forces. The threshold drag velocity, for the initiation of motion can be derived:

$$u_{t*} = A \sqrt{Dg(\rho_s - \rho)/\rho} \quad (2.3)$$

with D is the reference grain diameter, ρ_s is the density of the sand grains, ρ is the density of the air, g is the gravitational acceleration and A is an empirical coefficient based on the Shields function, derived by Bagnold varying for various conditions of interest [Bagnold, 1954].

Aeolian Transport Modes

As the shear stress velocity exceeds the threshold shear velocity, sediment transport will force the particles into suspension, saltation or surface creep mode as shown in Figure 2.2. When the particles are lifted from the surface and carried by the wind without having contact with the bed, the grains are in suspension. Saltation occurs when the grains are lifted from the bed, accelerated by the wind and ejecting new grains. During the creep mode the particles will move along the surface and stay in contact with the bed [Muller, 2011]. Sand moving in suspension is barely possible and thus saltation and creep are the most common modes on beaches and coastal dunes. The greatest fraction of aeolian sand transport is transported in saltation mode [Bagnold, 1954].

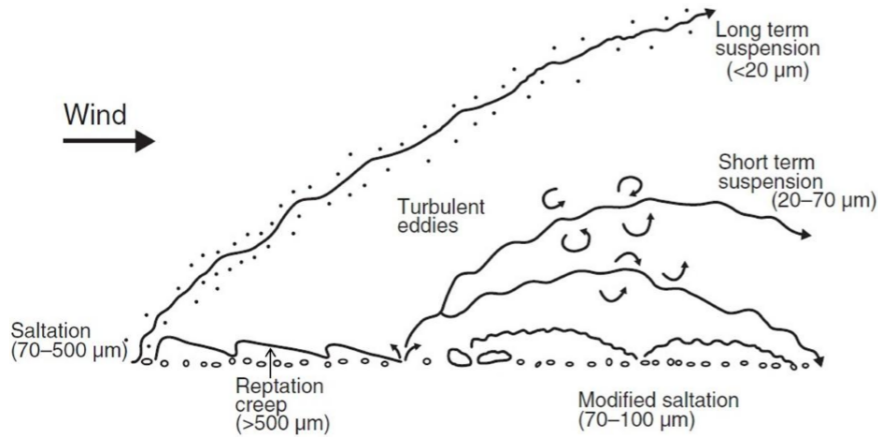


Figure 2.2: Modes of aeolian sediment transport, adapted from (Pye,1987).

2.2. Aeolian Sediment Transport Equation

2.2.1. Wind Driven Sediment Transport

The best conditions for aeolian sediment transport are horizontal and dry surface without vegetation or obstacles [Nordstrom et al., 1970]. For these circumstances, a large number of equations has been arrived. The formulae for wind driven sediment transport was firstly derived by Bagnold (1954). The rate of aeolian sediment transport [kg/s/m] over a dry beach can be described by:

$$q = C_b \frac{\rho}{g} \sqrt{\frac{d}{D}} (u_*)^3 \quad (2.4)$$

where C_b is an empirical coefficient related to the sediment size distribution (varying from 1.5 for nearly uniform sand, to 1.8 for typical dune sands, to 2.8 for moderately to poorly sorted sand, to more than 3.5 for a relatively immobile surface, for example cobbles or rock surfaces), d is the grain diameter of the sand [μm] relative to a reference grain diameter D of $250 \mu\text{m}$, ρ is the air density [$\text{kg} \cdot \text{m}^{-3}$], g is the gravitational acceleration [$\text{m} \cdot \text{s}^{-2}$] and u_* is the drag velocity [m/s]. Bagnold was followed by Kawamura (1951) who slightly reformulated the equation and added a threshold drag velocity u_{*t} at which dry and non-cohesive sand start to move:

$$q = C_k \frac{\rho}{g} (u_* - u_{*t})(u_* + u_{*t})^2 \quad (2.5)$$

Combining equations 2.2 and 2.4 a formulation can be obtained that relates wind velocity to estimated sediment transport:

$$q = \alpha C_b \frac{\rho}{g} \sqrt{\frac{d}{D}} (u_z - u_t)^3 \quad (2.6)$$

where

$$\alpha = \left(\frac{0.174}{\log z/k'} \right)^3 \quad (2.7)$$

α is a constant to account for the conversion of the measured wind velocity to the near-bed shear velocity following Prandtl's surface law. This relationship between wind speed and sediment transport assumes that there is sufficient sediment supply and steady wind conditions [de Vries et al., 2012].

2.2.2. Application to Coastal Areas

The assumptions valid for the description of aeolian sediment transport in the desert may not be automatically translate to a beach. The description of aeolian transport on a beach needs to include additional processes like moisture content, grain size sorting, storm surges, small-scale topography and vegetation cover [Muller et al., 2012] which will influence the sediment available for transport. Furthermore, the varying wind direction and wind velocity in combination with the tidal variations in water level will influence the effective fetch length and thus the wind transport capacity. Vegetation has an transport-limiting effect in the dunes,

Vegetation reduces the wind flow, capture the sediments and reduces erosion of the surface below and around the vegetation [Wolfe and Nickling, 1993]. Figure 2.3 shows an overview of the relevant processes and parameters involved in aeolian sediment transport in coastal areas.

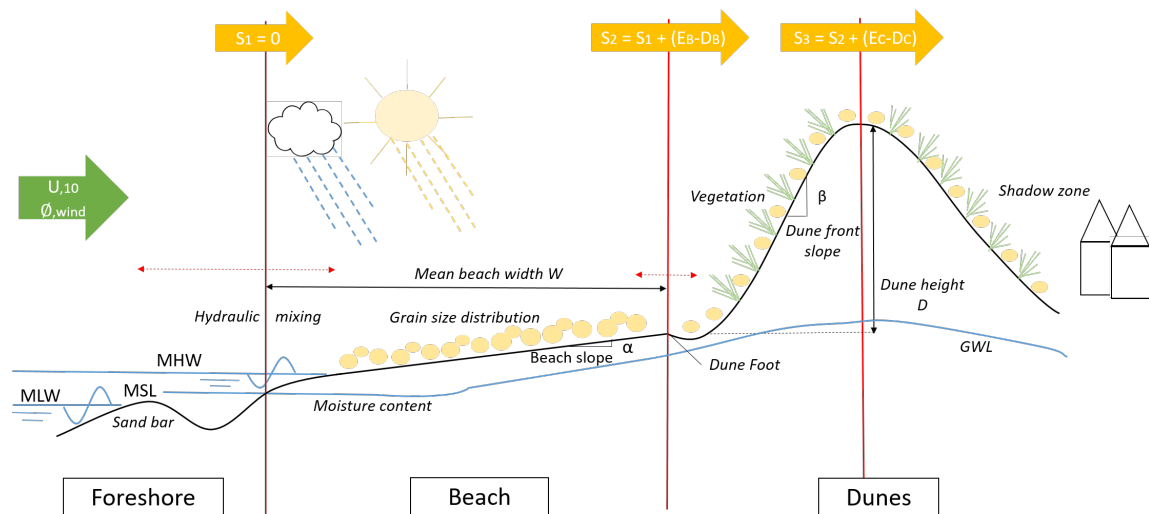


Figure 2.3: Cross-shore profile in which the important processes regarding aeolian sediment transport and dune development are mentioned.

Research studies using the Bagnold type formulation as described in equation 2.6, often assume wind speed as the only time-varying parameter. Other parameters in the formula are considered to be constant in time and space [Hoonhout et al., 2013]. This makes the temporal variability in aeolian sediment transport only dependent on changes in wind velocities [de Vries et al., 2012]. These studies often overestimate the sediment transport in coastal areas [Hoonhout et al., 2013]. A possible explanation for this overestimation are supply limitations like moisture content and grain size sorting which may act on different temporal and spatial scales. On beaches, a parameter like the moisture content or beach slope can also vary as a result of meteorological (rainfall) or hydrodynamic conditions (tides), independently of the wind conditions [de Vries et al., 2012].

Current research [de Vries et al., 2014] and [Hoonhout and de Vries, 2017] focus on the inclusion of spatio-temporal variations of supply limiting parameters in the aeolian transport formula. This approach forms an alternative for the traditional approach in which sediment capacity and/or availability is included through the velocity threshold [Hoonhout and de Vries, 2017] or the concept of critical fetch F_c . The latter concept distinguishes between saturated sediment transport, the fetch length F larger than the critical fetch F_c , and unsaturated sediment transport situations in which the fetch length F is smaller than the critical fetch F_c .

2.3. Aeolian Transport Model- AeoliS

In this research two different model approaches had been evaluated. The process-based model AeoliS and the cellular automata model DUBEVEG. A process-based model is characterized by physical external processes that forces the internal dynamics. A cellular automata model is rule-based model that uses a set of rules that represent a complex set of interacting physical laws [Keijsers, 2015]. The strength of AeoliS is to quantify sedimentation and erosion in supply-limited situations. The model DUBEVEG attempts on an accurate description of the interaction between vegetation and dune growth. It can predict the amount of sedimentation for two types of vegetation including the effect of seasonality on the quality and density of the vegetation. The model that is used in this study is the process-based model AeoliS. Figure 2.4 shows the similarities and the differences between both models. Both models are studying aeolian sediment transport under influence of climatic forcing. However, the model AeoliS attempt to understand aeolian sediment transport under supply-limited conditions and DUBEVEG analyse aeolian sediment transport regarding to dune development. In Appendix B more information about the model DUBEVEG can be found.

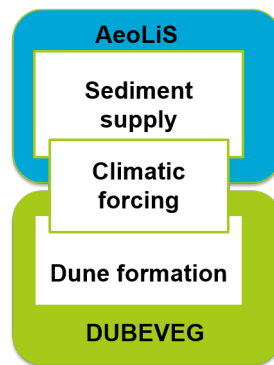


Figure 2.4: Similarities and differences between the process-based model AeoliS and cellular automata model DUBEVEG. AeoliS strength is to analyse the aeolian sediment supply under climatic forcing, whereas DUBEVEG strength is to analyse the dune formation under influence of climatic forcing.

2.3.1. Introduction to AeoliS

AeoliS is a process-based model which is developed by Sierd de Vries and Bas Hoonhout of Delft University of Technology [Hoonhout, 2016]. AeoliS includes a new model approach for aeolian sediment transport that focus on a distinction between the sediment availability and sediment transport capacity in a coastal environment. Compared to current sediment transport models, this approach includes a relatively smaller dependence of transport on wind speed (1^{st} order) and a higher dependence on sediment supply. This approach suggest a shift of focus on aeolian transport studies from solving complex wind field towards modelling source parameters when sediment transport rates are of interest [de Vries et al., 2014]. The model is able to describe aeolian sediment transport from the mean waterline till the dune foot.

2.3.2. Model Description

The model simulates spatio-temporal variations in bed surface properties and sediment availability instead of parametrizing through the shear velocity threshold or critical fetch. It is the first model that simulates the processes of sediment sorting and beach armouring. Furthermore, the model includes hydraulic mixing, infiltration and evaporation. The model distinguishes between transport-limited (due to limited fetch length) and availability-limited transport (due to varying bed surface properties).

Modelling Climatic Forcing

The AeoliS model is able to simulate erosion and deposition under influence of varying climatic conditions. Real time series of wind direction and wind speed, wave height and tidal level can be imposed to the model. The wind time series defines the capacity of the wind to simulate aeolian sediment transport. The tidal elevations and wave heights influence the aeolian sediment availability in the intertidal zone.

Modelling Sediment supply

The potential sediment supply is determined by the imposed topography under influence of climatic forcing. Marine processes influence the morphological development of the beach. The marine forcing reduces the beach width and steepens the beach slope resulting in a lower sediment availability for aeolian sediment transport towards the dunes. The tide influence the beach width such that during low tides more sediments comes available due to an extension of the beach width. Supply limiting processes are included in the model that influence the sediment availability in the intertidal zone. Evaporation lowers the moisture content and hence the sediments become available for aeolian sediment transport. The opposite behaviour is infiltration during high tide. This increases the moisture content and hence reduces the sediment availability. The main processes in coastal areas that influence the moisture content at the beach are the tide and wave run-up, rain showers and ground water. Wave forcing can also mix the beach surface near the water line enhances the availability of sand for transport.

The grain size distribution in the top layer of beach is exposed to wind and will therefore change over time. Fines may be eroded from the bed first, leaving the large grains behind. Therefore the beach surface become coarse and the threshold of motion increases. In calm periods, sediment sorting may lead to an armoured beach that is only mobilized after a storm surge [Hoonhout et al., 2013]. Shells and cobbles forms

non-erodible roughness elements which may shelter the erodible bed from wind erosion, resulting in reduced sediment availability.

Modelling Dune Formation

Dune formation is not included in the current stage of the model. Instead the shear threshold velocity is increased at the dune area to impose the effect of vegetation on deposition in the dunes. This simulates the transport-limiting effect of vegetation in the dunes. Aeolian sediment transport that passes the boundary between beach and dunes is assumed to deposit in the dunes and used to determine the dune growth rates.

2.3.3. Application to the Hondsbossche Dunes

A site as the HD with detailed and frequent topographic measurements is a good site for assessing the performance of the model compared to other model approaches.

1. **Strengths** - The model provide accurate information about the sediment fluxes from the beach to the dunes with an accurate description of the influence of beach surface properties on aeolian sediment transport.
2. **Weaknesses or lacks** - The spatial variations in wind velocity are not solved yet and hence no morphological feedback is included in the simulation. This means that the model is not able yet to simulate dune formation. Furthermore, the interaction between vegetation and sediment transport is not described in detail yet.

3

Methods

The previous chapter gives the general processes of aeolian sediment transport and dune development. The method to describe these processes for the Hondsbossche Dunes are shown in this chapter. The methodology consists of two parts; a data analysis and the application of a numerical model. The aim of the data analysis is to derive spatial and temporal volume changes of the beach and the dunes in order to analyse the morphological development of the system since construction. Furthermore, spatial and temporal variations in aeolian sediment supply towards these dunes are derived. The aim of the model application is to study the influence of the alongshore variations in sediment supply parameters on the aeolian transport towards the dunes.

3.1. Method: Data analysis

The conceptual framework in Figure 1.6, addressed in Chapter 1, presents the parameters and possible relations of interest between the forcing conditions and dune change. The method to derive changes and possible relations in morphological development of the beach and dunes consists of six steps:

1. Zonation of the cross-shore domain - subsection 3.1.2
2. Definition of the cross-shore transects - subsection 3.1.3
3. Derivation of volume changes for each zone - subsection 3.1.4
4. Derivation of the beach slope - subsection 3.1.5
5. Derivation of the beach width - subsection 3.1.6
6. Relation between sediment availability parameters and dune volume changes 3.1.7

Four different data sources have been used in order to derive the parameters of interest which will be elaborated upon first. Thereafter, the six method steps will be extensively described.

3.1.1. Data

Table 3.1 provides an overview of all the post-construction measurements including the location and frequency of measurements between May 2015 and December 2016. The individual data sources are elaborated upon below.

Table 3.1: Data-availability of post-construction measurements

Data	Coverage	Location	Frequency	Source
LiDAR	Topography	Petten- Camperduin	5 times	Contractor
LiDAR	Topography	Petten- Camperduin	1 time	Rijkswaterstaat
Single - beam	Bathymetry	Petten- Camperduin	every month	Contractor
Sieving curves	Grain size distribution	Petten-Camperduin	1 time	Contractor
RTK - GPS	Topography dune valley	Petten- Camperduin	2 times	HHNK

Morphology measurements

The morphology measurements, i.e. topographic and bathymetry, span the foreshore and the beach and dunes from -3.5 m NAP to landward of the previous sea dike. Surveys were executed using three different techniques, all based on global positioning systems. The bathymetry of the lower shoreface was measured using single beam echo sounder monthly by the contractor within the period June 2015 and September 2016 for eleven transects along the HD system. This covers a domain of about eight kilometres alongshore. Figure C.1 in Appendix C provides the aerial picture of the HD system which shows the location of the eleven transects. The topography of the beach and dunes were measured by Airborne LiDAR for five times in 19 months, the survey dates are¹

1. T0 - 24 May 2015
2. T1 - 28 December 2016
3. T2 - 21 March 2016
4. T3 - 1 September 2016
5. T4 - 5 December 2016

The surveyed domain spans at least the dry beach and dunes landward of the mean high water line (+0.8 m NAP) till beyond the HPZ between RSP 17.08 in the North and RSP 28.32 in the South [van Kesteren and Smit, 2013] as displayed in Figure 1.2 in Chapter 1. The coordinates are based on the Rijkswaterstaat reference system 'RijksStrandPaal'. The surveyed domain was 11.2 km by at least 340 m in along- and cross-shore direction, respectively. The measurements have a spatial resolution of 0.5 m and a vertical accuracy with an order of magnitude of a few centimetres. LiDAR does not penetrate through water and therefore the surveyed domain of the dune valley are not reliable for further analysis. Instead, additional surveys took place for the bed elevation data of the dune valley and the lagoon using RTK-GPS in Autumn 2016 and Spring 2016. The locations are provided in Appendix C.

Rijkswaterstaat, the Dutch Ministry of Infrastructure and Environment, executes annual coastline surveys to determine the deviation compared to the reference coastline of 1990 (Basal Coast Line). In March 2016 the first LiDAR flight took place above the new domain of the HD system. This survey is converted to 143 cross-shore transects which are identical to the so-called 'JARKUS' cross-shore profiles. The LiDAR survey of 21 March 2016, executed by the contractor, has been converted to the same cross-shore transects, in order to verify the reliability of the dataset. An example can be found in Appendix C for 3 cross-shore transects.

Grain size measurements

Sediment grains will start to move when the threshold shear velocity depending on the grain size, is exceeded as shown in section 2.1.1. The grain size alongshore are therefore studied. A total of 67 soil samples till a depth of -1 m NAP took place on site after completion of the project. These samples are used to determine the grain size distribution for five subdomains along the HD system [Brandenburg, 2015]. Figure 3.1 shows the median grain size D_{50} for the beach of the five subdomains S1- S5. A D_{50} of 290 μm was found for the entire project domain. Figure G.2 in Appendix C depicts the median grain size measured at the dunes by where a D_{50} of 328 μm was found.

¹The datasets does not show pre- and post storm season measurements, which is from October 1st till March 31st.

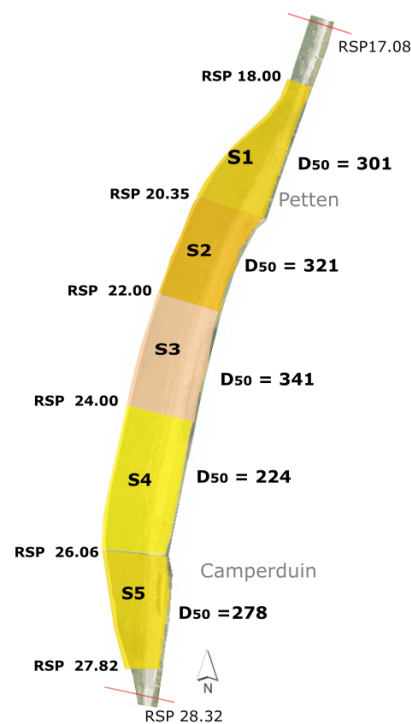


Figure 3.1: Aerial picture of the Hondbossche Dunes showing the median grain size D_{50} [μm] for each sampled subdomain S1 - S5. The location of the subdomains are indicated by RSP-coordinates.

3.1.2. Zonation of the Cross-shore Profile

The cross-shore profile has been distinguished into four different zones in order to derive spatial and temporal variations in morphological development. The four zones are distinguished by horizontal boundaries in vertical direction and a vertical landward boundary. This vertical landward boundary varies along the project domain from -35 m along the sea dike to -250 m RSP along the natural dunes Northwards and Southwards of the HD system. Exceptions will be individually appointed in the next steps. Figure 3.2 depicts the four zones that are defined.

1. Dunes: +3.5 m NAP
2. Dry beach zone: +0.8 m NAP till +3.5 m NAP
3. Intertidal zone: -0.75 m NAP till +0.8 m NAP
4. Surf zone: -3.5 m NAP till -0.75 m NAP

The surf zone and the intertidal zone together provide information about the spatial and temporal variations in marine supply along the HD system.

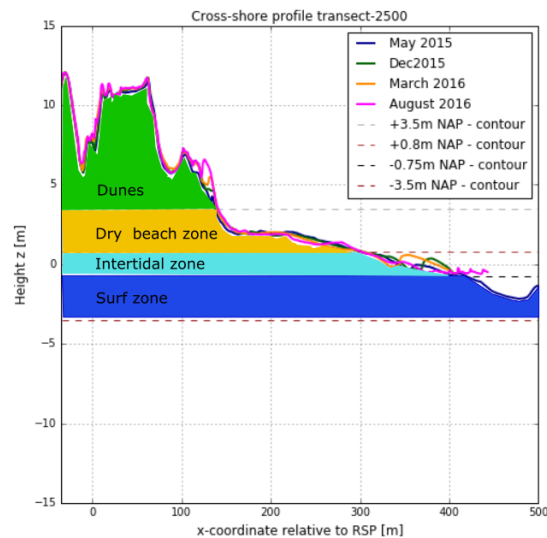


Figure 3.2: Definition of cross-profile zones used in this research. Four zones are distinguished: (1) Dunes, (2) Dry beach zone, (3) Intertidal zone and (4) Surf zone.

3.1.3. Definition of the Cross-shore Transects

The transect definition for the dry beach and dunes are identical to the so-called 'JARKUS' profiles, used for the annual coastline surveys executed by Rijkswaterstaat. A total of 135 transects have been used between transect RSP 17.08 in the North and transect RSP 28.32 in the South. Appendix F provides a map of the locations of all transects in Figure E.1 and an overview of the corresponding profile types in Table E.2. Originally, 143 transects were used, eight transects were discarded for different reasons, for example construction works, see Table E.1 in Appendix E. Five LiDAR surveys between May 2015 - December 2016, executed by the contractor, have been used to determine the parameters of interest of the dry beach and zone. The transect definition of the intertidal zone and the surf zone are identical for the eleven cross-shore profiles between RSP 19.10 and RSP 27.22, surveyed by the contractor using single-beam echo sounder. The locations of the 11 transects are coupled to the 135 transects of the beach and dunes. The five different profile types are distinguished for each analysis. See also section 3.1.1 for details about the measurements.

3.1.4. Volumes Changes of the Zones

Temporal volume changes have been determined for the beach and dunes by extracting cross-shore transects between successive time steps. Also cumulative volume change are derived between the first survey, T0 in May 2015 and the last survey, T4 in December 2016. Figure I.1 till Figure I.5 in Appendix I depict the sedimentation and erosion patterns for each measurement period which is used for the derivation. Only cumulative volume changes have been derived for the intertidal zone and the surf zone. The individual volumes per cross-shore zone are elaborated below.

Volume of the Dunes

The dune volume is enclosed by a vertical static point at the landward side and a horizontal line at the dune foot level, see Figure 3.2. The dune foot level is determined as the designed dune foot at +3.5 m NAP. The 135 cross-shore transects were evaluated for the dune foot level. Small deviations exist, but on average the dune foot position is in line with the designed dune foot level. Appendix E shows the dune volume enclosure for the individual profile types. Three exceptions are discussed here.

Connection with Northern dunes

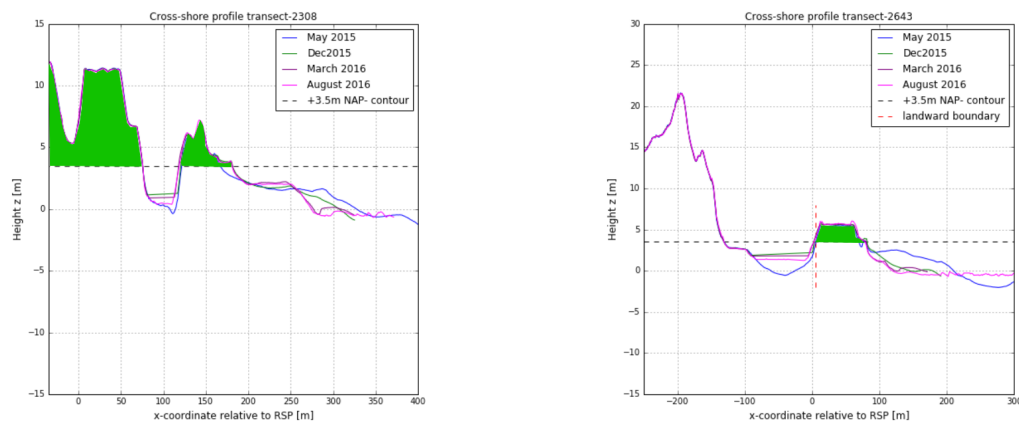
In between the first and the second survey (May 2015 - December 2016) additional construction works took place along the connection between the HD system and the natural dunes at Petten. Figure E.2 in Appendix E depicts a map of this location. At the map low dunes, some of them with a height above + 3.5 m NAP, can be observed at the beach. The low dunes are considered to be part of the dry beach and therefore the dune

volume change for the cross-shore transects between RSP 19.96 and RSP 20.29 had to be corrected. The survey of December 2015 (T1) is considered to be the baseline only for the transect between RSP 19.96 and RSP 20.29. Volume changes in between the period T0-T1 caused by the construction works were excluded. The correction volumes are listed in Table E.3 in Appendix E.

Profile type 4

Figure 3.3a depicts the dune enclosure for profile type 4. The dune valley is located between a lower foredune and a higher landward dune. Sediment that is transported by the wind into the valley is not considered to be part of the derived dune volume changes for this profile type.

Profile type 5 Figure 3.3b depicts the dune enclosure for profile type 5. At the location of the lagoon, the vertical landward boundary is defined at the seaward dune front of the lagoon and thus the only seaward dune front is considered. It is expected that minor changes will occur at the landward side of the lagoon in the first years after construction.



(a) Profile type 4

(b) Profile type 5

Figure 3.3: Two exceptions on the defined methodology for the dune enclosure: profile type 4 and 5.

Volume of the Dry Beach Zone

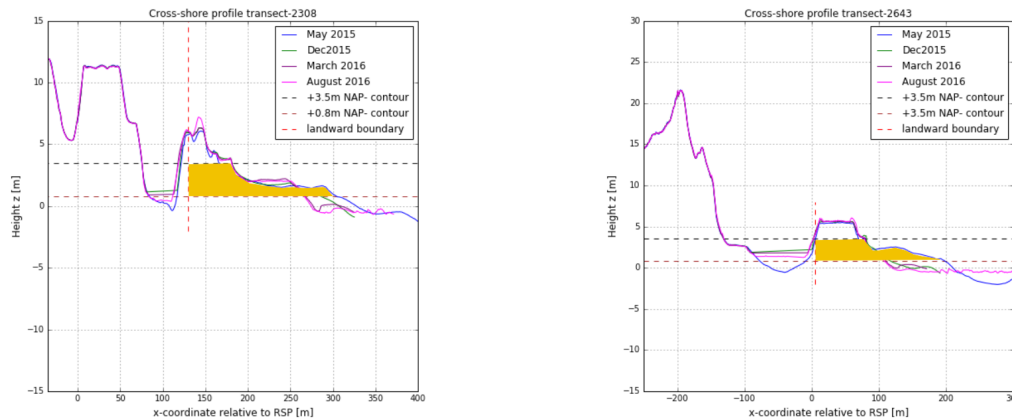
The volume of the dry beach zone is defined as the volume between the MHW level at +0.8 NAP meter and the dune foot level at +3.5 m NAP, see Figure 3.2. Appendix E shows the beach volume enclosure for the individual profile types. Two exceptions are mentioned here.

Profile type 4

Figure 3.4a depicts the beach enclosure for profile type 4. Note that the landward boundary is chosen at the dune crest of the seaward side of the Dune valley since only the first dataset includes the bathymetry of the dune valley. Sand that is transported by the wind into the valley is not considered as part of the volume changes of this profile type.

Profile type 5

Figure 3.4b depicts the beach enclosure for dune profile 5. At the location of the lagoon, the vertical landward boundary is defined at the seaward dune front of the lagoon and thus the beach volume seaward of the dune front is considered, see Figure 3.4b.



(a) Dune profile 4

(b) Dune profile 5

Figure 3.4: Two exceptions on the defined methodology for the dry beach enclosure: dune profile 4 and 5.

Volume of the Intertidal Zone

The volume of the intertidal zone is defined by the volume between mean high water (MHW) and mean low water (MLW). The mean tidal range at Petten is -0.75 to $+0.80$ m NAP.

Volume of the Surf Zone

The volume of the surf zone is defined by the volume between MLW at -0.75 m NAP and a depth contour of -3.5 m NAP.

3.1.5. Beach Slope

The beach slope has been derived for each of the five surveys between T0 in May 2015, and the last survey, T4 in December 2016. also the mean beach slope is determined. The beach slope is defined as the best fit line through the topography of the dry beach zone from MHW at $+0.8$ m NAP till the dune foot level at $+3.5$ m NAP, see Figure 3.5a.

3.1.6. Beach Width

The beach width has been derived for each of the five surveys between, T0 in May 2015, and the last survey, T4 in December 2016. The beach width is defined as the horizontal distance between the dune foot and the mean high waterline (MHW), see Figure 4.7. Cumulative change in beach width has been determined between the first May 2015 (T0) and the last December 2016 (T4) survey. In order to obtain insight into the forcing that causes the changes in beach width, the position of the MHW-line and dune foot is plotted for the five surveys.

Connection with Northern dunes

Between the first and the second survey (May 2015 - December 2016) additional construction works took place along the connection between the HD system and the natural dunes at Petten. Figure E.2 in Appendix C depicts a map of this location. At the map low dunes, some of them with a height above $+3.5$ m NAP can be observed at the beach. Between RSP 19.83 and RSP 20.29 the beach width reduces significantly when the defined derivation of the dry beach width is applied. In order to reduce the influence of these construction works, the dune foot position measured at December 2015, at the landward side of the low dunes, is the baseline for the transects between RSP 19.83 and RSP 20.29. The consequence is that no change in dune foot position in the period T0-T1 are measured.

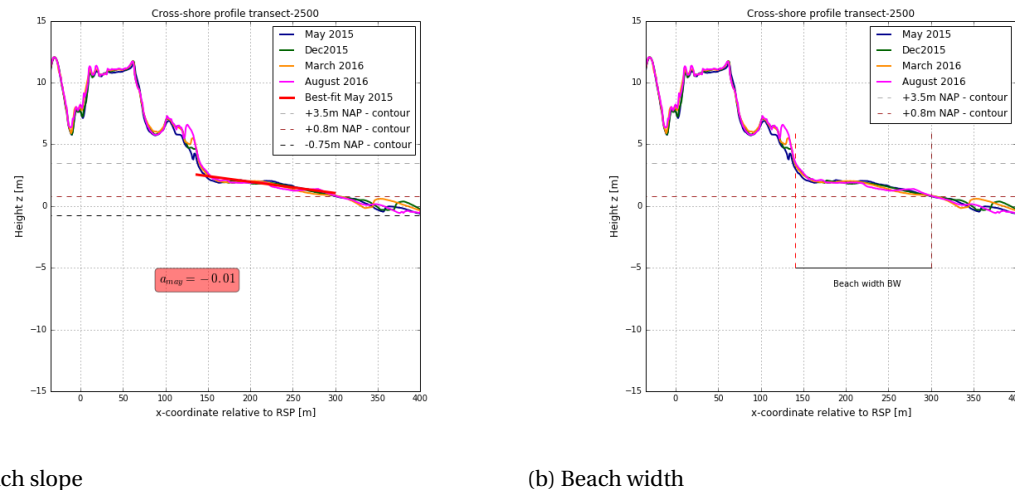


Figure 3.5: Dry beach zone definition used in this thesis

3.1.7. Relation Aeolian Sediment Availability and Dune Volume Change

The four sediment supply parameters: beach volume change, beach slope, beach width and median grain size of the beach are plotted against dune volume changes in order to test the conceptual framework on dependencies between sediment supply parameters and dune volume change. The analysis was only performed for the cross-shore transects along the new constructed beach-dunes system between RSP 20.25 and RSP 27.00, see Figure 1.2. The expected relation for each parameter is discussed:

- When significant sediment exchange between the dry beach zone and the dunes takes place a strong negative correlation is to be expected.
- For both the beach slope and the beach width it is expected that they show similar behaviour and therefore a positive correlation. When the beach slope becomes milder (resulting in a more positive value) or the beach become wider more sediment becomes available for sediment transport. This increases the potential dune growth. Beach slope is often a more constant parameter than beach width and therefore it is chosen to plot both. parameters.
- When the median grain size of the beach increases it is expected that the potential dune growth is less and therefore a negative correlation is to be expected. The median grain size is derived from soil samples that took place after construction of the works, there are five representative subdomains with a different median grain size D_{50} , see Figure 3.1.

3.2. Method: Modelling

The objective of the numerical modelling is to obtain a model hindcast that is able to reproduce (1) the observed erosion and sedimentation patterns and (2) the magnitude of dune volume changes along the HD system under influence of alongshore variations in aeolian sediment supply. The two-dimensional AeLiS model proved to successfully capture limitations in sediment availability on the aeolian sediment transport for the sand engine [Hoonhout and de Vries, 2017]. The model's strength for the Hondsbossche domain is to contribute to the effect of the variation in alongshore grain size distribution on the dune change. The method consists of four steps:

1. Model schematization of the HD system - subsection 3.2.1
2. Comparison of measured and modelled erosion and deposition patterns - subsection 3.2.2
3. Quantification and of modelled dune volume changes - subsection 3.2.3
4. Verification of the modelled dune volume changes - subsection 3.2.4

3.2.1. Model Schematization

A test simulation with the topography of the HD system provided insight into the modifications that have to be accounted for in the model code before the morphological development of the HD system can be simulated. Figure G.3 depicts the overview of the required model input for the HD system. The model input is divided into five categories related to:

- Topography
- Time
- Climatic forcing
- Sediment characteristics
- Vegetation

The model configuration files are given in Appendix G.

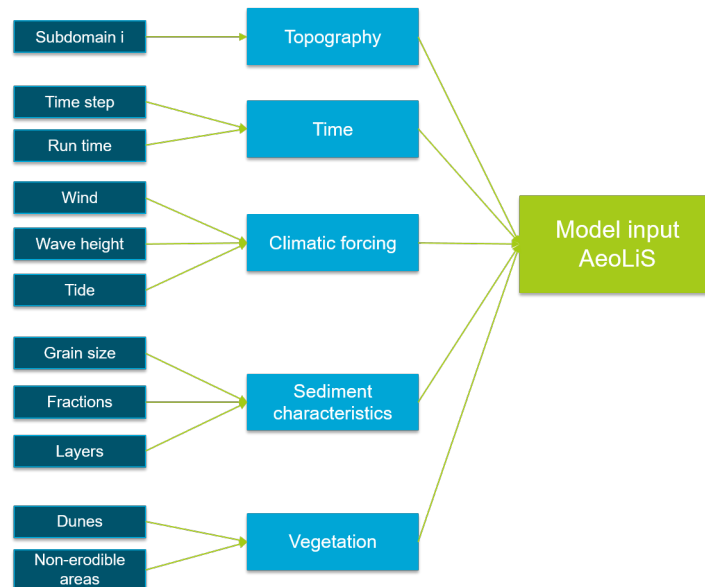


Figure 3.6: Schematic overview model input which is divided into five categories: Topography, Time, Climatic forcing, Sediment characteristics and Vegetation.

Topography

The topography of the first LiDAR survey, T0 in Mei 2015, has been imposed to the model. The bed elevation data were rotated with 15 degrees to a local orthogonal coordinate system in which x is defined in cross-shore direction and y in alongshore direction. The origin is located Northwards of RSP 17.08 with $x = 107218$ and $y = 535679$. The collected x, y, z point data of the survey were combined and interpolated to a 10 by 10 m grid. The project domain is divided into five subdomains S1 - S5 in order to impose alongshore variations in grains size characteristics. Each subdomain is simulated separately by selecting the local topography which is interpolated to a 10 by 10 m grid and imposing the measured grain size distribution. Figure 3.7 provides a schematic overview of the location the median grain size of each of the five subdomains. Note that the natural dunes North and South of the HD system are not included in the modelling. The topography of each subdomain is given in Appendix G.

Time

The model was run with an hourly time step, over the total period of the available surveys, i.e. 562 days (24 May 2015 to 5 December 2016).

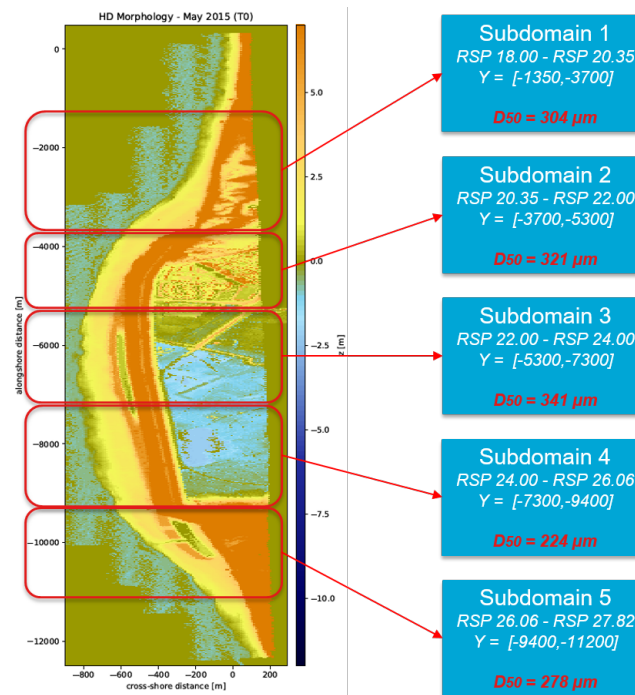


Figure 3.7: Schematic overview of the model runs. The HD system is divided into five subdomains in order to simulate alongshore variations in median grain size.

Climatic forcing

Hourly measured wind speed and direction are imposed to the model for the period May 2015 - December 2016. The dataset was rotated with + 75 degrees in order to fit with the local orthogonal conditions. Hourly wave height and ten-minutes water levels are imposed to the model for the same period May 2015 - December 2016. Water levels and wave heights are initially uniformly imposed to every grid cell in the model domain. Consequently, the water levels and wave heights are also present at cells that are lower than measured water level. This will influence the erosion and deposition pattern simulated by the model. To account for these issues a tide and wave mask is implemented in the simulation which locally lowers the water level in a grid cell.

Table 3.2 provides an overview of the data that has been used including the location and frequency of the measurements. The three locations used for the climatic data, are given in Figure 3.8. The wind data were obtained from the wind station 'IJmuiden' located 35 kilometres southwards of the HD system. This location was chosen as representative even though it is further away as 'De Kooy' which is located 30 kilometres North of the HD system. This decision was made because 'De Kooy' is not located along the (Dutch) coastline, see Appendix D for measured wind conditions at Den Helder.

Table 3.2: Data-availability used for input model

Data	Coverage	Location	Frequency	Source
Wind station	Wind conditions	IJmuiden	every hour	KNMI
Wave buoy	Wave height	Ijmuiden Munitiestortplaats	every hour	Rijkswaterstaat
Tidal levels	Tidal levels	Petten- Zuid	every 10 minutes	Rijkswaterstaat
Sieving curves	Grain size distribution	Petten - Camperduin	1 time	Contractor

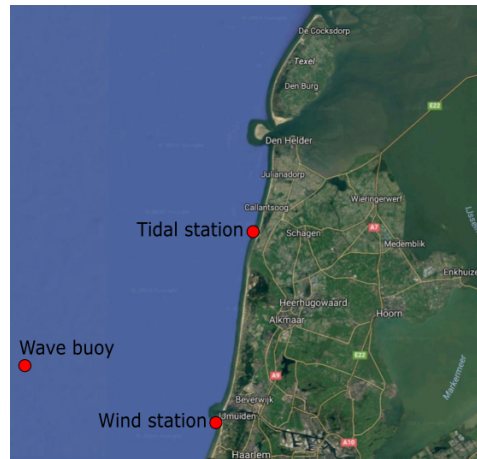
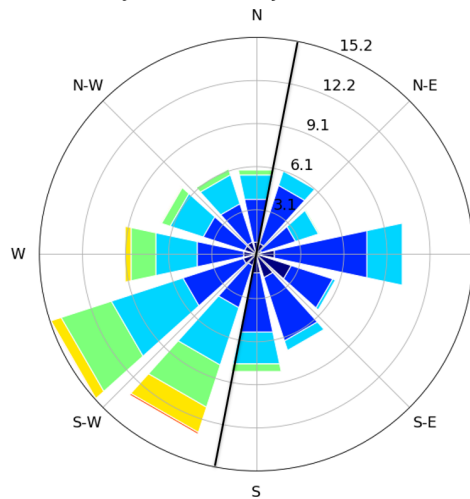


Figure 3.8: The location of the wind, wave and tidal level stations are indicated by red dots.

Wind conditions

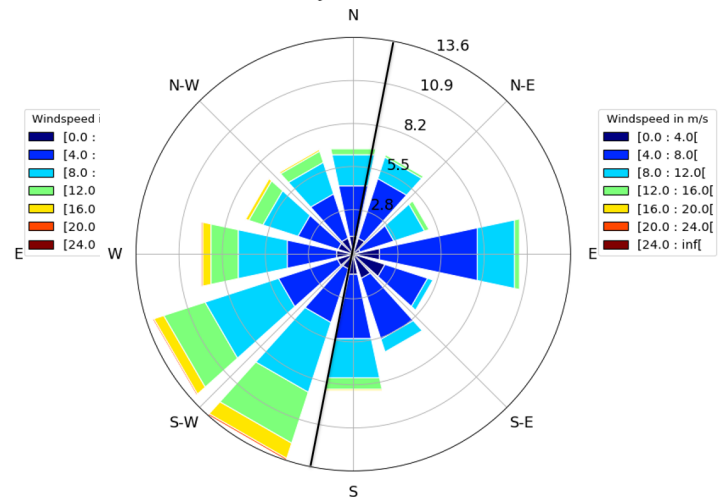
Figure 3.9a depicts the wind climate for the period May 2015 - December 2016 at 10 m above the bed. The orientation of the coastline of 15 degrees is plotted as a black line in both figures. The wind direction was mainly southwest for the period T0-T4. This is similar to the long term averaged wind climate in the period 1981-2015, see Figure 3.9b, but real stormy conditions are missing in both datasets. The maximum recorded wind speed over the first 19 months was 26 m/s which is equal to wind force 10 on the Beaufort scale. Appendix D provides also more information about the wind conditions measured between successive measurements. It shows that the maximum average wind speed was measured in the period December 2015 - March 2016 which were mostly from the south and west sectors. In contrast, during the the summer period March 2016 - September 2016 and the fall period September 2016 - December 2016 wind speeds were low and mostly from the north and west sectors (T2-T3) and the north and east sectors (T3-T4). The highest occurrence of wind speeds are between 4-8 m/s. This is typically found to be the wind speed found for aeolian sediment transport [de Vries et al., 2012].

Wind climate IJmuiden, 24 May 2015 - 5 December 2016



(a) Period May 2015 - December 2016

Wind climate IJmuiden, 1981 - 2015



(b) Period 1981 - 2015

Figure 3.9: The wind climate for station IJmuiden, the average coastline orientation of 15 degrees of the HD system is plotted.

Tidal levels

Figure 3.10 depicts the recorded water levels at the station of Petten-Zuid. In the period between November 2015 and January 2016 the highest water levels were measured with a highest recorded water level of 195 centimetres. Figure 3.11 shows the yearly recorded maximum sea level at the station of Petten-Zuid. The maximum sea level of 195 cm above NAP, is in contrast to the long term averaged sea level 13 cm lower. Two recorded storms have happened for this coastal stretch with a force of 8 on Beaufort scale in November 2015 [Watermanagementcentrum, 2015a], [Watermanagementcentrum, 2015b]. Appendix D contains more information about the conditions during these storms and the minimum recorded water levels at Petten-Zuid.

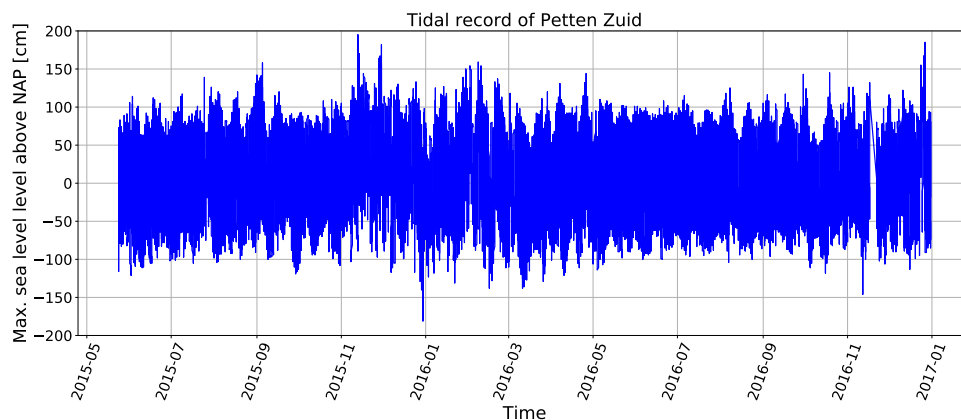


Figure 3.10: Recorded water levels at Petten-Zuid in the period 24 May 2015-5 December 2016.

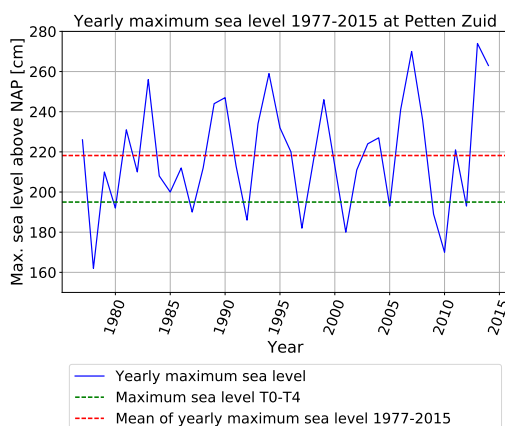


Figure 3.11: Yearly maximum sea level for the period 1977-2015 at Petten-Zuid. The red dashed line depicts the mean of the yearly maximum sea level for the period 1977-2015. The green dashed line depicts the maximum recorded sea level between May 2015 - June 2016.

Sediment characteristics

Figure 3.12 depicts the imposed grain size fraction for each subdomain. The sand fractions cover a range of 0.03 mm to 8 mm. The sediment characteristics are derived for each of the five subdomains based on 10-16 samples for each subdomain. This has result in minor deviations regarding to the measurements as shown in Figure 3.1. The deviations are given in Table 3.3. The grain size distribution is imposed to the initial bed that consist of 10 bed composition layers with a thickness of 1 cm each. Figure G.5 in Appendix G provides the grains size distribution.

Vegetation

In reality, vegetation is able to capture and hold the sediments. As the dune area is not included in the current stage of the model domain, a vegetation mask is implemented in the simulation. At measured topographies

Table 3.3: Deviations between measured grain size distribution and the derived grain size in the model.

	Subdomain 1	Subdomain 2	Subdomain 3	Subdomain 4	Subdomain 5
D ₅₀ - measurements	291	327	341	229	277
D ₅₀ - model	304	321	341	224	278

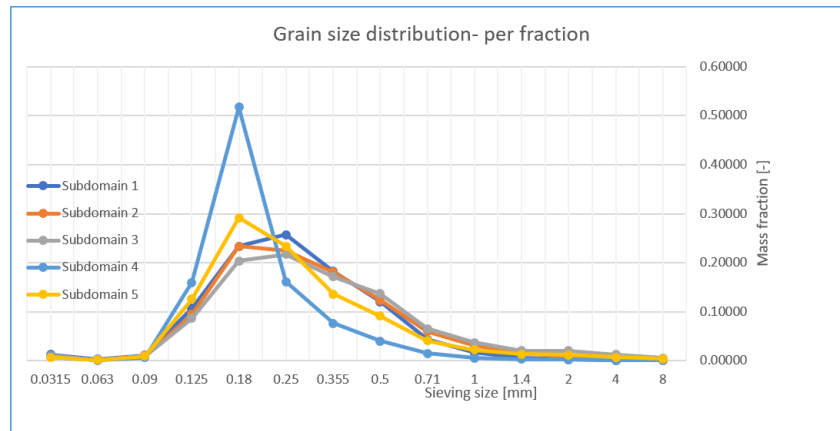


Figure 3.12: Grain size fraction for the five subdomains S1- S5. Subdomain S4 contains the finest fraction of sediment grains whereas subdomain S2 the coarse fraction.

higher than +3.5 m NAP, the location of the dune foot, the threshold velocity is increased by fifty % to impose the effect of vegetation on deposition in the dunes. The assumption is compared to the research of Keijsers [Keijsers, 2015] in which no strong correlation between vegetation density and deposition was calculated. Although high values of sedimentation are most common for a vegetation cover between 20 and 80 percent. The shear threshold velocity is assumed to be constant over time and alongshore. By implementing this vegetation mask a boundary is made between the beach zone and the dunes. Moreover, it reduces aeolian sediment transport in the dune area.

For grid cells that are not part of the project domain, for example landward of the Hondsbossche Dunes, an infinite value for the threshold velocity is defined. Aeolian sediment transport is therefore impossible. The same procedure is applied to the dune valley where in reality no aeolian sediment transport could take place due to the water level in the dune valley.

3.2.2. Measured and Modelled Sedimentation and Erosion Patterns

Measured and modelled sedimentation and erosion patterns are compared to test the capability of the model to reproduce the morphological development of the system. This comparison is made for the four measurement periods and the cumulative measurement period between May 2015 - December 2016. Section 4.2.1 presents the measured and modelled results. The measured topography at the seaward side and at the dune valley are not reliable since the LiDAR is not able to penetrate through the water. The location of the MHW-line and the dune foot position at +3.5 m are indicated in the figures of the measured topography.

3.2.3. Quantification of Modelled Dune Volume Change

To calculate the modelled dune volume changes it is assumed that all sediments passing the dune foot boundary at +3.5 m NAP will settle in the dunes. The dune growth rates [$\text{m}^3/\text{m}/\text{y}$] are based on the modelled bed level changes between successive measurements along the dune foot. The dune growth is determined for every 100 meters alongshore (5 grid cells) for the four measurement periods and cumulative measurement period between May 2015 - December 2016. The formulation that has been applied is:

$$\Delta V_{dunes} = \sum_{t_0}^{t_{end}} A_g \frac{1}{dy} \frac{365}{t_{end} - t_0} \quad (3.1)$$

where A_g is the surface of the grid cell which is 10 by 10 m, dy is the alongshore distance of the grid cell which is 10 m and t_0 is 0 and t_{end} the amount of days between successive LiDAR surveys. The total amount of the

days between the the first, T0 in May 2015, and T4, in December 2016, is 562 days.

3.2.4. Verification of the Modelled Dune Volume Change

The modelled dune growth rates are compared to other dune growth rates derived from three different methods to verify the results. These other dune growth rates combined with a short description, are given below.

Measured dune growth rates

Periodic and cumulative measured dune growth rates derived from LiDAR surveys are compared, see subsection 3.1.4.

Design calculation

A constant design value of 35 m³/m/y in the first year after construction is obtained from previous research and expertise of the Holland coast [de Vries et al., 2012], [van der Wal, 2004], the extension of the port of Rotterdam 'Tweede Maasvlakte' and the coastal reinforcement project 'Spanjaardse Duinen' along the Delfland coast [?].

Theoretical calculation

The formulation of Bagnold has been used for a theoretical description for the capacity of the wind to transport sediments towards dune dunes under absence of supply limited processes. The potential dune growth for the Hondsbossche domain [m³/m/y] is calculated based on hourly wind conditions in the period May 2015 - December 2016, obtained from the weather station of IJmuiden. The median grain size D_n of 290 μm measured for the entire Hondsbossche domain is assumed for this derivation. The Bagnold formula provides the upper limit of aeolian sediment transport capacity in [kg/m/s] and can be described according to:

$$q = \alpha C_b \frac{\rho}{g} \sqrt{\frac{d_n}{D_n}} (u_z - u_t)^3 \quad (3.2)$$

where C_b is an empirical coefficient related to the sediment size distribution (typically 1.8 for dune sands), d_n is the nominal grain diameter of the sand [μm] relative to a reference grain diameter D_n of 250 μm , ρ_a is the air density and is taken for a temperature of 20 degrees Celsius as 1.2 kg m³, g is the gravitational acceleration [m s⁻²], u_z is the measured wind velocity at a height of 10 meters above the bed and u_t is the threshold velocity according to $u_{th} = 5.75 A \sqrt{D} g (\rho_s - \rho_a) / \rho_a \log \frac{k}{k'}$ [m/s] in which $A = 0.08$ [-] for air flow, $k' = 0.01$ m and $k = \frac{1}{30} d_n$ m. $\alpha = \left(\frac{0.174}{\log z / k'} \right)^3$ is a constant to account for the conversion of the measured wind velocity to the near-bed shear velocity following Prandtl's surface law in which z is taken as 0.5 m.

To indicate the dune growth along the HD system there is only an interest in the onshore component of the wind direction. Therefore, the upper limit of the sediment transport capacity of the wind has been calculated by only taken into account the onshore component of the wind measurements between 195 and 15 degrees, in line with the orientation of the coastline. Every measurement i with an orientation angle varying from shore normal direction, needs to be corrected according to:

$$u_{z,cor} = u_{z,i} \cos(\theta_{cor} - \theta_{z,i}) \quad (3.3)$$

The sediment transport capacity in shore-normal direction for an individual measurement i becomes:

$$q_{x,i} = q_{sat,i} \cos(\theta_{cor} - \theta_{z,i}) \quad (3.4)$$

in which $\theta_{z,i}$ is the wind direction and θ_{cor} the correction angle between north and the shore normal. The total sediment transport capacity [m³/m] in onshore direction is the summation of the individual **positive** measurements and defined as:

$$q_{x,tot} = \sum_{n=1}^{\infty} q_{x,i} \frac{1}{(\rho_s - \rho_a)(1 - p)} * dt \quad (3.5)$$

in which p is the porosity [-] and typically 0.4, required to transform the mass transport into a volume transport. ρ_s is the density of the grains and chosen as 2650 kg/m³ and dt is the time between two wind measurements which is 1 day or 86400 seconds. Using these equations result in the following answers for the total onshore directed transport capacity of 216 m³/m/y.

4

Results

This chapter presents the results about the morphological development of the HD system for the nineteen months after construction. The results are derived from a data analysis and the application of a numerical model. Reference is made to Chapter 3 for the methodology applied and the assumptions that were taken to obtain the results. Section 4.1 presents the data analyses of (1) the spatial and temporal variations in the four different zones of the cross-shore profile and (2) spatial and temporal variations in aeolian sediment availability. The five different dune profile types are distinguished within the results. Section 4.2 demonstrates the model results of (1) measured and modelled sedimentation and erosion patterns and (2) measured and predicted dune growth rates.

4.1. Results: Data Analysis

4.1.1. Measured Erosion and Deposition over the Project Domain

Figure I.1 shows the measured nett erosion (in blue) and deposition (in red) for the full project domain above 0 m NAP during the period May 2015 - December 2016 (T0-T4). The figure clearly shows that erosion is pronounced at the beach area and deposition at the dunes. In alongshore direction, beach erosion is mostly observed along the Northern shoulder, between $y = -3200$ m and $y = -5000$ m, and along the Southern shoulder, between alongshore coordinate $y = -8500$ m and $y = -10500$ m. However, deposition at the beach is also found Northwards ($y = -3200$ m) and Southwards of the HD system ($y = -10500$ m). Deposition in the dunes is strongly pronounced along the Southern part of the HD system between alongshore coordinate $y = -6000$ m and $y = -9000$ m. Further information about the system is obtained by calculating spatial and temporal variations for a total of 135 cross-shore profiles derived from the data, see Figure I.1 and the measured erosion and deposition plots between consecutive surveys which are depicted in Appendix I. Table 4.1 presents an overview of the derived parameters.

Table 4.1: Overview of derived parameters and associated section

Parameter of interest	Section
ΔV Surf zone	4.1.2
ΔV Intertidal zone	4.1.2
ΔV Dry beach zone	4.1.3
ΔV Dunes	4.1.4
Beach slope	4.1.5
Beach width	4.1.6

4.1.2. Volume Change of the Surf Zone and the Intertidal Zone

Figure 4.1 shows the alongshore distribution of the morphological changes [m^3/m] of the surf zone and the intertidal zone within the period May 2015 to September 2016. The surf zone is defined between -3.5 m NAP and -0.75 m NAP (MLW) and the intertidal zone between -3.5 m NAP and -0.75 m NAP. The figure shows that the volume changes derived in the surf zone are always larger than the derived volume changes in the intertidal zone, except for two locations: (1) between RSP 21.00 and RSP 21.46 and (2) near RPS 27.00. Along the HD system, i.e. the area within the blue horizontal lines at RSP 20.25 and RSP 27.00, mainly erosion of the surf zone and the intertidal zone is observed, respectively, except for two locations: (1) near RSP 22.38, where deposition is observed in the surf zone and small erosion in the intertidal zone and (2) between RSP 24.15 and RSP 25.57, where deposition is observed in the surf zone and comparable erosion in the intertidal zone.

Table 4.2 provides an overview of the yearly average volume changes [$m^3/m/y$] per area. Although higher volume changes were derived in the surf zone, the average volume changes of both zones are comparable. The mean volume change observed in the period May 2015 - September 2016 is $-48 m^3/m$ for the surf zone which corresponds to $-39 m^3/m/y$ yearly, and for the intertidal zone $-45 m^3/m$ which is $-35 m^3/m/y$. However, it should be noted that high erosion rates were observed within the first months after construction due to: (1) the initial adaptation of the system to the climatic forcing and (2) event driven sediment transport due to more and higher south-western waves. This can be seen in the large erosion volume in particular along the Southern shoulder which is located between RSP 25.57 and RSP 27.72. The maximum erosion of the surf zone measured in this period is $-198 m^3/m$ and of the intertidal zone of $-123 m^3/m$ at this location. Deposition took place Northwards and Southwards of the HD system with a maximum of $110 m^3/m$ in the surf zone and $24 m^3/m$ in the intertidal zone.

Table 4.2: Cumulative net volume change for the intertidal zone and the surf zone between May 2015 - September 2016. The RSP coordinates indicate the alongshore locations in Figure 4.2 from North (first row) to South (last row).

	RSP coordinates	Surf zone <i>[$m^3/m/y$]</i>	Intertidal zone <i>[$m^3/m/y$]</i>
Northern Dunes	17.08 - 20.25	+90	+20
HD system	20.25 - 27.00	-61	-50
Southern Dunes	27.00 - 28.32	+49	+3
Full project domain	17.08 - 28.32	-39	-35

The derivation is limited to the eleven transects measured by the contractor and show only cumulative net volume changes for the period May 2015 - September 2016, whereas derived parameters of the dry profile covers the entire project domain from RSP 17.08 till RSP 23.32 and show temporal variations for the four surveys between May 2015 - December 2016. In section 4.1.8 the results are compared to the other three zones of the cross-shore profile.

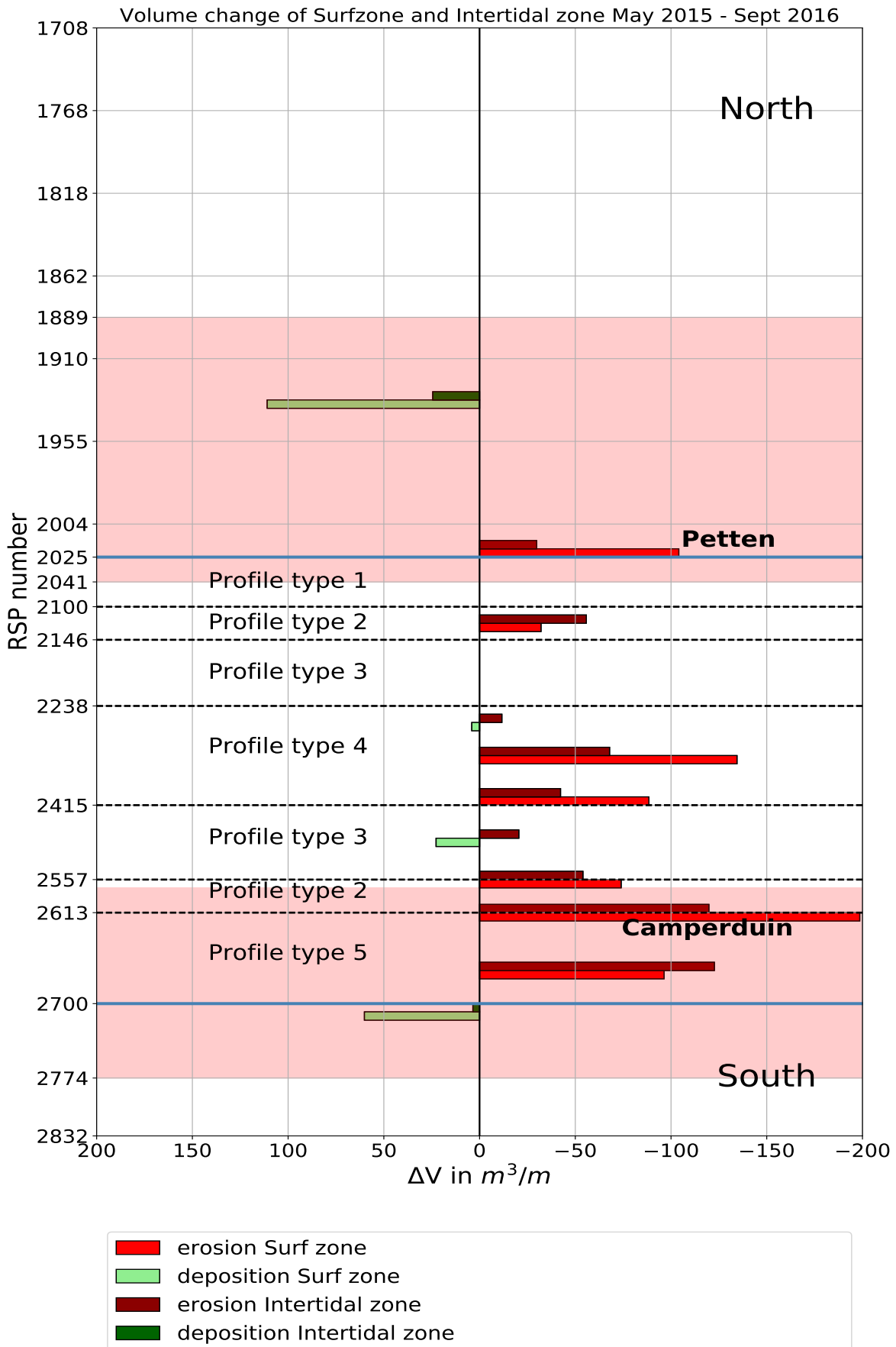


Figure 4.1: Derived cumulative net volume change of the surf zone and the intertidal zone in the period June 2015 - September 2016. Note that the figure has the same orientation as the Dutch coastline which means that the North is at the upper part of the figure and the South at the lower part of the figure. The sea is located at the left side of the origin and dry land is located at the right side of the origin; erosion (red coloured) means that the coastal area retreats and is therefore depicted towards the right into landward direction and deposition (green coloured) means that the coastal area extends and is therefore depicted toward the left into seaward direction. Difference in height of the bars indicates spatial variability in volume changes. The blue lines indicate the boundaries of the new HD system and the red shaded areas indicate the locations of the Northern and Southern shoulder. The black dashed lines distinguish the five different dune profile types.

4.1.3. Volume Change of the Dry Beach Zone

Temporal variability in volume changes

Figure 4.2 shows the alongshore distribution in morphological change of the dry beach zone [m^3/m] in the four measurement periods. The dry beach zone is defined as the zone between +0.8 m NAP (MHW) and +3.5 m NAP (dune foot). Beach volume changes for the cross-shore transects varies between $-125 m^3/m$ and $50 m^3/m$. Table 4.3 provides an overview of the spatio-temporal variability in beach volume change [$m^3/m/y$] per profile type alongshore derived from Figure 4.2. The results show that a strong erosion of $-21 m^3/m/y$ was measured in the first period after construction, between May 2015 - September 2016 (T0-T1), along the full project domain. This is $-64 m^3/m/y$ when only the HD system is considered. Moreover, the obtained results show that a significant response was measured in the between March 2016 - September 2016 (T2-T3). In this period, mainly deposition was observed along the project domain with an average value of $+28 m^3/m/y$, except for profile type 2 (South) and 5. In the last period, between September 2016 - December 2016 (T3-T4), a relatively large decrease in the beach volume was obtained, except for profile type 4 and 3 (South). It is worth noting that along profile type 2 (South) and profile type 5 only erosion is measured in time and along profile type 4 and the Southern dunes only deposition is measured in time. Within the surveys, there is significant alongshore variability in beach volume change which will be described in more detail below for each of the successive surveys.

Table 4.3: Temporal Dry beach volume changes per profile type in the four measurement periods. The RSP coordinates indicate the alongshore location in Figure 4.2 from North (first row) to South (last row). Left column shows the cumulative net volume change between May 2015 - December 2016.

	RSP coordinates	T0-T1 [$m^3/m/y$]	T1-T2 [$m^3/m/y$]	T2-T3 [$m^3/m/y$]	T3-T4 [$m^3/m/y$]	T0-T4 [$m^3/m/y$]
Northern Dunes	17.08 - 20.25	-1	+30	+47	+14	+20
Profile type 1	20.25 - 21.00	-46	-1	+24	-24	-15
Profile type 2 North	21.00 - 21.46	-69	-19	+32	-37	-27
Profile type 3 North	21.46 - 22.38	-79	+44	+2	-22	-27
Profile type 4	22.38 - 24.15	+9	+2	+5	+9	+7
Profile type 3 South	24.15 - 25.57	-17	-18	+17	+24	-0.1
Profile type 2 South	25.57 - 26.13	-109	-88	-17	-27	-65
Profile type 5	26.13 - 27.00	-162	-103	-9	-40	-88
Southern Dunes	27.00 - 28.32	+41	+23	+32	+37	+35
Full project domain	17.08 - 28.32	-21	+7	+28	+6	+2
HD system	20.25 - 27.00	-64	-25	+6	-13	-29

Spatial variability in volume changes

In this paragraph the spatial variability in dune volume changes is presented for the four measurement periods, as shown in Figure 4.2.

May 2015 - December 2015 Along the Northern dunes, a small decrease in volume was observed for T0-T1 (green line). However, locally deposition is observed between approximately RSP 18.62 and RSP 19.55. In the Northern part of the HD system, along profile type 1, 2 and 3, a strong decrease in the beach volume is observed. This result is less pronounced along profile type 3 (South) and 4; for profile type 4 even deposition is measured. For profile type 2 (South) and 5 a decrease in beach volume a strong decrease in beach volume was measured with values up to $-97 m^3/m$. Accretion of the beach volume is found for the Southern Dunes, located southwards of RSP 27.00 and indicated by the blue horizontal line. The mean volume change in the period T0-T1 is $-13 m^3/m$ which is equivalent to $-21 m^3/m/y$.

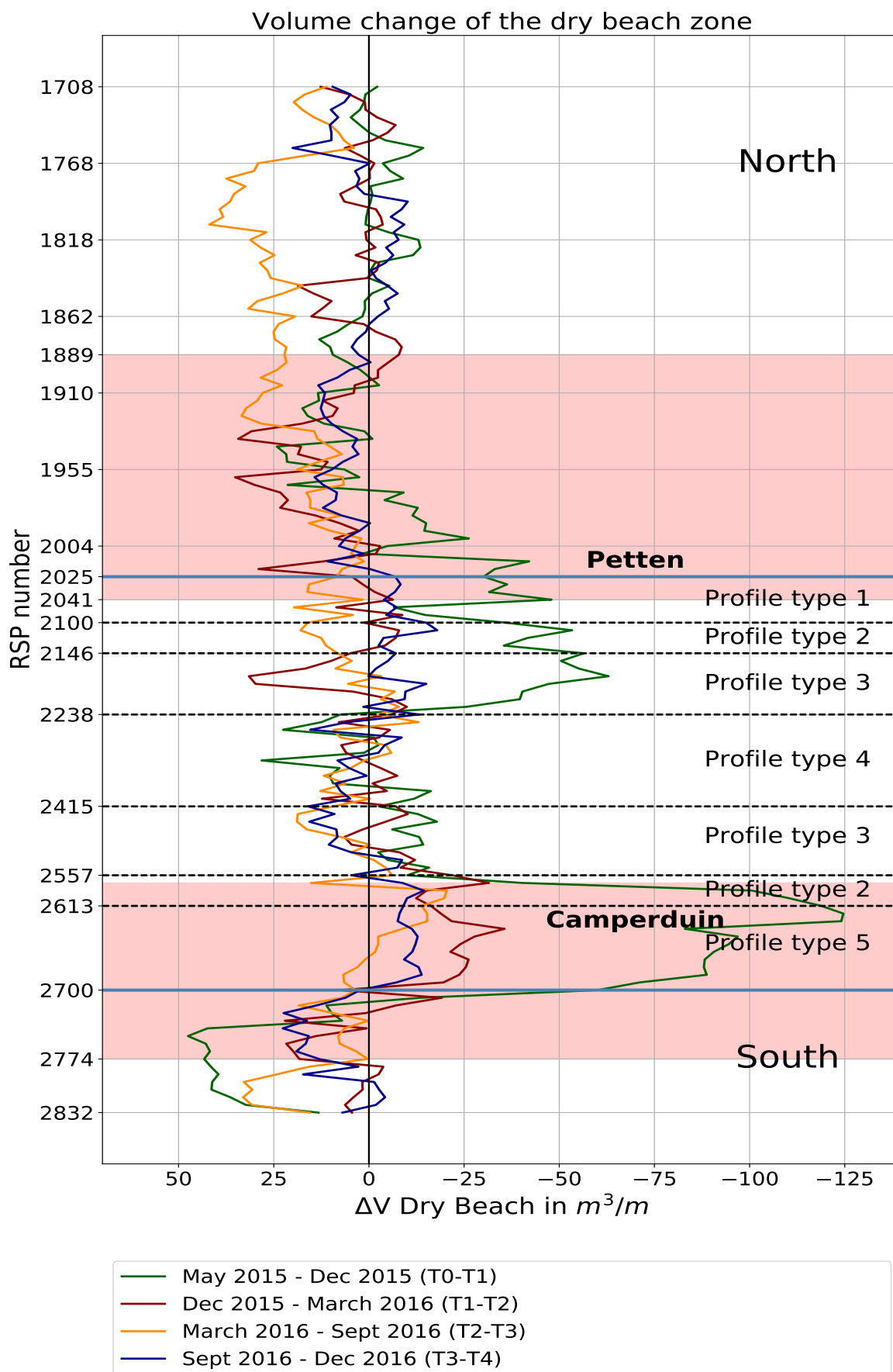


Figure 4.2: Temporal volume change of the dry beach zone in the four measured periods. Note that the figure has the same orientation as the Dutch coastline which means that the North is at the upper part of the figure and the South at the lower part of the figure. The sea is located at the left side of the origin and dry land is located at the right side of the origin; erosion (negative values) of the surf zone or the intertidal zone means that the coastal area retreats and is therefore depicted towards the right into landward direction and deposition (positive values) means that the coastal area extends and is therefore depicted toward the left into seaward direction. The blue lines indicate the boundaries of the new HD system and the red shaded areas indicate the locations of the northern and Southern shoulder. The black dashed lines distinguish the five different dune profile types.

December 2015 - March 2016 Along the Northern Dunes, an increase in beach volume is observed locally for T1-T2 (red line), which shows the highest values along the Northern shoulder. In the Northern part of the HD system, along profile type 1 and 2 spatial variations in beach volume changes are relatively constant and erosive. However, along dune profile type 3 (North) a large spatial variation and deposition is measured. The Southern shoulder shows erosion along profile type 2 and 5. Accretion of the beach volume is derived for the Southern dunes. The mean volume change in the period T1-T2 is $+2 \text{ m}^3/\text{m}$ which is equivalent to $+7 \text{ m}^3/\text{m}/\text{y}$.

March 2016 - September 2016 A large increase in beach volume is observed for the Northern Dunes between RSP 17.08 and approximately RSP 19.10, for T2-T3 (yellow line). The increase in beach volume is smaller, but still present along the Northern shoulder till RSP 20.25. In the Northern part of the HD system increase in beach volume is relatively large for profile type 1 and 2 (North). Along profile type 3 (North) and 4 and, spatial variation in erosion and deposition is observed; on average a small increase in beach volume was observed. Erosion along profile type 2 (South) and 5 is relatively constant. For the Southern Dunes, located southwards of RSP 27.00, a large increase in beach volume was observed. The mean volume change in the period T2-T3 is $+13 \text{ m}^3/\text{m}$ which is equivalent to $+28 \text{ m}^3/\text{m}/\text{y}$.

March 2016 - December 2016 Along the Northern Dunes, locally erosion is observed between approximately RSP 18.02 and RSP 18.89. However, on average an increase in beach volume is derived for T3-T4 (blue line). In the Northern part of the HD system, along profile type 1, 2 (North) and 3 (North), a decrease of the beach volume is found. A relatively small increase in beach volume is observed along profile type 4 (small) and a relatively large increase along profile type 3 (South). Along profile type 2 (South) and 5 decrease in beach volume is observed which is larger than in the third period. A large accretion of the beach volume is derived for the Southern Dunes. The mean volume change in the period September 2016 and December 2016 is $+2 \text{ m}^3/\text{m}$ which is equivalent to $+6 \text{ m}^3/\text{m}/\text{y}$.

Cumulative net volume changes

Figure 4.3 depicts the cumulative net volume change of the dry beach zone derived for the period May 2015 - December 2016 (T0-T4). In general, mainly erosion is observed along the HD system, the stretch between the two blue horizontal boundaries at RSP 20.25 and RSP 27.00, and deposition is observed along the Northern and Southern Dunes. However, locally deposition is observed along profile type 1, 4 and 3 (South). The mean beach volume change shows a small positive result of $3 \text{ m}^3/\text{m}$ along the full project domain which is equivalent to $+2 \text{ m}^3/\text{m}/\text{y}$, see Table 4.3. If only the HD system is considered, a negative result of $45 \text{ m}^3/\text{m}$ is derived which is equivalent to $-29 \text{ m}^3/\text{m}/\text{y}$. The largest negative volume changes have occurred along the Southern shoulder for profile type 2 (South) and 5, indicated by the red shaded area. Locally, beach erosion up to $-169 \text{ m}^3/\text{m}$ is derived along profile type 5. The largest positive volume changes have occurred along the Southern dunes for which beach accretion up to $89 \text{ m}^3/\text{m}$ is derived and an average value for this domain of $+35 \text{ m}^3/\text{m}/\text{y}$, see Table 4.3. Along the HD system still beach accretion up to $42 \text{ m}^3/\text{m}$ is observed for profile type 4 and an average value for this domain of $+9 \text{ m}^3/\text{m}/\text{y}$. In section 4.1.8 the results are compared to the other three zones of the cross-shore profile.

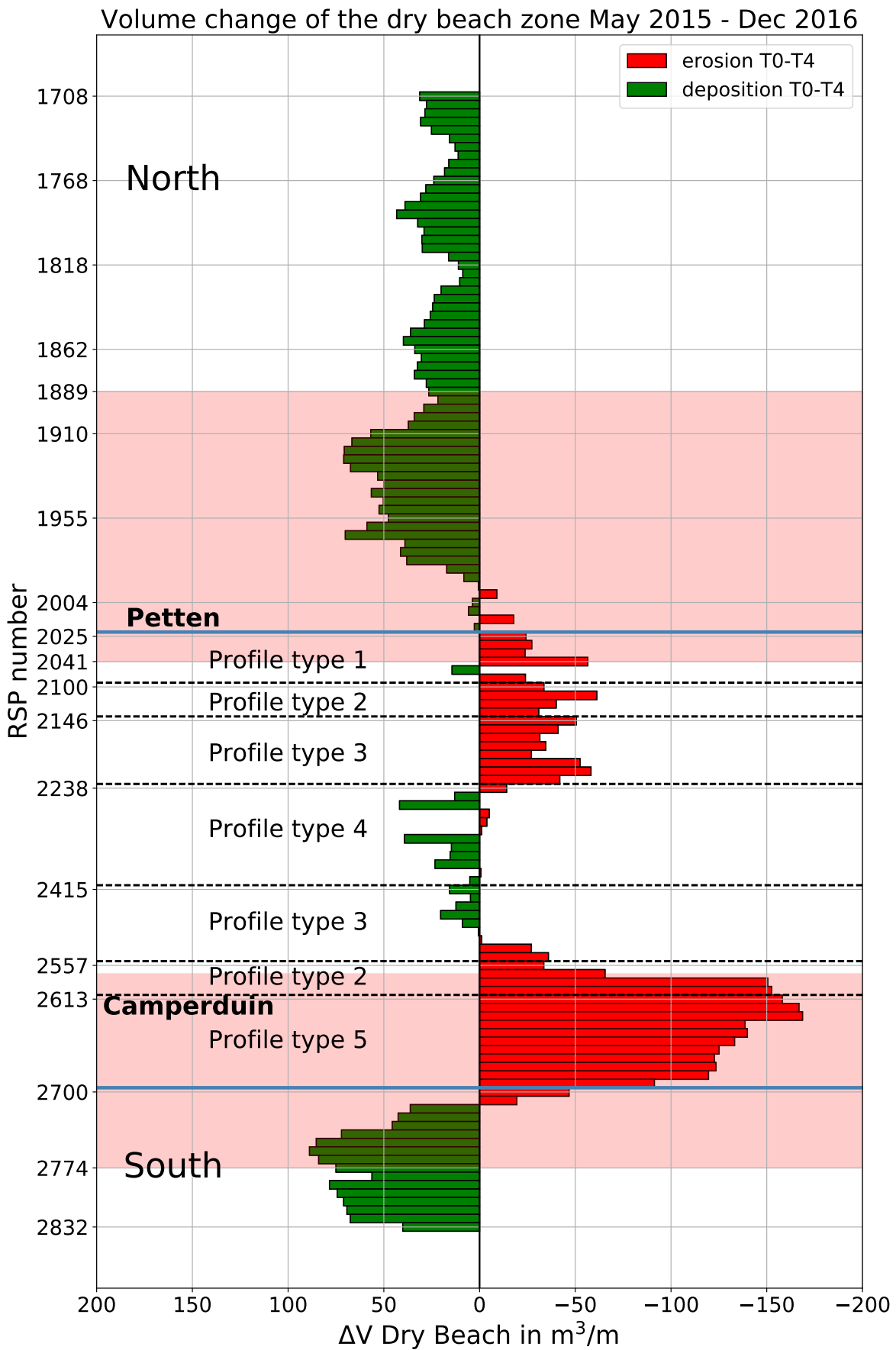


Figure 4.3: Cumulative net volume change of the dry beach zone between May 2015 - December 2016. Note that the figure has the same orientation as the Dutch coastline which means that the North is at the upper part of the figure and the South at the lower part of the figure. The sea is located at the left side of the origin and dry land is located at the right side of the origin; erosion (red coloured) of the dry beach zone means that the coastal area retreats and is therefore depicted towards the right into landward direction and deposition (green coloured) means that the coastal area extends and is therefore depicted toward the left into seaward direction. Difference in height of the bars indicates spatial variability in volume changes. The blue lines indicate the boundaries of the new HD system and the red shaded areas indicate the locations of the Northern and Southern shoulder. The black dashed lines distinguish the five different dune profile types.

4.1.4. Volume Change of the Dunes

Temporal variability in volume changes

Figure 4.4 shows the alongshore distribution in morphological change of the dunes [m^3/m] in the four measurement periods. The dunes are defined as the zone above +3.5 m NAP (dune foot). Dune volume changes for the cross-shore transects varies between $-10 m^3/m$ and $+55 m^3/m$. Table 4.4 provides an overview of the spatio-temporal variability in dune volume change [$m^3/m/y$] per profile type alongshore. The results show that a large dune growth rate of $+25 m^3/m/y$ was measured in the first period after construction, between May 2015 and December 2015 (T0-T1), along the full project domain. However, the result also shows a large dune growth rate of $+26 m^3/m/y$ in the third period, between March 2016 - September 2016 (T2-T3), along the full project domain. The dune growth rate decreases in time when only the HD system is considered from $+35 m^3/m/y$ in the first period to $+22 m^3/m/y$ in the last period and it has become more constant. It is worth noting that the derived dune volume changes are mainly positive in time and alongshore, except for profile type 5 in the period Dec 2015 - March 2016. Large dune growth rates are observed along profile type 2 (South) and profile type 3 (North and South). There is significant alongshore variability in dune growth within the surveys. This will be described in more detail below for each of the successive surveys.

Table 4.4: Dune volume changes per profile type in the four measurement periods. The RSP coordinates indicate the alongshore location in Figure 4.4 from North (first row) to South (last row). Left column shows the cumulative net volume change between May 2015 - December 2016.

	RSP coordinates	T0-T1 [$m^3/m/y$]	T1-T2 [$m^3/m/y$]	T2-T3 [$m^3/m/y$]	T3-T4 [$m^3/m/y$]	T0-T4 [$m^3/m/y$]
Northern Dunes	17.08 - 20.25	+20	+19	+29	+9	+21
Profile type 1	20.25 - 21.00	+8	+16	+13	+25	+14
Profile type 2 North	21.00 - 21.46	+27	+23	+9	+21	+20
Profile type 3 North	21.46 - 22.38	+45	+46	+11	+26	+32
Profile type 4	22.38 - 24.15	+22	+8	+25	+35	+23
Profile type 3 South	24.15 - 25.57	+57	+70	+39	+25	+48
Profile type 2 South	25.57 - 26.13	+54	+31	+62	+8	+45
Profile type 5	26.13 - 27.00	+34	-0.3	+11	+8	+18
Southern Dunes	27.00 - 28.32	+14	+7	+21	+6	+14
Full project domain	17.08 - 28.32	+25	+20	+26	+14	+23
HD system	20.25 - 27.00	+35	+26	+23	+22	+28

Spatial variability in volume changes

In this paragraph the spatial variability in dune volume changes is presented for the four measurement periods, as shown in Figure 4.4.

May 2015 - December 2015 Along the full project domain, large dune growth is observed between T0-T1 (green line), but alongshore variations are observed. Along the Northern Dunes, dune growth is mostly pronounced between RSP 18.18 and RSP 19.55. Locally, dune erosion is measured just Northwards of RSP 20.25. For the HD system, dune growth is relatively small for profile type 1. Profile type 2 (North) and 4 show relatively small dune growth compared to the adjacent dunes of profile type 2 (South) and 3 (North and South). Note that the volume changes of profile type 4 do not take into account any variations that have occurred in the dune valley due to limited reliability of the LiDAR measurements. LiDAR is not able to penetrate through the water, see section 3.1 of Chapter 3 for the applied methodology along this profile type. Figure H.2 till Figure H.8 in Appendix H shows indeed that morphological volume changes were observed at the seaward slope of the dune valley and indicate that more dune growth has occurred along profile type 4. For profile type 5 also a large dune growth was derived and a smaller accretion of the dune volume is observed for the Southern

Dunes, located Southward of RSP 27.00 and indicated by the blue horizontal line. The mean volume change in the period T0-T1 is $15 \text{ m}^3/\text{m}$ which is equivalent to $25 \text{ m}^3/\text{m}/\text{y}$.

December 2015 - March 2016 A similar, but less pronounced, pattern of dune volume change is observed along the full project domain between T1-T2 (red line), except for profile type 3 (North and South) which shows larger dune growth compared to the first period. Locally, dune erosion is observed, for example just Northwards and Southwards of the HD system, indicated by the blue horizontal lines at RSP 20.25 and RSP 27.00. Moreover, dune growth along profile type 1 has increased with respect to the first period and shows comparable results with the adjacent profile types. Profile type 4 shows again smaller dune growth rates compared to the adjacent profile types. Dune erosion is measured along profile type 5. The mean volume change in the period T1-T2 is $5 \text{ m}^3/\text{m}$ which is equivalent to $20 \text{ m}^3/\text{m}/\text{y}$.

March 2016 - September 2016 Large dune growth is also observed along the full project domain between T2-T3 (yellow line). In this period a similar pattern of dune growth is observed which is derived in the first two measurement periods. Dune growth is relatively large along the Northern and Southern Dunes. Along the HD system, dune growth is less pronounced for profile type 1, 2 (North) and 3 (North) than for profile type 4, 3 (South) and 2 (South). However, It is worth noting that the dune growth for profile type 3 (North and South) is less pronounced than in the earlier measurement periods. Dune growth along profile type 2 (South) is significantly larger than the the other profile types. A small and alongshore stable pattern of dune growth is observed for profile type 5. The mean volume change in the period T2-T3 is $12 \text{ m}^3/\text{m}$ which is equivalent to $26 \text{ m}^3/\text{m}/\text{y}$.

September 2016 - December 2016 A similar, but less pronounced, pattern of dune volume change is observed between T3-T4 (blue line) compared to the first (T0-T1) and third period (T1-T2) along the full project domain. A pattern of relatively constant spatial behaviour can be observed: along the Northern part of the HD system a comparable increase in dune volume is measured for: (1) profile type 1, 2 (North) and 3 (North) and 3 (South) and (2) profile type 2 (South), 5 and the Southern dunes. For profile type 4 significantly larger dune growth is measured than the other profile types. The mean volume change in the period T3-T4 is $4 \text{ m}^3/\text{m}$ which is equivalent to $14 \text{ m}^3/\text{m}/\text{y}$.

Cumulative net volume changes

Figure 4.5 depicts the cumulative net volume change of the dunes derived for the period May 2015 - September 2016 (T0-T4). Dune growth is observed along the full project domain with a mean volume change of $35 \text{ m}^3/\text{m}$ which is equivalent to $23 \text{ m}^3/\text{m}/\text{y}$ along the full project domain, see Table 4.4. This results in a total dune growth along the 11 kilometres project domain of $253.000 \text{ m}^3/\text{y}$. If only the HD system is considered, a result of $43 \text{ m}^3/\text{m}$ is derived. This is equivalent to $28 \text{ m}^3/\text{m}/\text{y}$ and a total dune growth of $189.000 \text{ m}^3/\text{m}/\text{y}$ along the 6.75 kilometres-long HD system. Dune growth is strongly pronounced along the Northern Dunes between RSP 18.18 and RSP 18.89. Along the HD system, dune growth is large for profile type 3 (North) and profile type 2 (South) and 3 (South) with an average rate of $32 \text{ m}^3/\text{m}/\text{y}$ (profile type 3 North), $45 \text{ m}^3/\text{m}/\text{y}$ (profile type 2 South) and respectively $48 \text{ m}^3/\text{m}/\text{y}$ (profile type 2 South). Locally, dune growth up to $100 \text{ m}^3/\text{m}$ is derived for profile type 2 (South). Note that the volume changes of profile type 4 do not take into account any variations that have occurred in the dune valley due to limited reliability of the LiDAR measurements. In section 4.1.8 the results are compared to the other three zones of the cross-shore profile.

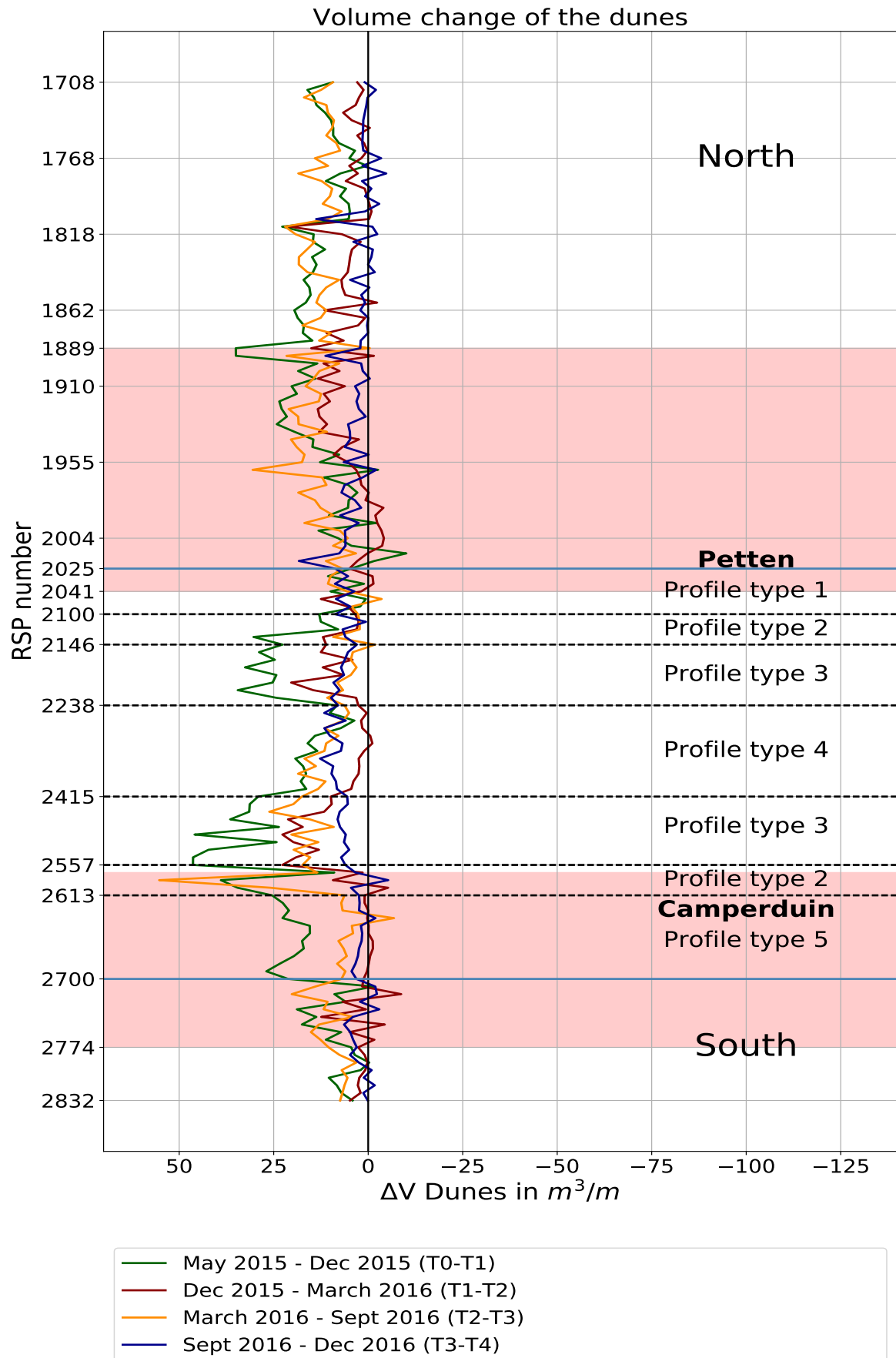


Figure 4.4: Temporal volume change of the dunes in the four measured periods. Note that the figure has the same orientation as the Dutch coastline which means that the North is at the upper part of the figure and the South at the lower part of the figure. The sea is located at the left side of the origin and dry land is located at the right side of the origin; erosion (negative values) of the dunes means that the coastal area retreats and is therefore depicted towards the right into landward direction and deposition (positive values) means that the coastal area extends and is therefore depicted toward the left into seaward direction. The blue line indicates the boundaries of the new HD system and the red shaded areas indicate the locations of the Northern and Southern shoulder. The black dashed lines distinguish the five different dune profile types.

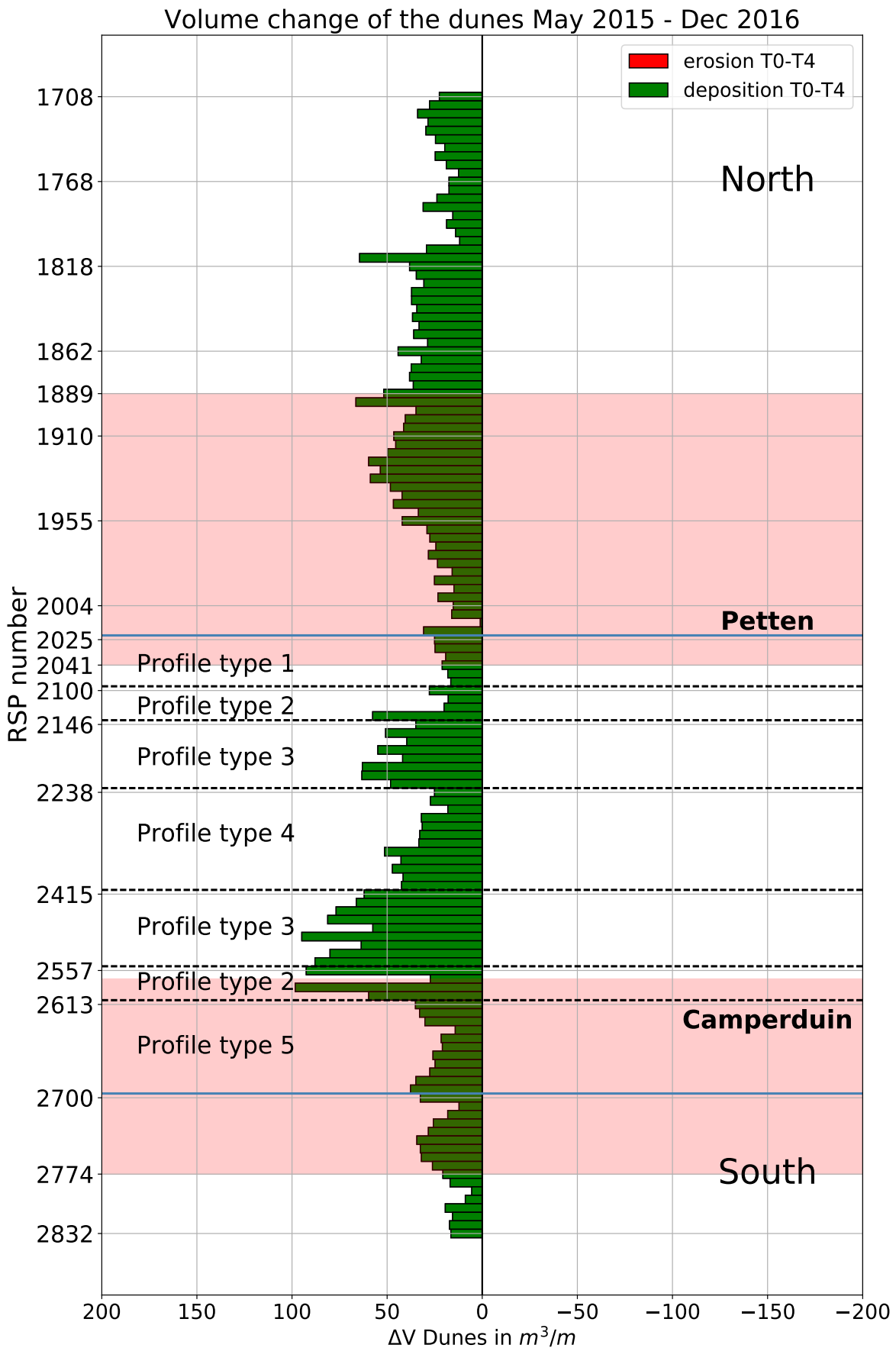


Figure 4.5: Cumulative net volume change of the dunes between May 2015 - December 2016. Note that the figure has the same orientation as the Dutch coastline which means that the North is at the upper part of the figure and the South at the lower part of the figure. The sea is located at the left side of the origin and dry land is located at the right side of the origin; deposition (green coloured) means that the coastal area extends and is therefore depicted toward the left into seaward direction. Difference in height of the bars indicates spatial variability in volume changes. The blue line indicates the boundaries of the new HD system and the red shaded areas indicate the locations of the Northern and Southern shoulder. The black dashed lines distinguish the five different dune profile types.

4.1.5. Dry Beach Slope

Spatio-temporal variability in beach slope

Figure 4.6 shows the beach slope for the five surveys, the beach slope is derived as a linear fit between +0.8 m NAP (MHW) and +3.5m NAP (dune foot). The mean beach slope varies between 1/10 (-0.1) up to 1/100 (-0.01). Table 4.5 provides an overview of the spatio-temporal variability in beach slope per profile type along-shore. The initial constructed beach slope was approximately constant along the HD system and was milder for the Northern and Southern dunes (green line). The results show that the cross-shore profiles along the HD system have become steeper in time, except for the profile type 3 (South) for which the beach slope on average did not change in time. The beach slope of the Northern and Southern Dunes became milder in time. It is striking that the beach of dune profile type 5 became significantly steeper compared to the profile type 1 to 4. Locally, a beach slope of 1/10 (-0.01) was observed at RSP 26.29. The mean beach slope is depicted in Appendix H and in the left column of Table 4.5; a mean value of 1/33 (-0.03) was found along the full project domain with a maximum beach slope up to 1/25 (-0.04) along profile type 5 and a minimum beach slope up to 1/250 (-0.004) along the Northern dunes. Appendix H depicts cross-sectional plots for the largest erosive and/or accretive profiles for each dune type. The largest change in beach slope is found to occur around the intertidal zone. In section ?? the influence of the beach slope on the dune volume changes is presented.

Table 4.5: Mean beach slope per profile type for the five surveys. The RSP coordinates indicate the alongshore location in Figure 4.6 from North (first row) to South (last row). Left column shows the cumulative mean beach slope between May 2015 - December 2016.

	RSP coordinates	T0 [-]	T1 [-]	T2 [-]	T3 [-]	T4 [-]	T0-T4 [-]
Northern Dunes	17.08 - 20.25	-0.03	-0.03	-0.03	-0.02	-0.02	-0.03
Profile type 1	20.25 - 21.00	-0.01	-0.01	-0.01	-0.01	-0.02	-0.03
Profile type 2 North	21.00 - 21.46	-0.01	-0.03	-0.03	-0.03	-0.03	-0.03
Profile type 3 North	21.46 - 22.38	-0.01	-0.02	-0.02	-0.02	-0.02	-0.02
Profile type 4	22.38 - 24.15	-0.01	-0.02	-0.02	-0.02	-0.02	-0.02
Profile type 3 South	24.15 - 25.57	-0.01	-0.01	-0.01	-0.01	-0.01	-0.01
Profile type 2 South	25.57 - 26.13	-0.01	-0.02	-0.02	-0.03	-0.03	-0.02
Profile type 5	26.13 - 27.00	-0.01	-0.05	-0.06	-0.07	-0.07	-0.05
Southern Dunes	27.00 - 28.32	-0.02	-0.01	-0.01	-0.01	-0.01	-0.01
Full project domain	17.08 - 28.32	-0.02	-0.03	-0.03	-0.02	-0.02	-0.03
HD system	20.25 - 27.00	-0.01	-0.03	-0.03	-0.03	-0.03	-0.03

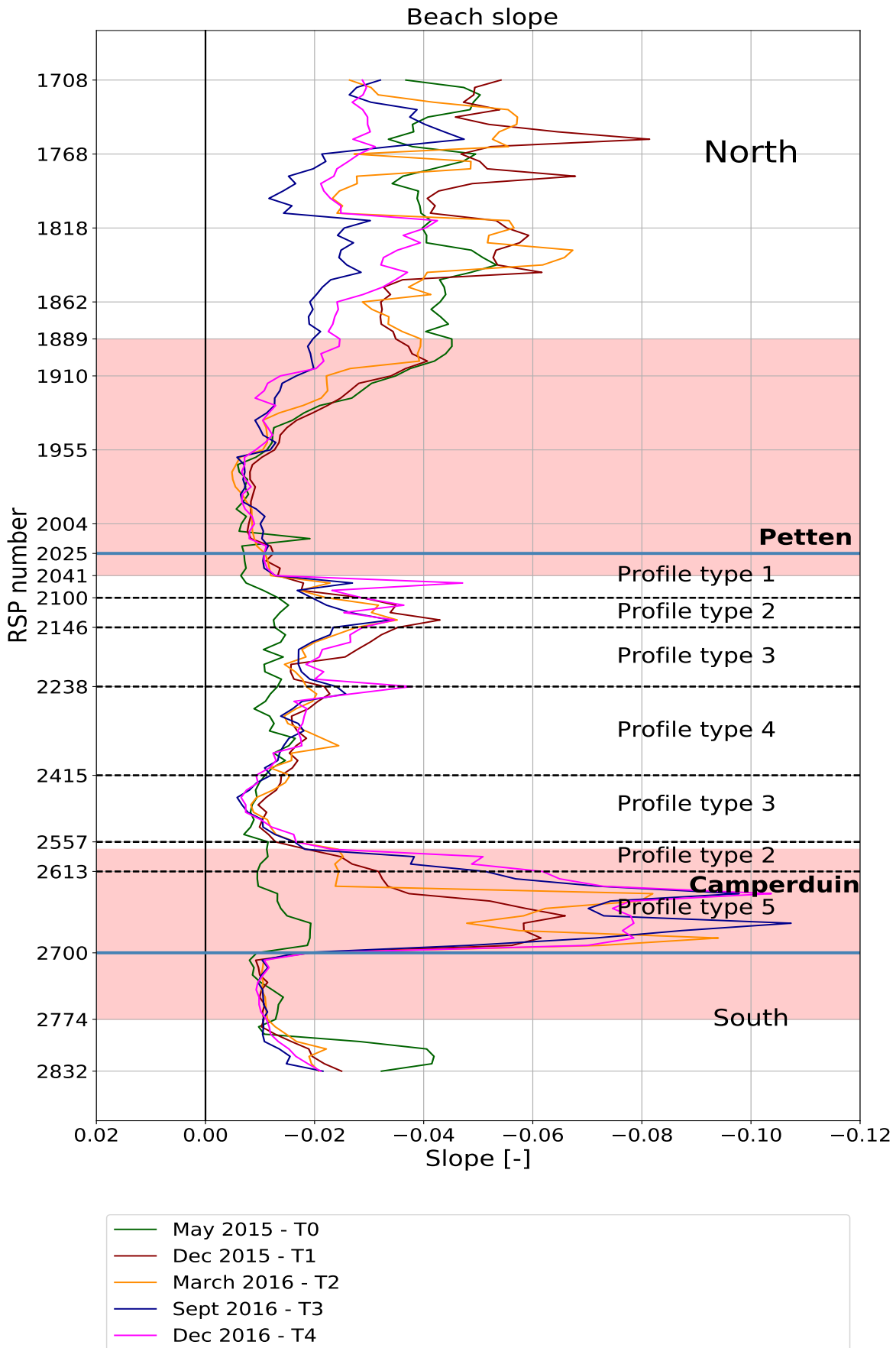


Figure 4.6: Beach slope of the dry beach zone for the five surveys. Note that the figure has the same orientation as the Dutch coastline which means that the North is at the upper part of the figure and the South at the lower part of the figure. The sea is located at the left side of the origin and dry land is located at the right side of the origin. Steepening of the beach, resulting in a more negative value, means that the coastal area retreats and is therefore depicted towards the right into landward direction. Flattening of the beach, resulting in a more positive value, means that the coastal area extends and is therefore depicted toward the left into seaward direction. The blue line indicates the boundaries of the new HD system and the red shaded areas indicate the locations of the Northern and Southern shoulder. The black dashed lines distinguish the five different dune profile types.

4.1.6. Dry Beach Width

Spatio-temporal variability in beach width

Figure 4.7 shows the beach width for the five surveys. The beach width is derived as the horizontal distance between +0.8 m NAP (MHW) and +3.5 m NAP (dune foot). Table 4.6 provides an overview of the spatio-temporal variability in beach width [m]. The initial constructed beach width varies alongshore, see also the green line in Figure 4.7. The beach width is large along the Northern dunes, between RSP 19.55 and 20.25, profile type 1, profile type 2 (South) and 3 (South)) and the Southern dunes between RSP 27.00 and RSP 27.74. The beach width is of similar order in size along dune profile type 2 (North), 3 (North), 4 and 5. Along the Northern Dunes the beach width is small compared to the other profile types. The results show that on average the beach width has decreased along the the full project domain, a large response was measured in T0-T1. An alongshore variability in beach width development is measured in and this will be described in more detail below for three subdomains: (1) Northern Dunes, (2) HD system and (3) Southern Dunes.

Along the Northern dunes, the beach width has increased in time. Increase in beach width is pronounced between RSP 17.38 till RSP 19.75 whereas a decrease in time is found between RSP 19.75 and RSP 20.25. Figure H.16 in Appendix H shows that the increase in beach width is caused due to shifting of the MHW-line in seaward direction. Note that a fixed dune foot position is chosen at the Northern Shoulder, between RSP 19.89 and RSP 20.29, to reduce the effect of the construction works that took place in the period T0-T1, see section 3.1 for methodology considerations.

Along the HD system, a reduction of the beach width is found in time. This effect is mostly pronounced along profile type 1, 2 (North), 3 (North), 2 (South) and 5 and between T0-T1. However, a small increase in beach width is derived for profile type 1 and 2 (North) in T2-T3. Figure H.16 in Appendix H shows that for profile type 1, 2 (North) and 3 (North) the decrease in beach width is mainly caused by a landward shift of the MHW-line, but also due to a seaward shift of the dune foot position. For profile type 2 (South) and 5 it is observed that the decrease in beach width is strongly caused by shoreline movement in landward direction. Along dune profile 3 (South) a rather constant beach width is measured while this position deviates strongly from equilibrium, also shown in Figure H.16 in Appendix H.

Along the Southern dunes, between RSP 27.00 and RSP 27.47, the beach width has decreased in time. This is caused by a seaward movement of the dune foot. Southwards of RSP 27.47 the beach width has increased in time. This observation is caused by a combination of two processes; a shift of the MHW-line and a shift of the dune foot in seaward direction. Both observations can be seen in Figure H.16 in Appendix H.

Table 4.6: Mean beach width per profile type for the five surveys. The RSP coordinates indicate the alongshore location in Figure 4.7 from North (first row) to South (last row). Most left column shows the cumulative change in beach width between May 2015 - December 2016.

	RSP coordinates	T0 [m]	T1 [m]	T2 [m]	T3 [m]	T4 [m]	T0-T4 [m]	Δ T0-T4 [m/y]
Northern Dunes	17.08 - 20.25	94	88	93	107	105	98	+7
Profile type 1	20.25 - 21.00	197	140	141	148	124	150	-48
Profile type 2 North	21.00 - 21.46	131	74	74	87	76	88	-36
Profile type 3 North	21.46 - 22.38	128	90	84	84	89	95	-25
Profile type 4	22.38 - 24.15	129	104	97	95	93	104	-24
Profile type 3 South	24.15 - 25.57	168	146	152	148	141	151	-17
Profile type 2 South	25.57 - 26.13	171	107	102	90	81	110	-58
Profile type 5	26.13 - 27.00	125	52	46	33	29	57	-63
Southern Dunes	27.00 - 28.32	152	150	154	148	156	150	+9
Full project domain	17.08 - 28.32	121	101	103	108	105	107	-10
HD system	20.25 - 27.00	145	100	97	96	88	105	-37

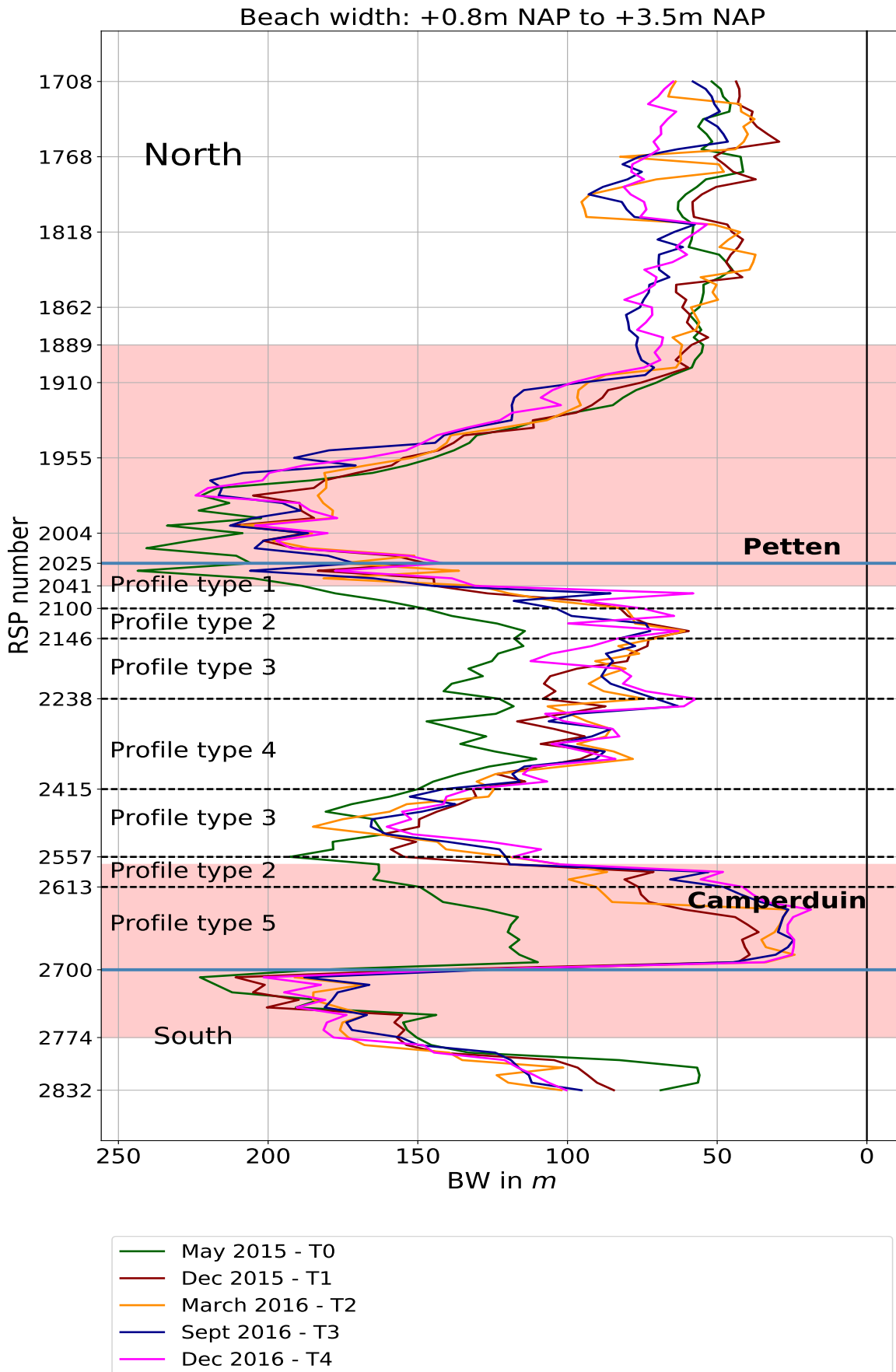


Figure 4.7: Beach width of the dry beach zone for the five surveys. Note that the figure has the same orientation as the Dutch coastline which means that the North is at the upper part of the figure and the South at the lower part of the figure. The sea is located at the left side of the origin and dry land is located at the right side of the origin. Decrease of the beach width, resulting in a more negative value, means that the coastal area retreats and is therefore depicted towards the right into landward direction. Increase of the beach width, resulting in a more positive value, means that the coastal area extends and is therefore depicted toward the left into seaward direction. The blue lines indicate the boundaries of the new HD system and the red shaded areas indicate the locations of the Northern and Southern shoulder. The black dashed lines distinguish the five different dune profile types.

Cumulative change in beach width

Figure 4.8 depicts the cumulative change in beach width derived for the period May 2015 - December 2016 (T0-T4). In general, mainly shoreline retreat is measured along the HD system, the stretch between the two blue horizontal boundaries at RSP 20.25 and RSP 27.00, and shoreline advance is observed along the Northern and Southern dunes. Locally, along the Northern Dunes at RSP 18.16, a small decrease in beach width is found. The mean shoreline retreat is -16 m which is equivalent to -10 m/y along the full project domain, see Table 4.6. If only the HD system is considered, a mean of -57 m is derived which is equivalent to -37 m/y. The largest change in beach width are pronounced along dune profile 1 in the North and dune profile 2 (South) and 5 with minimum decrease of -65 m and a maximum decrease up to -120 m. Shoreline extension up to 80 m are observed along the Northern and Southern dunes. Figure H.17 and Figure H.18 in Appendix ?? depicts the cumulative change of the MHW-position and the dune foot position. The figures show that the decrease or increase in beach width is mainly caused by a landward shift of the MHW-position rather than a seaward movement of the dune foot. The average landward shift of the MWH-line is -11 m and the seaward shift of the dune foot position is 5 m. In section ?? the influence of the beach width on the dune volume changes is presented.

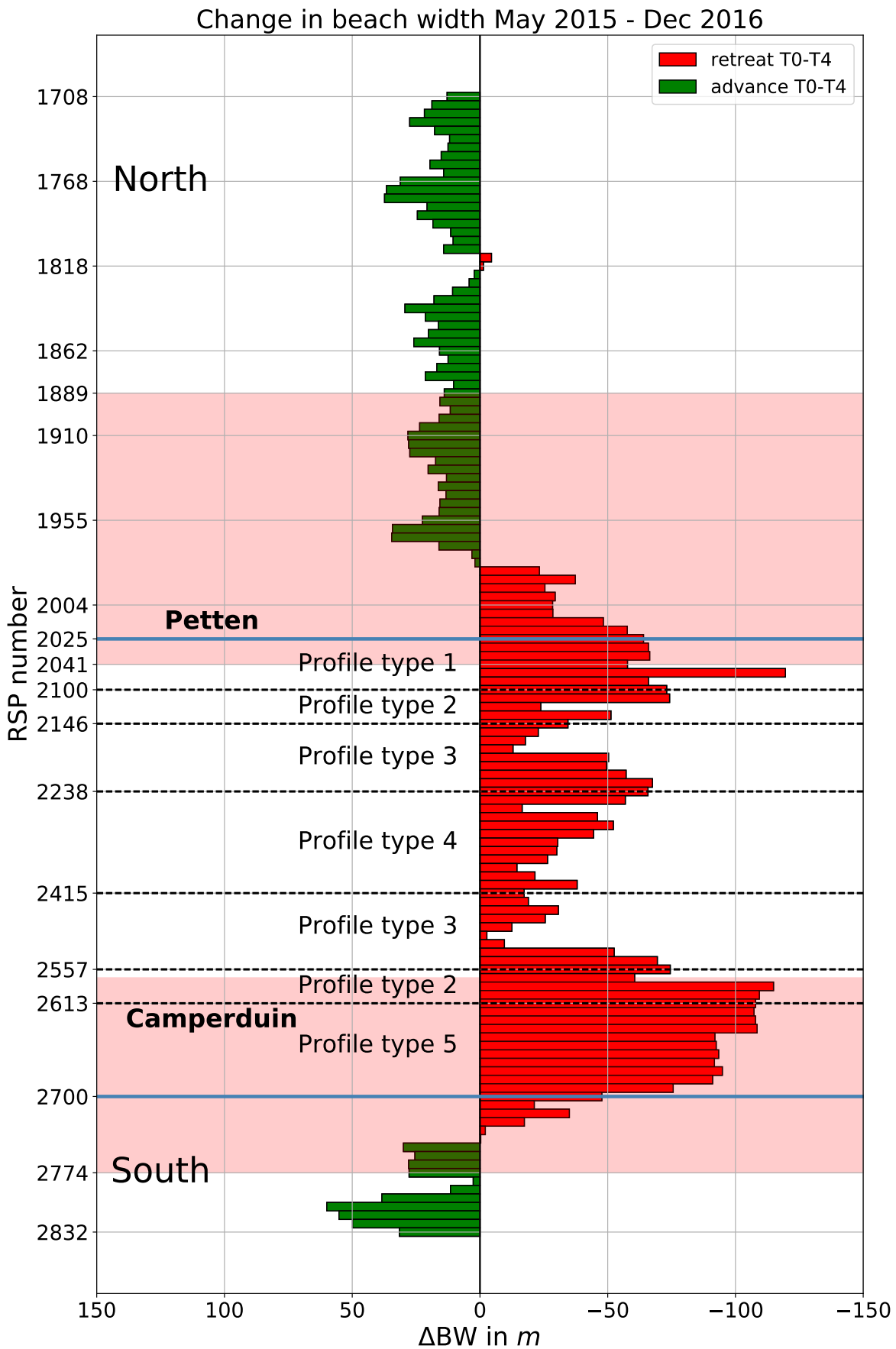


Figure 4.8: Cumulative change of the beach width of the Dry beach zone between May 2015 - December 2016. Note that the figure has the same orientation as the Dutch coastline which means that the North is at the upper part of the figure and the South at the lower part of the figure. The sea is located at the left side of the origin and dry land is located at the right side of the origin; decrease (red coloured) of the dry beach width means that the coastal line retreats and is therefore depicted towards the right into landward direction and increase (green coloured) means that the coastal line extends and is therefore depicted toward the left into seaward direction. Difference in height of the bars indicates spatial variability in change of beach width. The blue lines indicate the boundaries of the new HD system and the red shaded areas indicate the locations of the Northern and Southern shoulder. The black dashed lines distinguish the five different dune profile types.

4.1.7. Relation Aeolian Sediment Availability and Dune Volume Change

Figure 2.8 shows spatial variations. In this section four sediment parameters that influence the aeolian sediment availability are plotted against dune volume changes to identify the relation between sediment availability and dune volume changes. The parameters of interest are given in Table 4.7 in which also the expected relation between the sediment availability parameter and the dune volume change is given. This analysis has only focused on the man-made dune profile types along the HD system.

Table 4.7: This table shows the four correlated parameters and the expected correlation between the parameter and dune volume change.

Parameter	Expected correlation	Plot type	Reference
Dry beach volume change T0 - T4	-	Scatter plot	Figure H.19
Mean dry beach slope	+	Scatter plot	Figure H.20a
Mean dry beach width	+	Scatter plot	Figure H.20b
Median grain size T0	-	Box plot	Figure 4.11

Dry beach volume change vs dune volume change

Figure ?? shows the relation between the average dry beach volume change and the dune volume change in T0-T4. Intuitively, in cross-shore direction a negative correlation between beach volume changes and dune volume changes is expected. Dune growth is only expected when sediments are transported from the beach towards the dunes by the wind. Hence, a decrease in beach volume is expected to result in a similar dune growth. However, a significant statistical relation is not found for the full project domain, see Figure H.19 in Appendix H. This could be related to the importance of marine processes which governs the beach volume change. To detect if this mechanism is present, the MHW-line is measured, see Appendix H. It was found that the shoreline retreated landward which confirms that marine processes have been involved. The actual dune growth along the system is related to small changes in beach volume, see the right half of the figure. Moreover, spatial variation in dune growth is observed for smaller beach volume changes which indicates that besides sediment exchange rates between beach and dunes there also other properties of the system involved that determine the actual or measured dune growth. The potential dune growth and the spatial variations in dune growth are larger when variations in beach volume are small, see the right part of the figure.

Dry beach slope versus dune volume change

A positive correlation between beach slope and dune volume changes is expected: a milder and therefore wider beach increases the aeolian sediment availability for transport towards the dunes. Figure 4.10a shows the relation between the average dry beach slope and the dune volume change. Based on the results presented here it is suggested that there is certain potential for dune growth which is associated with a certain beach slope. The envelop (brown line) is a graphical representation of the upper limit of the potential dune growth under influence of a varying beach slope. The envelope of maximum empirical dune growth is obtained from the data. It is expected that dune growth higher than the upper limit is rather possible. It is shown that a milder beach slope is associated with more dune growth and more spatial variation in dune growth, see the right part of the figure. A flatter beach slope would activate more aeolian sediment transport and therefore increases the potential dune growth. Spatial differences in dune geometry and other processes that influence aeolian sediment transport, for example the location with respect to the wind conditions or the sediment characteristics, could explain that the potential dune growth is not always reached for a beach slope with a similar magnitude. Note that the beach slope varies within small boundaries, only for profile type 5 significantly steeper slopes are found compared to the other profile types. To test how well a statistical correlation between beach slope and dune volume change exists, a linear trend was fitted at the dataset. A positive correlation coefficient of $r = 0.4$ is found, see Figure H.20a in Appendix H. The relatively low correlation could be possibly caused by forcing of processes on shorter time scales that dominates the initial development of the system.

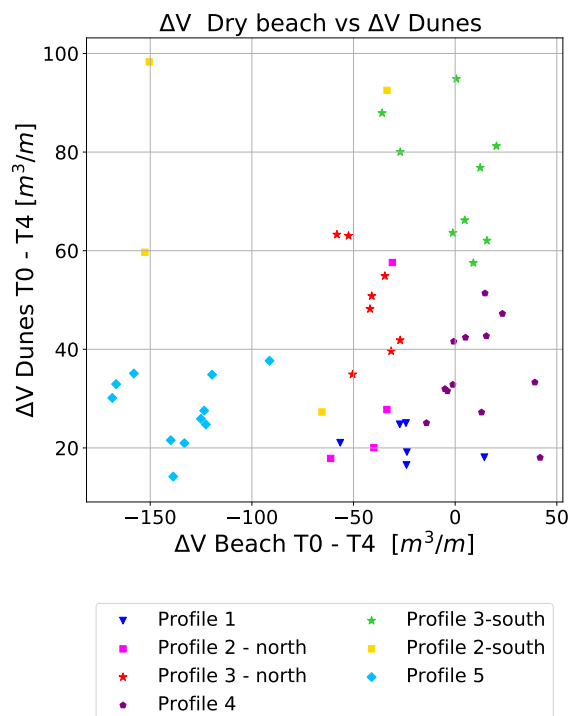


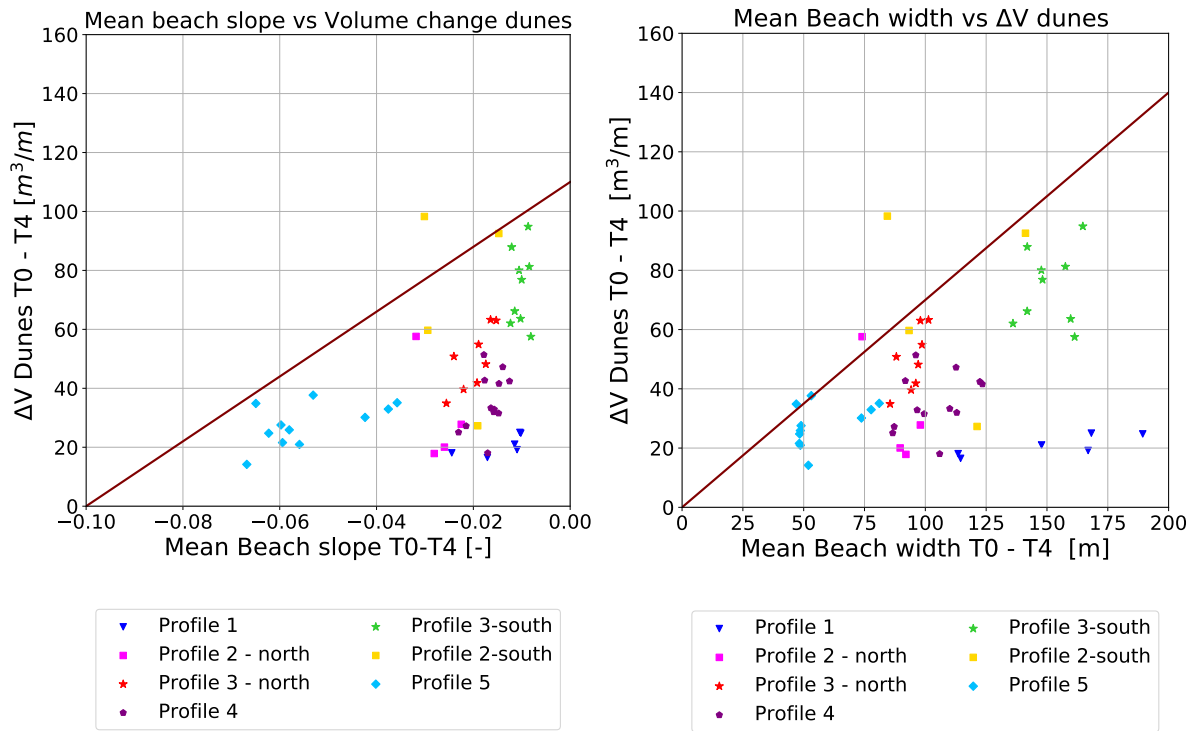
Figure 4.9: Beach volume change (x-axis) against the volume change of the Dunes (y-axis) along the HD system in the period T0-T4. Profile type 1-5 are indicated by different colors and markers. Dune growth is pronounced for smaller beach volume changes.

Dry beach width versus dune volume change

For the beach width also a positive correlation is expected: a wider beach increases the aeolian sediment availability for transport towards the dunes. Figure 4.10b shows the relation between the average dry beach width and the dune volume change. Following the results of the relation between dry beach slope and dune volume change, which is often a more constant parameter, a similar procedure is applied here to identify the influence of beach width on dune volume change. It is suggested that there is a certain potential dune growth associated with a certain beach width. The envelope (brown line) is a graphical representation of the upper limit of the potential dune growth under influence of a varying beach width. The envelope of maximum empirical dune growth is obtained from the data. It is expected that dune growth higher than the upper limit is not or rather possible. Higher dune growth rates are related to wider beaches. A wider beach would activate more sediment into transport towards the dunes. Alongshore variation in dune growth for a beach width of similar size could be explained by the fact that the potential dune growth is not reached due to the spatial differences in dune geometry or other processes that govern the aeolian sediment transport towards the dunes, for example the location with respect to the wind conditions and sediment characteristics. To test how well a statistical correlation between beach width and dune volume change exists, a linear trend was fitted at the dataset. A positive correlation coefficient of $r = 0.39$ is found, see Figure H.20b in Appendix H. The relatively low correlation could be possibly caused by forcing of processes on shorter time scales that dominates the initial development of the system.

Median grain size versus dune volume change

A negative correlation is expected between median grain size and dune growth: coarser grains are more difficult to be picked-up and transported by the wind resulting in smaller dune growth. Figure 4.11 identifies the relation between the measured median grain size for five distinct subdomains and the measured cumulative dune volume change for each cross-shore transect between May 2015 - September 2016. Based on the results a relation between median grain size and dune growth is difficult to identify. The largest dune growth is indeed pronounced for the finest median grain size, but the four other subdomains shows comparable results for variation in median grain size. The location of the measured D_{50} is given in Figure 3.1 in Chapter ???. The finest grains are located along the Northern and Southern shoulder, while the middle section along the HD system consists of larger grains. The largest spatial variation in dune growth is also found for the subdomain with the finest median grain size. However, still 75 % of the derived cross-shore transects in this domain has



(a) Mean beach slope vs volume change dunes

(b) Mean Beach width vs volume change dunes

Figure 4.10: Mean beach slope or beach width of the Dry beach zone (x-axis) against the volume change of the Dunes (y-axis) along the HD system in the period May 2015 - December 2016 (T0-T4). The envelope (brown line) is a graphical representation of the upper limit of the potential dune growth under influence of a varying beach slope or beach width. Profile type 1-5 are indicated by different colors and markers.

a dune growth rates of more than $40 m^3/m/y$. In subdomain 5 for which a median grain size of $277 \mu m$ was found, the black circle indicates a cross-shore transect along profile type 2 at RSP 26.06, see also Figure 4.5 The other data-locations in this subdomain represents cross-shore transects of profile type 5 which show much lower dune growth rates. In subdomain 1 for which a median grain size of $291 \mu m$ was found, the black circle indicates a cross-shore transect just northwards of the HD system. For this cross-shore transect at RSP 20.09 relatively low dune growth rates were measured compared to the other cross-shore transects in the subdomain, see also 4.5.

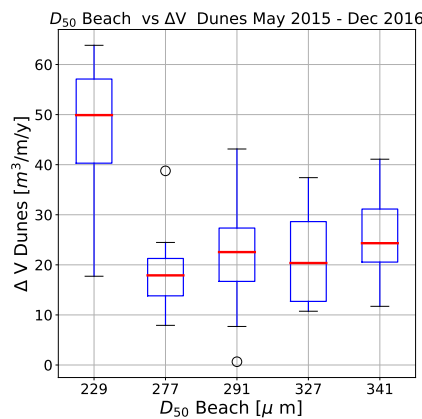


Figure 4.11: Median grain size of the Dry beach zone (x-axis) for each subdomain against the volume change of the Dunes (y-axis) along the HD system in the period May 2015 - December 2016 (T0-T4). Each boxplot represents the upper and lower quartile and median of dune volume changes within a subdomain. The height of the boxes indicates spatial variability in dune volume changes. The black circles indicates cross-shore locations that are at least 1.5 times smaller than the first quartile (lower horizontal line of box), or 1.5 times larger than the third quartile (upper horizontal line of box).

4.1.8. Differences between Profile Types

Table 4.8 provides an overview of the derived parameters of interest for the five profile types and the natural dunes located Northwards and Southwards of the HD system in the period May 2015 - December 2016 (T0-T4). The most significant results are presented.

The volumetric losses of the surf zone, the intertidal zone and the beach zone are compensated by accretion along the Northern and Southern Dunes. Based on the result it can be derived that on average 20 percent of the volumetric losses in the cross-shore profile along the HD system ($-214 \text{ m}^3/\text{m}$) are compensated by accretion in the new dunes ($+43 \text{ m}^3/\text{m}$). However, it should be noted that there is a strong influence of the alongshore location with respect to volumetric losses in the lower profile and growth in the dunes. The volumetric losses of the dry beach zone were associated with a decrease in beach width and a steepening of the beach slope. This effect is strongly pronounced for profile type 5 along the Southern shoulder. The volumetric increase of the dry beach zone along the Northern and Southern dunes were associated with an increase in beach width and a milder beach slope in time.

The average dune growth rate ($+28 \text{ m}^3/\text{m}/\text{y}$) is comparable to design expectations ($+35 \text{ m}^3/\text{m}/\text{y}$), see subsection 3.2.4. The dune growth rate is largest for profile type 3-South ($+48 \text{ m}^3/\text{m}/\text{y}$). The dune growth along profile type 3 (South) is characterized by parameters that stimulate the actual sediment transport towards the dunes: a milder beach slope, a larger beach width, and lower median grain size compared to the other profile types 1-5. In the North the dune growth rate is also larger for profile type 3-North ($+32 \text{ m}^3/\text{m}/\text{y}$) than the adjacent profile types 2 (North) and 4. A comparison is made between profile types 1-5 and profile type 3 (North or South). The observations are listed below:

1. For profile type 1 a similar beach width is derived compared to profile type 3 (South). However, dune growth is significantly smaller for profile type 1. Profile type 1 is characterized by: a steeper beach slope, a lower median grain size and a higher and steeper dune front compared to profile type 3 (South). The sediment supply towards the dunes could be explained by the steeper beach slope and the high and steep dune front.
2. The dune growth rate for profile type 2 (North) is significantly smaller compared to the adjacent profile type 3 (North). This is possibly influenced by a steeper beach slope, a smaller beach width, and a higher and steeper dune front (1:2) [V/H] compared to profile type 3 (North) (1:4).
3. The dune growth rate is also high for profile type 2 (South). However, this profile type is characterized by: a large decrease in beach volume, a smaller beach width and a higher decrease in beach width which reduces the aeolian sediment availability for transport towards the dunes.
4. The dune growth for profile type 4 is significantly smaller compared to the adjacent profile type 3 (North) while the profile type 4 is characterized by parameters that stimulates the aeolian sediment supply towards the dunes: an constant beach slope, a wider beach width, a coarser grain size and a bit higher and steeper dune front (1:3) compared to profile type 3 (1:4).
5. The dune growth rate is small for profile type 5 compared to profile type 2 (South) and 3 (South). However, this profile type is characterized by a significant decrease in beach volume, steeper beach slope, a smaller beach width and a higher decrease in beach width, compared to the profile type 2 (South) and 3 (South). This might reduces the aeolian sediment supply towards the dunes.

In Appendix 4.11 box plots are presented to obtain insight into the spatial variations within the profile types itself. In subsection 4.2.2 the measured dune volume changes, are compared to the predicted dune growth rates simulated by the model.

Table 4.8: Overview of derived parameters of interest for the five different profile types in the period May 2015 - December 2016 (T0-T4). '-' indicates that there is no specific data available for the profile type.

	RSP coordinates	ΔV Surf zone [m ³ /m/y]	ΔV Intertidal zone [m ³ /m/y]	ΔV Dry beach zone [m ³ /m/y]	ΔV Dunes ^a [m ³ /m/y]	Beach slope mean [-]	Beach width mean [m]	Δ Beach width [m/y]	D ₅₀ [μm]
Northern Dunes	17.08 - 20.25	-	-	+20	+21	-0.03	98	+7	304
Profile type 1	20.25 - 21.00	-	-	-16	+14	-0.03	150	-48	304-321
Profile type 2 North	21.00 - 21.46	-	-	-27	+20	-0.03	88	-36	304-321
Profile type 3 North	21.46 - 22.38	-	-	-27	+32	-0.02	95	-25	321-341
Profile type 4	22.38 - 24.15	-	-	+7	+23	-0.02	104	-24	341
Profile type 3 South	24.15 - 25.57	-	-	-0.1	+48	-0.01	151	-17	224
Profile type 2 South	25.57 - 26.13	-	-	-65	+45	-0.02	110	-58	224-278
Profile type 5	26.13 - 27.00	-	-	-88	+18	-0.05	57	-63	278
Southern Dunes	27.00 - 28.32	-	-	35	+14	-0.01	150	+9	-
Full project domain	17.08 - 28.32	-39	-35	2	+23	-0.03	107	-10	-
HD system	20.25 - 27.00	-60	-50	-29	+28	-0.03	105	-37	-

^aIn the design phase a ΔV of 35 m³/m/y was derived for the first year after construction based on earlier research and expertise obtained from reference projects [?].

4.2. Results: Modelling

4.2.1. Measured and Modelled Sedimentation and Erosion Patterns

This section presents the measured and modelled sedimentation and erosion patterns for the HD system. For each of the five subdomains, that represents a different median grain size and alongshore domain, the periodic and cumulative measurements and model results are presented for the four measurement periods between May 2015 and December 2016. The most important assumptions that needs to be considered for interpretation of the results are:

1. No marine sediment transport is modelled.
2. A constant vegetation cover in time and in space is imposed to the dune area.
3. A representative grain size distribution is imposed to each subdomain.
4. Soil moisture content at the beach is not included.

Reference is made to section 3.2 of Chapter 3 for the methodology that is applied to obtain the results, Figure 4.12 shows the location for each of the five subdomains. Note that the noise in the measurements are seen as a result of LiDAR survey that not penetrate through water at sea or the dune valley. Therefore, the intertidal zone and the position of the dune foot are indicated in the figures.

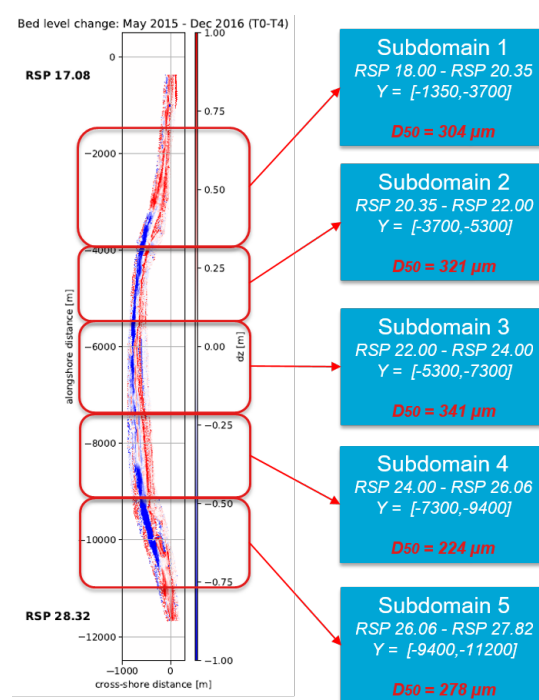


Figure 4.12: Schematic overview of the model domains. The HD system is divided into five subdomains in order to simulate alongshore variations in median grain size.

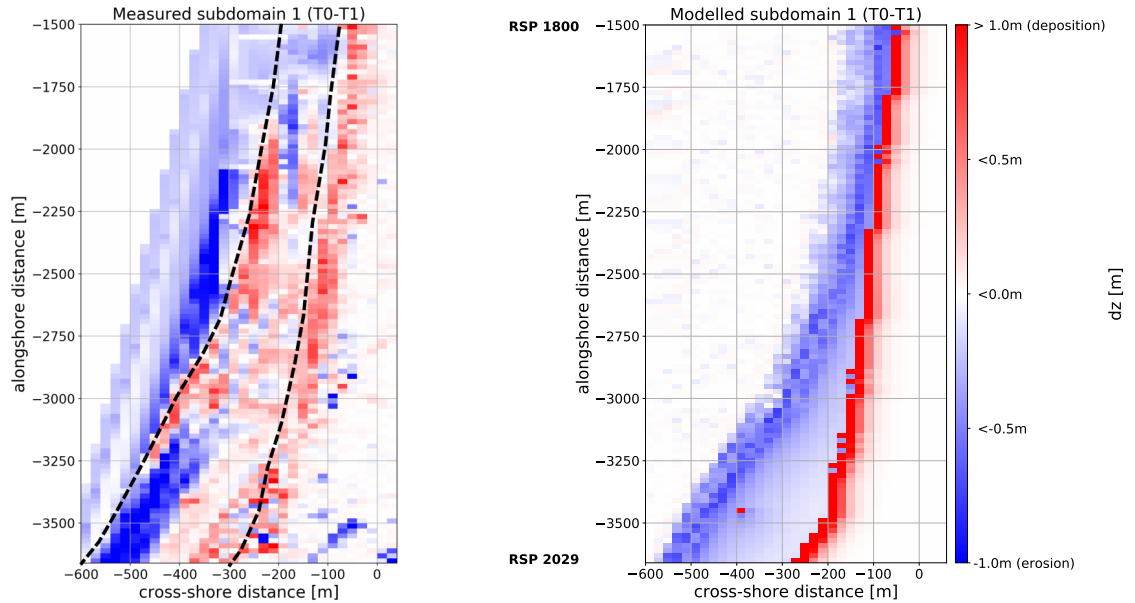
Periodic changes

Subdomain 1 with median grain size $D_{50} = 304 \mu\text{m}$

Subdomain 1 is located along the Northern shoulder of the HD system at Petten, Figure 4.12 shows the location for this domain along the HD system. The model is imposed with a median grain size of $304 \mu\text{m}$ for this subdomain derived from post-construction grain size measurements, see section 3.2.1. An overview of the measured and modelled morphological development is given in Figure 4.13 till Figure 4.16. The domain of interest is at the right side of the alongshore line that fits between cross-shore coordinate $x = -280 \text{ m}$ in the North and $x = -600 \text{ m}$ in the South and is located between RSP 18.00 and RSP 20.29.

Figure 4.13a illustrates a rapid redistribution of sediments in the first measurement period. This is pronounced in both the measurements and the model results. The deposition of aeolian sediment in the dunes is more localized in the model than in the measurements which is indicated in the model results by the small dense alongshore red line. The observed large deposition at the beach in the period May 2015 - December

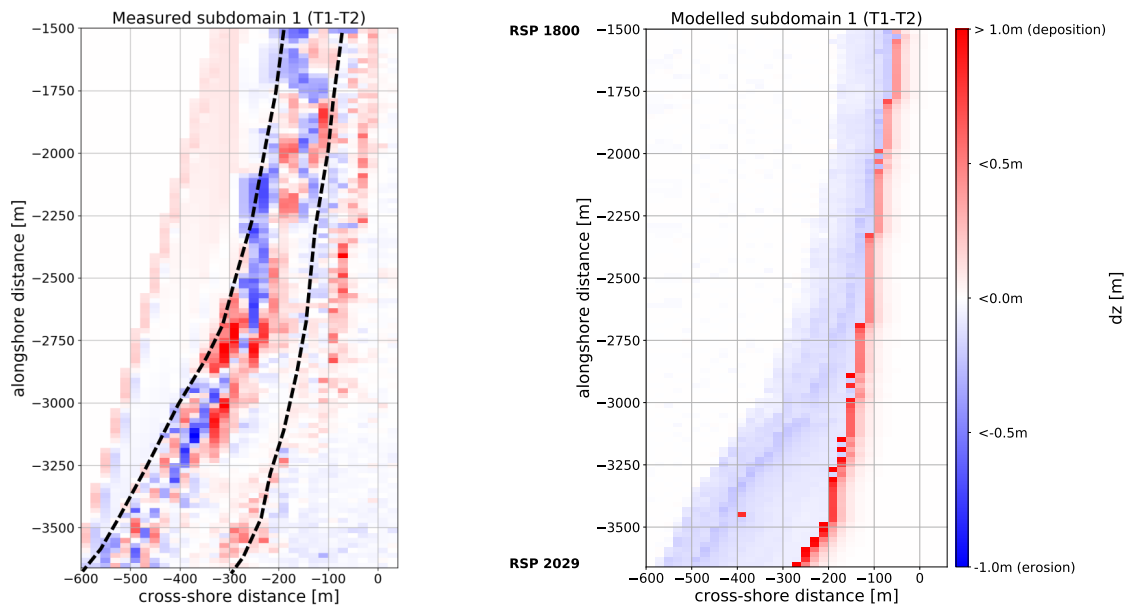
2015, shown in Figure 4.13a, between the cross-shore location $x = -400$ m and $x = -200$ m and the alongshore location $y = -3750$ m and $y = -3250$ m, are additional construction works and are not present in the model. The observed deposition in the intertidal zone in the period May 2015 - September 2016, shown in Figure 4.13a till Figure 4.15a, and at the beach in the period May 2015 - December 2015, see Figure 4.13a, between alongshore location $y = -1750$ m and $y = -3100$ m of the subdomain, is also not presented in the model results as marine sediment transport is not simulated. This is also observed from the less pronounced erosion of the intertidal zone in the model results in the period September 2016 - December 2016 as shown in Figure 4.16b. Moreover, the dune growth is more pronounced in the period September 2016 - December 2016, shown in Figure 4.16a. The model result show one red cell at the coordinates $y = -3500$ m and $x = -400$ m, this is a seasonal beach building. The model simulated this cell as a deposition area since the cell is larger than his surrounding cells and therefore able to capture sediments.



(a) Measured sedimentation and erosion in T0-T1.

(b) Modelled sedimentation and erosion in T0-T1.

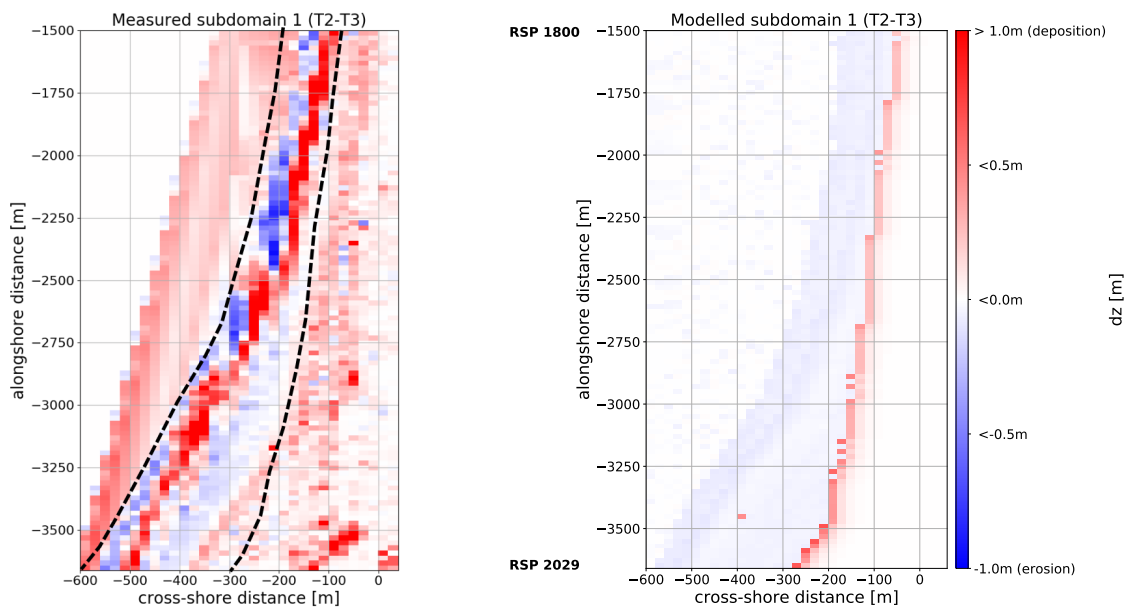
Figure 4.13: Measured and modelled sedimentation and erosion between May 2015 - Dec 2015 of subdomain 1 along the Northern shoulder of the HD system between RSP 18.00 and RSP 20.29. The black dashed lines in the measurement indicate the position of the intertidal zone (left) and the dune foot (right), Northern direction upwards. Model results only include aeolian sediment transport and dune development as a result of measured climatic forcing and a constant influence of vegetation for this period.



(a) Measured sedimentation and erosion in T1-T2.

(b) Modelled sedimentation and erosion in T1-T2.

Figure 4.14: Measured and modelled sedimentation and erosion between Dec 2015 - March 2016 of subdomain 1 along the Northern shoulder of the HD system between RSP 18.00 and RSP 20.29. The black dashed lines in the measurement indicate the position of the intertidal zone (left) and the dune foot (right), Northern direction is upwards. Model results only include aeolian sediment transport and dune development as a result of measured climatic forcing and a constant influence of vegetation for this period.



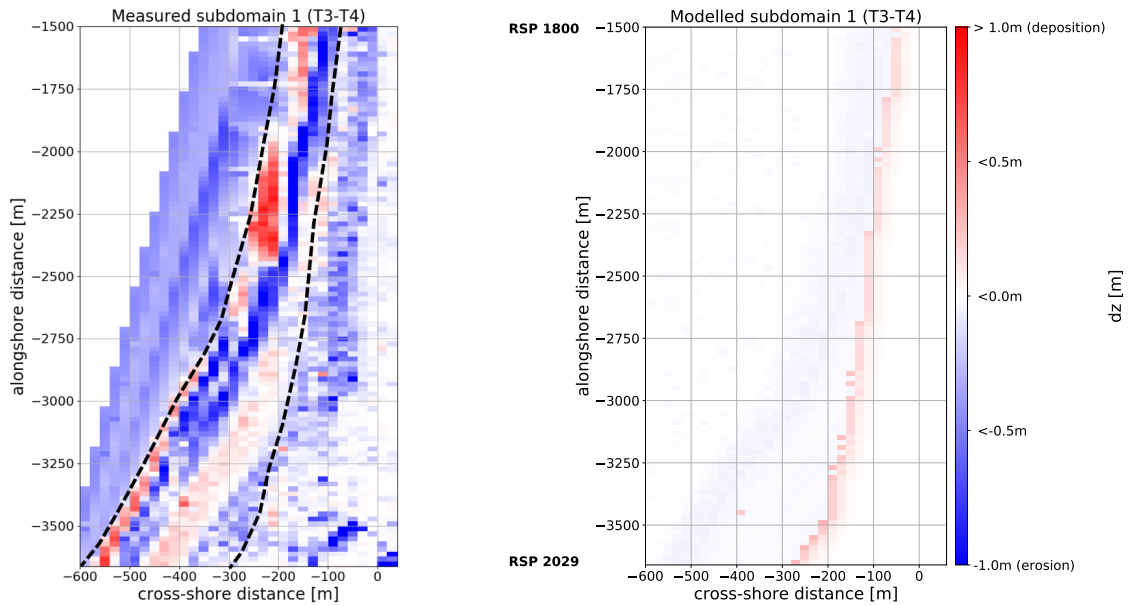
(a) Measured sedimentation and erosion in T2-T3.

(b) Modelled sedimentation and erosion in T2-T3.

Figure 4.15: Measured and modelled sedimentation and erosion between March 2016 - September 2016 of subdomain 1 along the Northern shoulder of the HD system between RSP 18.00 and RSP 20.29. The black dashed lines in the measurement indicate the position of the intertidal zone (left) and the dune foot (right), Northern direction is upwards. Model results only include aeolian sediment transport and dune development as a result of measured climatic forcing and a constant influence of vegetation for this period.

Subdomain 2 with median grain size $D_{50} = 321 \mu m$

Subdomain 2 is located along the Northern straight section of the HD system, Figure 4.12 shows the location for this domain along the HD system. The model is imposed with a median grain size of $321 \mu m$ for this subdomain derived from post-construction grain size measurements, see section 3.2.1. An overview of the measured and modelled morphological development is given in Figure 4.17 till Figure 4.20. The domain of



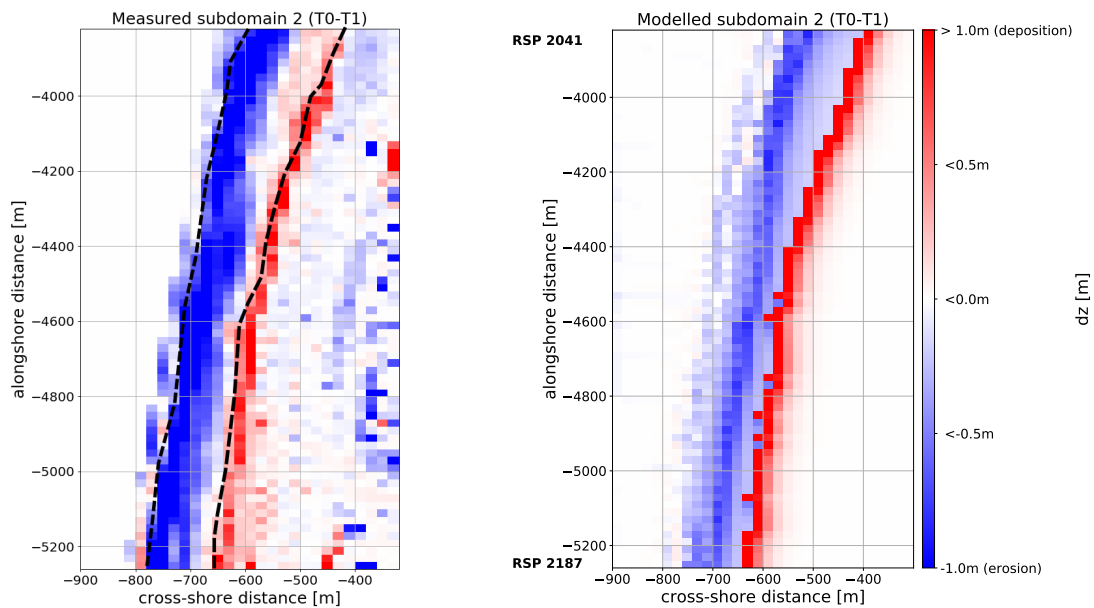
(a) Measured sedimentation and erosion in T3-T4.

(b) Modelled sedimentation and erosion in T3-T4.

Figure 4.16: Measured and modelled sedimentation and erosion between September 2016 - December 2016 of subdomain 1 along the Northern shoulder of the HD system between RSP 18.00 and RSP 20.29. The black dashed lines in the measurement indicate the position of the intertidal zone (left) and the dune foot (right), Northern direction is upwards. Model results only include aeolian sediment transport and dune development as a result of measured climatic forcing and a constant influence of vegetation for this period.

interest is at the right of the alongshore line that fits between cross-shore coordinate $x = -700$ m in the North and $x = -800$ m in the South and located between RSP 20.41 and RSP 21.87.

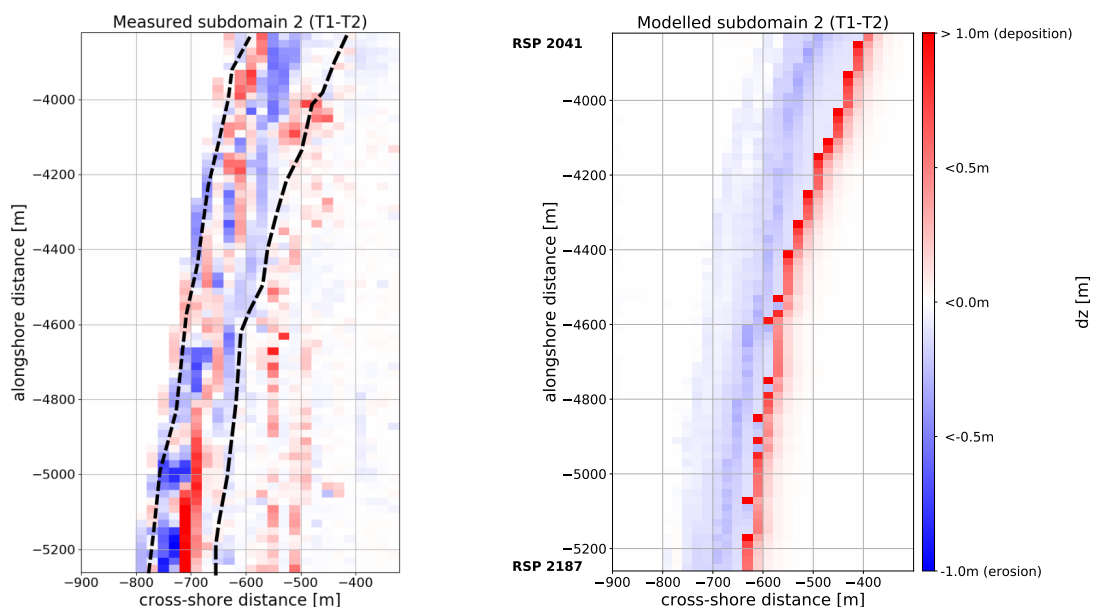
Figure 4.17a illustrates a rapid redistribution of sediments in the first measurement period. This is pronounced in both the measurements and the model results. The measurements show alongshore and cross-shore variations in bed level change of the intertidal zone and the beach as shown in Figure 4.18a till Figure 4.20a. This could be observed along the line of cross-shore coordinate $x = -800$ m. This is not correctly presented in the model as marine sediment transport is not included in the model, although it does show alongshore and cross-shore spatial variations in bed level change. The deposition of aeolian sediment in the dunes is more localized in the model than in the measurements at the location of the dune foot position in the period Dec 2015 - September 2016, shown in Figure 4.18 till Figure 4.19. The dune growth is smaller and show more spatial variations in the measurements than in the model results in the period December 2015 - September 2016.



(a) Measured sedimentation and erosion in T0-T1.

(b) Modelled sedimentation and erosion in T0-T1.

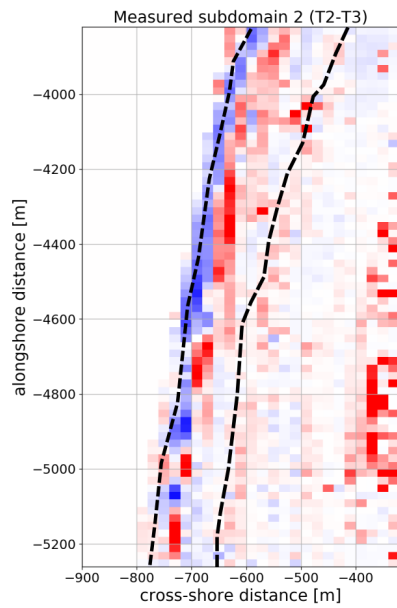
Figure 4.17: Measured and modelled sedimentation and erosion between May 2015 - Dec 2015 of subdomain 2 along the Northern area of the HD system between RSP 20.41 and RSP 21.87. The black dashed lines in the measurement indicate the position of the intertidal zone (left) and the dune foot (right), Northern direction is upwards. Model results only include aeolian sediment transport and dune development as a result of measured climatic forcing and a constant influence of vegetation for this period.



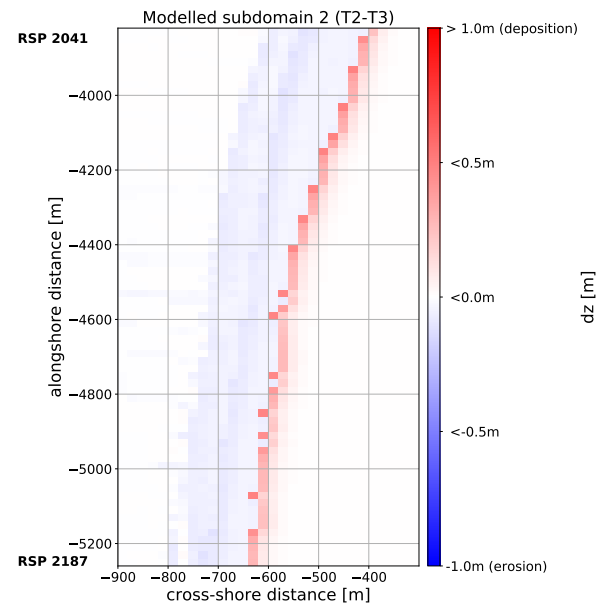
(a) Measured sedimentation and erosion in T1-T2.

(b) Modelled sedimentation and erosion in T1-T2.

Figure 4.18: Measured and modelled sedimentation and erosion between Dec 2015 - March 2016 of subdomain 2 along the Northern area of the HD system between RSP 20.41 and RSP 21.87. The black dashed lines in the measurement indicate the position of the intertidal zone (left) and the dune foot (right), Northern direction is upwards. Model results only include aeolian sediment transport and dune development as a result of measured climatic forcing and a constant influence of vegetation for this period.

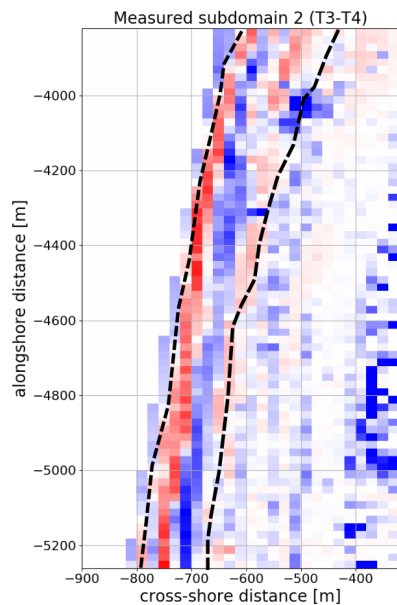


(a) Measured sedimentation and erosion in T2-T3.

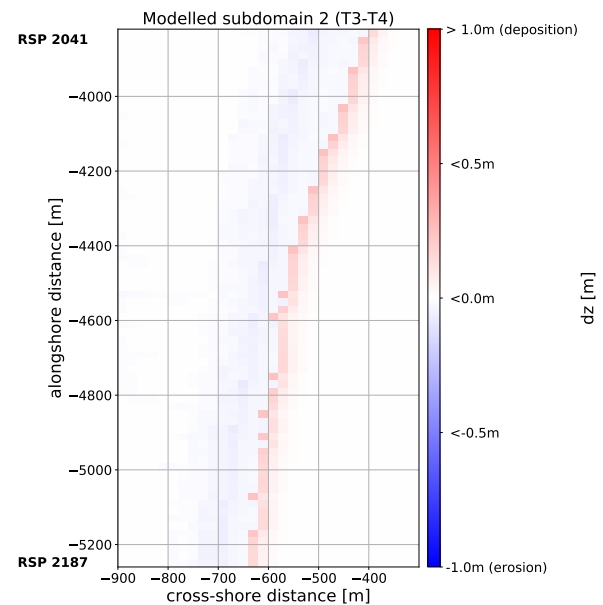


(b) Modelled sedimentation and erosion in T2-T3.

Figure 4.19: Measured and modelled sedimentation and erosion between March 2016 - September 2016 of subdomain 2 along the Northern area of the HD system between RSP 20.41 and RSP 21.87. The black dashed lines in the measurement indicate the position of the intertidal zone (left) and the dune foot (right), Northern direction is upwards. Model results only include aeolian sediment transport and dune development as a result of measured climatic forcing and a constant influence of vegetation for this period.



(a) Measured sedimentation and erosion in T3-T4.



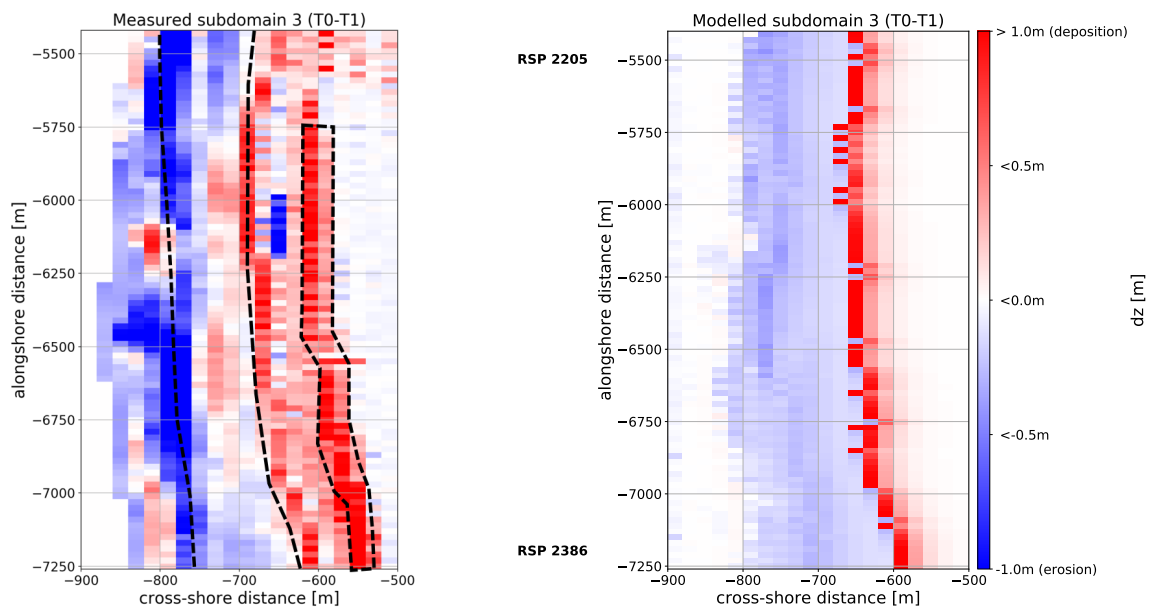
(b) Modelled sedimentation and erosion in T3-T4.

Figure 4.20: Measured and modelled sedimentation and erosion between September 2016 - December 2016 of subdomain 2 along the Northern area of the HD system between RSP 20.41 and RSP 21.87. The black dashed lines in the measurement indicate the position of the intertidal zone (left) and the dune foot (right), Northern direction is upwards. Model results only include aeolian sediment transport and dune development as a result of measured climatic forcing and a constant influence of vegetation for this period.

Subdomain 3 with median grain size $D_{50} = 341 \mu\text{m}$

Subdomain 3 is located along the straight section in the middle part of the HD system, Figure 4.12 shows the location for this domain along the HD system. The model is imposed with a median grain size of $341 \mu\text{m}$ for this subdomain derived from post-construction grain size measurements, see section 3.2.1. An overview of the measured and modelled morphological development is given in Figure 4.21 till Figure 4.24. The domain of interest is at the right of the alongshore line that fits between cross-shore coordinate $x = -800 \text{ m}$ in the North and $x = -760 \text{ m}$ in the South and located between RSP 22.05 and RSP 23.86. The dune valley is located between the alongshore distance $y = -5750 \text{ m}$ and $y = -7250 \text{ m}$ and the cross-shore distance $x = -600 \text{ m}$ and $x = -500 \text{ m}$.

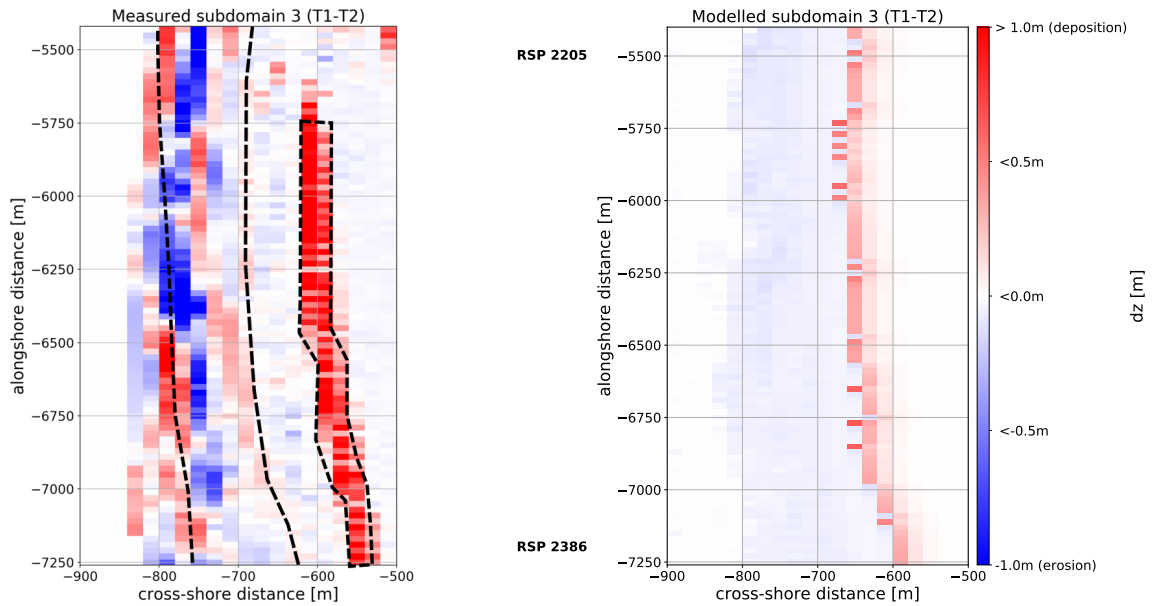
Figure 4.21a illustrates a rapid redistribution of sediments in the first measurement period. This is pronounced in both the measurements and the model results. The observed strong local erosion and deposition in the intertidal zone and beach in the period December 2015 - December 2016, shown in Figure 4.22a till Figure 4.24a, is not correctly presented in the model results as marine sediment transport is not simulated. This could be observed along the line of cross-shore coordinate $x = -700 \text{ m}$ in the North and $x = -800 \text{ m}$ in the South. The deposition of aeolian sediment in the dunes is in the first period May 2015 - December 2015, shown in Figure 4.21, more localized in the model than in the measurements. The spatial spreading in the measurements can be noticed when observing east of the dashed line between cross-shore coordinate $x = -680 \text{ m}$ in the North and $x = -620 \text{ m}$ in the South, which indicates the location of the dune foot position at $+3.5 \text{ m NAP}$. This is where the dune valley is located. This area is considered in the model simulations as an area with an infinite threshold velocity to avoid numerical errors. Hence, in the model simulation no morphological changes in the dune valley are observed. The location of deposition in the dunes in the remaining periods between December 2015 and December 2016, see Figure 4.22 till Figure 4.24 is correctly simulated by the model; morphological changes occur at the seaward side of the dune valley.



(a) Measured sedimentation and erosion in T0-T1.

(b) Modelled sedimentation and erosion in T0-T1.

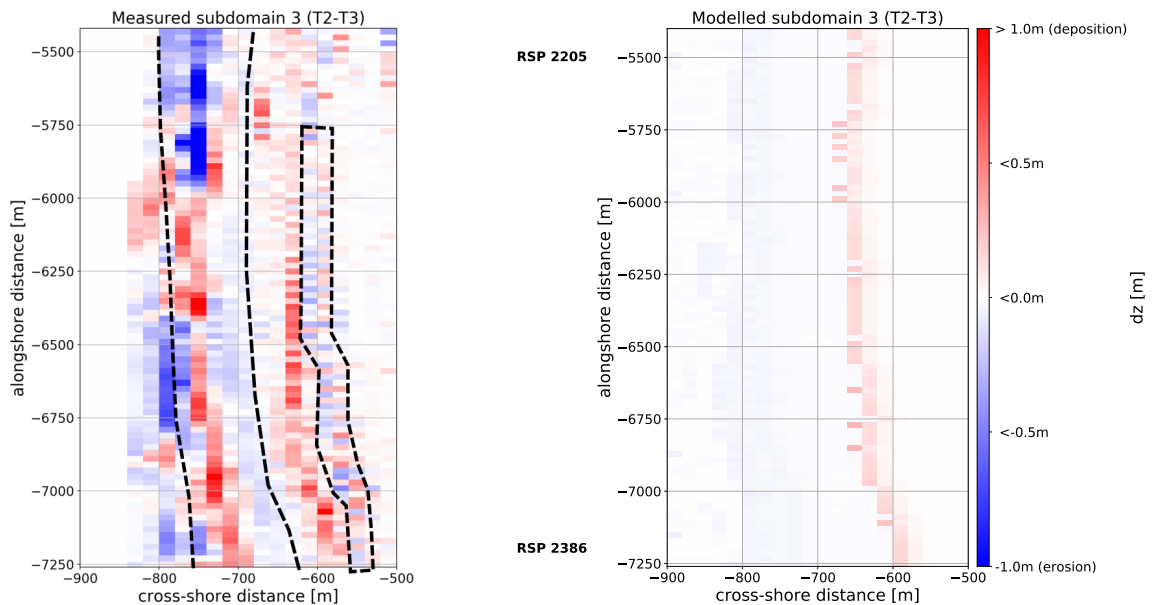
Figure 4.21: Measured and modelled sedimentation and erosion between May 2015 - Dec 2015 of subdomain 3 along the middle area of the HD system between RSP 22.05 and RSP 23.87. The black dashed lines in the measurement indicate the position of the intertidal zone (left) and the dune foot (right), Northern direction is upwards. Model results only include aeolian sediment transport and dune development as a result of measured climatic forcing and a constant influence of vegetation for this period.



(a) Measured sedimentation and erosion in T1-T2.

(b) Modelled sedimentation and erosion in T1-T2.

Figure 4.22: Measured and modelled sedimentation and erosion between Dec 2015 - March 2016 of subdomain 3 along the middle area of the HD system between RSP 22.05 and RSP 23.87. The black dashed lines in the measurement indicate the position of the intertidal zone (left) and the dune foot (right), Northern direction is upwards. Model results only include aeolian sediment transport and dune development as a result of measured climatic forcing and a constant influence of vegetation for this period.



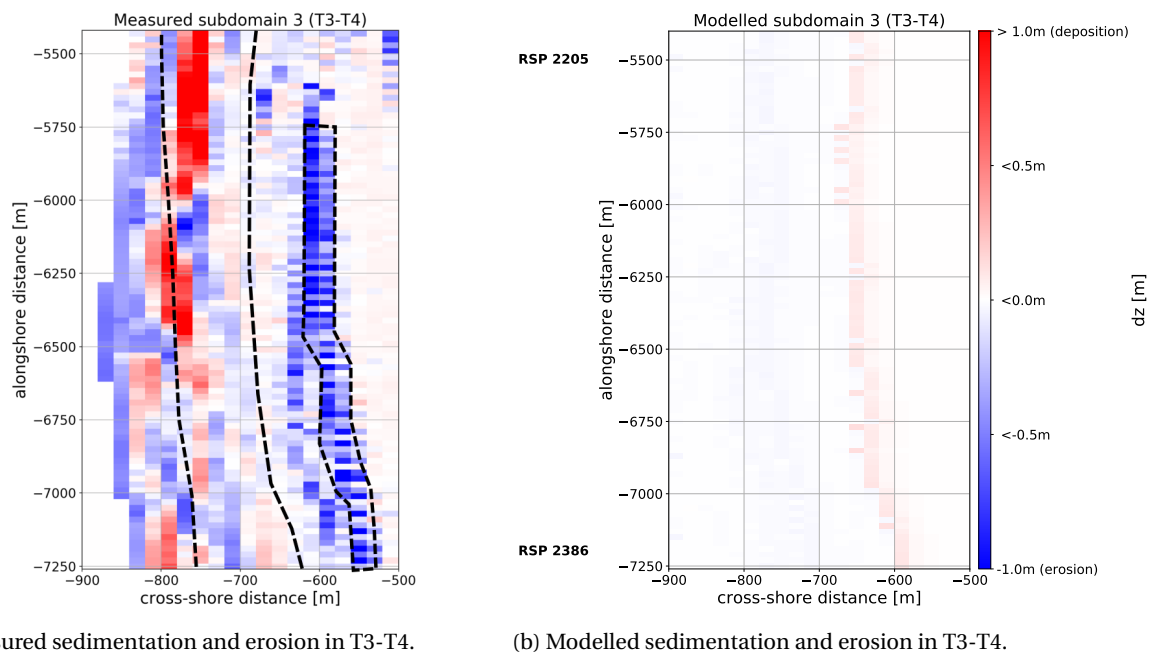
(a) Measured sedimentation and erosion in T2-T3.

(b) Modelled sedimentation and erosion in T2-T3.

Figure 4.23: Measured and modelled sedimentation and erosion between March 2016 - September 2016 of subdomain 3 along the middle area of the HD system between RSP 22.05 and RSP 23.87. The black dashed lines in the measurement indicate the position of the intertidal zone (left) and the dune foot (right), Northern direction is upwards. Model results only include aeolian sediment transport and dune development as a result of measured climatic forcing and a constant influence of vegetation for this period.

Subdomain 4 with median grain size $D_{50} = 224 \mu\text{m}$

Subdomain 4 is located along the Southern straight section of the HD system, Figure 4.12 shows the location for this domain along the HD system. The model is imposed with a median grain size of $224 \mu\text{m}$ for this subdomain derived from post-construction grain size measurements, see section 3.2.1. An overview of the measured and modelled morphological development is given in Figure 4.25 till Figure 4.28. The domain of



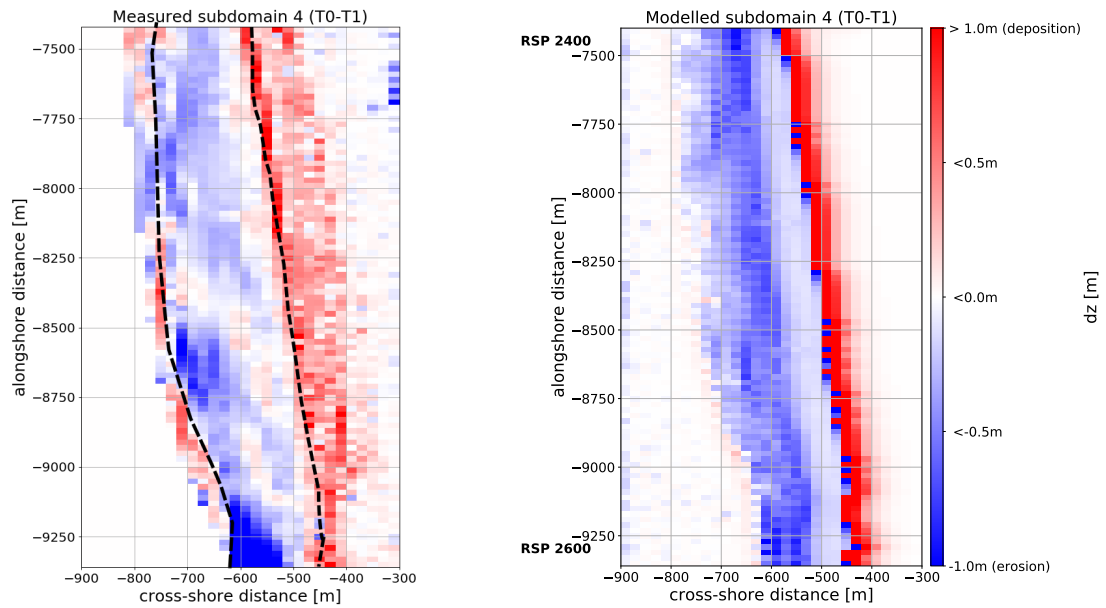
(a) Measured sedimentation and erosion in T3-T4.

(b) Modelled sedimentation and erosion in T3-T4.

Figure 4.24: Measured and modelled sedimentation and erosion between September 2016 - December 2016 of subdomain 3 along the middle area of the HD system between RSP 22.05 and RSP 23.87. The black dashed lines in the measurement indicate the position of the intertidal zone (left) and the dune foot (right), Northern direction is upwards. Model results only include aeolian sediment transport and dune development as a result of measured climatic forcing and a constant influence of vegetation for this period.

interest is at the right of the alongshore line that fits between cross-shore coordinate $x = -700$ m in the North and $x = -600$ m in the South and located between RSP 24.00 and RSP 26.00.

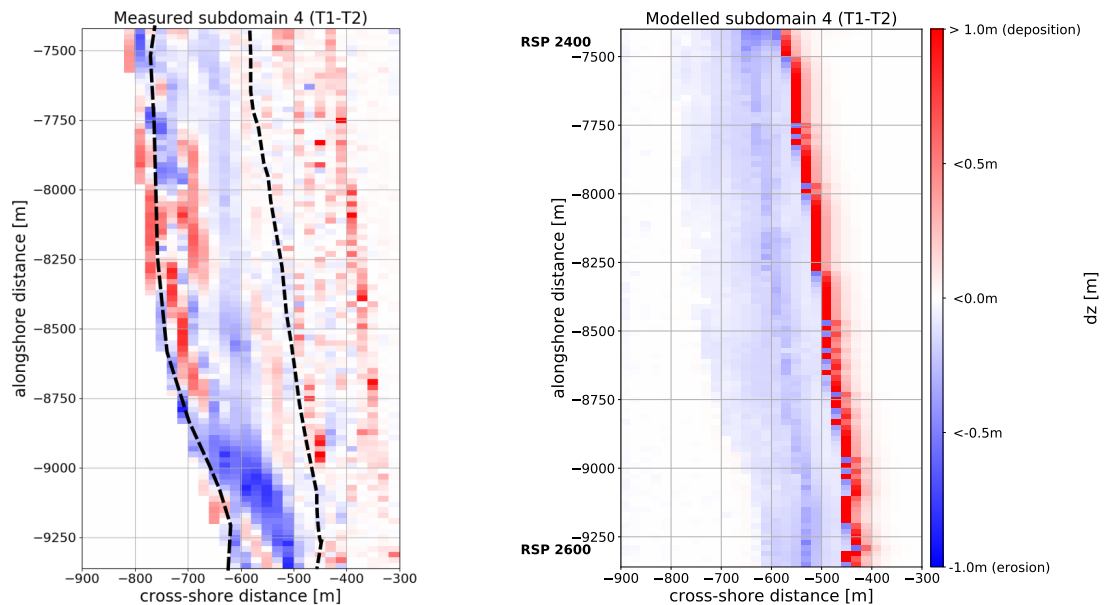
Figure 4.25a illustrates the redistribution of sediments in the first measurement period. In contrast to the other subdomains, rapid bed level changes are less pronounced and smaller in the measurements than in the model results for the first measurement period May 2015 - December 2015. The spatial variability in the erosion and deposition patterns of the intertidal zone are larger in the measurements than in the model results for the full period between May 2015 - December 2016. This is shown in Figure 4.25 till Figure 4.28. The observed strong deposition in the intertidal zone and at the beach in in the period September 2016 - December 2016, shown in Figure 4.28a, between alongshore location $y = -8500$ m and $y = -9250$ m of the subdomain, is also not present in the model results as marine sediment transport is not simulated. The deposition of aeolian sediment in the dunes is more localized in the model, along the dune foot, than in the measurements. When only the temporal variations in modelled dune volume changes are considered, cross-shore spatial spreading of dune growth is also larger in the model results in the period May 2015 - December 2015, see Figure 4.25b, than in the subsequent measurement periods between December 2015 - December 2016, as can be seen in Figure 4.26b till Figure 4.28b. Furthermore, the main cross-shore position of deposition in the dunes at approximately $x = -450$ m is correctly presented in the model. The observed small dune growth in the period September 2016 - December 2016 is not correctly presented in the model results.



(a) Measured sedimentation and erosion in T0-T1.

(b) Modelled sedimentation and erosion in T0-T1.

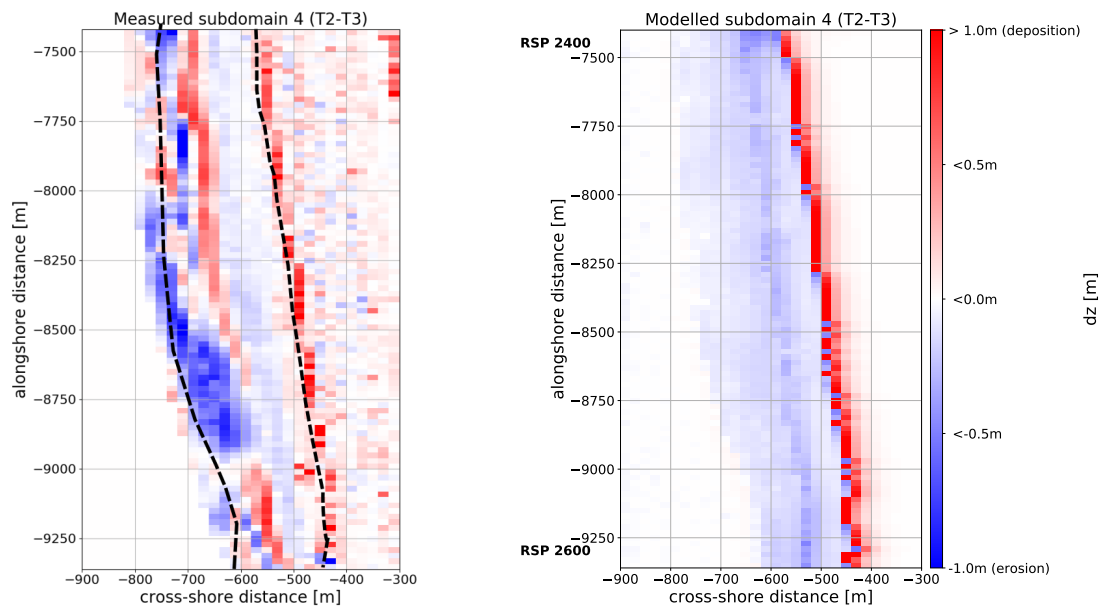
Figure 4.25: Measured and modelled sedimentation and erosion between May 2015 - Dec 2015 of subdomain 4 along the Southern area of the HD system between RSP 24.00 and RSP 26.00. The black dashed lines in the measurement indicate the position of the intertidal zone (left) and the dune foot (right), Northern direction is upwards. Model results only include aeolian sediment transport and dune development as a result of measured climatic forcing and a constant influence of vegetation for this period.



(a) Measured sedimentation and erosion in T1-T2.

(b) Modelled sedimentation and erosion in T1-T2.

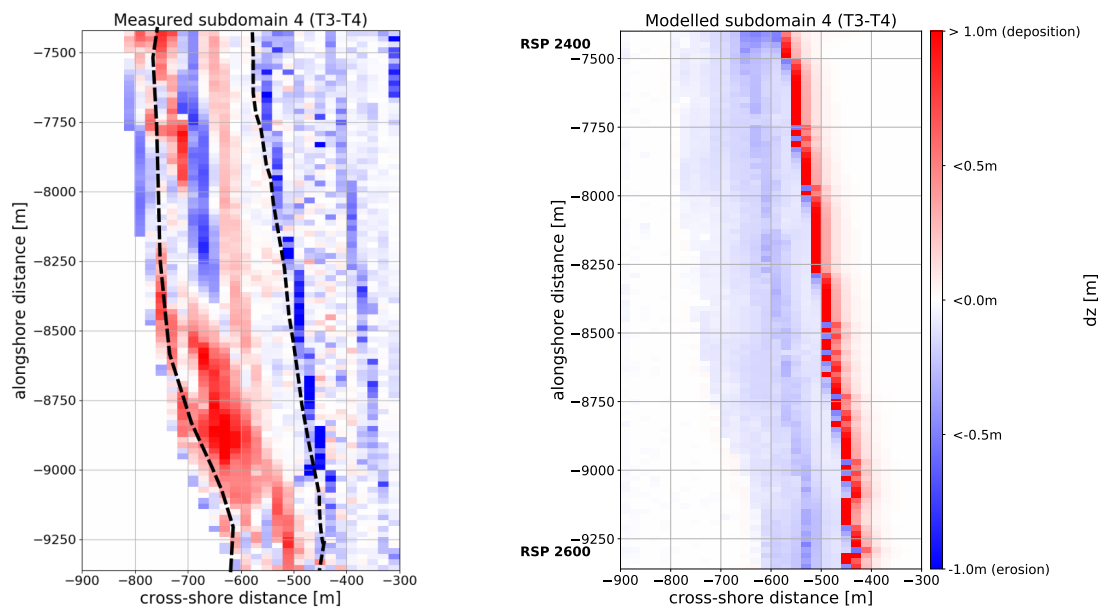
Figure 4.26: Measured and modelled sedimentation and erosion between Dec 2015 - March 2016 of subdomain 4 along the Southern area of the HD system between RSP 24.00 and RSP 26.00. The black dashed lines in the measurement indicate the position of the intertidal zone (left) and the dune foot (right), Northern direction is upwards. Model results only include aeolian sediment transport and dune development as a result of measured climatic forcing and a constant influence of vegetation for this period.



(a) Measured sedimentation and erosion in T2-T3.

(b) Modelled sedimentation and erosion in T2-T3.

Figure 4.27: Measured and modelled sedimentation and erosion between March 2016 - September 2016 of subdomain 4 along the Southern area of the HD system between RSP 24.00 and RSP 26.00. The black dashed lines in the measurement indicate the position of the intertidal zone (left) and the dune foot (right), Northern direction is upwards. Model results only include aeolian sediment transport and dune development as a result of measured climatic forcing and a constant influence of vegetation for this period.



(a) Measured sedimentation and erosion in T3-T4.

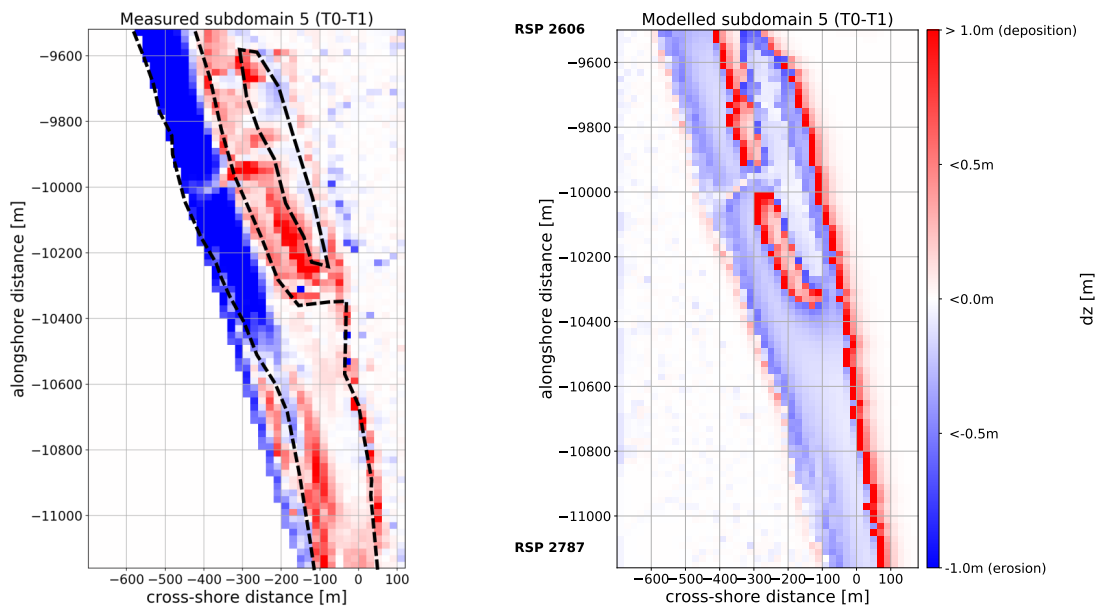
(b) Modelled sedimentation and erosion in T3-T4.

Figure 4.28: Measured and modelled sedimentation and erosion between September 2016 - December 2016 of subdomain 4 along the Southern area of the HD system between RSP 24.00 and RSP 26.00. The black dashed lines in the measurement indicate the position of the intertidal zone (left) and the dune foot (right), Northern direction is upwards. Model results only include aeolian sediment transport and dune development as a result of measured climatic forcing and a constant influence of vegetation for this period.

Subdomain 5 with median grain size $D_{50} = 278 \mu\text{m}$

Subdomain 5 is located along the Southern shoulder of the HD system at Camperduin, Figure 4.12 shows the location for this domain along the HD system. The model is imposed with a median grain size of $278 \mu\text{m}$ for this subdomain derived from post-construction grain size measurements, see section 3.2.1. An overview of the measured and modelled morphological development is given in Figure 4.29 till Figure 4.32. The domain of interest is at the right side of the alongshore line that fits between cross-shore coordinate $x = -500 \text{ m}$ in the North and $x = -100 \text{ m}$ in the South and located between RSP 26.06 and RSP 27.82. The lagoon is located between the alongshore distance $y = -9400 \text{ m}$ and $y = -10300 \text{ m}$ and the cross-shore distance $x = -300 \text{ m}$ and $x = -50 \text{ m}$.

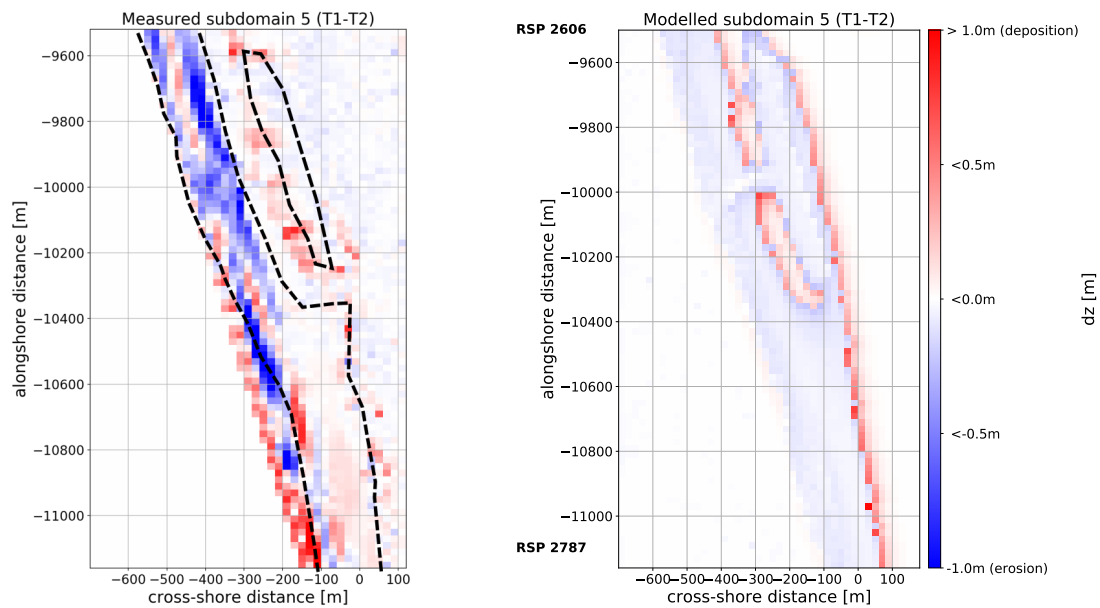
Figure 4.29a illustrates a rapid redistribution of sediments in the first measurement period. The spatial variability in and the quantity of the bed level changes are larger in the measurements than in the model results. The observed erosion of the intertidal zone and the beach in the period May 2015 - December 2015 and the deposition in the period September 2016 - December 2016, see Figure 4.32, between alongshore location $y = -9500 \text{ m}$ and $y = -10500 \text{ m}$ of the subdomain, is not present in the model results as marine sediment transport is not simulated. The same is observed for the deposition in the intertidal zone in the period May 2015 - December 2015 between the along shore location $y = -11000 \text{ m}$ and $y = -11500 \text{ m}$, as shown in Figure 4.29. The location of deposition of aeolian sediment in the dunes is correctly presented in the model along the lagoon and along the Southern natural dunes between alongshore location $y = -10300 \text{ m}$ and $y = -11200 \text{ m}$. The dune growth is smaller and shows more spatial variation in the measurements than in the model results in the period December 2015 - September 2016.



(a) Measured sedimentation and erosion in T0-T1.

(b) Modelled sedimentation and erosion in T0-T1.

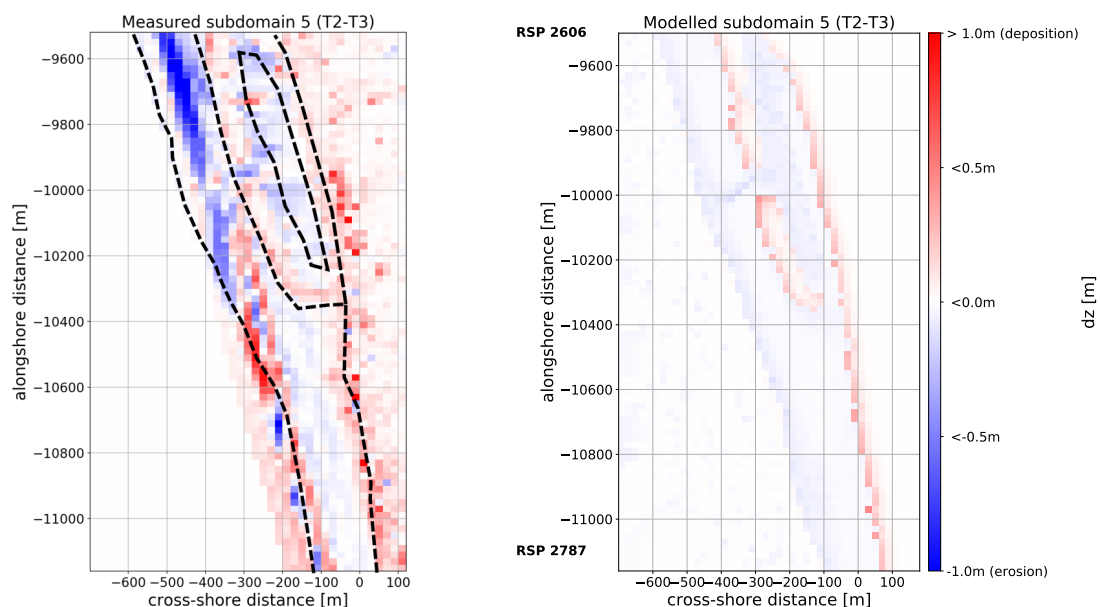
Figure 4.29: Measured and modelled sedimentation and erosion between May 2015 - Dec 2015 of subdomain 5 along the Southern shoulder of the HD system between RSP 26.06 and RSP 27.87. The black dashed lines in the measurement indicate the position of the intertidal zone (left) and the dune foot (right), Northern direction is upwards. Model results only include aeolian sediment transport and dune development as a result of measured climatic forcing and a constant influence of vegetation for this period.



(a) Measured sedimentation and erosion in T1-T2.

(b) Modelled sedimentation and erosion in T1-T2.

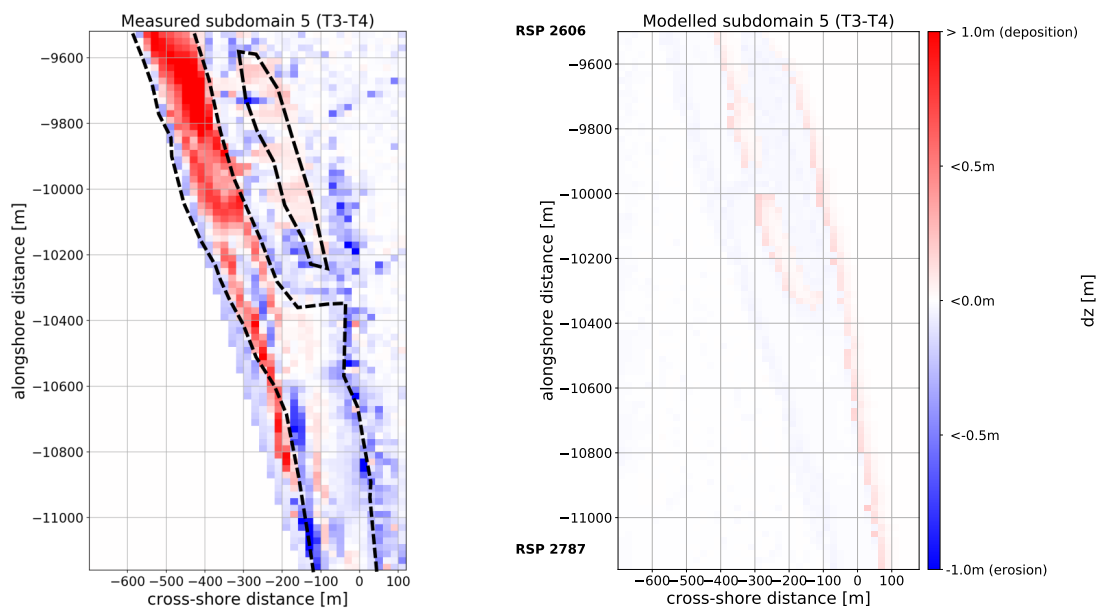
Figure 4.30: Measured and modelled sedimentation and erosion between Dec 2015 - March 2016 of subdomain 5 along the Southern shoulder of the HD system between RSP 26.06 and RSP 27.87. The black dashed lines in the measurement indicate the position of the intertidal zone (left) and the dune foot (right), Northern direction is upwards. Model results only include aeolian sediment transport and dune development as a result of measured climatic forcing and a constant influence of vegetation for this period.



(a) Measured sedimentation and erosion in T2-T3.

(b) Modelled sedimentation and erosion in T2-T3.

Figure 4.31: Measured and modelled sedimentation and erosion between March 2016 - September 2016 of subdomain 5 along the Southern shoulder of the HD system between RSP 26.06 and RSP 27.87. The black dashed lines in the measurement indicate the position of the intertidal zone (left) and the dune foot (right), Northern direction is upwards. Model results only include aeolian sediment transport and dune development as a result of measured climatic forcing and a constant influence of vegetation for this period.



(a) Measured sedimentation and erosion in T3-T4.

(b) Modelled sedimentation and erosion in T3-T4.

Figure 4.32: Measured and modelled sedimentation and erosion between September 2016 - December 2016 of subdomain 5 along the Southern shoulder of the HD system between RSP 26.06 and RSP 27.87. The black dashed lines in the measurement indicate the position of the intertidal zone (left) and the dune foot (right), Northern direction is upwards. Model results only include aeolian sediment transport and dune development as a result of measured climatic forcing and a constant influence of vegetation for this period.

Cumulative changes

An overview of the cumulative measured and modelled morphological development for each subdomain is given in Figure 4.33 till Figure 4.37. Reference is made to Figure 4.12 for the locations of the subdomains along the HD system. The model results do not accurately fit the measurements in the intertidal zone. This can be seen clearly in subdomain 1, 4 and 5 where deposition (red) in the intertidal zone is measured, but not predicted by the model. This could be explained by the fact that marine sediment transport is not imposed to the model in this research. The main location of the dune growth is correctly predicted by the model along the dune foot. However, the deposition is localized along the dune foot in the model whereas the measurements show spatial spreading in cross-shore direction at the dunes. In the Southern area of subdomain 1, between cross-shore coordinates $x = -400$ m and $x = -300$ m, shown in Figure 4.33a, dunes have been constructed. This explains the deviation between measured and modelled position of dune growth. In subdomain 5, the lagoon has a negative influence on sediment transport towards the dunes landwards of the dunes. This is not accurately predicted by the model, as seen in Figure 4.37.

Subdomain 1 with median grain size $D_{50} = 304 \mu\text{m}$

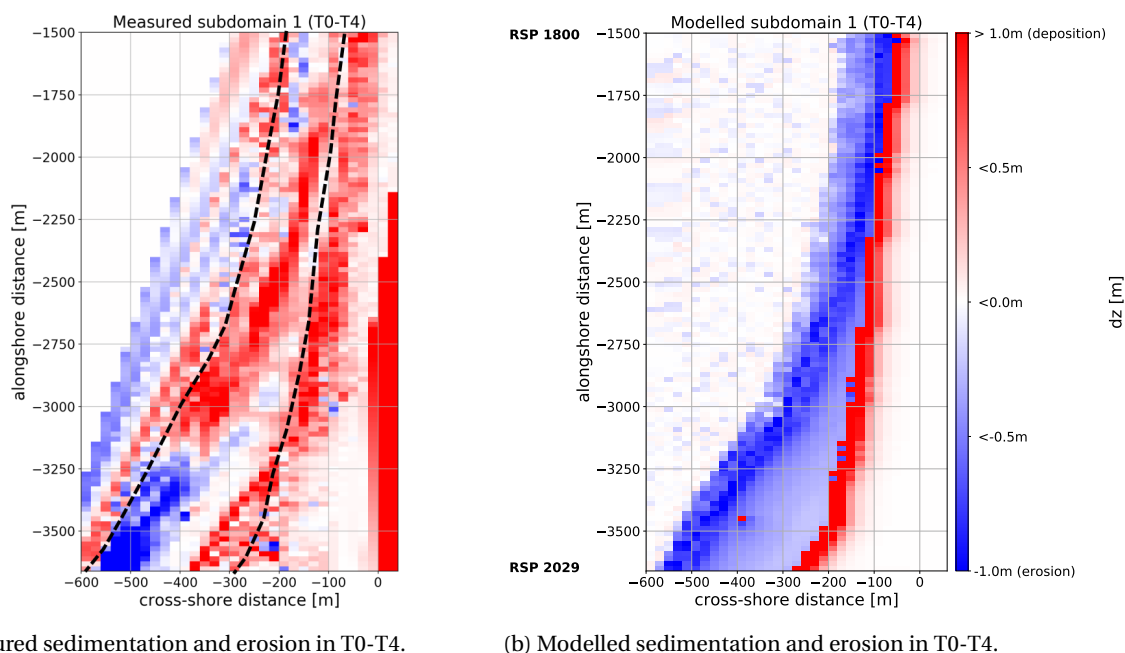
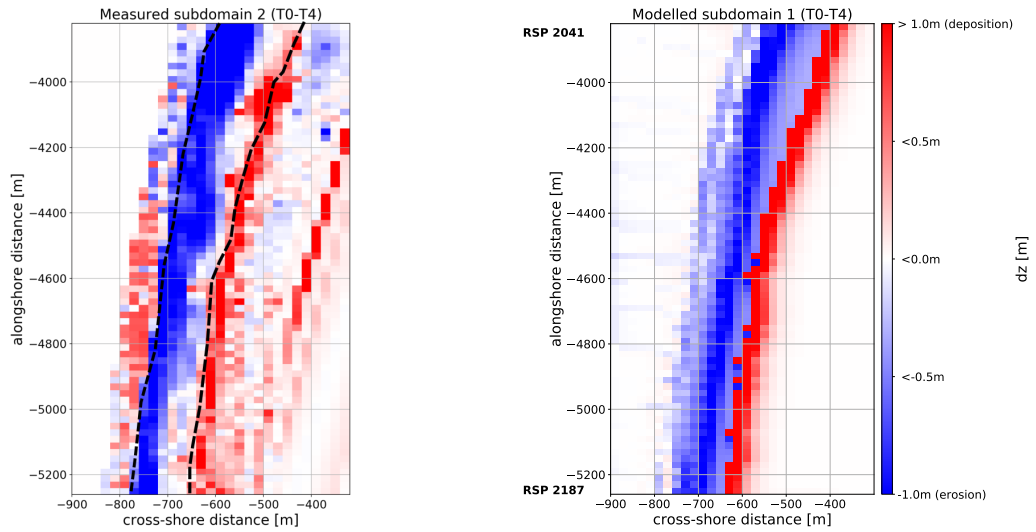


Figure 4.33: Measured and modelled sedimentation and erosion between May 2015 - Dec 2016 of subdomain 1 along the Northern shoulder of the HD system between RSP 18.00 and RSP 20.29. The black dashed lines in the measurement indicate the position of the intertidal zone (left) and the dune foot (right), Northern direction is upwards. Model results only include aeolian sediment transport and dune development as a result of measured climatic forcing and a constant influence of vegetation for this period.

Subdomain 2 with median grain size $D_{50} = 321 \mu\text{m}$

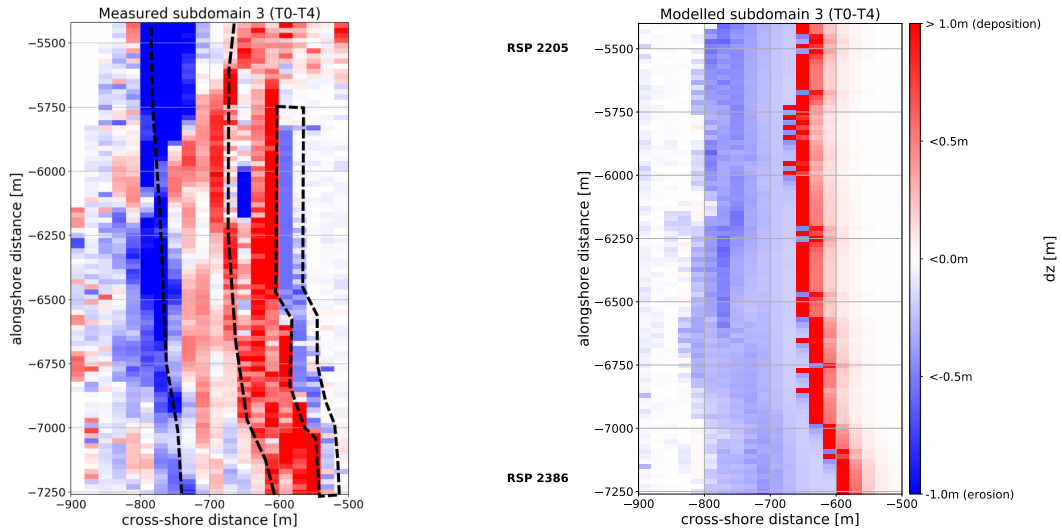


(a) Measured sedimentation and erosion in T0-T4.

(b) Modelled sedimentation and erosion in T0-T4.

Figure 4.34: Measured and modelled sedimentation and erosion between May 2015 - Dec 2016 of subdomain 2 along the Northern area of the HD system between RSP 20.41 and RSP 21.87. The black dashed lines in the measurement indicate the position of the intertidal zone (left) and the dune foot (right), Northern direction is upwards. Model results only include aeolian sediment transport and dune development as a result of measured climatic forcing and a constant influence of vegetation for this period.

Subdomain 3 with median grain size $D_{50} = 341 \mu\text{m}$

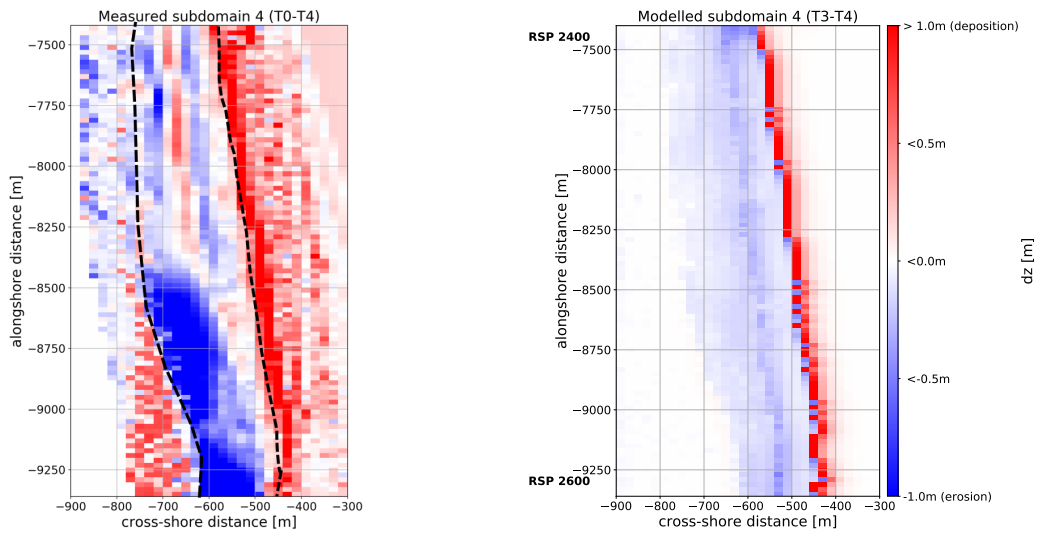


(a) Measured sedimentation and erosion in T0-T4.

(b) Modelled sedimentation and erosion in T0-T4.

Figure 4.35: Measured and modelled sedimentation and erosion between May 2015 - Dec 2016 of subdomain 3 along the middle area of the HD system between RSP 22.05 and RSP 23.86. The black dashed lines in the measurement indicate the position of the intertidal zone (left) and the dune foot (right), Northern direction is upwards. Model results only include aeolian sediment transport and dune development as a result of measured climatic forcing and a constant influence of vegetation for this period.

Subdomain 4 with median grain size $D_{50} = 224 \mu m$

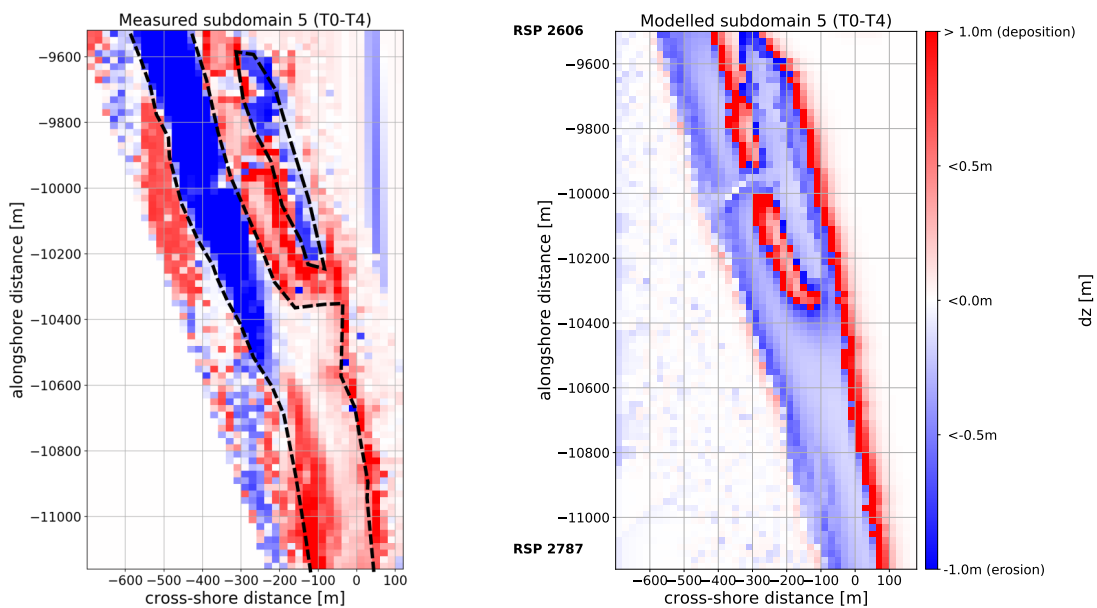


(a) Measured sedimentation and erosion in T0-T4.

(b) Modelled sedimentation and erosion in T0-T4.

Figure 4.36: Measured and modelled sedimentation and erosion between May 2015 - Dec 2016 of subdomain 4 along the Southern area of the HD system between RSP 24.00 and RSP 26.00. The black dashed lines in the measurement indicate the position of the intertidal zone (left) and the dune foot (right), Northern direction is upwards. Model results only include aeolian sediment transport and dune development as a result of measured climatic forcing and a constant influence of vegetation for this period.

Subdomain 5 with median grain size $D_{50} = 278 \mu m$



(a) Measured sedimentation and erosion in T0-T4.

(b) Modelled sedimentation and erosion in T0-T4.

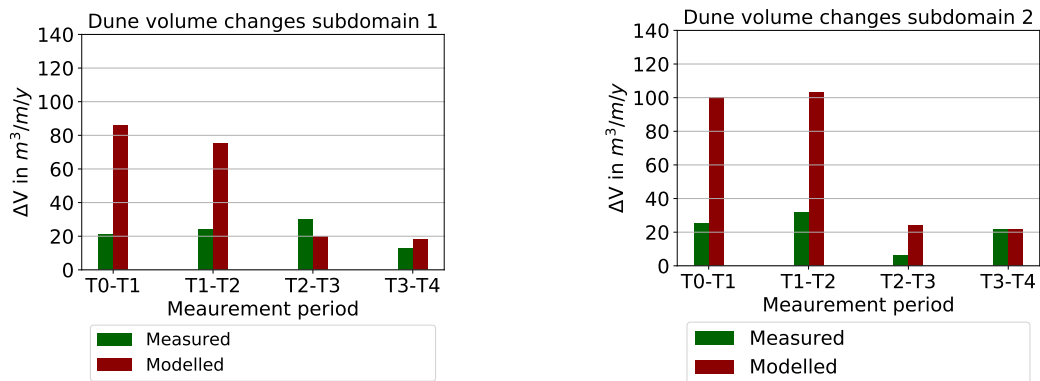
Figure 4.37: Measured and modelled sedimentation and erosion between May 2015 - Dec 2016 of subdomain 5 along the Southern shoulder of the HD system between RSP 26.06 and RSP 27.87. The black dashed lines in the measurement indicate the position of the intertidal zone (left) and the dune foot (right), Northern direction is upwards. Model results only include aeolian sediment transport and dune development as a result of measured climatic forcing and a constant influence of vegetation for this period.

4.2.2. Measured and Predicted Dune Volume Changes

This section presents the measured and modelled net dune volume changes for the HD system. The section is divided into five parts. The first part presents the periodic measured and modelled dune volume changes for each subdomain. The second part presents the cumulative measured and modelled dune volume changes for the period May 2015 - December 2016. The third part presents the comparison between the cumulative changes predicted by the model AeoliS for the five subdomains. The fourth part presents the comparison between the measured and modelled dune volume change for the five different profile types. The last part presents the comparison of the measured and modelled results to the prediction during the design phase and a theoretical prediction of the wind transport capacity. Reference is made to Chapter 3 for the methodology that is applied to obtain the results.

Periodic Volume Changes

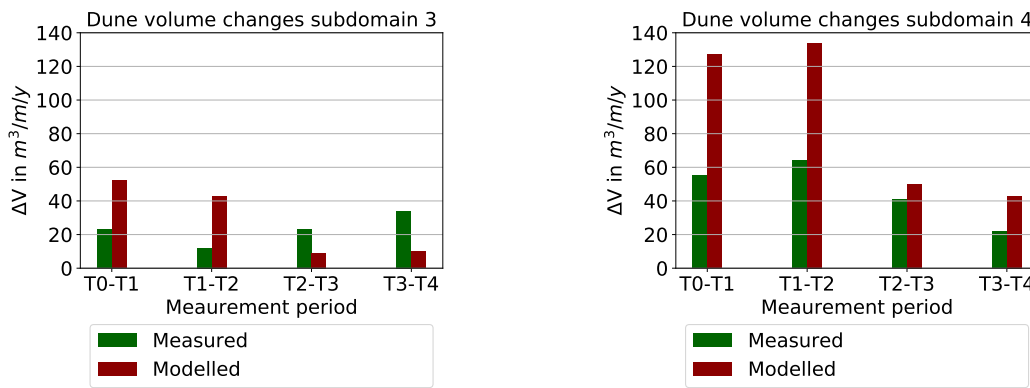
Figure 4.38 till Figure 4.40 present the periodic averaged measured and modelled dune volume changes for each of the five subdomains. Reference is made to Figure 4.12 for the locations of the subdomains along the HD system. The figures show that the model significantly overestimates the measurements in the first two periods May 2015 - December 2015 (T0-T1) and December 2015 - March 2016 (T1-T2) for each subdomain. The model overestimates and underestimates the measurements to a less extent for the last two periods March 2016 - September 2016 (T2-T3) and September 2016 - December 2016 (T3-T4). The model results mainly show a decrease in aeolian sediment transport in time. This could be explained by the fact that the measured wind conditions in the first two periods T0-T1 and T1-T2 show higher and more onshore directed winds compared to, respectively the last two periods T2-T3 and T3-T4. The periodic measured wind conditions are provided in Appendix D. Appendix J provides the alongshore spatial variation for each subdomain over the different measurement periods. The figures show that the model does predict alongshore variations in dune growth but to a less extent than the measurements. This can also be seen in the next paragraph, which discuss spatial variations over the full measurement period T0-T4.



(a) Periodic dune growth rates subdomain 1.

(b) Periodic dune growth rates subdomain 2.

Figure 4.38: Periodic measured and modelled dune growth rates between May 2015 - Dec 2016 for subdomain 1 along the Northern shoulder (left figure) and subdomain 2 along the Northern area (right figure) of the HD system. The left bar depict the measured average dune volume change as obtained from the LiDAR measurements. The right bar depicts the modelled averaged dune volume change as obtained from the AeoliS model.



(a) Periodic dune growth rates subdomain 3.

(b) Periodic dune growth rates subdomain 4.

Figure 4.39: Periodic measured and modelled dune growth rates between May 2015 - Dec 2016 for subdomain 3 along the middle stretch (left figure) and subdomain 4 along the Southern area (right figure) of the HD system. The left bar depict the measured average dune volume change as obtained from the LiDAR measurements. The right bar depicts the modelled averaged dune volume change as obtained from the AeoliS model.

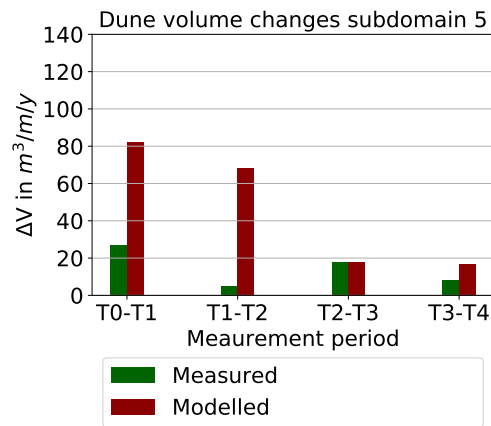


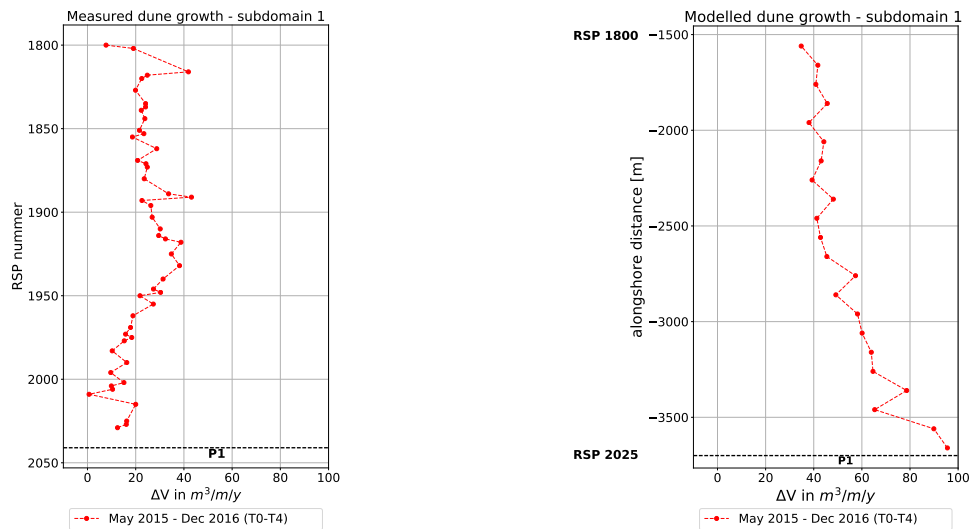
Figure 4.40: Periodic measured and modelled dune growth rates between May 2015 - Dec 2016 for subdomain 5 along the Southern shoulder of the HD system. The left bar depict the measured average dune volume change as obtained from the LiDAR measurements. The right bar depicts the modelled averaged dune volume change as obtained from the AeoliS model.

Cumulative net Volume Changes

Subdomain 1 with median grain size $D_{50} = 304 \mu m$ references

Subdomain 1 is located along the Northern shoulder of the HD system at Petten, Figure 4.12 shows the location for this domain along the HD system. Figure 4.33 presents the cumulative measured and modelled morphological development in the period May 2015 - December 2016 (T0-T4) which has been used to derive the net dune volume changes.

Figure 4.41 presents the cumulative measured and modelled dune volume changes between May 2015 - December 2016. The measurements present a large constant dune growth in the Northern area of the domain and a decreasing growth towards the South, whereas the model results show a relative constant dune growth in the Northern area which increases towards the Southern area of the subdomain. Larger dune growth in the North could be the effect of the constructed low dunes in the period May 2015 - December 2015 that are not considered as part of the dune area in the simulations, but as part of the beach system. A wider beach increase the sediment availability for aeolian sediment transport in the model, see Chapter 3 for method considerations. The average dune growth is $23 m^3/m^3/y$ according to the measurements and $54 m^3/m^3/y$ according to the model.



(a) Cumulative measured dune growth rates in T0-T4.

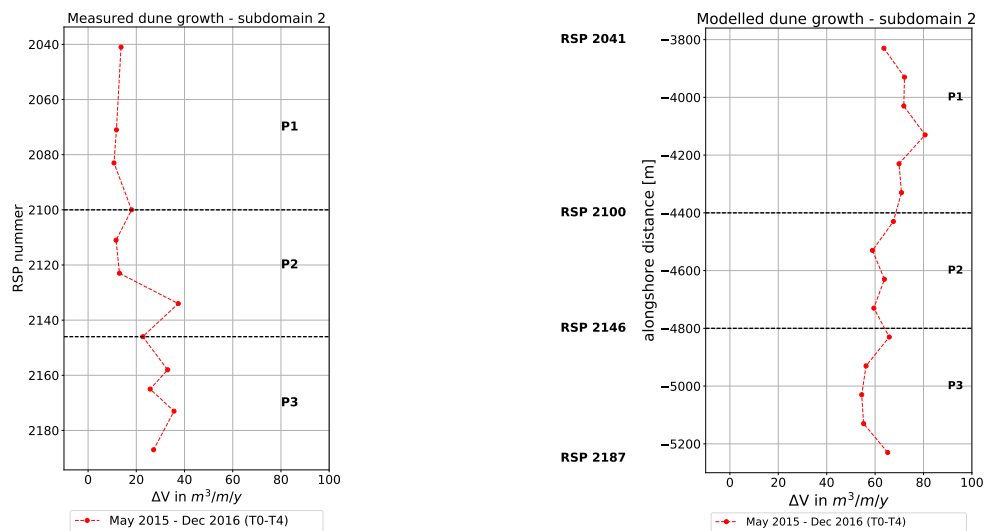
(b) Cumulative modelled dune growth rates in T0-T4.

Figure 4.41: Cumulative measured and modelled dune growth rates between May 2015 - Dec 2016 of subdomain 1 along the Northern shoulder of the HD system between RSP 18.00 and RSP 20.25. Note that the figures have the same orientation as the Dutch coastline: North is upwards and the South is downwards. The dashed horizontal black lines indicates the locations of the five different dune profiles P1-P5. Furthermore, the vertical labels differ and therefore the reference locations are given in RSP coordinates at the left side of the y-axis in the model results (right figure).

Subdomain 2 with median grain size $D_{50} = 321 \mu\text{m}$

Subdomain 2 is located along the Northern straight section of the HD system, Figure 4.12 shows the location for this domain along the HD system. Figure 4.34 presents the cumulative measured and modelled morphological development in the period May 2015 - December 2016 (T0-T4) which has been used to derive the net dune volume changes.

Figure 4.42 presents the cumulative measured and modelled dune volume changes between May 2015 - December 2016. The measurements present a small constant dune growth in the Northern area of the subdomain, indicated by the upper horizontal dashed line at RSP 21.00, and dune growth increases towards the Southern area of the subdomain, indicated by the lower black dashed line at RSP 21.46. The model results show the opposite behaviour with a relative larger dune growth in the Northern area than in the middle and Southern area of the subdomain. Larger dune growth in the North could be the effect of an initially larger beach at T0 and therefore a larger sediment availability for aeolian sediment transport in the model, see also Figure 4.7 in which the green line shows the initial beach width. The average dune growth is $22 \text{ m}^3/\text{y}$ according to the measurements and $65 \text{ m}^3/\text{y}$ according to the model.



(a) Cumulative measured dune growth rates in T0-T4.

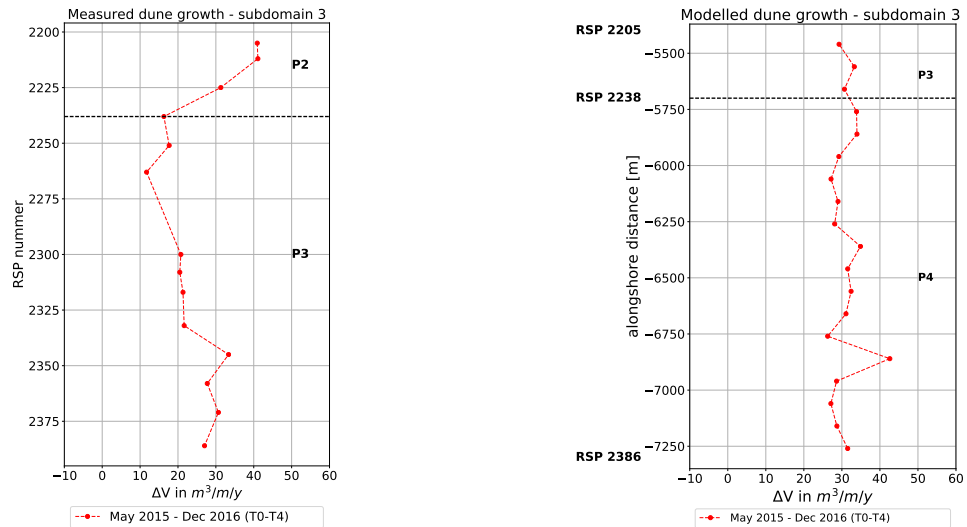
(b) Cumulative modelled dune growth rates in T0-T4.

Figure 4.42: Cumulative measured and modelled dune growth rates between May 2015 - Dec 2016 of subdomain 3 along the Northern area of the HD system between RSP 20.41 and RSP 21.87. Note that the figures have the same orientation as the Dutch coastline: North is upwards and the South is downwards. The dashed horizontal black lines indicates the locations of the five different dune profiles P1-P5. Furthermore, the vertical labels differ and therefore, the reference locations are given in RSP coordinates at the left side of the y-axis in the model results (right figure).

Subdomain 3 with median grain size $D_{50} = 341 \mu\text{m}$

Subdomain 3 is located along the straight section of the HD system, Figure 4.12 shows the location for this domain along the HD system. Figure 4.35 presents the cumulative measured and modelled morphological development in the period May 2015 - December 2016 (T0-T4) which has been used to derive the net dune volume changes.

Figure 4.43 presents the cumulative measured and modelled dune volume changes between May 2015 - December 2016. The model predicts a relatively constant dune growth rate along the entire domain. This prediction fits the measurements more in the Southern part of the domain than around RSP 22.38 (black dashed line). The average dune growth is $25 \text{ m}^3/\text{m}^3/\text{y}$ according to the measurements and $31 \text{ m}^3/\text{m}^3/\text{y}$ according to the model. It should not be forgotten that the capacity of the dune valley to capture sediments is not included in the model, see Chapter 3 for method considerations, which could increase the prediction quality of the model. Furthermore, beach width is relatively constant along this subdomain which reduces substantial changes in sediment availability of the system, see also Figure 4.7 in which the temporal variations in beach width are shown.



(a) Cumulative measured dune growth rates in T0-T4.

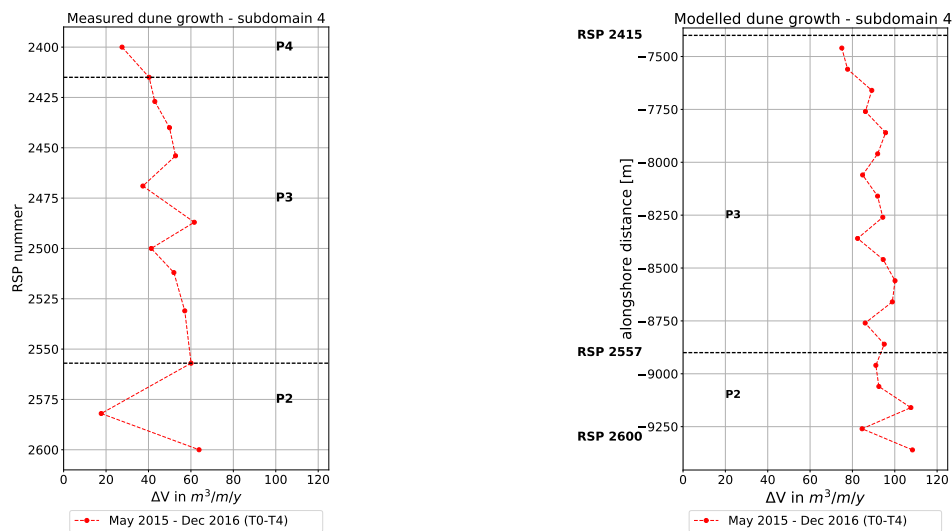
(b) Cumulative modelled dune growth rates in T0-T4.

Figure 4.43: Cumulative measured and modelled dune growth rates between May 2015 - Dec 2016 of subdomain 2 along the middle area of the HD system between RSP 22.05 and RSP 23.86. , Northern direction is upwards. Note that the figures have the same orientation as the Dutch coastline: North is upwards and the South is downwards. The dashed horizontal black lines indicates the locations of the five different dune profiles P1-P5. Furthermore, the vertical labels differ and therefore the reference locations are given in RSP coordinates at the left side of the y-axis in the model results (right figure).

Subdomain 4 with median grain size $D_{50} = 224 \mu m$

Subdomain 4 is located along the Southern straight section of the HD system, Figure 4.12 shows the location for this domain along the HD system. Figure 4.36 presents the cumulative measured and modelled morphological development in the period May 2015 - December 2016 (T0-T4) which has been used to derive the net dune volume changes.

Figure 4.44 presents the cumulative measured and modelled dune volume changes between May 2015 - December 2016. Both the measurements and the models results show an alongshore variation in dune growth as a result of alongshore variations in beach width at T0, see Figure 4.7 in which the green line shows the initial beach width. This influence the spatial variations in sediment availability for aeolian sediment transport. The average dune growth is $46 \text{ m}^3/\text{y}$ according to the measurements and $91 \text{ m}^3/\text{y}$ according to the model.



(a) Cumulative measured dune growth rates in T0-T4.

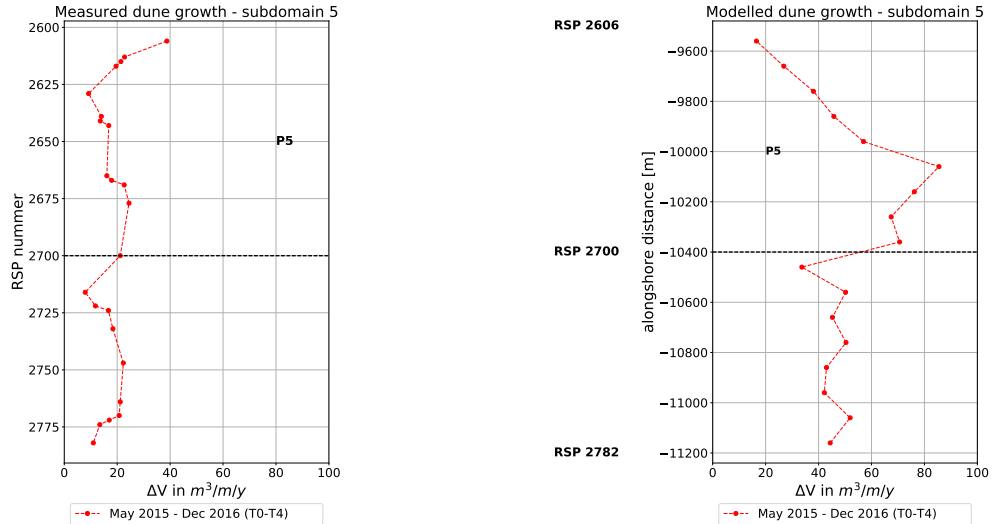
(b) Cumulative modelled dune growth rates in T0-T4.

Figure 4.44: Cumulative measured and modelled dune growth rates between May 2015 - Dec 2016 of subdomain 4 along the Southern area of the HD system. Note that the figures have the same orientation as the Dutch coastline: North is upwards and the South is downwards. The dashed horizontal black lines indicates the locations of the five different dune profiles P1-P5. Furthermore, the vertical labels differs, Furthermore, the vertical labels differ and therefore the reference locations are given in RSP coordinates at the left side of the y-axis in the model results (right figure).

Subdomain 5 with median grain size $D_{50} = 278 \mu\text{m}$

Subdomain 5 is located along the Southern shoulder of the HD system at Camperduin, Figure 4.12 shows the location for this domain along the HD system. Figure 4.37 presents the cumulative measured and modelled morphological development in the period May 2015 - December 2016 (T0-T4) which has been used to derive the net dune volume changes.

Figure 4.45 presents the cumulative measured and modelled dune volume changes between May 2015 - December 2016. The measurements show a relatively constant dune growth along the entire subdomain, whereas the model results show an increase in dune growth from the North towards the middle part of the subdomain and a constant dune growth along the Southern part of the domain. The large dune growth in the middle part of the domain might be the effect of dune growth at the landward side of the lagoon. This is not a dune area of interest yet, due to the large sediment volume that resides at the lagoon and beach. Hence, no analysis has been derived based on the LiDAR measurements, see Chapter 3 for method considerations. The average dune growth is $18 \text{ m}^3/\text{y}$ according to the measurements and $50 \text{ m}^3/\text{y}$ according to the model.



(a) Cumulative measured dune growth rates in T0-T4.

(b) Cumulative modelled dune growth rates in T0-T4.

Figure 4.45: Cumulative measured and modelled dune growth rates between May 2015 - Dec 2016 of subdomain 5 along the Southern shoulder of the HD system. Note that the figures have the same orientation as the Dutch coastline which means that the North is at the upper part of the figure and the South at the lower part of the figure. The dashed horizontal black lines indicates the locations of the five different dune profiles P1-P5. Furthermore, the vertical labels differ and therefore the reference locations are given in RSP coordinates at the left side of the y-axis in the model results (right figure).

Comparison of Subdomains

Figure 4.46 shows the comparison of the cumulative measured and modelled dune volume changes for the five subdomains. The figure shows that the model overestimates the measurements for each subdomain. The overestimation varies between each subdomain: the difference is with a factor 1.2 lowest for subdomain 3 ($D_{50} = 341 \mu\text{m}$), and with a factor 3 highest for subdomain 2 ($D_{50} = 321 \mu\text{m}$), see also Table 4.9. For subdomain 1 ($D_{50} = 304 \mu\text{m}$) an overestimation of a factor 2.3 is found. The model results present for subdomain 4 ($D_{50} = 224 \mu\text{m}$) an overestimation with a factor 2. Lastly, for subdomain 5 ($D_{50} = 278 \mu\text{m}$) an overestimation with a factor 2.8 is found. A distinct relation between the median grain size and the quantity of overestimation of the model does not exist. The results show that subdomain 2 is most sensitive to the assumptions that are made for the simulations, as seen by the highest overestimation of the measurements, see also section 5.2.2. Besides, modelled dune growth rates are higher for subdomain 2 than for subdomain 1 and subdomain 5 in the South while the imposed median grain size is higher for subdomain 2 than subdomain 1 and 5.

Table 4.9: Overview of the measured and modelled dune growth in the left and middle column. The right column shows the overestimation by the model.

Subdomain	Average dune growth Measurements	Average dune growth Model	Overestimation by Model
1	23	54	2.3
2	22	65	3
3	25	31	1.2
4	46	91	2
5	18	50	2.8

Comparison of Dune Profile Types

Figure 4.47 shows the comparison of the cumulative dune volume changes for the five profile types based on the measurements and the model results for the five different subdomains. Subdomain 1 does not show any results since no profile types are represented in this subdomain. Subdomain 2 represents three different profile types: profile type 1, 2 and 3. The model results show the largest overestimation for profile type 1 with a factor 5.5 and the smallest overestimation for profile type 3 with a factor 2.6. The volume change of profile type 2 is overestimated by the model with a factor 3.1. Subdomain 3 represents two different profile types: profile 3 and 4 along the dune valley. The model results show an equivalent overestimation of dune growth for

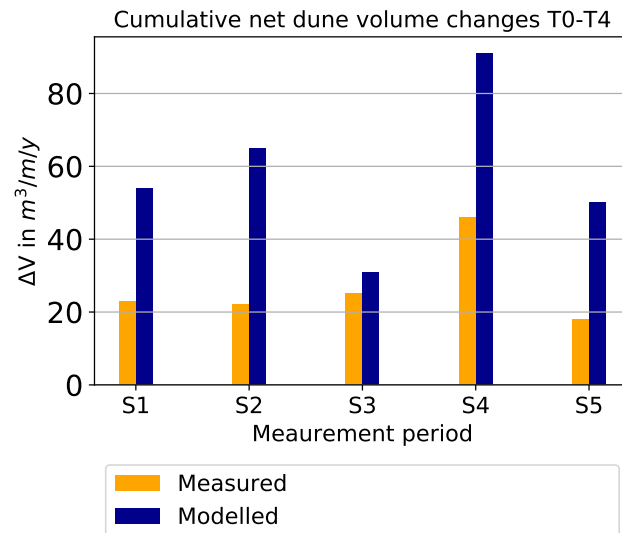
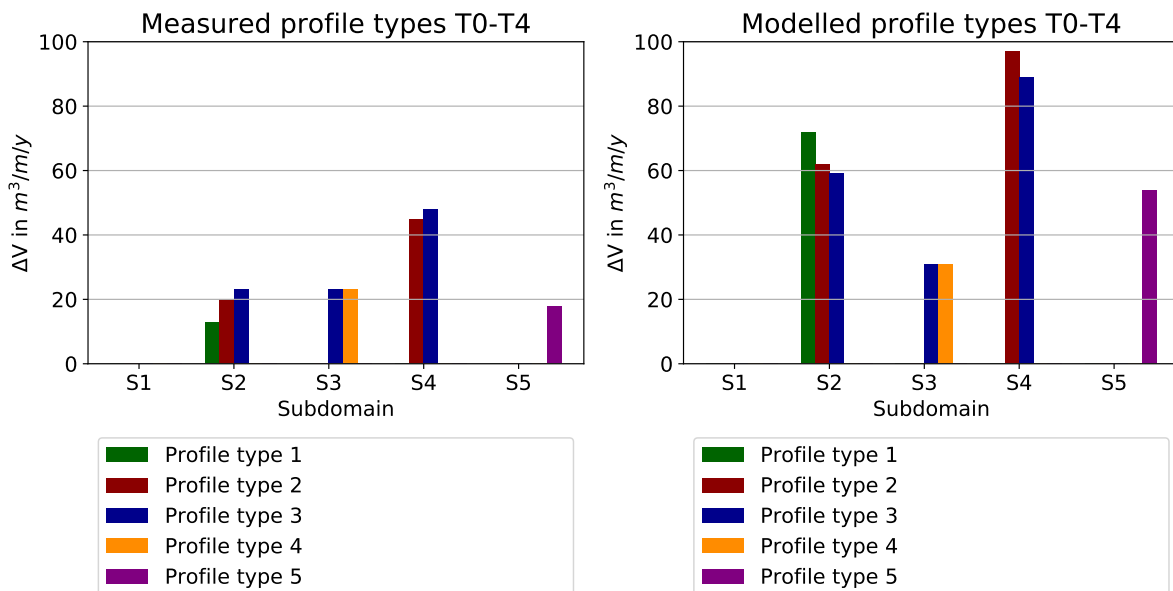


Figure 4.46: Comparison of cumulative dune volume changes for the five subdomains S1-S5. Subdomain 1 is in the North of the HD system and Subdomain 5 is located in the South of the HD system. The left bar depicts the measured dune volume changes derived from LiDAR measurements and the right bar depicts the modelled dune volume changes predicted by the AeoliS model. The overestimation is highest for subdomain 2 with a median grain size of $D_{50} = 321 \mu\text{m}$ and lowest for subdomain 3 with a median grain size of $D_{50} = 341 \mu\text{m}$.

both profile types with a factor 1.4. Subdomain 4 represents two different profile types: profile 2 and profile 3. The model results show a larger overestimation with a factor 2.2 for profile type 2 than for profile type 3, which shows an overestimation of a factor 1.9. Subdomain 5 presents only profile type 5 along the lagoon. The model results show an overestimation of the measurements with a factor 3. By comparing subdomain 2 and subdomain 4, a larger overestimation by the model is found for profile type 2 and 3 in subdomain 2 than in subdomain 4. The comparison between measurement and model result shows that profile type 1 and 5 are most sensitive to the assumptions that are made for the model simulations, as seen in the highest overestimation by the model.



(a) Average measured dune growth per dune profile.

(b) Average modelled dune growth per dune profile.

Figure 4.47: Average measured and modelled dune growth per profile type 1-5 for the five subdomains S1-S5. The five different colours each indicate a different profile types. Note that certain dune profiles only exist in certain subdomains.

Comparison of Methods for Quantification of Dune Volume Changes

Figure 4.48 shows the comparison of the cumulative dune volume changes obtained from four distinguished methods:

1. Measurements derived from LiDAR.
2. Model results predicted by supply limited model AeoliS.
3. Design calculation based on empirical knowledge obtained from previous research and reference projects.
4. Theoretical description (Bagnold's formula) for the capacity of the wind to transport sediments under absence of supply limited processes.

The design calculations and the theoretical description are constant along the entire HD system with a dune volume change of $35 \text{ m}^3/\text{y}$ and respectively, $216 \text{ m}^3/\text{y}$. Neglecting sediment supply limiters results in a large overestimation of the measurements; the theoretical model shows an overestimation of the measurement by a factor 4.7 for subdomain 4 till a factor 12 for subdomain 5. The model results are also largely overestimated by the theoretical model with a factor 2.4 for subdomain 4 till a factor 7 for subdomain 3. The design calculation ($35 \text{ m}^3/\text{y}$) is on average equivalent to the measurements ($28 \text{ m}^3/\text{y}$): the design prediction shows an overestimation of subdomain 1, 2, 3 and underestimation of subdomain 4.

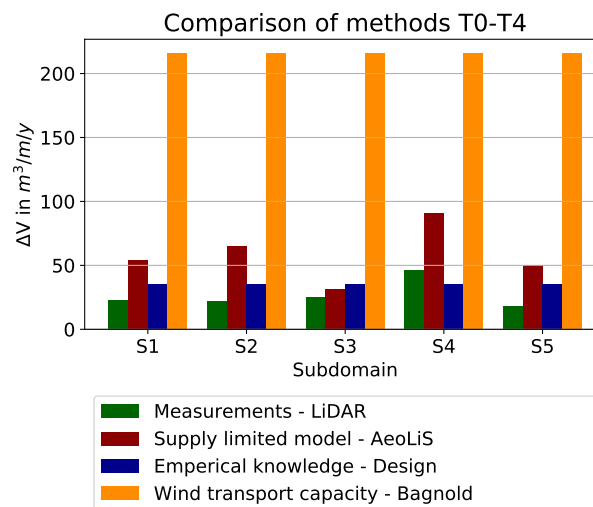


Figure 4.48: Comparison of methods for quantification of dune volume changes. The two most left bars depict the measured and modelled dune volume changes as obtained from LiDAR measurements and the supply limited model AeoliS. The third bar depicts the expectation of dune growth according the design based on empirical knowledge. The most right bar depicts the theoretical prediction of the wind driven transport capacity according to Bagnold's formula in which a constant uniform median grain size of $D_{50} = 290 \mu\text{m}$ is applied.

5

Discussion

In this research the nature of aeolian sediment transport on beach and dune development is explored at the man-made Hondsbossche Dunes. Here, the assumptions and the found results are critically discussed. First, the morphological development of the dunes is discussed. Second, the importance of marine sediment supply on the beach and dune development. Last, the assumptions that are made to hindcast the dune development are discussed.

5.1. Spatio-Temporal Variations in Dune Growth

The aim of this research was to study the morphological development of the Hondsbossche Dunes. The results give insight into the volume changes of the different dune profile types. Dune growth rates show temporal and alongshore variation and varies within the different profile types, an increase is found within the nineteen months after construction. The results of the morphological analysis are first discussed, and the assumptions underlying the derivations are explained in the second part of this section.

5.1.1. Results of Dune Development

The average dune growth is $28 \text{ m}^3/\text{y}$ for the HD system and $23 \text{ m}^3/\text{y}$ for the full project domain in the first nineteen months. This magnitude corresponds with the values reported by Van der Wal [van der Wal, 2004] $14 \text{ m}^3/\text{y}$ for nourished beaches, De Vries [de Vries et al., 2012] $0\text{-}40 \text{ m}^3/\text{y}$ at the Dutch coast, and De Schipper [de Schipper et al., 2016] $15 \text{ m}^3/\text{y}$ at the Sand Engine in the first eighteen months. Aeolian sediment transport has strongly decreased in time at the Sand Engine due to a reduction in aeolian sediment supply which is likely due to the development of a beach armour layer [Hoonhout, 2017].

Spatio-temporal variability in sediment availability

The spatio-temporal variability in dune volume changes is best explained by the temporal and alongshore variation in sediment availability at the beach. The average dune growth rate is with $25 \text{ m}^3/\text{y}$ along the full project domain, which is considered to be high within the first period after construction (May 2015 - December 2015). The large dune growth rate in the first period could be explained by the high content of fine grains of the nourished sand. The finer grains can be easily transported towards the dunes resulting in a fast development of the dunes. Due to sorting processes the dune growth decreases in time, unless new sediments are available for aeolian transport. The latter process is observed between the third and fourth survey (March 2016 - September 2016). In this period an average increase in beach volume of $28 \text{ m}^3/\text{y}$ was observed along the project domain. This increase in beach volume was pronounced along the Northern Dunes and profile type 1 and 2 (North) of the HD system, but is also found at profile type 3 (South). Locally, an increase in beach width was also measured along the Northern dunes and profile type 1. This increase in sediment availability could explain to some degree the high dune growth rate, respectively $26 \text{ m}^3/\text{y}$, measured along the Northern dunes and parts of the HD system for profile type 4 and 3 (South) in the period March 2016 - September 2016.

The dune growth along the Northern dunes seems to be under influence of the construction of the HD system. The volume analysis shows that the beach volume started to increase between the second and third

survey (March 2016 - September 2016). Erosion of the beach along the HD system in the first period after construction might have increased the marine sediment transport towards the Northern located beaches. Therefore, the sediment availability for dune growth has increased. To detect this process an comparison of the dune growth rates in the Northern dunes and the annual surveys of the coastal stretch adjacent to the Northern project domain (Northwards of RSP 17.08). The derivation shows a two times smaller dune growth rate along the coastal stretch Northwards of the project domain. This indicates indeed that dune growth along the Northern Dunes is under influence of the HD system. The derivation of the dune volume changes can be found in Appendix H.

The spatial variability in dune growth can be explained to some extent by the variability in median grain size at the beach. Looking at the differences in dune growth between profile type 2 and 3 (North) and profile type 2 and 3 (South), it can be seen that higher dune growth rates were derived for dune profile type 2 and 3 in the South where also the finer grains were observed.

Spatial variability in dune geometry

The relation between the sediment availability parameters (beach volume, beach width, and beach slope) suggests there is a potential dune growth associated with the quantities of the sediment availability parameters. However, the derived dune volume analysis shows that the potential dune growth is not always reached. This could be related to spatial differences in dune geometry or other processes that dominates the aeolian sediment supply towards the dunes. The influence of: (1) dune geometry, (2) vegetation, and (3) alongshore location with respect to the wind, are discussed here.

The presented results show indeed that there is a appreciable different response in dune growth for the five distinguished dune profile types. There is a considerably positive effect of a lower foredune and a relatively mild slope on dune growth. In this research it is observed that dune growth rates are considerable larger for profile type 3. The gradually increase in height stimulates the potential sediment transport of the finer grains into suspension to higher parts of the dunes.

The absence of a dense vegetation cover control to some degree the spatial variations in dune growth rates. Visual observations proved that the dune vegetation is denser along the Southern part of the HD system compared to the Northern part of the HD system. Vegetation reduces the wind flow, capture the sediments and reduces erosion of the surface below and around the vegetation [Wolfe and Nickling, 1993]. The difference in vegetation cover between North and South could be explained to the fact that the construction of the new HD system started in the South and was finished after one year in the North.

The alongshore location of the profile type with respect to the dominant wind direction also influence the dune growth. The measured wind conditions are predominantly coming from the southwest. The results show indeed a larger dune growth for profile type 2 and 3 along the Southern shoulder compared to the Northern shoulder. During south-west winds sediment is eroded from the downwind located beach and transported towards the dunes. The vegetation near the dune foot decelerates the wind flow and blocks further transport unless the induced flow conditions stimulates uphill transport of the fine sediments to the higher parts of the dunes. The coarser sediment will deposit along the dune foot. Just northwards of the HD system, between RSP 19.83 and RSP 20.25, a small dune growth is found compared to the adjacent stretches. The section is located in the shadow zone of the new developed dunes and thus the transport of sediments towards these dunes is blocked. See Figure 5.1 for a schematization of this situation. The dunes located northward of this stretch at RSP 19.83 the dunes are also positively located with respect to the dominant wind direction and downwind availability of sediments due to wide beaches. It must be realised that the small observed dune growth could be explained in some degree by the methodology chosen. Low dunes were constructed between May 2015 and December 2015, see Figure E.2 in Appendix C. The low dunes set a limit to the sediment transport towards the natural dunes, due to their height and the marram grass which captures and reduces the erosion of sediments in between the vegetation.

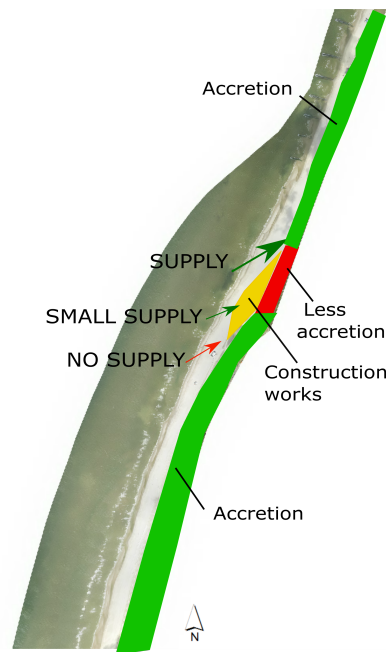


Figure 5.1: Schematization of the dune growth along the northern shoulder between RSP 19.83 and RSP 20.35. The red arrow indicates that there is less sediment supply toward the red coloured area compared to adjacent stretches. Supply is also limited due to the constructed smaller dunes in front of the natural dunes.

5.1.2. Interpretation of the Assumptions

The impact of the two main assumptions on the results found are discussed here.

Representation by cross-shore transects

Dune volume changes were derived at 138 cross-shore transects of the Dutch JARKUS dataset (yearly coast measurements). The derived morphological changes represents a larger domain in alongshore direction in which major local changes within adjacent cross-shore transects are cancelled out by this approach. However, the overall pattern of dune volume changes fits well to the observations reported by [Verheijen, 2017]. Verheijen used a more dense and equidistant cross-shore transects, resulting in area-averaged dune volume changes. The results show an equal pattern of volume changes for the the five different profile types. Profile type 1 shows a locally decrease in dune volume, which was the only exception. It appears that the JARKUS-transects have a lower resolution along this profile type and therefore did not capture local features in development here.

Subsidence of the subsoil

The influence of subsidence of the sand on dune volume analysis is not considered in this research. It is thought that larger dune growth rates would be seen if this influence was taken into account. Subsidence is a time-based process in which a volumetric cubic of sand decrease in time, resulting in more densely packed sand. The collected LiDAR surveys only give insight into momentary volumetric results and does not consider the effect of subsidence within successive surveys. Additional analysis into this process is done by executing measurements at several project locations before construction [de Jongh, 2017]. An average subsidence of 0.1 m was measured [Leenders et al., 2016]. This has resulted into a total subsidence of the sand estimated at 200.000 m³/y of which 150.000 m³/y takes place in the dunes. The increase in dune growth would be 22 m³/y along the HD system if subsidence is included in the analysis. This would result in a total dune growth of 45 m³/y, a factor 2 higher than the average dune growth of 28 m³/y derived for the HD system in this research. However, it would be likely that there is a rather alongshore variation in subsidence. This depends on the local conditions, like the drying rates and the sediment characteristics of the sand.

5.1.3. Importance of Marine Sediment Supply

Although the focus of this research is on aeolian sediment transport, the influence of marine processes on the aeolian sediment availability cannot be neglected. The dry beach zone shows a similar pattern of morphological development compared to the intertidal zone and the surf zone: volumetric losses and deposition Northwards and Southwards of the HD system. The marine sediment supply is simplified and derived from eleven cross-shore transects along the curved coastline. The bathymetry between the surveyed transects is not available, which limits the analysis of the relation between marine sediment supply and aeolian sediment availability on a local scale. This influences the alongshore variation in aeolian sediment availability and the dune growth.

The volumetric losses in the cross-shore profile of the beach, intertidal zone, and the surf zone are derived to have an average of $139 \text{ m}^3/\text{y}$. High volumetric losses in the first year after construction (April 2015 - April 2016) were predominantly determined by: (1) the initial adaptation to the climatic forcing and (2) event driven sediment transport due to more and higher south-western waves in this period compared to the average in long term. The latter effect has led to a net transport potential which was 2.5 times larger than the long term yearly average [?]. The volumetric losses decrease in time: the first half of the second year (April 2016-September 2016) show smaller losses compared to the same period in the first year ¹. The majority of the volumetric losses were transported in alongshore direction towards the Northern and Southern stretches of the project domain leading to accretion of the beaches. The volumetric losses can also be attributed to aeolian sediment transport in cross-shore direction. On average 20 percent ($28 \text{ m}^3/\text{y}$) of the cross-shore volumetric losses can be attributed to aeolian sediment transport towards the dunes. However, it should be noted that alongshore variation in marine sediment supply determine the actual dune growth. The magnitude corresponds with the value reported by Schippers [de Schipper et al., 2016] of 20 percent compensation of losses in the survey domain due to aeolian sediment transport at the Sand Engine. It should be noted that the coastal system at the Sand Engine differs in terms of the morphological development since it is under influence of the port of Rotterdam.

In particular for dune profile type 5 along the Southern shoulder, marine processes are strongly dominating the morphological development of the beach. The marine forcing reduces the beach width and steepens the beach slope, which disables to accommodate aeolian sediment transport towards the dunes. This can be seen by a lower dune growth rate for profile type 5 compared to the adjacent profile type 3 (South). However, marine forcing might also positively contribute to the accommodation of aeolian sediment transport by a constant hydraulic mixing of the top layer of the bed which increases the availability of fine grains and therefore the potential dune growth.

5.2. Modelling Dune Growth

The aim of the hindcast was to simulate the large-scale morphological development of the HD system and to predict the dune growth. The results show that the overall observed erosion and deposition patterns are accurate reproduced by the supply limited model. Adding to this, the model results show an overestimation of the measured dune growth rates. The overestimation with respect to the measurements is a factor 1.2 - 3 varying between the five different modelled subdomains. The model assumptions made and the negligence of system characteristics and climatic forcing, explains the discrepancy between measurements and the model results regarding erosion and deposition patterns and dune growth rates. The main assumptions are distinguished between: (1) the model schematization and (2) the interpretation of the results.

5.2.1. Model Schematization

Division of the project domain

In order to simulate the effect of alongshore variation in grain size on the aeolian sediment transport, the domain is divided into five subdomains. The influence of sediment exchange between adjacent sub-domains under varying wind conditions is thus neglected. However, the model can reproduce the large-scale erosion and deposition patterns and show alongshore variations in dune growth rates under influence of varying grain sizes. Thus, the division in the project domain influences the results to a minimal extent.

¹Email conversation with A. Kroon, Phd-candidate TU Delft, date May 17th, 2017.

Effect of vegetation

The dune area is not included in the model domain, instead the shear threshold velocity is increased landward of the location of the dune foot by fifty % to impose the effect of vegetation on deposition in the dunes. The assumption is compared to the research of Keijsers [Keijsers, 2015] in which no strong correlation between vegetation density and deposition was calculated. Although high values of sedimentation are most common for a vegetation cover between 20 and 80 %. The shear threshold velocity is assumed to be constant over time and alongshore. This simulates the transport-limiting effect of vegetation in a simplified manner; alongshore variations and density are not considered. However, the results proved that the model is able to properly simulate the location of main deposition along the dune foot and show alongshore variations in dune growth under constant influence of vegetation.

Synchronisation of the climatic time series

The influence of the climatic forcing on the system is modelled by imposing real times series of wind, wave and tidal conditions. The wind data is available for the total measurement period (562 days) between May 2015 and December 2016, however the time series of the tidal elevations and the wave heights have some gaps in the time series. The model compresses therefore the time series of tidal elevations and wave heights resulting in a shorter period. In order to derive a time series of 562 days for those, the model adds the missing days by repeating the measured data starting at the beginning of the time series. The wind time series defines the extent of the aeolian sediment transport, whereas the tidal elevations and wave heights influence the aeolian sediment availability in the intertidal zone. Since calm climatic conditions were observed during the measurement period, the effect of the missing data of time series of tidal and wave is not significant in this research. If large storm event would occur, then the absence of data are certainly of relevance for the model results.

5.2.2. Model Results

Subsidence of the subsoil

The influence of subsidence of the sand on dune volume analysis is not considered, resulting in higher dune growth rates, expected up to factor 2, see subsection 1.1.2. The inclusion of this process could improve the performance of the model with respect to the measurements. In particular in the first period (May 2015 - December 2016) after construction, where the model overestimation is higher compared to the successive periods.

Precipitation

No precipitation has imposed to the model which could explain the discrepancy between the temporal or seasonal variations in measured and modelled dune growth rates. Additionally, high water levels increases the moisture content of the beach surface and therefore decreases the sediment availability for aeolian transport. The model results largely overestimates the first and second period of measurements compared to the third and fourth period. This is due to that the wind speeds are higher and the wind direction is more onshore, see Figure D.2a till Figure D.3b in Appendix D which shows the wind climate for each measurement period. A higher wind speed increases the capacity of the wind to transport sediment towards the dunes. Simultaneously, the occurrence of more wet periods highly influences the pick-up of sediments and, therefore, reducing the actual transport of sediments towards the dunes. Weather data obtained from the KNMI weather station 'De Kooy' at Den Helder shows that the combination of (1) onshore wind with speeds higher than 5 m/s and (2) precipitation, results in a frequency of occurrence of 13 percent of the time in the period between May 2015 and December 2016. The weather data shows availability of sediments is limited at certain moments due to the precipitation. Subdomains with a relative large beach surface, for example subdomain 2, are more sensitive to the negligence of moisture content in the simulation of the model. A large beach surface increases the aeolian sediment availability and thus the deposition in the dunes.

Figure 5.2 depicts part of the HD system where a wet area is located in front of the dunes. The wet area reduces the aeolian sediment transport towards the dunes for two reasons: (1) the high moisture content of this part reduces the sediment availability and (2) aeolian transport in onshore direction is trapped by the wet surface. This effect was most present in the first period after construction and could therefore partly the large overestimation in this period.



Figure 5.2: The beach at the Hondsbossche Dunes in September 2016. The dunes are located at the left side with wet areas just in front. These wet areas influence the aeolian sediment transport towards the dunes negatively for two reasons: (1) the high moisture content of this part reduces the sediment availability and (2) aeolian transport in onshore direction is trapped by the wet surface.

Representation without morphological feedback

Changes in topography in time are not simulated by the model since there is no changes in topography in time are not simulated by the model since there is no morphological feedback included. Instead, the model simulates aeolian sediment transport rates starting from the topography of the first survey, May 2015 (T0). The negligence of an update in the topography might causes the model to overestimates the measured dune growth rates at locations where large temporal variations in beach topography were measured. Two additional simulations proved that an update of the bed topography reduces the overestimation of the model. Therefore, the topography of the second survey was imposed to the model taking into account that the largest morphological response of the system was observed between the first and the second survey. The overestimation reduced with 8 percent for subdomain 2, along the Northern shoulder, which shows large temporal variations in beach width and thus sediment availability. The overestimation reduced with 4 percent for subdomain 4, along the Southern shoulder, which shows a relative constant beach width in time and thus sediment availability. Though the effect on the results is limited, the inclusion of all four measured topographies in the period between May 2015 and December 2016 might reduce the overestimation further. This will contribute to an accurate description of the sedimentation and deposition in the intertidal zone and beach as a result of marine sediment transport, which improves the description of the aeolian sediment availability. It is expected that a bed topography update will be less effective for subdomain 2, where a relative constant aeolian sediment availability in terms of beach width was measured.

A comparison is made to the aeolian sediment transport rates predicted for the Sand Engine in which the bed topography was updated with measurements. The overestimation for deposition in the dune was in the order of a factor 1.2 for the Sand Engine reported by [Hoonhout, 2017]. This indicates already the good performance of the model prediction in this research without a bed update; an overestimation of a factor 1.2-3 was derived.

6

Conclusions & Recommendations

In this chapter the conclusions and recommendations are given based on the results presented in Chapter 4 and the discussion in Chapter 5. First, the conclusion is given which is subdivided into answers to the three research sub-questions and the main research question. Thereafter, recommendations for further research into aeolian sediment transport and modelling are. The main research question is:

How do different man-made dune geometries responds to the aeolian sediment transport towards the dunes?

The sub-questions related to this main research question are:

1. What is the observed morphological development of the dry beach and dunes since construction?
2. What are the processes and parameters that influence the morphological development of the dry beach and dunes?
3. To what extent are existing models able to reproduce and predict the measured alongshore variations in dune growth?

6.1. Conclusions

6.1.1. Morphological Development since Construction

The morphological development of the beach and dunes along the Hondsbossche Dunes is analysed for the nineteen months after construction using four LiDAR surveys in the period May 2015 - December 2016.

The observations show an alongshore variation in volume changes of the dry beach. High beach volume losses are observed along the HD system, for which the highest response is measured in the seven months after construction. The measured losses are on average $29 \text{ m}^3/\text{m}/\text{y}$ in the period May 2015 - December 2016. Locally, hardly any erosion is observed at profile type 3 along the Southern shoulder and accretion of $7 \text{ m}^3/\text{m}/\text{y}$ is observed at profile type 4 at the middle of the HD system. The volumetric losses of the dry beach are transported in alongshore direction towards the Northern and Southern stretches of the project domain leading to accretion of the beaches. The average volume changes along the entire project domain show a positive result of $2 \text{ m}^3/\text{m}/\text{y}$. The volumetric losses of the intertidal zone and the surf zone confirms this alongshore adjustment, where volumetric losses of $74 \text{ m}^3/\text{m}/\text{y}$ are measured. The accretion is found up to $109 \text{ m}^3/\text{m}/\text{y}$ just Northwards and Southwards of the system. This is predominantly occurred due to: (1) the initial adaptation to the climatic forcing and (2) more and higher south-western waves in storm season (November 2015 - March 2016) [de Jongh, 2017]. The latter effect is strongly pronounced along the Southern shoulder where large erosion is observed.

The volumetric losses of the dry beach is associated with a shoreline retreat of on average $37 \text{ m}/\text{y}$ and with a maximum up to $48 \text{ m}/\text{y}$ for profile type 1. However, decrease in beach width is mostly pronounced for profile type 2 and 5 along the Southern shoulder. Simultaneously, an increase in beach width is observed Northwards and Southwards with a shoreline extension up to $9 \text{ m}/\text{y}$. Spatio-temporal variations in beach width are mainly caused by marine forcing resulting in retreat or progradation of the shoreline, rather than a seaward

movement of the dune foot. The beach width along profile type 3 (South) stayed relatively constant in time. This is notable since the shoreline is most seaward located here and under influence of the predominately south-western wave forcing. The initial beach slope was rather constant along the HD system, but temporal and alongshore variations are derived. Steepening of the beach slope is observed for the eroding beach profiles. Locally, values up to 1:10 and an average value of 1:5 were derived for profile type 5 along the Southern shoulder. The shoreline has increased Northwards and Southwards of the system. This is associated with a development of milder beach slopes.

On average 20 percent of the cross-shore volumetric losses can be attributed to aeolian sediment transport towards the dunes. The average dune growth is $28 \text{ m}^3/\text{m}/\text{y}$. The dune growth rate is in the same order of magnitude compared to the design expectations ($35 \text{ m}^3/\text{m}/\text{y}$) derived the studies of the Holland coast [van Kesteren and Smit, 2013]. Alongshore variations in dune growth are significant with a minimum of $14 \text{ m}^3/\text{m}/\text{y}$ at profile type 1 in the North up to $45\text{-}48 \text{ m}^3/\text{m}/\text{y}$ at profile type 2 and 3 in the South. Moreover, dune growth is pronounced along the Northern and Southern dunes which has result in an average dune growth of $23 \text{ m}^3/\text{m}/\text{y}$ for the full project domain. The morphological response of the dunes is strong between the first survey, in May 2015, and the second survey, December 2015. This is likely be occurred as a result of a high content of fine sand in the nourished sands which can be easily transported towards the dunes. Besides, between the third survey in March 2016 and the fourth survey in September 2016, high dune growth rates are measured. This is a result of an increase in sediment availability due to an increase in beach volume, respectively beach width alongshore. This effect is strongly pronounced along the Northern Dunes and profile type 1 and 2 in the North and profile type 3 in the South.

6.1.2. Governing Processes and Parameters

The morphological development of the beach is governed by the alongshore variations in marine sediment transport. The dry beach zone shows a similar pattern compared to the intertidal zone and the surf zone: volumetric losses are derived along the HD system and deposition Northwards and Southwards of the system. Locally, deposition is found in the surf zone and small erosion in the intertidal zone. At these locations also an increase in beach volume took place (profile type 4). High erosion rates are measured after construction, between May 2015 - December 2015, which is a result of: (1) the initial adaptation of the system and (2) severe marine forcing due to more frequently and high south-western waves. The construction of the HD system is likely to has increased sediment deposition in the surf zone, intertidal zone, and the beach along the Northern dunes. This is caused by the Northwards directed sediment transport that transports the eroding sediment from the beach along the HD system. In the results this effect is shown by a large increase in beach volume in the second period after construction (December 2015 - March 2016).

The alongshore variability in morphological development of the dunes is governed by the interaction of: (1) spatio-temporal sediment availability at the beach and (2) alongshore variation in dune geometry. The beach characteristics regarding the sediment availability are the beach width, beach slope and median grain size which are correlated to the measured dune growth per profile type, but a unique relation could not be defined. Often higher dune growth rates are reached when the beach width is larger and the beach slope milder. In this case, the beach activates more aeolian sediment transport and therefore increases the dune growth. However, a spatial variation in dune growth is observed for equivalent beach width or slope. The maximum or potential dune growth is often not reached due to alongshore variation in local conditions that block the aeolian sediment transport paths towards the dunes. The local factors that show their influence on the development of the dunes are:

1. location with respect to the dominant wind direction
2. beach width
3. beach slope
4. median grain size
5. dune geometry

The first four factors governs the sediment availability at the beach, whereas the dune geometry determines the performance of the dune type to capture and transports the sediment to higher parts of the beach. The model shows that the negligence of the moisture content of the beach, f.e. precipitation, seems to overestimate the actual dune growth rates. This factor seems to be of large importance for the first period after construction in which large wet surfaces were observed at the higher parts of the beach. The topography of

the beach blocks the discharge of water, resulting in low drying time scales at the beach. These areas reduce the sediment availability at particular these places, besides potential aeolian sediment transport towards the dunes is trapped. The local factors that dominates the dune growth for each profile type is described in subsection 6.1.4. The effect of vegetation and local measurements, f.e. willow screens, is not included in the measured dune development.

6.1.3. Modelling Alongshore Variation in Dune Growth

The model strategy used is the process-based model AeoliS. The model strength is simulating instead of parametrizing spatial and temporal variation in beach properties and their influence on aeolian sediment transport towards the dunes. The model can predict aeolian sediment transport rates for large spatial and temporal scales under supply-limited conditions.

The AeoliS-model provides a first framework for the description of aeolian sediment transport and dune development at the Hondsbossche dunes. The Hondsbossche domain is divided into five subdomains in order to impose the measured alongshore variation in grain size. The initial topography of the survey of May 2015 is imposed to the model together with real time series of wind, waves and tides. The AeoliS model is able to reproduce large scale spatial patterns of erosion and deposition under influence of varying climatic conditions. Deposition in the intertidal zone as an effect of marine forcing is not simulated, since this is not included in the model yet. The dune area is not included, instead a vegetation mask is imposed that increases the shear velocity threshold for the dune area in order to simulate the effect of vegetation on deposition in the dunes. Aeolian sediment transport that passed the alongshore boundary of the dune foot (at +3.5m NAP) is assumed to deposit in the dunes and used to determine the dune growth rates.

The AeoliS model shows to predict alongshore variations in dune growth as a result of spatial variations in sediment availability. The model overestimates the measurements with a factor varying from 1.2 to 3. Subdomain 2, located along the north part, is most sensitive for the assumed conditions, since the initial beach width was large compared to other domains. This results in a large sediment availability in time while the measurements show a relatively large decrease in beach width. The model overestimation is lowest for subdomain 3, at the middle of the HD system, which is characterized by a relative small and constant beach width alongshore and in time. Furthermore, a comparison of modelled and measure dune growth rates for each measurement period shows that the overestimation reduces in time. The overestimation is highest in the first period as a result of high and onshore directed wind forcing and a large sediment availability. High wind speed increases the capacity of the wind to transport sediment, whereas the large sediment availability is likely to be a result of the negligence of soil moisture and marine sediment transport in the model. In particular, the negligence of both factors could have a severe influence in the first period in which large marine erosion of the beach are pronounced and large wet surface with small drying time scales were observed at the higher parts of the beach. The overestimation is less pronounced in the last period in which low and offshore wind is measured which reduces the pick-up of sediment into aeolian transport towards the dunes.

6.1.4. Conclusion on Main Research Question

How do different man-made dune geometries responds to the aeolian sediment transport towards the dunes?

Based on the findings, it can be concluded that the five man-made constructed profile types show an appreciable different response to the aeolian sediment transport towards the dunes. The morphological response of the dunes is most pronounced in the first seven months after construction with an average rate of $35 \text{ m}^3/\text{m}/\text{y}$ and has decreased in time to $22 \text{ m}^3/\text{m}/\text{y}$ in the last period. The dune growth rate is largest for profile type 3 - South ($48 \text{ m}^3/\text{m}/\text{y}$), since it is characterized by parameters that stimulate the actual transport towards the dunes. The dune geometry consists of a low foredune with a relatively mild slope which stimulates the transport of sediments to the higher parts of the dunes. Limited temporal and spatial variations in beach width and beach slope were observed resulting in a beach width of 151 m and slope of 1/100 at the last survey. Moreover, a fine grain size with a $D_{50} = 224 \mu\text{m}$ was derived at the beach. These factors positively contribute to the aeolian sediment availability at profile type 3. The important characteristics of the four other profile types with respect to the (1) dune geometry and (2) the sediment availability are compared here. The effect of vegetation and local measurements, f.e. willow screens, is not taken into account.

Profile type 1 is located along the Northern shoulder for which the dune geometry is characterized by a steep and high dune front (1:1.3 - 1:1.7). The average dune growth is $14 \text{ m}^3/\text{m}/\text{y}$. The dune growth is considered to be low with respect to profile type 3, but also to the adjacent profile type 2. This seems to be related to the lower capacity of the profile type to capture the sediments due to the higher and steeper front slope of the dune. The potential transport of fine grains towards higher parts of the dunes is therefore limited. The sediment availability is characterized by an equivalent order of magnitude with respect to the beach width (150 m). However, a steep beach slope of 1/30 is derived and a coarser grain size of $D_{50} = 304 \mu\text{m}$ reducing the sediment availability of the beach.

Profile type 2 is located at two stretches along the HD system: in the North adjacent to profile type 1 and in the South adjacent to profile type 2 and profile type 3. This profile type is characterized by a steep (1:1.7) and high dune front. Spatial differences in dune growth were found between the two sections: the average dune growth is $20 \text{ m}^3/\text{m}/\text{y}$ in the North and $45 \text{ m}^3/\text{m}/\text{y}$ in the South. The spatial differences in dune growth within the two locations is related to local conditions along the Southern dunes in terms of (1) the location with respect to the predominantly south-west wind and (2) a finer median grain size ($D_{50} = 224 \mu\text{m}$) of the dry beach, (3) a milder beach slope (1:50) and (4) wider beach (110 m). These factors result in higher aeolian sediment availability in the South. However, marine forcing is likely to have a severe influence on the beach development in time, large volumetric losses and shoreline retreat are seen. The most remarkable difference between profile type 2 and 3 is related to the dune geometry itself, minor differences were found in the sediment availability.

Profile type 3 is located at two stretches along the HD system: it is located between profile type 2 and 4 in the North and the South, respectively. Spatial differences in dune growth were found between the two sections: the average dune growth is $23 \text{ m}^3/\text{m}/\text{y}$ in the North. The spatial differences in dune growth are committed to favourable conditions along the Southern dunes in terms of: (1) the location with respect to the predominantly south-west wind and (2) a finer median grain size of the dry beach, a milder beach slope and wider beach. These factors result in higher aeolian sediment availability.

Profile type 4 is located along the straight part of the HD system in between profile type 3 at the North and at the South. This profile type is characterized by the dune valley that is constructed between a low foredune with a mild front slope (1:2.9), and a high landward located dune. The average measured dune growth is $23 \text{ m}^3/\text{m}/\text{y}$. This is considered to be low with respect to profile type 3. However, the capture of sediments in the dune valley is not considered due to the limited reliability of the LiDAR when penetrating through water. Other factors that could explain the lower dune growth rate are: (1) a coarser median grain size of the dry beach ($D_{50} = 341 \mu\text{m}$), (2) a steeper beach slope (1:50), and (3) a smaller beach (104 m). Marine forcing is likely to have a small influence on the beach development in time, a volumetric increase of the beach and small shoreline retreat are seen.

Profile type 5 is located along the Southern shoulder of the HD system, the dunes are the barrier between the lagoon and the beach. The dune geometry is characterized by a steep (1:2) and low dune front. The average dune growth is $18 \text{ m}^3/\text{m}/\text{y}$. This is considered to be low with respect to profile type 2 and 3. The stimulating conditions in terms of: (1) the location with respect to the predominantly south-west wind and (2) the fine grains of the dry beach in front of the area, does not dominate the dune growth. For this profile type, it is likely that the marine forcing has dominated the dune growth as a consequence of a severe reduction in aeolian sediment availability. The temporal development of the beach zone shows that the beach volume and width has significantly decreased. Locally, a shoreline retreat up to more than 100 metres and a beach slope of 1/10 was measured.

Overall, it can be concluded that the dune growth of a profile type is likely to be determined by: (1) a temporal variability in local processes that determines the aeolian sediment availability and transport towards the dunes and (2) the dune geometry that determines the capacity of the profile type to capture the sediments and transport the sediments to higher parts of the dunes. The capacity of aeolian sediment transport to build dunes is experienced to be higher if the beach slope and beach width suffer from low spatial and temporal variations as a result of marine forcing. Besides, fine grains at the beach promote the pick-up and transport of sediment. Dune growth is higher if the dune consists of a lower foredune with a mild slope, equivalent to profile type 3 and a large supply of sediments towards the dunes. A large supply is stimulated during high and onshore directed winds and a favourable location with respect to the dominant wind direction.

6.2. Recommendations

This section gives scientific and management recommendations for the coastal area 'Hondsbossche Dunes'. The scientific recommendations suggests research related to data and to model. The management recommendations give advice to maintain required the safety level that is associated with this coastal area. The recommendation for each topic are ranked based on two till four criteria, as shown in table 6.1. The criteria are classified into a five point scale for which the ranking is defined based on the expertise obtained during this research.

Table 6.1: Overview of the criteria that are used to evaluate the recommendations.

Criteria	Scale = 1	Scale = 5
Importance of the recommendation for further research	very	moderate
Laborious to execute the recommendation	most	least
Equipment or devices required to execute the recommendation	highest	least
Materials needed to execute the recommendation	Much materials needed	less materials needed

6.2.1. Scientific Recommendations

This section is separated into two parts: recommendations regarding the data analysis and recommendations regarding the application of the numerical model AeoliS.

Improvements of the data analysis

Four LiDAR measurements were used to obtain insight into the morphological development of the Hondsbossche dunes. Recommendations regarding to the data-analysis are given in Table 6.2. For the criteria *importance* the recommendations are distinguished between enhancing the current data and the additions of new data to get a better understanding in the relationship between aeolian sediment transport and dune development. The criteria *labourious* indicates the effort by employees or researchers that is required to achieve the recommendation. Some of the recommendations ask for more or higher quality equipment which could result in higher costs.

Improvements of the numerical model

The AeoliS model was applied at the Hondsbossche Dunes. The model is a convenient first step to simulate variations in alongshore aeolian sediment availability on dune growth rates. Suggestions for future model studies using this model are given in Table 6.3. These recommendations are only ranked on *importance* and *labourious*. High *importance* is given to the recommendations which lead to a better understanding of the current model, whereas lower *importance* is apportioned to recommendation for future morphological development. The criteria *labourious* indicates the effort by employees or researchers that is required to achieve the recommendation.

6.2.2. Management Recommendations

Table 6.4 shows the recommendations for the managing the Hondsbossche Dunes. All the four criteria are applied to rank the recommendations. The most *important* suggestion is given to the recommendations with the highest consequences. The recommendations are also ranked based on the criteria *materials* to indicate requirement of additional costs.

Table 6.2: Proposed recommendations regarding to data

#	Recommendation	Importance	Labourious	Equipment	Proposed approach	Proposed frequency	Expected outcome
1	LiDAR surveys	2	5	1	Execute flights during low water to obtain topographic data including the intertidal zone	twice per year: March and October	Less morphological response of dunes and improved relation between beach and dune development
2	Grain size measurements	2	1	4	Take samples for each sub-domain in cross-shore and alongshore direction	1. once per year 2. post nourishment (maintenance)	Improved relation between grain size and dune growth Post nourishment: a finer content of sediments is expected leading to an impulse in dune growth
3	Morphological change dune valley	3	2	2	Analyse current available data and monitor the development with RTK-GPS device	once per year	The dune valley continues with capturing sediments
4	Subsidence of the dunes	1	3	3	Use a fixed reference point to derive deviations in subsidence in alongshore and cross-shore direction and per profile type	once per year	Alongshore variability in loosely and densely packed sand. Loosely packed sand areas are expected along the dune foot and densely packed sand in landward direction. The knowledge could improve dune volume.
5	Relation beach between foreshore development	1	4	1	Use LIDAR surveys and single beam monitoring to analyse development of bathymetry measurements in relation to beach development based on temporal and spatial variability	twice per year: March and October	More apparent relation between beach development and bathymetry as result of marine forcing.
6	Soil moisture measurements	2	3	1	Analyse the effect of high water levels and precipitation rates on the moisture content by using e.g. a laser scanner.	once per year i	Improved understanding into seasonal aeolian sediment availability at the beach

#	Recommendation	Importance	Labourious	Equipment	Proposed approach	Proposed frequency	Expected outcome
7	Statistical analysis of relation between sediment availability and dune growth	4	5	5	(i) Overcome the spatial lack between the current surveys of the available parameters and dune growth to capture 2D sediment transport due to predominantly South-Western winds better. (ii) Derive longer time series of aeolian sediment parameters (beach slope, beach width and median grain size) to improve the statistical evidence for the relationship between sediment availability and dune growth.	-	Better understanding into the parameters of sediment availability that restrict dune growth.
8	Dune volume analysis Northern Shoulder	3	5	5	Consider low constructed dunes along Northern shoulder (between RSP 19.96 and RSP 20.29) as a feature of the dune system for the period May 2015 till December 2015, and evaluate their response to sediment transport.	-	The occurrence of dune growth is more present for this area than was expected.
9	Dune geometry	5	5	5	Quantify the relation between dune front parameters (height and slope) and measured dune growth.	-	Quantified evidence for the positive performance of profile type 3.

Table 6.3: Proposed recommendations regarding to model

#	Recommendation	Importance	Labourious	Proposed approach	Expected outcome
1	Sensitivity analysis of model input parameters	1	4	-	Understand the effect of model parameters on the model results
2	Inclusion of marine sediment transport	2	3	Impose measured topographies of T1-T4 to capture the effects of erosion and sedimentation in the intertidal zone	Improve prediction of aeolian sediment availability and dune growth rates
3	Inclusion of soil moisture content	2	2	Increase the shear velocity threshold locally	Improve prediction of aeolian sediment availability and dune growth rates. Especially, the overestimation of the first period in which higher precipitation rates occurred and larger wet beach areas were observed
4	Develop large-scale domain	3	1	Develop an approach to include alongshore variation in grain size distribution	One model domain in which sediment exchange in the alongshore direction could be captured
5	Total dataset for climate conditions	3	4	Apply method for to fill missing data points	Synchronisation of the time series
6	Prediction of future morphological development	5	5	Simulation of 10 year development on average climatic conditions	A possible trend in the morphological development might be found
7	Inclusion of seasonal effects in vegetation	4	2	1. Impose temporal and alongshore variation in the shear velocity threshold of the dune area	Notable alongshore and temporal effect of aeolian sediment transport on dune vegetation
		4	1	2. Coupling with DUBEVEG	Accurate description of the influence of vegetation on dune growth
8	Simulations regarding to the impact of climate change	5	5	High, moderate or low climate scenario runs	Prediction for different climate scenarios on dune development

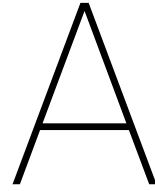
Table 6.4: Proposed recommendations for coastal management

#	Recommendation	Stage	Importance	Labourious	Equipment	Materials	Approach	Purpose
1	Monitor connection HD system - Petten	maintenance	2	2	2	3	Monitor the development of the lower dunes regarding to vegetation cover and sediment volumes	Achievement of the critical dune volume to comply with the used design storm
2	Recovery of dune geometry after storm	storm recovery	1	1	1	1	Construct a lower foredune with a mild slope	Fast storm recovery in case of large amount of dune erosion during storm
3	Yearly assessment of dune volume change	maintenance	3	3	5	5	(i) Conduct the assessment using the JARKUS reference system. (ii) If safety based on this assessment is not longer guaranteed create in collaboration with Rijkswaterstaat and contractor a maintenance plan	To check whether the safety level of the Hondsbossche Dunes is met
4	Monitor profile type 1	maintenance	3	2	3	3	Conduct calculation on future data in which dune volume is computed .	Identify if there is still enough dune volume to comply with the prescribed values.
5	Invest in long-term analysis of future morphological development	-	3	4	5	5	(i) Create budget to execute research in the future morphological development. (ii) Assign this to a research institute . (iii) React on the identified critical points from the research	Early discover of problems in the morphological development regarding to coastal safety

Bibliography

- Bagnold, R. (1954). *The Physics of Blown Sand and Desert Dunes*. METHUEN & CO. LTD., London.
- Brandenburg, P. (2015). Keuringsrapport 145347-KF-015. Technical report, Van Oord and Boskalis.
- College, C. (2003). Wind flow over dunes. <https://www.calvin.edu/academic/geology/coastaldunes/processes/wind3.htm>. Accessed: 2016-06-01.
- de Jongh, L. (2017). Initial morphological evolution of a mega nourishment.
- de Schipper, M., de Vries, S., Ruessink, G., de Zeeuw, R., Rutten, J., van Gelder-Maas, C., and Stive, M. (2016). Initial spreading of a mega feeder nourishment: Observations of the sand engine pilot project. *Coastal Engineering*, 111:23 – 38.
- de Vries, S., Southgate, H., Kanning, W., and Ranasinghe, R. (2012). Dune behavior and aeolian transport on decadal timescales. *Coastal Engineering*, 67:41–53.
- de Vries, S., van Thiel de Vries, J., van Rijn, L., Arens, S., and Ranasinghe, R. (2014). Aeolian sediment transport in supply limited situations. *Aeolian Research*, 12:75–85.
- Durán, O. and Moore, L. J. (2013). Vegetation controls on the maximum size of coastal dunes. *Proceedings of the National Academy of Sciences*, 110(43):17217–17222.
- Google (2016). Google Earth. https://www.google.co.uk/intl/en_uk/earth/. Accessed: 2016-07-05.
- Hoonhout, B. (2017). *Aeolian Sediment Availability and Transport*. PhD thesis.
- Hoonhout, B. M. (2016). AeoliS. <http://aeolis.readthedocs.io/en/latest/>. Accessed: 2016-10-10.
- Hoonhout, B. M. and de Vries, S. (2017). A Process-based Model for Aeolian Sediment Transport and Spatiotemporal Varying Supply. not published yet.
- Hoonhout, B. M., de Vries, S., Baart, F., van Thiel de Vries, J., van der Weerd, L., and Wijnberg, K. (2013). Monitoring of beach surface properties with remote sensing.
- Informatiecentrum Kust, Z. t. Z. (2012). Hondsbossche zeedijk. <https://www.hhnk.nl/portaal/informatiecentrum-kust-zand-tegen-zee>. Accessed: 2016-07-05.
- Joosten, R. (2005). Toetsing primaire waterkeringen 2005. Technical report, Hoogheemraadschap Hollands Noorderkwartier.
- Keijsers, J. (2015). *Modelling foredune dynamics in response to climate change*. PhD thesis.
- Kroon, A., van Leeuwen, B., Walstra, D., and Loman, G. (2015). Dealing with uncertainties in long-term predictions of a coastal nourishment. pages 1–10.
- Lancaster, N. (1970). *Geomorphology of desert dunes*. Routledge, London.
- Leenders, J., Bodde, W., and Smit, M. (2016). Inventarisatie optimalisatiemogelijkheden kustversterking HPZ.
- Leenders, J. and Smit, M. (2016). Inventarisatie maatregelen ontwerp HPZ.
- Luijendijk, A., Ranasinghe, R., de Schipper, M., Huisman, B., Swinkels, C., Walstra, D., and Stive, M. (2017). The initial morphological response of the Sand Engine: A process-based modelling study. *Coastal Engineering*, 119:1–14.
- Ministerie van Infrastructuur en Milieu (2016). Achtergrond bij de normering van de primaire waterkeringen in Nederland. Technical report, Ministerie van Infrastructuur en Milieu.

- Muller, M. (2011). Process-Based Modeling of Coastal Dune Development.
- Muller, M., Roelvink, D., L. A., De Vries, S., and Van Thiel de Vries, J. (2012). Process-Based Modeling of Coastal Dune Development. *Coastal Engineering Proceedings*, 1(33):1–8.
- Nordstrom, K., Psuty, N. P., and Carter, B. (1970). *Coastal dunes: form and process*. Wiley, Chichester, England.
- Oudeluis, C. (2012). Hondsbossche zeedijk. <http://campingoudesluis.nl/petten/hondsbossche-zeedijk>. Accessed: 2016-07-05.
- Roos, R., van der Wel, N., and van Wijngaarden, M. (2011). *Duinen en Mensen - Noordkop en Zwanenwater*. Uitgeverij Natuurmedia, Amsterdam.
- Smit, M., van Kester, D., and Olijslagers, F. (2015). ZSNH: aeolian processes in dune design.
- van der Wal, D. (2004). Beach-dune interaction in nourishment areas along the dutch coast. *Journal of Coastal Research*, pages 317–325.
- van Kesteren, D. and Smit, M. (2013). Initieel Aanlegprofiel, Prognose van eolisch zandverlies. Technical report, Van Oord en Boskalis.
- Verheijen, A. (2017). Aeolisch transport en duinontwikkeling in de Hondsbosshe en Pettermerduinen.
- Watermanagementcentrum, D. W. (2015a). Watermanagementcentrum Nederland - Stormvloedflits 2015-05 van 13 en 14 november 2015.
- Watermanagementcentrum, D. W. (2015b). Watermanagementcentrum Nederland - Stormvloedflits 2015-05 van 29 en 30 november 2015.
- Wolfe, S. A. and Nickling, W. G. (1993). The protective role of sparse vegetation in wind erosion. *Progress in Physical Geography*, 17(1):50–68.



Background Design

A.1. New Approach to Failure Probabilities

The rejected HPZ became part of a larger reinforcement project, the 'weak links', in which a total of ten locations were recommended for adaptations in order to comply with the Water Law that since January 2017 has included a new approach to failure probabilities of the primary sea defences and the secondary dike systems [Ministerie van Infrastructuur en Milieu, 2016]. So far the safety standard for a certain dike or dune has been expressed in a probability of exceedance of the designated water levels. Since studies proved that the consequences of a flooding is strongly dependent on the location within a dike system, the safety standard has been expressed in terms of flood risk: the probability that a certain section of a dike system will fail when the load is higher than the strength [Ministerie van Infrastructuur en Milieu, 2016]. Therefore, the probability of failure of one section is independently determined by the separate failure mechanisms. Combining the failure probabilities of one section results in a flood risk for a certain area within this dike-system. The probability of flooding safety for the new design of the Hondsbossche Dunes has therefore changed from 1/10.000 to 1/3.000 years [Ministerie van Infrastructuur en Milieu, 2016].

A.2. History of Construction

For almost 600 years this five-kilometre-long HPZ section showed its weaknesses. Different types of defences were constructed to protect the low-lying hinterland against flooding. In the early Middle Ages the closed dune system was under attack from the sea. This resulted in a retreating coastline for many centuries. Between 1350 and 1850 the erosion was 3.5 meters per year on average. The involved aeolian sediment transport had caused problems for the village of Petten.

Since the 'Sint-Elizabeth' flooding of 1421 this weakest section in the defence of the Dutch coast got many improvements. The dunes had to remain bare on the sea side to positively contribute to sand transport in landward direction. This aeolian process resulted in new dunes. Since the dune erosion was faster than the dune accretion, people chose for a different approach. Groynes were constructed perpendicular to the coastline.

After the 'Allerheiligen' flooding of 1570 the responsible authorities concluded that the fixed Hondsbossche & Pettemer section formed an outcrop on the coastline. This made it sensitive for storm surges. In 1624 a new sea dike was constructed 350 meters behind the previous sea defence. In the 17th and 18th century these sea dike was made up of sand and grass. The wide beach in front of the sea defence reduced the wave impact on the new sea dike. The beach width was yearly assessed after the storm season. Strengthening of the sea dike occurred at the landward side which resulted in regressive coastline. The sand dike itself formed part of the adjacent and moving soft coastal system.

The next large improvement was developed in the 19th century. It was first decided to construct a wall consisting of wooden piles to break the waves in front of the sea dike, but still many problems arose. Therefore, the current sea dike composed of clay and basalt was designed and constructed [Roos et al., 2011]. This dike survived many storms, but again formed a hard and fixed outcrop on the coast line.

The newest version of the dike was realised in 1981. It stands at a height of 12 meters above NAP and has groynes in place to reduce the wave impact. After so many improvements the HPZ-section still formed a fixed outcrop and has influenced the adjacent erosive coastline.

A.3. Design Requirements and Methodology

The design requirement for strengthening the Hondsbossche & Pettermer sea defence was to develop a coastal profile that meet the legal coastal safety requirements for the coming fifty years taking into account climate change and land subsidence. The secondary objective was to create an appealing coastal zone for recreation with favourable conditions for ecology [Leenders and Smit, 2016]. These requirements have resulted in a design philosophy based on two perspectives. The first perspective aims to stabilize the sand where that is deemed necessary for safety purposes or to diminish the hindrance of windblown sand. The second perspective allows sand to be transported by wind to develop an ecologically interesting area with an appealing coastal zone [Smit et al., 2015]. All the existing knowledge about aeolian processes and the experiences from previous projects, for example the 'Maasvlakte 2', the 'Sand Engine' and the 'Spanjaardse duinen', in combination with the design requirements, resulted in three types of measures based on [Smit et al., 2015]:

1. large geometric features - Large elevation will create shadow zones where sand will accumulate.
2. small geometric features - Local small elevations will create differences in deposition patterns and thus stimulates a local variable evolving dune.
3. plants and objects - Plants will reduce locally the wind velocity and thus enhance deposition and containment of sand.

Large geometric measures are the construction of the dunes itself. In combination with small geometric features (low-lying deposition areas) and plants (marram grass, buckthorn) a dune should develop that shows alongshore and cross-shore geometric variabilities. On a small-scale the irregular pattern of vegetated and non-vegetated areas should stimulate local sand transport and positively contribute to the development of different ecological systems [Smit et al., 2015].

A.4. Design of the Dunes

The project area of the is divided into three larger areas, namely the northern recreation zone from RSP 17.00 till RSP 22.51, the nature zone from RSP 17.00 till RSP 22.51 and the southern recreation zone from RSP 26.06 till RSP 28.32. The nature zone includes the dune slack (valley) behind the foredunes which is the only habitat requirement for the Hondsbossche & Pettermer Dunes.

A.4.1. Project boundaries

The average coastline orientation for this area is 18 degrees. In the north at approximately RSP 18.89 the coastline orientation start to deviate slowly from the average orientation angle. This process continues till RSP 20.41, the so-called the Northern shoulder. In the south the coastline orientation start to deviate again at approximately RSP 25.57 and continues to RSP 27.72, the so-called Southern shoulder. The figure clearly shows the curving shape of the new coastal area of which the cross-shore boundaries are defined as RSP 17.09 in the north and RSP 28.32 in the south [van Kesteren and Smit, 2013]. The landward project boundary is defined as -250 m RSP along the Northern and Southern natural dunes and as -35 m RSP along the sea defence (dike crest).

A.4.2. Dune Profile Types

Five different dune types have been designed for the HD system of which the design drawings are displayed in the next section. The seaward dune slope and the dune crest of all the five dune profile types are covered with vegetation with a minimum of 60 percent. The landward dune slope of dune profile type 1 till 4 is fully covered [Leenders and Smit, 2016]. This satisfy the requirement that the critical profile needs to be fully covered with vegetation. The characteristics for each dune profile type and the expectations of morphological development are given here.

Profile type 1- High dune with variations in height

The highest part of this dune section is at +26.20 m NAP with a dune slope of approximately 1:1.7 m forming the watch tower of this area. At both sides of the watch tower lower dunes are constructed of which the layout is matching with profile type 2. Low-lying deposition areas have been constructed with a variation in height within a range of two meters. For profile type 1 it is expected that the dune foot will grow in height and in seaward direction. The low-lying areas at the dune crest will be totally filled up with sand.

Profile type 2- High dune with restricted variations in height

Profile type 2 has been constructed at two sections along the HD-system. The dune crest of profile type 2 varies around a height of +12.5 m NAP with a dune slope of approximately 1:2.1 m. The seaward and the landward slope are comparable to the lower part of profile type 1. At the dune crest no low-lying deposition areas were constructed, only areas without vegetation has been constructed. For profile type 2 it is expected that the entire cross-shore profile will grow in height.

Profile type 3- High dune with lower foredune

Profile type 3 has also been constructed at two sections along the HD system, see Figure 1.2. The dune profile consists of a lower foredune which varies around a height of +5.50 m NAP and with a dune slope of approximately 1:4 m. This lower foredunes stands in front of a higher landward dune which varies around a height of +10 m NAP and with a dune slope of 1:1.8 m. At the dune crests low-lying deposition areas have been constructed at a maximum depth of -0.5 m at the foredune and -2 m at the landward dune. Also variation in the amount and pattern of vegetation is constructed.

Initially, it was expected that the foredunes were wide enough to accumulate enough sand and thus reducing the aeolian losses landward of the system. During the construction phase it was experienced that the effectiveness of capturing sand by the foredunes was not enough. It was therefore chosen to place extra willow screens along the dunefoot of profile type 3. For profile type 3 it is expected that the largest morphological changes will occur at the seaward dune slope and dune crest of the foredunes.

Profile type 4- Dune slack or valley

Profile type 4 is located in the middle section of the HD system which is established as the nature area of the HD system. The profile consists of two rows of dune dived by a wet dune slack (or valley). The crest of the seaward (fore)dune varies around a height of +6 m NAP with a seaward dune slope of 1:3 m and a landward dune slope towards the valley of 1:1.1 m. At the dune crest small open areas have been constructed and at the landward slope a curling pattern of vegetation. This should stimulate local variations in morphological development. The seaward dune slope and the dune dune crest are covered for 75 percent by vegetation.

The crest of the landward dune varies around a height of +11 m NAP. The dune slope toward the valley consists of a milder and steeper part. It has a dune slope of approximately 1:1.6 m till a level of +7 m NAP and a slope of 1:1.3 m till the crest. Again, variation in vegetation pattern on the slope and low-lying deposition areas on the dune crest have been constructed to create initial variations in morphology. The dune crest itself is fully covered by vegetation except for the the location of the low-lying deposition areas. The largest profile changes are expected at the seaward dune. The dune slack (valley) will capture onshore windblown sand and thus prevent aeolian sediment transport towards the higher landward dune.

Profile type 5- The lagoon

Profile type 5 is located at the lagoon and therefore a total different profile. At the sea side of the lagoon a small and low dune (+5 m NAP) and initial dune slope of 1:2 was constructed of which only the seaward slope and dune crest is covered by vegetation.

A.4.3. Overview of the Profile Characteristics

Table A.1 gives the overview of the parameters about the small and large geometric features for the different dune profile types and the extra measurements that were constructed [Leenders and Smit, 2016]. Along the dune foot of the entire HD system willow screens have been placed to capture the sand. The willow screens have also been installed on several places at the dune crest to prevent locally hindrance of wind-blowing sand. The low-lying deposition areas have been constructed according to a strict pattern of squares in the southern part of the HD system. This has changed to a randomly pattern in northern direction. The constructed dimensions of the areas are approximately 10 * 10 meters.

During the construction phase two extra measurements have been taken to prevent aeolian transport: shredded wet paper and screens at the previous sea dike. The last measures reduced the hindrance for the hinterland of the sand that has already passed the landward boundary of the dune profile.

Table A.1: Overview of measurements- as built. Adapted from: [Leenders and Smit, 2016]

Profile type	RSP number	Length [m]	Width [m]	Vegetation		Low-lying deposition areas		Wind screens [m]
				Buckthorn [m ²]	Marram grass [m ²]	[#]	[m ²]	
1	20.17-20.94	750	80	14494	34901	18	1504	1566.9
2	20.94-21.46	500	100	11184	28580	46	3879	1263.7
3	21.46-22.47	1000	125	15355	36260	23	3086	2894.6
4	22.47-23.94	1500	160	13781	112331	148	16318	1817.0
3	23.94-25.40	1500	125	27638	103687	151	18758	2566.6
2	25.40-25.89	500	100	6878	27605	50	6709	702.1
5	25.89-26.91	1000	100	1463	57321	50	3666	1360.3

A.4.4. Design Drawings

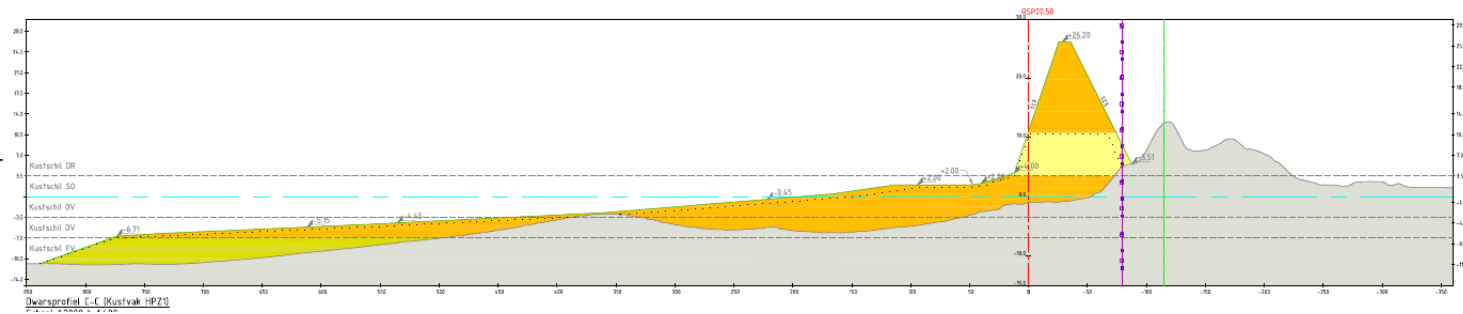


Figure A.1: Design drawing of dune profile type 1, adapted from: [van Kesteren and Smit, 2013].

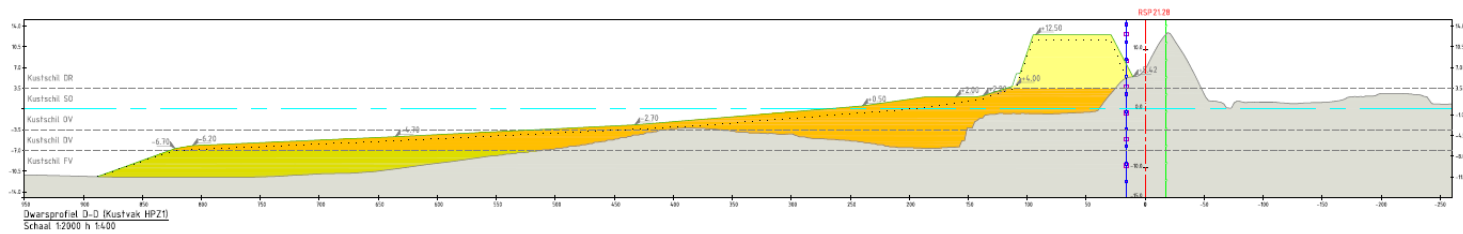


Figure A.2: Design drawing of dune profile type 1, adapted from: [van Kesteren and Smit, 2013].

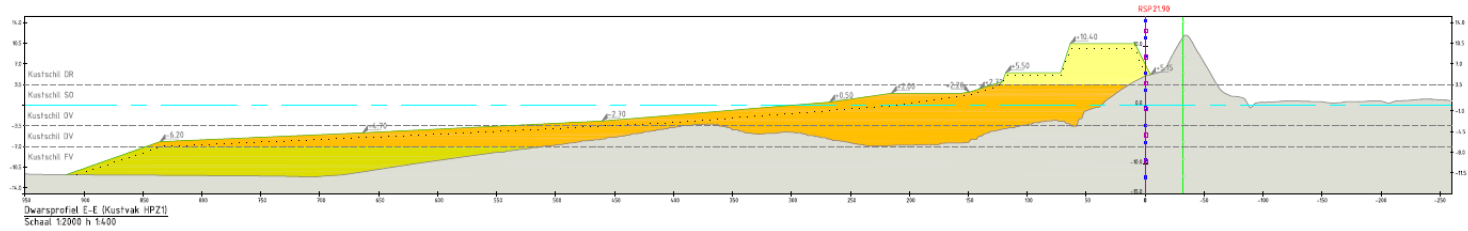


Figure A.3: Design drawing of dune profile type 1, adapted from: [van Kesteren and Smit, 2013].

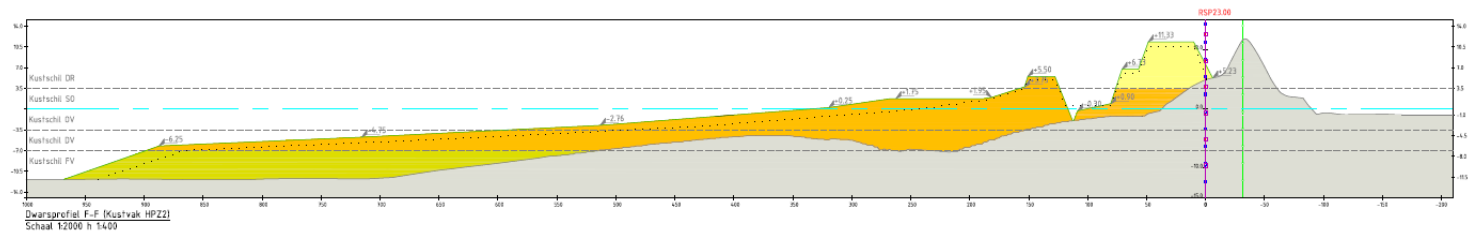


Figure A.4: Design drawing of dune profile type 1, adapted from: [van Kesteren and Smit, 2013].

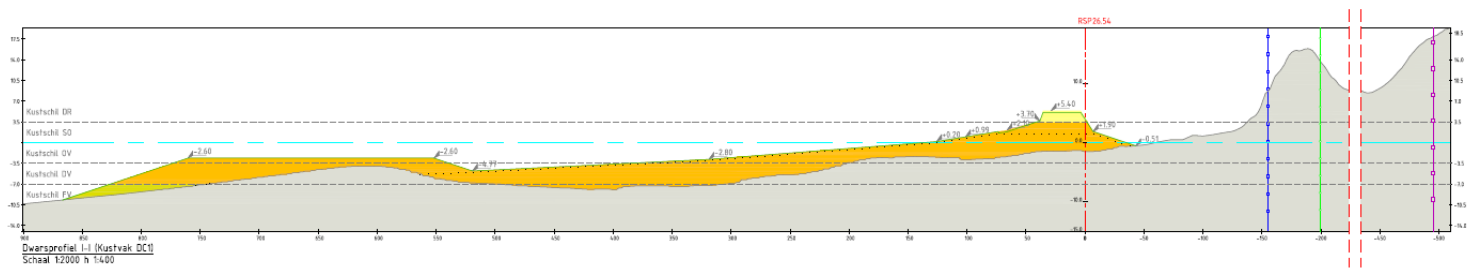


Figure A.5: Design drawing of dune profile type 1, adapted from: [van Kesteren and Smit, 2013].

A.4.5. Expected Aeolian Transport and Morphological Development

Table?? provides information about the expected aeolian sediment transport and accumulation for the different dune profile types for the first year after construction. This expectation is built during the design phase and based on literature, expert judgement and reference projects [Leenders and Smit, 2016].

The expected growth of the dunes is $35 \text{ m}^3/\text{m}/\text{y}$. A distinction is made between the seaward dune slope, dune crest and landward dune slope. These numbers are not known for profile type 5. It is expected that the dune crest of dune profile type 3 and the seaward dune of profile type 4 will increase largely in volume compared to profile type 1 and 2. For profile 1 and profile 2 the expected increase in volume is located at the landward dune slope. This also include a higher expected aeolian losses along these two profiles.

Table A.2: Overview of volume changes according to the design. Adapted from [Leenders and Smit, 2016] ^a This value represents the total accumulation on the seaward dune. ^b This value represents the total accumulation on the seaward slope and dune crest of the landward dune row.

Area of interest	Full section [m ³ /m/y]	Profile type 1 [m ³ /m/y]	Profile type 2 [m ³ /m/y]	Profile type 3 [m ³ /m/y]	Profile type 4 [m ³ /m/y]	Profile type 5 [m ³ /m/y]
<i>Dunes</i>	35.0	35.0	35.0	35.0	35.0	35.0
<i>Dune slope seaward</i>	-	6.0	15.0	7.5	24.5 ^a	-
<i>Dune crest</i>	-	12.5	6.5	29	1.4 ¹	-
<i>Dune slope landward</i>	-	16.5	16.0	2.0	1.8	-
<i>Aeolian losses</i>	-	16.5	17.9	2.0	1.9	-

Table A.3: Overview of volume changes according to the design. Adapted from [Leenders and Smit, 2016]

Area of interest	Full section [m ³ /m/y]	Profile type 1 [m ³ /m/y]	Profile type 2 [m ³ /m/y]	Profile type 3 [m ³ /m/y]	Profile type 4 [m ³ /m/y]	Profile type 5 [m ³ /m/y]
<i>Dunes</i>	35.0	35.0	35.0	35.0	35.0	35.0
<i>Dune slope seaward</i>	-	6.0	15.0	7.5	24.5 ^a	-
<i>Dune crest</i>	-	12.5	6.5	29	1.4 ^b	-
<i>Dune slope landward</i>	-	16.5	16.0	2.0	1.8	-
<i>Aeolian losses</i>	-	16.5	17.9	2.0	1.9	-

^aThis value represents the total accumulation on the seaward dune. ^b This value represents the total accumulation on the seaward slope and dune crest of the landward dune row.

A.4.6. Monitoring EcoShape

Five cross-profiles will be monitored from 2016 till 2018 by the EcoShape consortium. The research goal of this consortium is to monitor the morphological development of the dunes and the effect of the large geometric features (dune slope, lower foredunes) as well as the small geometric features measurements, for example the low-lying deposition areas and the vegetation. There is a special interest for the habitat development of the nature area along dune profile type 4. The monitoring should provide insight into the occurred processes and if the development is line with the expectations. This knowledge will be used for the design of future large-scale sandy project.

B

Aeolian Transport Model- DUBEVEG

In many different branches of research, geology, ecology, agriculture and coastal engineering, research into aeolian transport modelling is conducted. Although there is considerable overlap, hydraulic engineers tend to concentrate on the mechanics of sediment transport and practical measures aimed at stabilizing blowing sand, while geologists have focused on the classification and changes of large scale features and covering large timescales. (Pye and Tsoar, 1990, cited in Muller, 2011, p.18) [Muller, 2011]. The model examined here represent the biogemorphological model (DUBEVEG).

B.1. Introduction to the model

DUBEVEG (DU = DUNE, BE = BEACH, VEG = Vegetation) is a cellular automata model which is developed by Alma de Groot and Joep Keijsers of Imares and Wageningen University. The model focus on how the interaction between hydrodynamics, aeolian sand transport and vegetation growth shapes the dunes. Therefore an existed dune formation module based on desert dunes is combined with the development of a beach module and a vegetation module. The model was originally developed to study the development of moist dune slacks for different nourishment scenarios. The development of the model continued on the biogeomorphic evolution of coastal dunes in response to climate change.

B.2. Model Description

The principal feature of the algorithm is that batches of sand are transported across a simulated 3D surface based on stochastic procedure, whereby deposition, transport and erosion are determined by change. Hence, a set of rules represent a complex set of interacting physical laws

The aeolian transport is described according to the DECAL (Discrete Ecogeomorphic Aeolian Landscapes Model) algorithm [?] which is an extension of the dune model of [?]. It consists of a collection of a regular grid of cells, all with an initial state that evolves through a number of discrete time steps, according to a set of rules based on the states of neighbouring cells. Moreover, it is a self-organising model which means that the dynamic dune development is controlled by local interactions and feedback mechanisms, automatically evolving towards a state of equilibrium. The model can be divided into three modules which interacts with each other.

1. Aeolian module - The topography consist of stacks of discrete slabs of sand on the grid of the model domain of which below the base layer no further erosion is possible. Wind will repeating pick up slabs of sediment one by one and moving them to the next downwind cell in onshore direction. If the slab will be eroded or deposited depends on the probability p_e and p_d which represent different supply parameters and is determined for each grid cell separately. If the slab is determined not to be deposited, the slab is moved to the next cell and a new deposition assessment will take place until the slab is deposited, see Figure B.1. Besides the main sand transport process, two constraints are simulated in the model: shadow zones and avalanching caused by a steep dune slope.
2. Hydraulic module - Once every two weeks the modules takes the highest offshore tide level recorded for this period. The module simplifies the processes occurring near the water line. The module determines

the associated vertical limit of wave run-up, calculates wave dissipation across the actual topography and adjust the topography accordingly.

3. **Vegetation module** - Vegetation decreases sand transport and enhances deposition. This is modelled by changing the probabilities for erosion and deposition proportional to the vegetation cover in a cell. Erosion of sand is virtually zero once vegetation cover exceeds 15-50 percent, but it is still possible for sand grains to pass densely covered cells. Vegetation increase the slope stability, so steeper angles can be maintained. Vegetation development within vegetated cells is controlled by the growth functions following the DECAL model in which two type of vegetation can be modelled. These give the response of vegetation by defining tolerance limits to deposition and erosion and the sedimentation balance for which growth is optimal. Once full surface cover is reached, no further growth is possible.

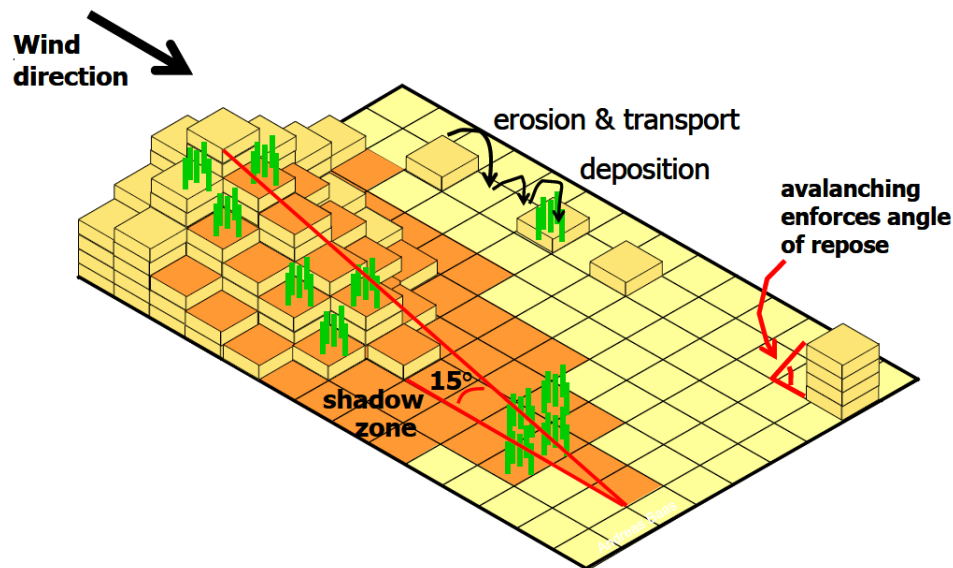


Figure B.1: Visual representation of DECAL - algorithm. Copied from

B.2.1. Spatial and temporal scales

- In cross-shore direction: mean water line till 50 m landwards of the original foredune crest and in along-shore direction: 25-100 meters
- Grid resolution: 1 m horizontal and 0.1 m vertical (slab height)
- Time steps: After a certain amount of iterations of the dune module, representing two weeks, the beach module will give an update. The vegetation module will give an update once a year.
- Simulation period: Years to decades

B.3. Application to Hondsbossche Dunes

1. **strengths** - The model successfully incorporates biogeomorphic and marine processes involved in dune building which allow for a realistic simulation of coastal dune development. It provides a connection between the description of large scale processes like wind flow and small-scale processes like sand transport and vegetation growth.
2. **weaknesses or lacks** - A detailed description of the supply processes near the water line and on the beach. Furthermore, the description of the wind forcing on sediment supply is rather simplified described.

C

Data Availability

C.1. Bathymetry

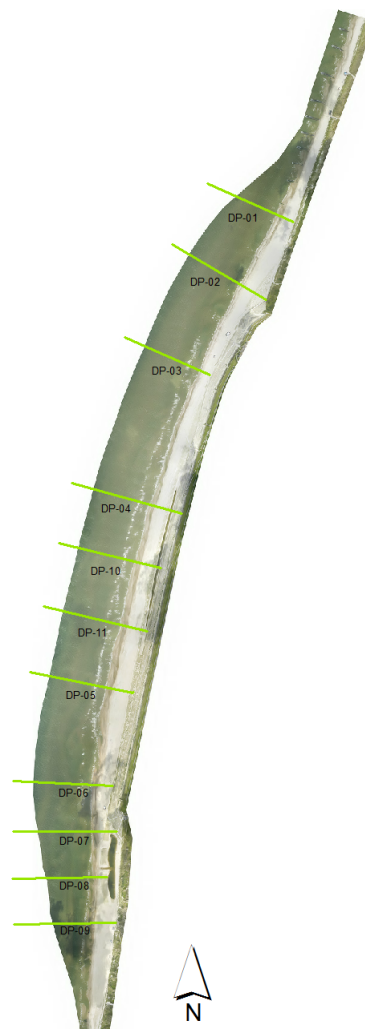


Figure C.1: Aerial picture of the Hondbossche Dunes with in green the 11 transects monitored for the bathymetry.

C.2. Topography

C.2.1. Comparison Two Airborne LiDAR Datasets

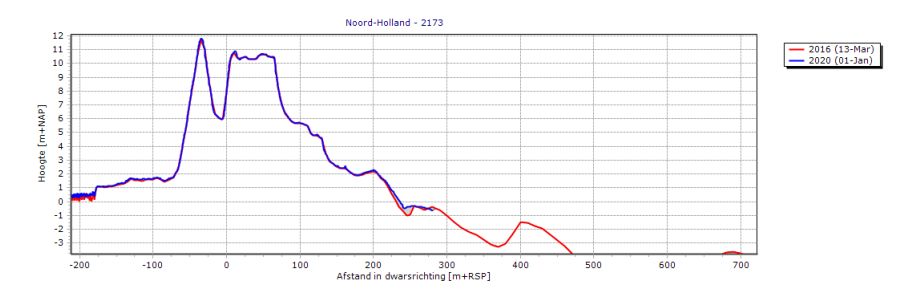


Figure C.2: Comparison of LiDAR surveys at RSP 21.73 executed by Rijkswaterstaat (in red) and the contractor (in blue) in Spring 2016.

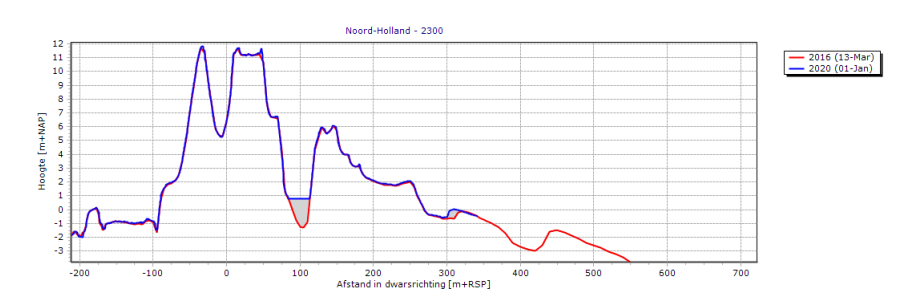


Figure C.3: Comparison of LiDAR surveys executed by Rijkswaterstaat at RSP 23.00 (in red) and the contractor (in blue.) in Spring 2016

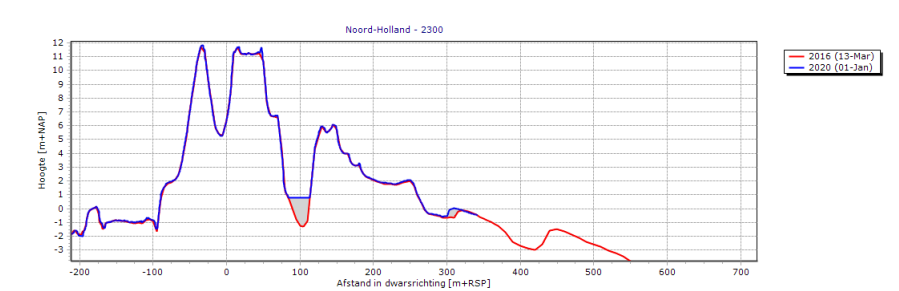


Figure C.4: Comparison of LiDAR surveys executed by Rijkswaterstaat at RSP 24.27 (in red) and the contractor (in blue) in Spring 2016.

C.2.2. Locations Dune Valley

Extra measurements has taken place at the location of dune valley and the lagoon to obtain information about the morphological development under water since may 2015. Only during the first measurement campaign in May 2015 (T0) the bathymetry of the dune valley and lagoon has been measured. The dune valley is measured for the second time on 6 October 2016 and and third time in March 2016 by using RTK GPS. In Figure C.5 the locations of the measured transects are provided.



Figure C.5: Measured transects dune valley at the location of profile type 4.

C.2.3. Grain Size Measurements

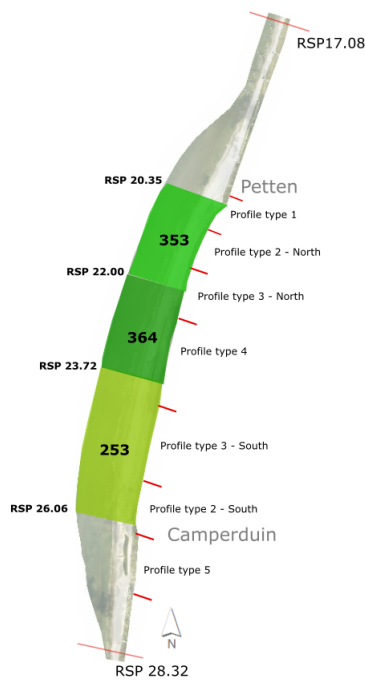


Figure C.6: Aerial picture of the Hondsbossche Dunes which shows the D_{50} per dune area. The five different dune profile types are indicated by the red lines.



Climatic Conditions

D.1. Wind

In order to choose a representative wind climate for the location of the HD-system, the data- locations of IJmuiden were compared with the data-locations of Den Helder. The station of Den Helder is located at the south-east side of Den Helder, at the airport 'De Kooy', and is 35 kilometres east of the HD-system. Figure D.1a and Figure D.1b provide information about the occurred wind climate for the location of Den Helder. The average climate for the period 1981-2015 in Figure D.1a shows that lower wind speeds were measured at the location of Den Helder compared to IJmuiden in Figure 3.9b. The wind climate within the period T0-T4 in Figure ?? does show a record of lower wind speeds as well. It is therefore chosen to use wind data of IJmuiden as a representative wind climate for Petten.

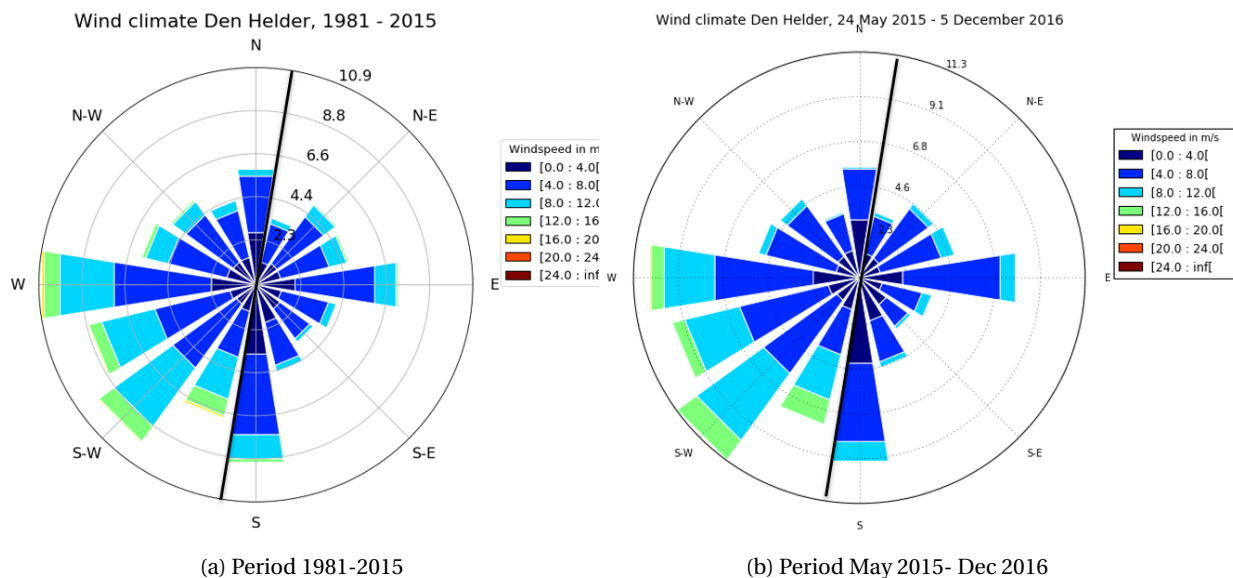
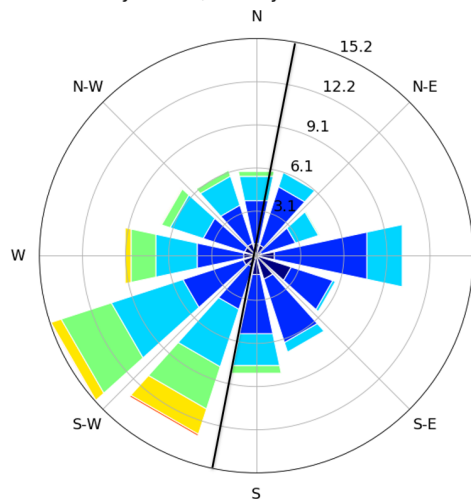


Figure D.1: Wind climate Den Helder, the average coastline orientation of the HD-system is plotted.

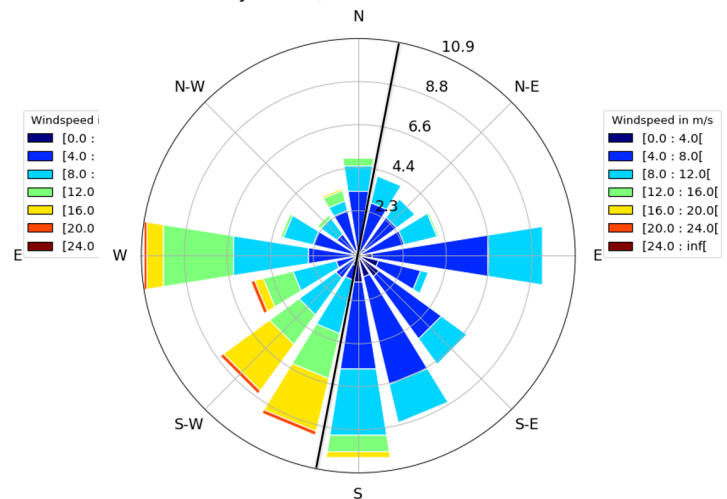
The wind rose for the period 24 May 2015 - 28 December 2015 (T0-T1) is plotted in Figure D.2a, the period 28 December 2016 - 21 March 2016 (T1-T2) in Figure D.2b, the period 21 March 2016 - 1 September 2016 (T2-T3) in Figure D.3a and the period 1 September 2016 - 5 December 2016 (T3-T4) in Figure D.3b. In each plot the average coastline orientation of approximately 15-20 degrees is plotted. In the period T0-T1 the wind blow predominantly from south-west direction, together with the highest wind speeds. This changed to west for the period T1-T2, but the largest frequency of high wind speed occurred for the south-west to south direction. Again, in the period T2-T3 there was a predominantly south-western wind. The wind rose for the period T3-T4 states that during this period wind was blowing from eastern direction. It can be noticed that within the period March 2016 to December 2016 T2-T4 lower wind speeds were measured.

Wind climate IJmuiden, 24 May 2015 - 5 December 2016



(a) Period May 2015-Dec 2015

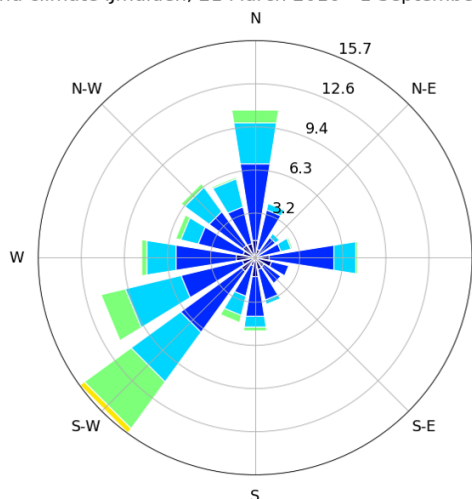
Wind climate IJmuiden, 28 Dec 2015 - 21 March 2016



(b) period Dec 2015 - March 2016

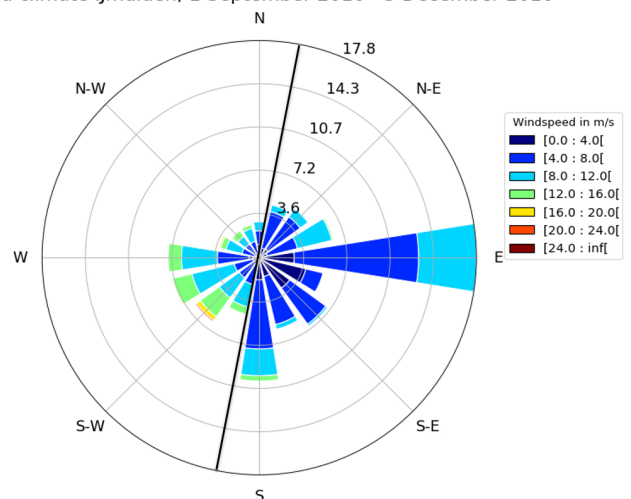
Figure D.2: Wind climate IJmuiden, the average coastline orientation of the HD-system is plotted.

Wind climate IJmuiden, 21 March 2016 - 1 September 2016



(a) Period March 2016 - September 2016

Wind climate IJmuiden, 1 September 2016 - 5 December 2016



(b) Period September 2016 - December 2016

Figure D.3: Wind climate IJmuiden, the average coastline orientation of the HD-system is plotted.

Figure D.5 shows the measured winds speed periodically in a histogram. All the histograms show that no wind speeds higher than 20 m/s were measured. The peak of the histograms is at a height with a speed of 4-8 m/s. As mentioned earlier a wind speed in the order of 5-10 m/s is needed to transport sediments by wind. Figure D.6 shows the wind speeds for only onshore directed winds in a histogram for the average climate within the period 1981-2015 and the period 24 May 2016 to 5 December 2016. Both histograms show a similar pattern, with a peak at 4 - 8 m/s, compared to the histogram considering all wind directions, displayed in Figure D.4

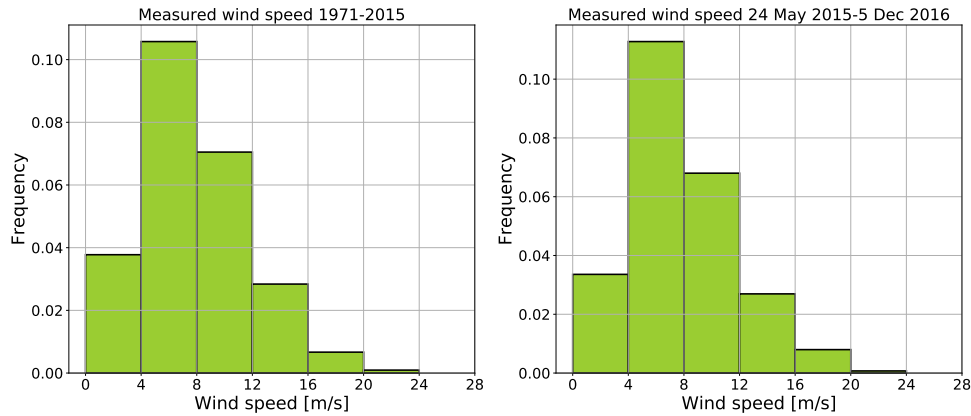


Figure D.4: Wind climate IJmuiden: the occurrence of wind speed. The left figure depicts the period 1981-2015 and the right figure depicts the period May 2015 - Dec 2016 (T0-T4).

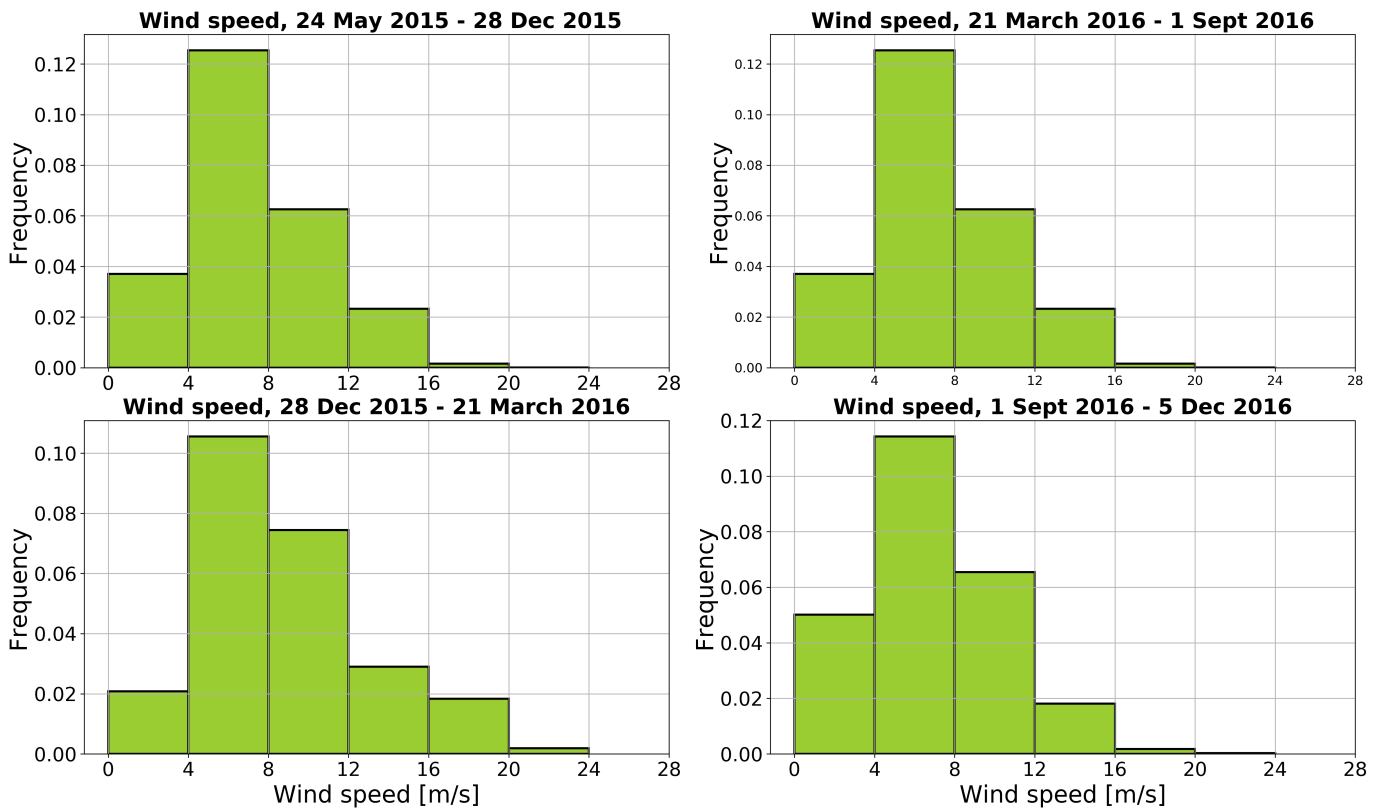


Figure D.5: Wind climate IJmuiden, occurrence of wind speed. Upper left: May 2015 - Dec 2015 (T0-T1), upper right: December 2015 - March 2016 (T1-T2), lower left: March 2016 - Sept 2016 (T2-T3), lower right: Sept 2016 - Dec 2016 (T3-T4).

D.2. Waves

The wave roses for the period 24 May 2015 - 28 December 2015 (T0-T1) is plotted in Figure D.7a), the period 28 December 2015 - 21 March 2016 (T1-T2) in Figure D.7b). The waves are predominantly coming from the south-west which also include the highest measured waves. This is also seen in the wind conditions. Furthermore, waves travelling from the North-West show a high frequency of occurrence. A detailed look into

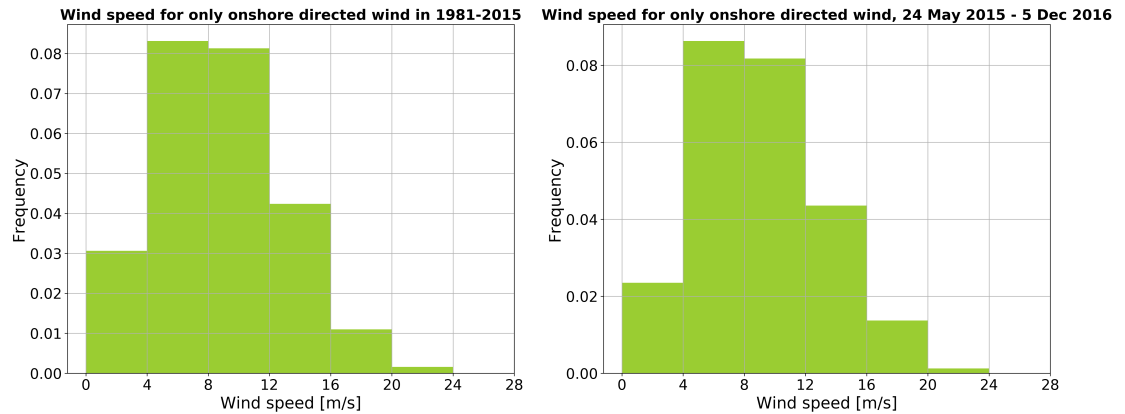


Figure D.6: Wind climate IJmuiden, occurrence of wind speed of onshore directed wind. Left: 1981-2015 and right: May 2015 - December 2016 (T0-T4).

the figures of the period T0-T1 (Figure D.7b) and the period T1-T2 (Figure D.7b), show that the highest waves were measured during the winter season from December 2015 - March 2016 (T1-T2).

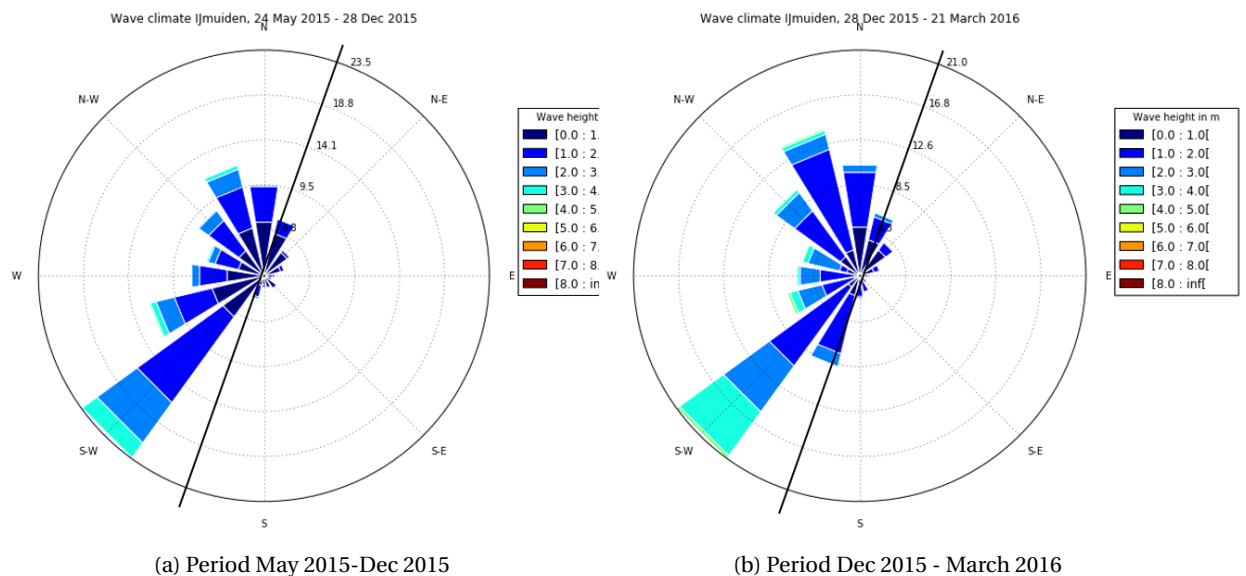


Figure D.7: Wave climate IJmuiden, period Dec 2015 - March 2016, the average coastline orientation of the HD system is plotted

D.3. Tidal Levels

Figure D.8 shows the yearly minimum recorded water levels at the location of Petten-Zuid for the period 1977-2015. The minimum water level for the period T0-T1 is approximately 10 centimetres higher than average.

Storm Surges

Data about storm surges stated that two relevant storms have happened for this coastal stretch. The first storm occurred at 13th and 14th of November 2015, it was a westerly storm on a Beaufort scale 7-8 [Watermanagementcentrum, 2015a]. The storm occurred during the lowest spring tide of the month. At Den Helder, 30 kilometres northwards the HD system, the measured water level was 2.11 meters which is a water level with a frequency of once in the year. The second storm occurred in the evening and night of 29 to 30 November 2015. Again, it was a western storm on a Beaufort scale of 8 [Watermanagementcentrum, 2015b]. It was a few

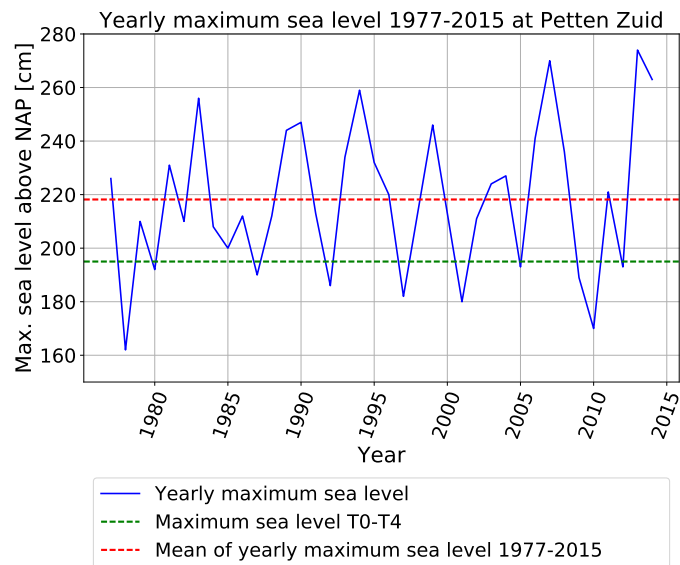
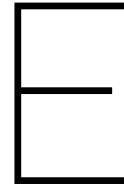


Figure D.8: Tidal level Petten-Zuid, yearly minimum sea level for the period 1977-2015. In red: the mean of the yearly minimum sea level for the period 1977-2015. In green: the minimum sea level recorded between May 2015 and December 2016.

days after spring tide and the measured water level at Den Helder was 1.92 meters. This maximum water level occurs 1-2 times a year.



Definition of Cross-shore Transects

E.1. Location of cross-shore transects

Figure E.1 provides depicts the locations of the 135-cross-shore transect along the HD system and the Northern and Southern located dunes.

E.1.1. Discarded transects transects

Originally, 143 transects were derived within the project boundaries of RSP 17.08 to RSP 28.32 within a distance of less than 250 meters from each other. The final data-analyses have taken place for 135 transects, see Figure E.1. Eight profile were discarded for different reasons, see Table E.1.

RSP- number	Reason
17.63	No data within the cross-profile
18.08	No data within the cross-profile
20.23	Construction works May 2015 - December 2015
20.58	Construction works May 2015 - December 2015
22.00	Construction works May 2015 - December 2015
22.83	Construction works May 2015 - December 2015
26.54	Location of the lagoon inlet
27.20	At the location of beach building- no data

Table E.1: Deleted transects for further analyses

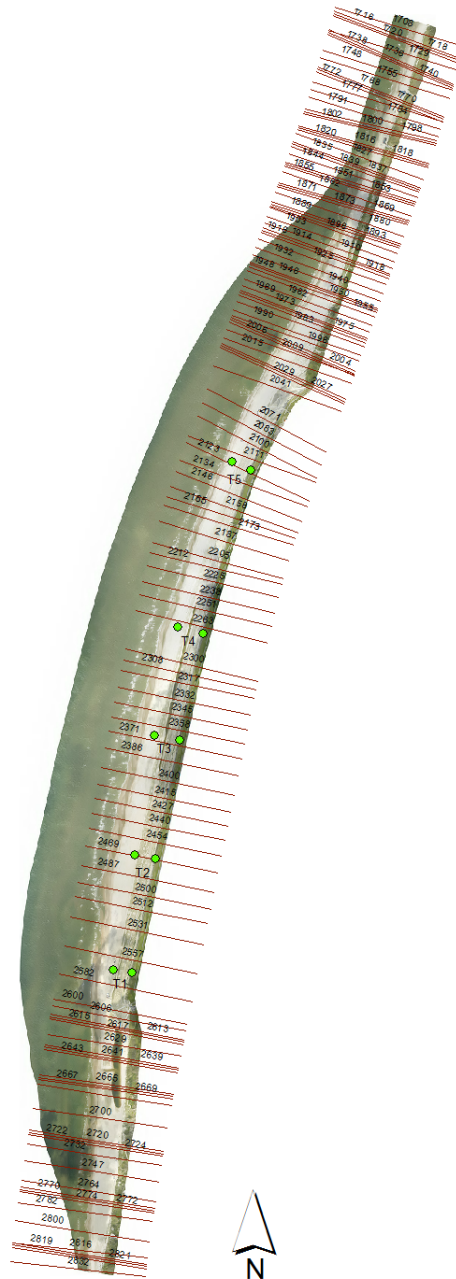


Figure E.1: Aerial picture of the Hondsbossche Dunes with in green the 135 transects analysed for aeolian sediment supply.

Table E.2: Overview of the cross-shore transects and related profile types and subdomains.

RSP number	Profile type	Subdomain	RSP number	Profile type	Subdomain
1708	Northern Dunes	-	2041	Type 1	2
1716	Northern Dunes	-	2071	Type 1	2
1718	Northern Dunes	-	2083	Type 1	2
1720	Northern Dunes	-	2100	Type 2	2
1729	Northern Dunes	-	2111	Type 2	2
1736	Northern Dunes	-	2123	Type 2	2
1738	Northern Dunes	-	2134	Type 2	2
1740	Northern Dunes	-	2146	Type 3	2
1748	Northern Dunes	-	2158	Type 3	2
1755	Northern Dunes	-	2165	Type 3	2
1768	Northern Dunes	-	2173	Type 3	2
1770	Northern Dunes	-	2187	Type 3	2
1772	Northern Dunes	-	2205	Type 3	3
1777	Northern Dunes	-	2212	Type 3	3
1784	Northern Dunes	-	2225	Type 3	3
1791	Northern Dunes	-	2238	Type 3	3
1798	Northern Dunes	-	2251	Type 4	3
1800	Northern Dunes	1	2263	Type 4	3
1802	Northern Dunes	1	2300	Type 4	3
1816	Northern Dunes	1	2308	Type 4	3
1818	Northern Dunes	1	2317	Type 4	3
1820	Northern Dunes	1	2332	Type 4	3
1827	Northern Dunes	1	2345	Type 4	3
1835	Northern Dunes	1	2358	Type 4	3
1837	Northern Dunes	1	2371	Type 4	3
1839	Northern Dunes	1	2386	Type 4	3
1844	Northern Dunes	1	2400	Type 4	4
1851	Northern Dunes	1	2415	Type 3	4
1853	Northern Dunes	1	2427	Type 3	4
1855	Northern Dunes	1	2440	Type 3	4
1862	Northern Dunes	1	2454	Type 3	4
1869	Northern Dunes	1	2469	Type 3	4
1871	Northern Dunes	1	2487	Type 3	4
1873	Northern Dunes	1	2500	Type 3	4
1880	Northern Dunes	1	2512	Type 3	4
1889	Northern Dunes	1	2531	Type 3	4
1891	Northern Dunes	1	2557	Type 2	4
1893	Northern Dunes	1	2582	Type 2	4
1896	Northern Dunes	1	2600	Type 2	4
1903	Northern Dunes	1	2606	Type 2	4
1910	Northern Dunes	1	2613	Type 2	5
1914	Northern Dunes	1	2615	Type 5	5
1916	Northern Dunes	1	2617	Type 5	5
1918	Northern Dunes	1	2629	Type 5	5
1925	Northern Dunes	1	2639	Type 5	5
1932	Northern Dunes	1	2641	Type 5	5
1940	Northern Dunes	1	2643	Type 5	5
1946	Northern Dunes	1	2665	Type 5	5
1948	Northern Dunes	1	2667	Type 5	5
1950	Northern Dunes	1	2669	Type 5	5
1955	Northern Dunes	1	2677	Type 5	5
1962	Northern Dunes	1	2700	Southern Dunes	5

RSP number	Profile type	Subdomain	RSP number	Profile type	Subdomain
1969	Northern Dunes	1	2716	Southern Dunes	5
1973	Northern Dunes	1	2722	Southern Dunes	5
1975	Northern Dunes	1	2724	Southern Dunes	5
1977	Northern Dunes	1	2732	Southern Dunes	5
1983	Northern Dunes	1	2747	Southern Dunes	5
1990	Northern Dunes	1	2764	Southern Dunes	5
1996	Northern Dunes	1	2770	Southern Dunes	5
2002	Northern Dunes	1	2772	Southern Dunes	5
2004	Northern Dunes	1	2774	Southern Dunes	5
2006	Northern Dunes	1	2782	Southern Dunes	5
2009	Northern Dunes	1	2800	Southern Dunes	-
2015	Northern Dunes	1	2816	Southern Dunes	-
2025	Type 1	1	2819	Southern Dunes	-
2027	Type 1	1	2821	Southern Dunes	-
2029	Type 1	1	2823	Southern Dunes	-
			2832	Southern Dunes	-

E.2. Connection HD system - Natural dunes Petten (North)

In Table E.3 the correction volumes for the dunes are listed because of the construction of lower dunes in the period May 2015 - December 2015 (T0-T1), as can be seen in Figure E.2.

RSP- number	Corrected volumes [m^3/m]
19.96	3
20.02	1
20.04	40
20.06	1
20.09	4
20.15	22
20.23	4
20.25	9
20.27	0
20.29	3

Table E.3: Correction for dune volumes at 10 transects, because of construction works that took place between T0-T1 at the Northern shoulder.

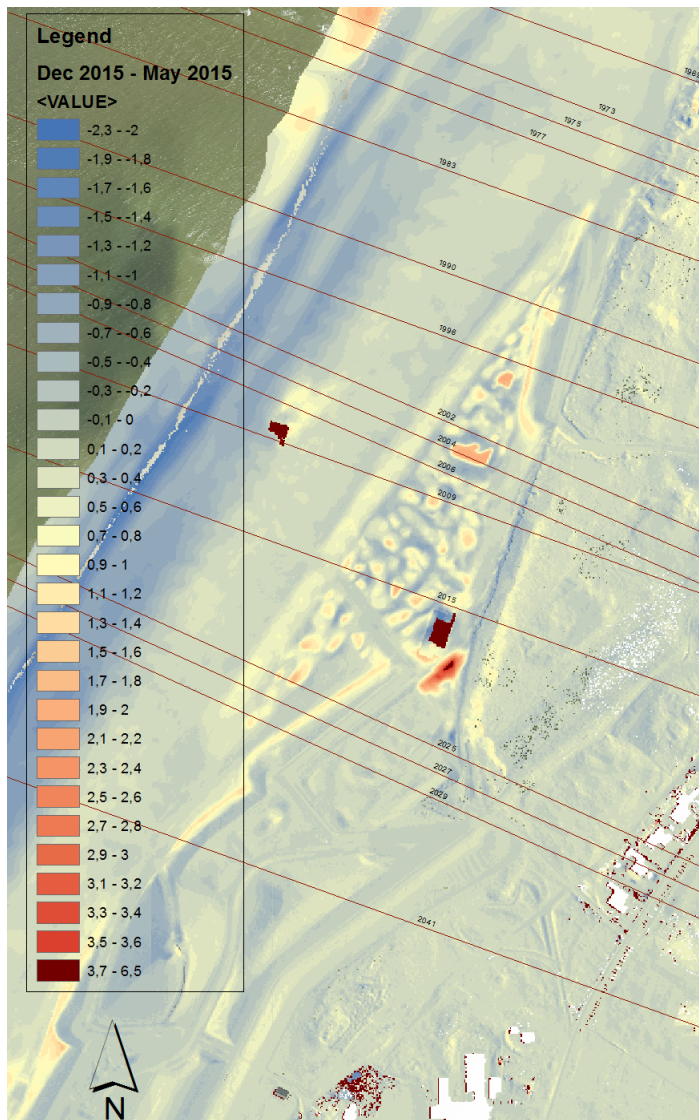
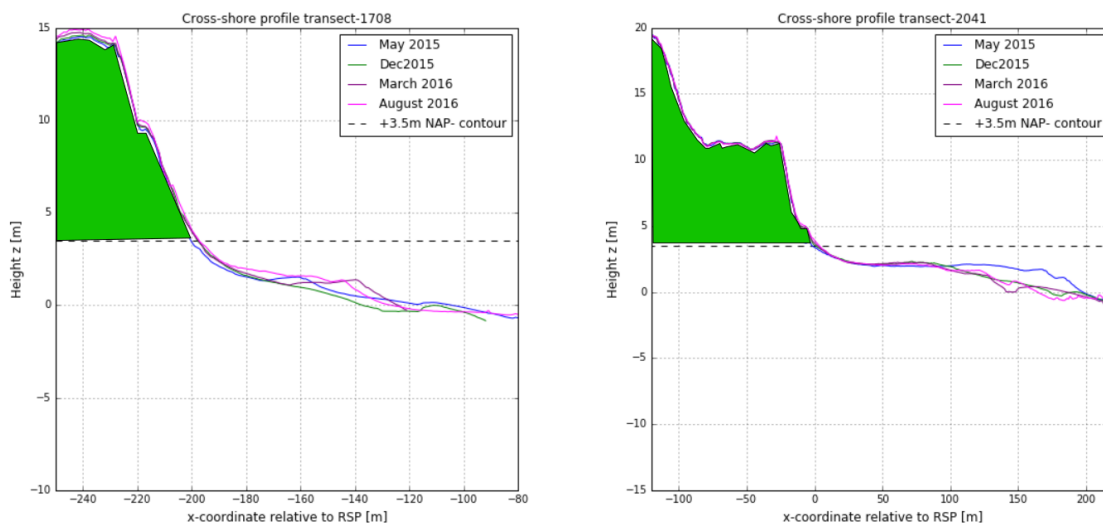


Figure E.2: Difference map of the connection between the HD system and the natural dunes North. The maps shows the bumpy pattern at the beach which is constructed between May 2015 and December 2015 (T0-T1).

F

Derivation of Beach and Dune Volumes

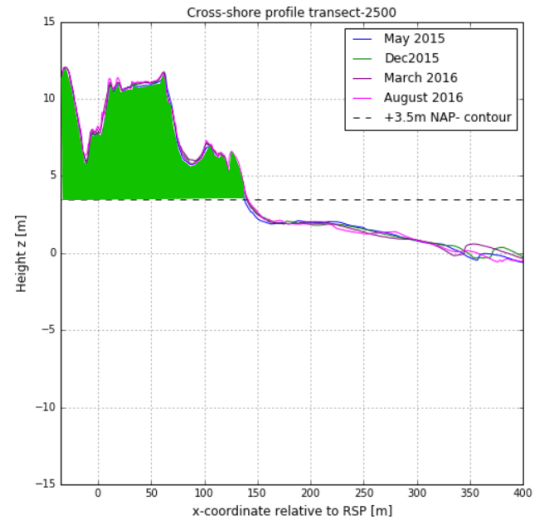
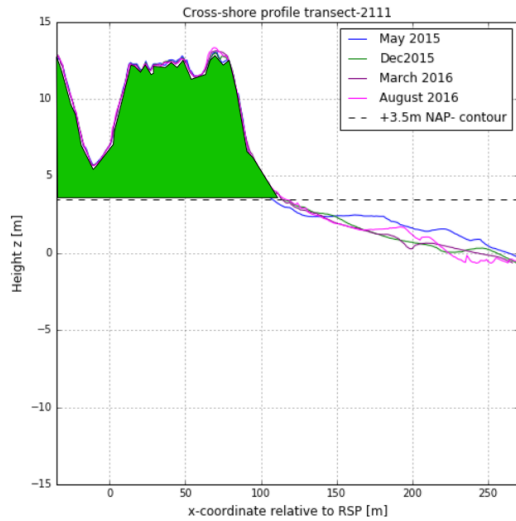
F.1. Dune volume per Profile Type



(a) Dune enclosure at Northern dunes

(b) Dune enclosure at profile type 1

Figure F.1: Dune enclosure at Northern dunes and profile type 1.

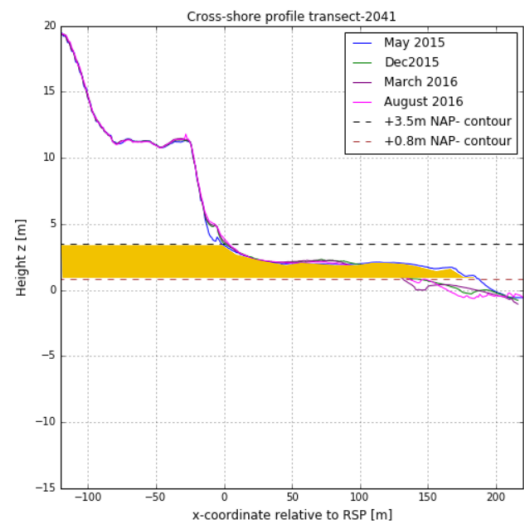
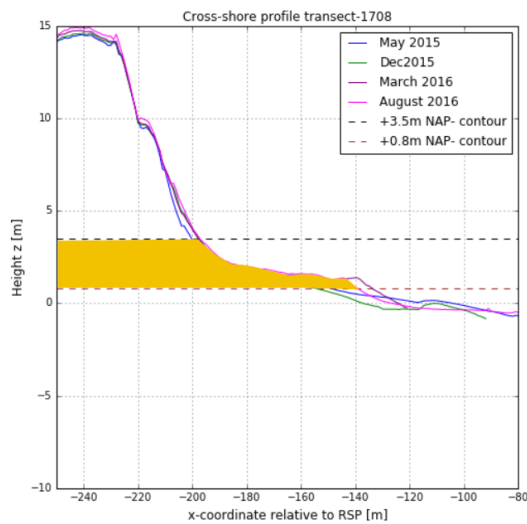


(a) Dune enclosure at profile type 2

(b) Dune enclosure at profile type 3

Figure E2: Dune enclosure at profile type 2 and 3.

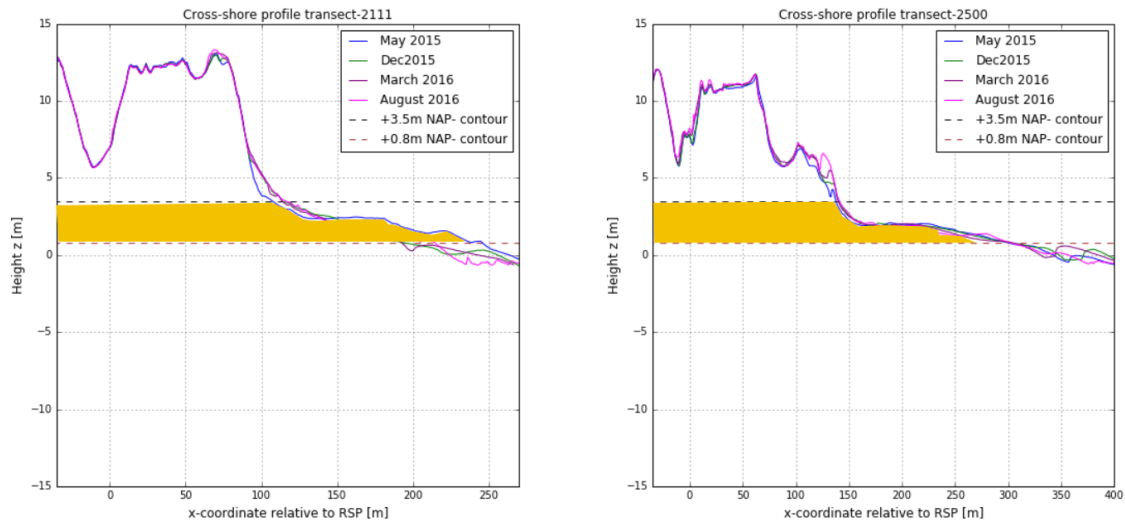
E.2. Beach volume per Profile Type



(a) Beach enclosure at Northern profiles

(b) Beach enclosure at profile 1

Figure E3: Beach enclosure at Northern dunes and profile 1.



(a) Beach enclosure at profile type 2

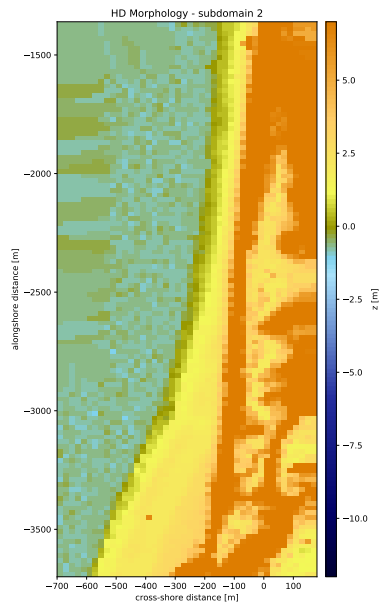
(b) Beach enclosure at profile type 3

Figure E4: Beach enclosure at profile type 2 and 3.

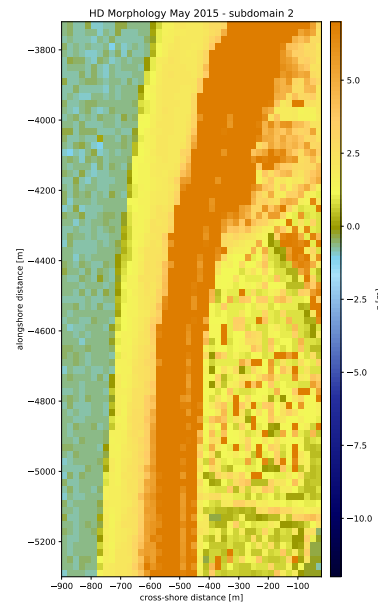
G

Model Input

G.1. Topography Hondsbossche Dunes



(a) Subdomain 1



(b) Subdomain 2

Figure G.1: Morphology May 2015 (T0) of the subdomain 1 and 2

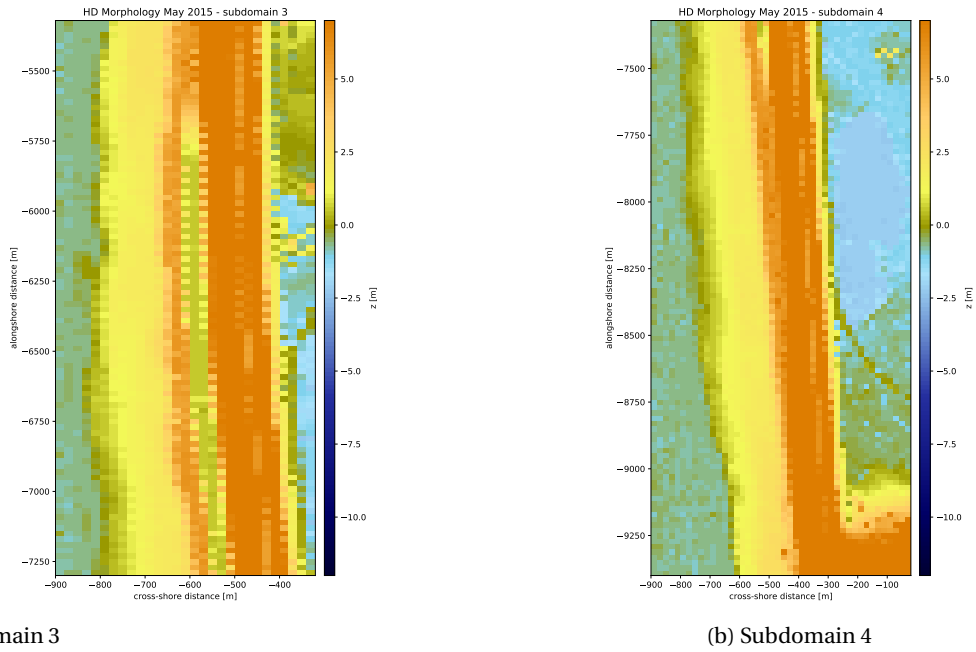


Figure G.2: Morphology May 2015 (T0) of the subdomain 3 and 4

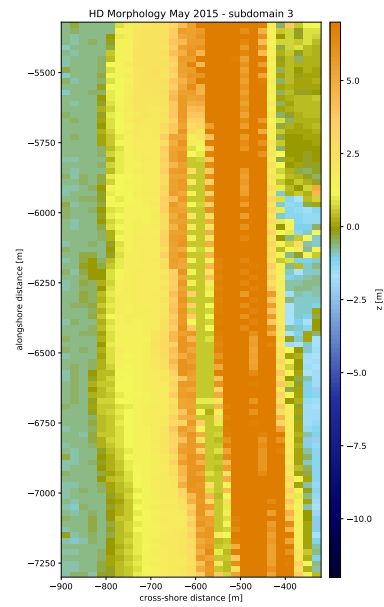


Figure G.3: Morphology May 2015 (T0) of the subdomain 5

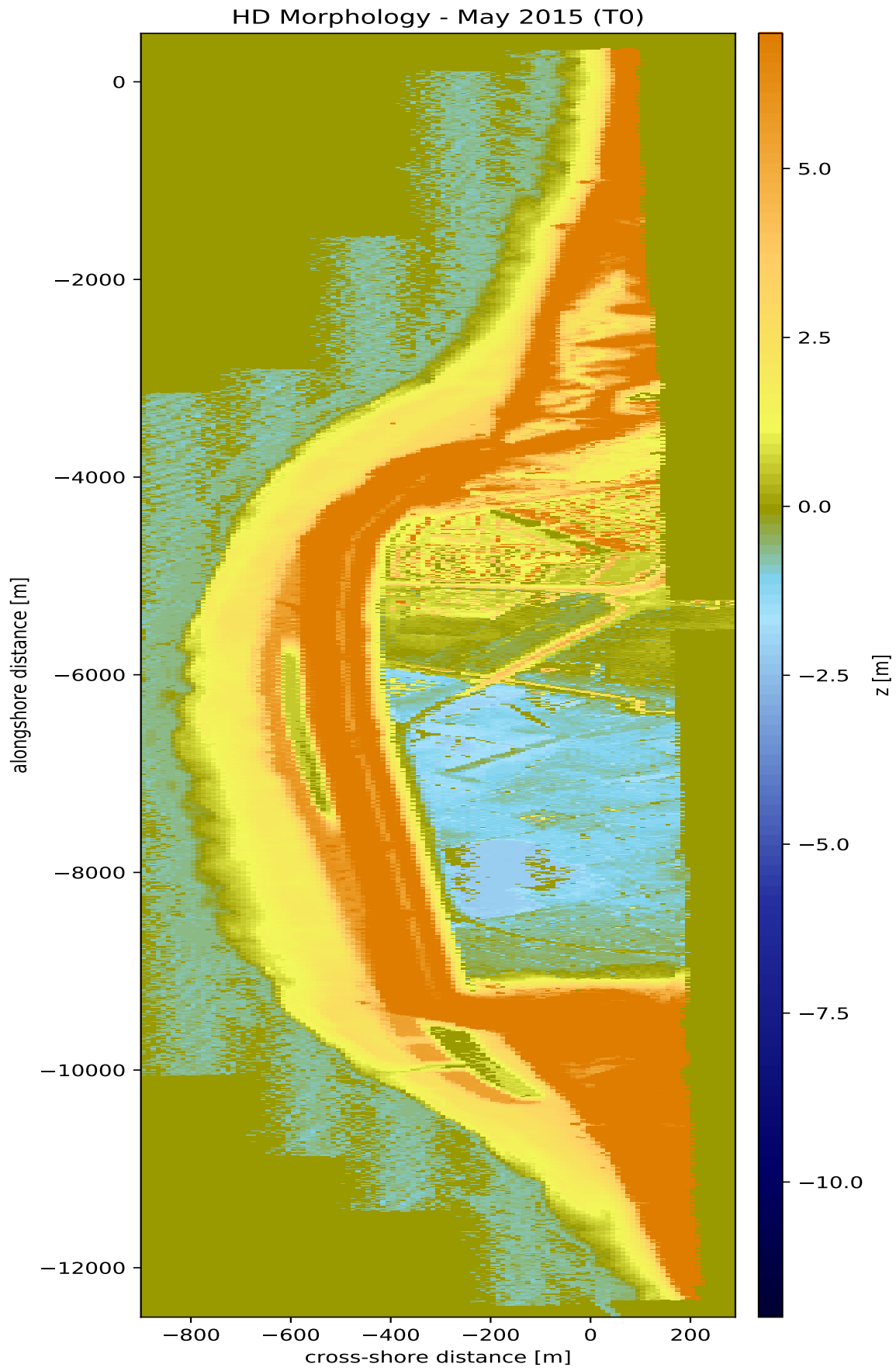


Figure G.4: Morphology May 2015 (T0) project domain

G.2. Sieving Curves

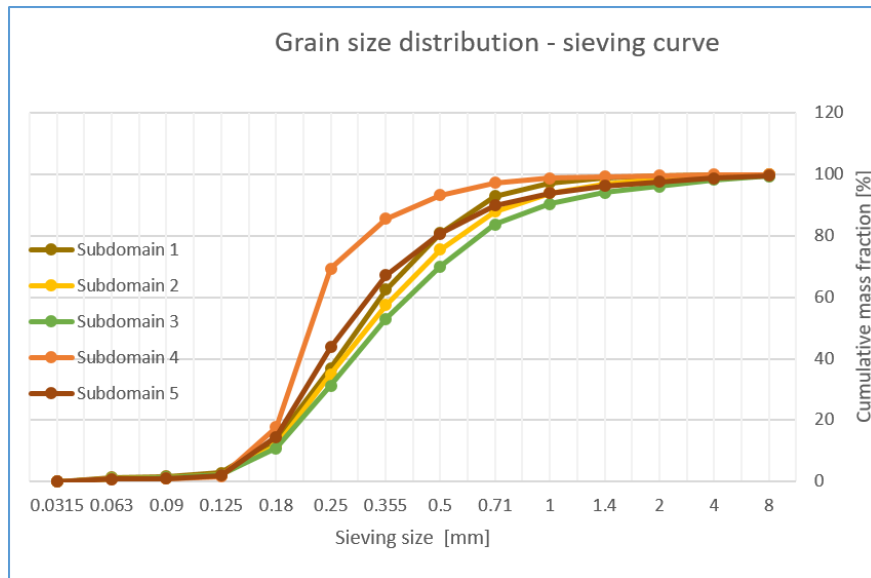


Figure G.5: Grain size distribution for the five subdomains

G.3. Model configuration files

G.3.1. Subdomain 1

Table G.1: Model input for subdomain 1

Parameter	Input or value
xgrid	x_HPZ2_may2015.txt
ygrid	y_HPZ2_may2015.txt
bed	z_HPZ2_may2015.txt
tide	tide_T0T4.txt
wave	waves_T0T4.txt
wind	wind_T0T4.txt
grain distribution	0.01038 0.00206 0.00944 0.08663 0.20413 0.21681 0.17131 0.13719 0.06550 0.03719 0.02088 0.02056 0.01281 0.00586
grain size	0.0000315 0.0000630 0.0000900 0.0001250 0.0001800 0.0002500 0.0003550 0.0005000 0.0007100 0.0010000 0.0014000 0.0020000 0.0040000 0.0080000
nfractions	14
nlayers	10
nx	29
ny	99
tstop	48556800
dt	3600
output variables	zb zs Ct Cu uw udir uth mass pickup w qs pickup.sum pickup.avg zb.sum zb.avg qs.sum qs.avg
output time	604800
T	1
bi	0.05
threshold mask	vegetation_dunes+polder_HPZ2.txt
tide mask	tides_mask_HPZ2.txt
wave mask	waves_mask_HPZ2.txt

G.3.2. Subdomain 2

Table G.2: Model input for subdomain 2

Parameter	Input or value
xgrid	x_HPZ1_may2015.txt
ygrid	y_HPZ1_may2015.txt
bed	z_HPZ1_may2015.txt
tide	tide_T0T4.txt
wave	waves_T0T4.txt
wind	wind_T0T4.txt
grain distribution	0.01000 0.00167 0.00967 0.09450 0.23367 0.22450 0.18067 0.12392 0.06008 0.03125 0.01583 0.01008 0.00350 0.00100
grain size	0.0000315 0.0000630 0.0000900 0.0001250 0.0001800 0.0002500 0.0003550 0.0005000 0.0007100 0.0010000 0.0014000 0.0020000 0.0040000 0.0080000
nfractions	14
nlayers	10
nx	44
ny	79
tstop	48556800
dt	3600
output variables	zb zs Ct Cu uw udir uth mass pickup w qs pickup.sum pickup.avg zb.sum zb.avg qs.sum qs.avg
output time	604800
T	1
bi	0.05
threshold mask	vegetation_dunes+polder_HPZ1.txt
tide mask	tides_mask_HPZ1.txt
wave mask	waves_mask_HPZ1.txt

G.3.3. Subdomain 3

Table G.3: Model input for subdomain 3

Parameter	Input or value
xgrid	x_DP2_may2015.txt
ygrid	y_DP2_may2015.txt
bed	z_DP2_may2015.txt
tide	tide_T0T4.txt
wave	waves_T0T4.txt
wind	wind_T0T4.txt
grain distribution	0.01314 0.00357 0.01129 0.10686 0.23371 0.25700 0.18243 0.12071 0.04357 0.01671 0.00571 0.00271 0.00150 0.00300
grain size	0.0000315 0.0000630 0.0000900 0.0001250 0.0001800 0.0002500 0.0003550 0.0005000 0.0007100 0.0010000 0.0014000 0.0020000 0.0040000 0.0080000
nfractions	14
nlayers	10
nx	44
ny	117
tstop	48556800
dt	3600
output variables	zb zs Ct Cu uw udir uth mass pickup w qs pickup.sum pickup.avg zb.sum zb.avg qs.sum qs.avg
output time	604800
T	1
bi	0.05
threshold mask	vegetation_dunes_DP2.txt
tide mask	-
wave mask	-

G.3.4. Subdomain 4

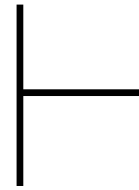
Table G.4: Model input for subdomain 4

Parameter	Input or value
xgrid	x_HPZ3_may2015.txt
ygrid	y_HPZ3_may2015.txt
bed	z_HPZ3_may2015.txt
tide	tide_T0T4.txt
wave	waves_T0T4.txt
wind	wind_T0T4.txt
grain distribution	0.00813 0.00140 0.00687 0.16013 0.51727 0.16173 0.07633 0.04067 0.01500 0.00593 0.00313 0.00247 0.00093 0.00030
grain size	0.0000315 0.0000630 0.0000900 0.0001250 0.0001800 0.0002500 0.0003550 0.0005000 0.0007100 0.0010000 0.0014000 0.0020000 0.0040000 0.0080000
nfractions	14
nlayers	10
nx	44
ny	104
tstop	48556800
dt	3600
output variables	zb zs Ct Cu uw udir uth mass pickup w qs pickup.sum pickup.avg zb.sum zb.avg qs.sum qs.avg
output time	604800
T	1
bi	0.05
threshold mask	vegetation_dunes+polder_HPZ3.txt
tide mask	tides_mask_HPZ3.txt
wave mask	waves_mask_HPZ3.txt

G.3.5. Subdomain 5

Table G.5: Model input for subdomain 5

Parameter	Input or value
xgrid	x_DC1_may2015.txt
ygrid	y_DC1_may2015.txt
bed	z_DC1_may2015.txt
tide	tide_T0T4.txt
wave	waves_T0T4.txt
wind	wind_T0T4.txt
grain distribution	0.00757 0.00164 0.00986 0.12614 0.29200 0.23393 0.13614 0.09171 0.04107 0.02243 0.01343 0.01221 0.00779 0.00407
grain size	0.0000315 0.0000630 0.0000900 0.0001250 0.0001800 0.0002500 0.0003550 0.0005000 0.0007100 0.0010000 0.0014000 0.0020000 0.0040000 0.0080000
nfractions	14
nlayers	10
nx	44
ny	89
tstop	48556800
dt	3600
output variables	zb zs Ct Cu uw udir uth mass pickup w qs pickup.sum pickup.avg zb.sum zb.avg qs.sum qs.avg
output time	604800
T	1
bi	0.05
threshold mask	vegetation_dunes_DC1.txt
tide mask	-
wave mask	-



Additional results - Data analysis

H.1. Natural dune growth north

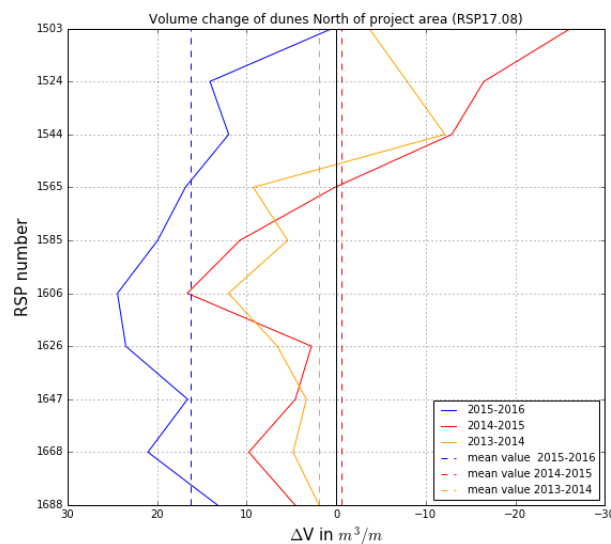


Figure H.1: Yearly dune volume change in the period 2013-2014, 2014-2015 and 2015-2016 for the transects northwards of the project area.

H.2. Morphological Change of Dune Valley

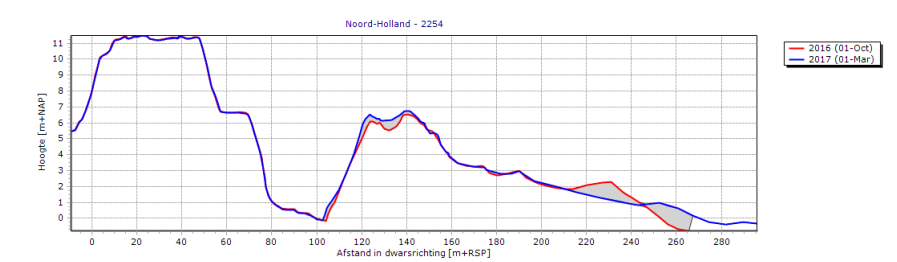


Figure H.2: Morphological change of the Dune valley at RSP 22.54 between October 2016 - March 2016

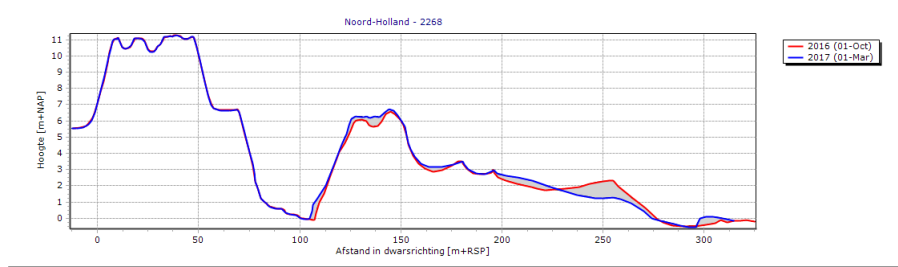


Figure H.3: Morphological change of the Dune valley at RSP 22.68 between October 2016 - March 2016

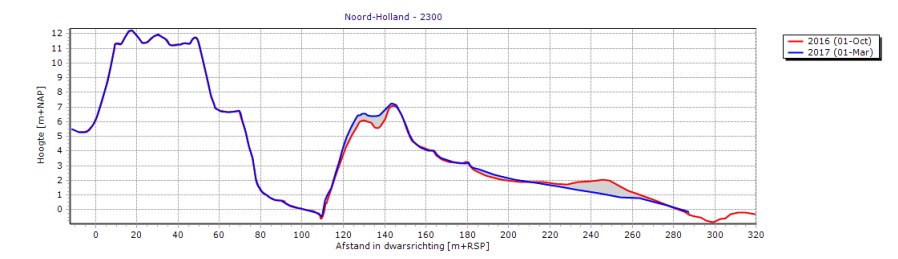


Figure H.4: Morphological change of the Dune valley at RSP 23.00 between October 2016 - March 2016

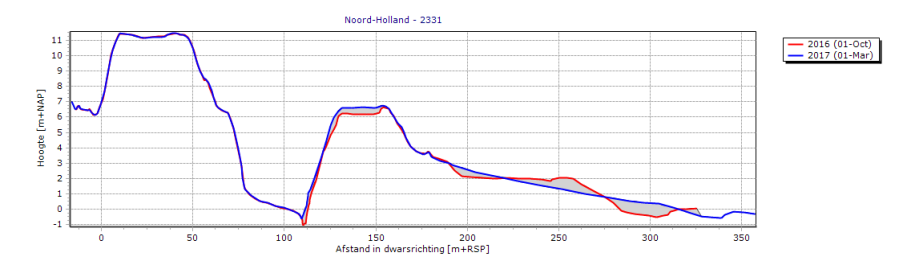


Figure H.5: Morphological change of the Dune valley at RSP 23.31 between October 2016 - March 2016

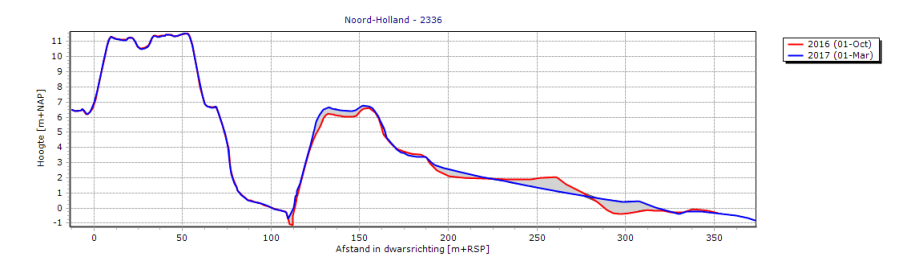


Figure H.6: Morphological change of the Dune valley at RSP 23.36 between October 2016 - March 2016

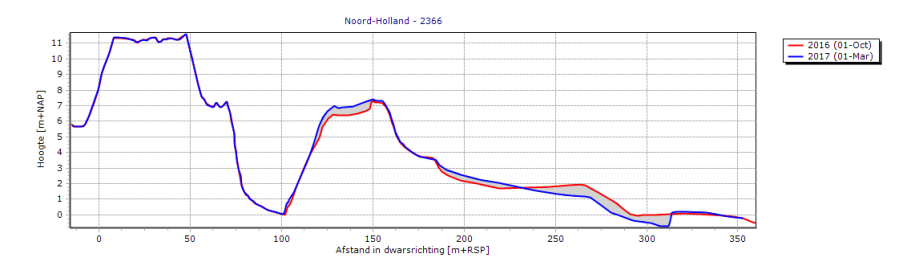


Figure H.7: Morphological change of the Dune valley at RSP 23.66 between October 2016 - March 2016

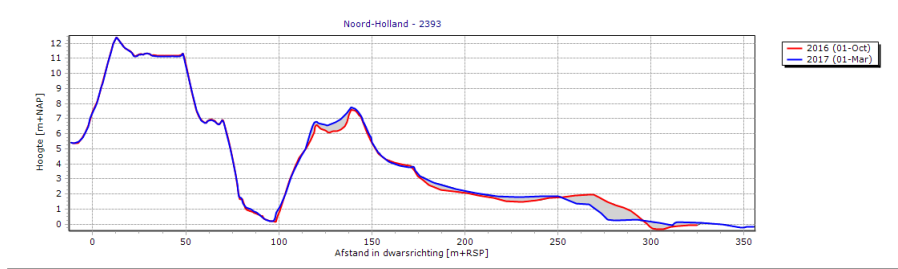
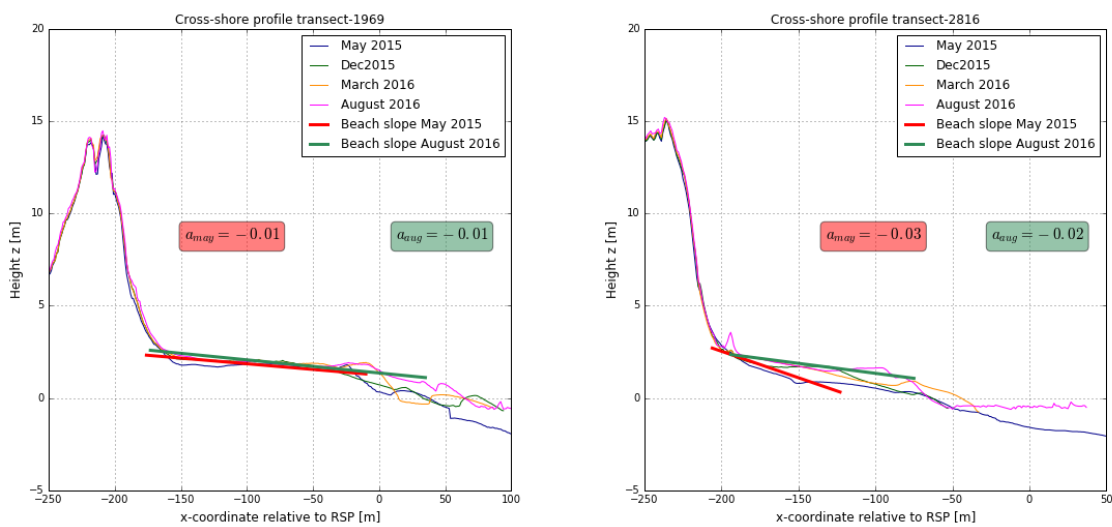


Figure H.8: Morphological change of the Dune valley at RSP 23.93 between October 2016 - March 2016

H.3. Beach Slope

H.3.1. Cross-shore profiles

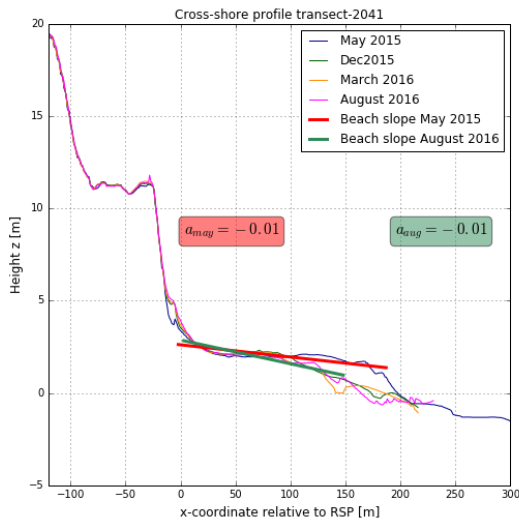


(a) Northern Dunes - accretive profile

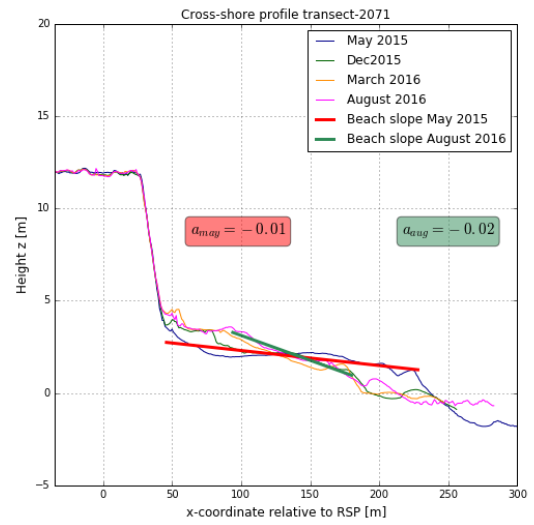
(b) Southern Dunes- accretive profile

Figure H.9: Cross-shore profile along Northern and Southern dunes.

H.3.2. Mean Beach Slope

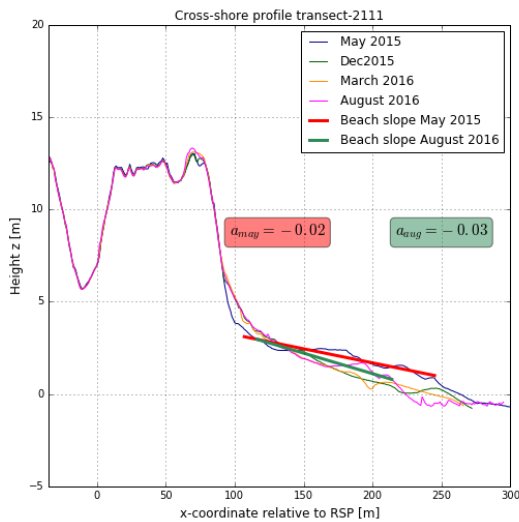


(a) Profile type 1 - erosive profile

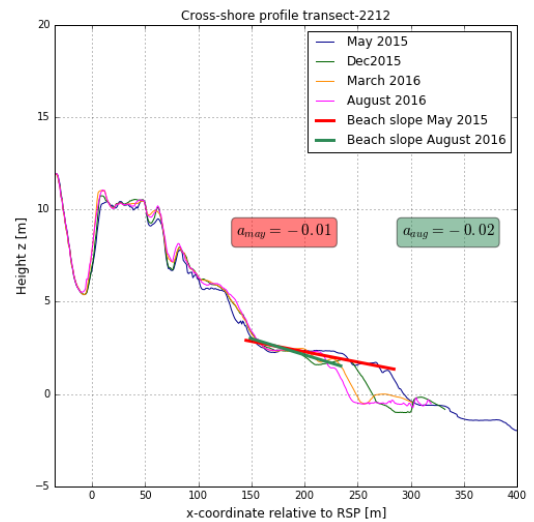


(b) Profile type 1 - erosive profile

Figure H.10: Cross-shore profile along profile type 1.

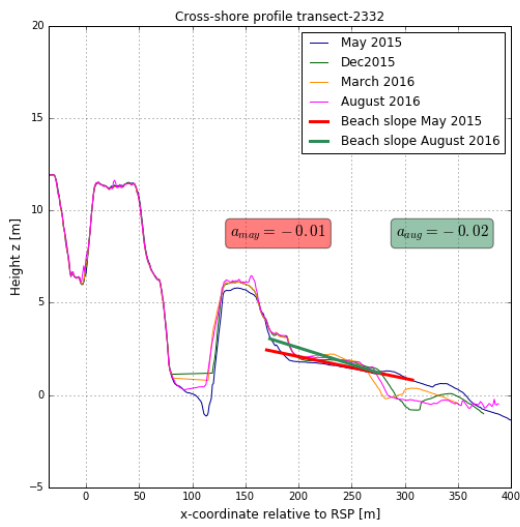


(a) Profile type 2 North - erosive profile

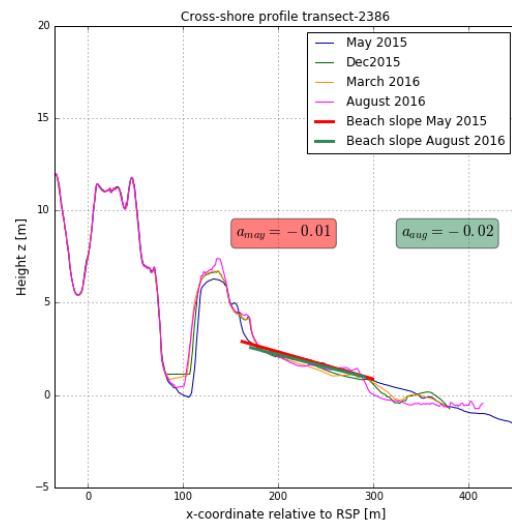


(b) Profile type 3 North - erosive profile

Figure H.11: Cross-shore profile along profile type 2 en 3 North.

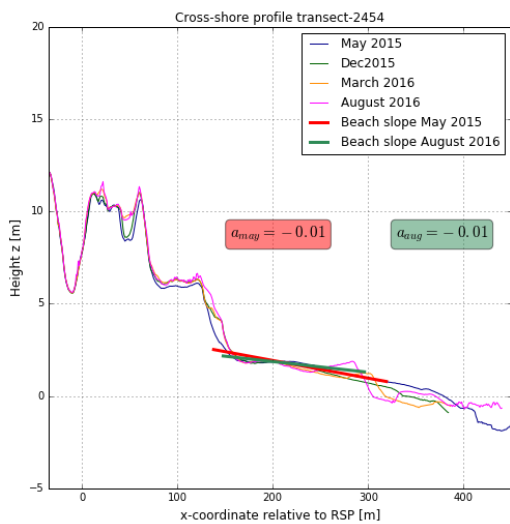


(a) Profile type 4- accretive profile

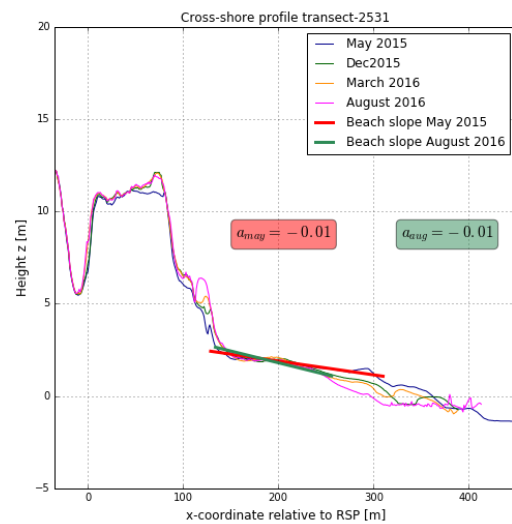


(b) Profile type 4 - erosive profile

Figure H.12: Cross-shore profile along profile type 4.

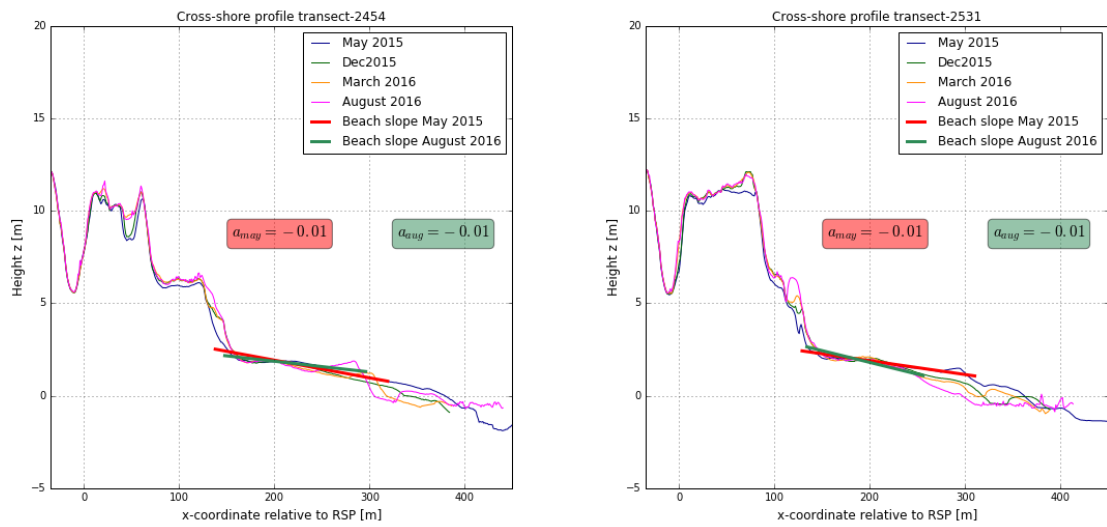


(a) Profile type 3 South- accretive profile



(b) Profile type 3 South - erosive profile

Figure H.13: Cross-shore profile along profile type 3 South.



(a) Profile type 2 South- erosive profile

(b) Profile type 5 - erosive profile

Figure H.14: Cross-shore profile along profile type 2 South and 5.

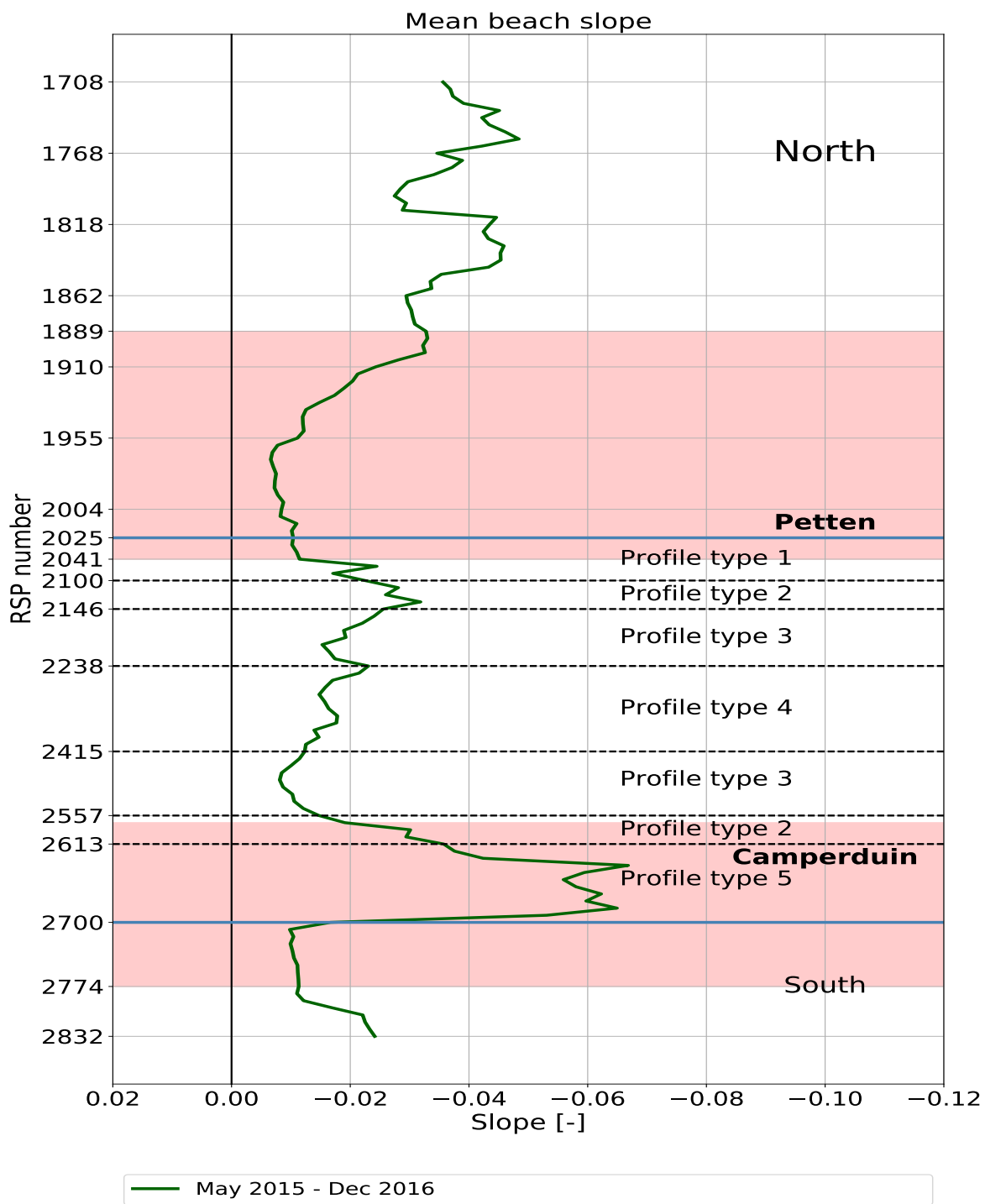


Figure H.15: Mean beach slope of the Dunes between T0-T4. The blue line indicates the boundaries of the new HD system.

H.4. Beach Width

H.4.1. MHW Position and Dune foot Position

Figure H.16 shows the position of the mean high water line (MHW) and the dune foot. Figure H.17 shows the cumulative change in MHW-position over the period T0-T4 and Figure H.18 shows the change in dune foot position over the period T0-T4. The gap in Figure H.18 is the result of the chosen method in which a fixed dune position is realized, to reduce the effect of the construction works that took place in the period T0-T1.

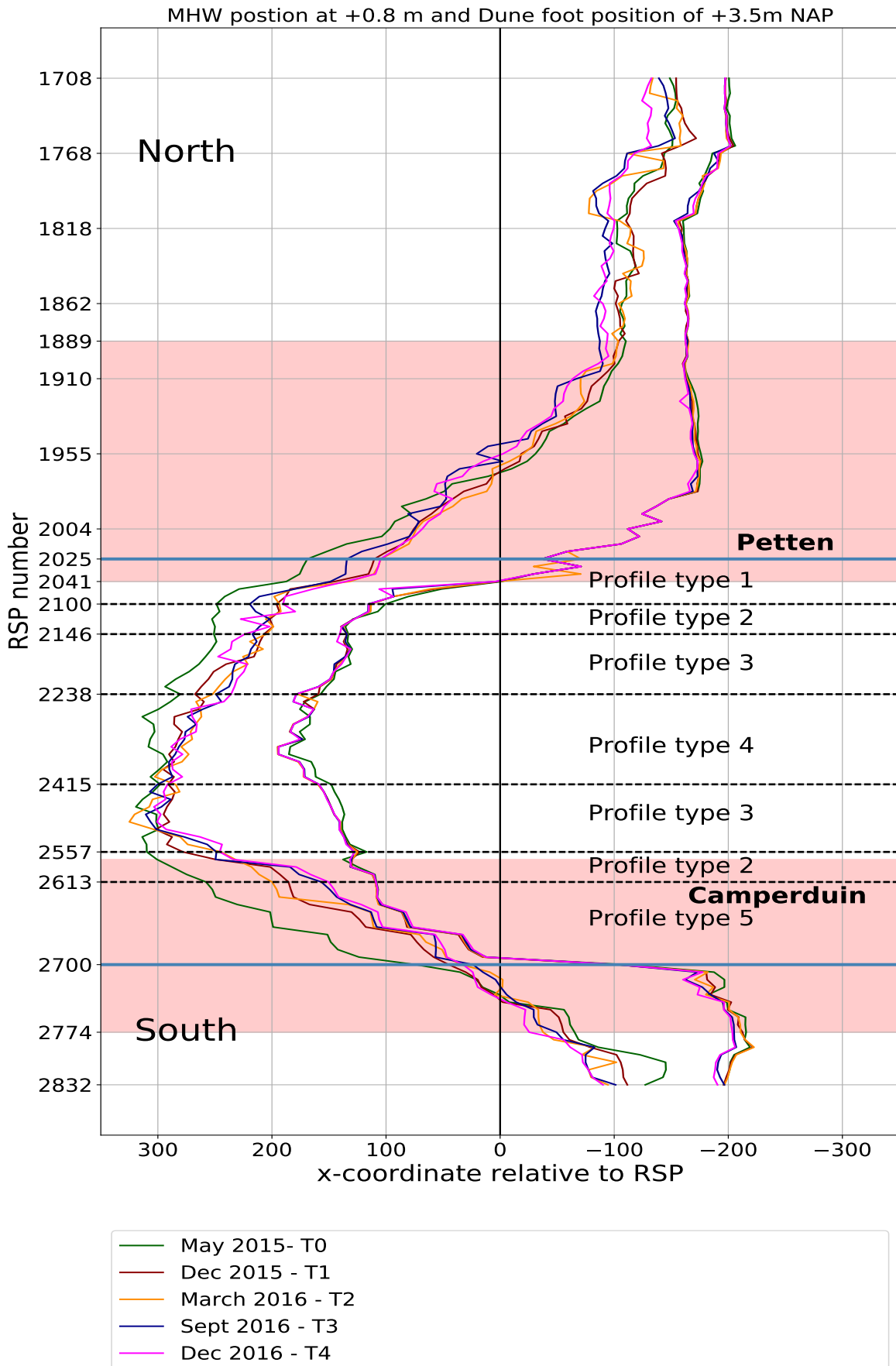


Figure H.16: Position of the MHW- line and dune foot for the four measured periods. Note that the figure has the same orientation as the Dutch coastline which means that the North is at the upper part of the figure and the South at the lower part of the figure. The sea is located at the left side of the origin and dry land is located at the right side of the origin; decrease (negative values) in beach width means that the coastal line retreats and is therefore depicted towards the right into landward direction and increase (positive values) means that the coastal line extends and is therefore depicted toward the left into seaward direction. The blue line indicates the boundaries of the new HD system and the red coloured areas indicates the locations of the northern and southern shoulder. The black dashed lines distinguish the five different dune profile types.

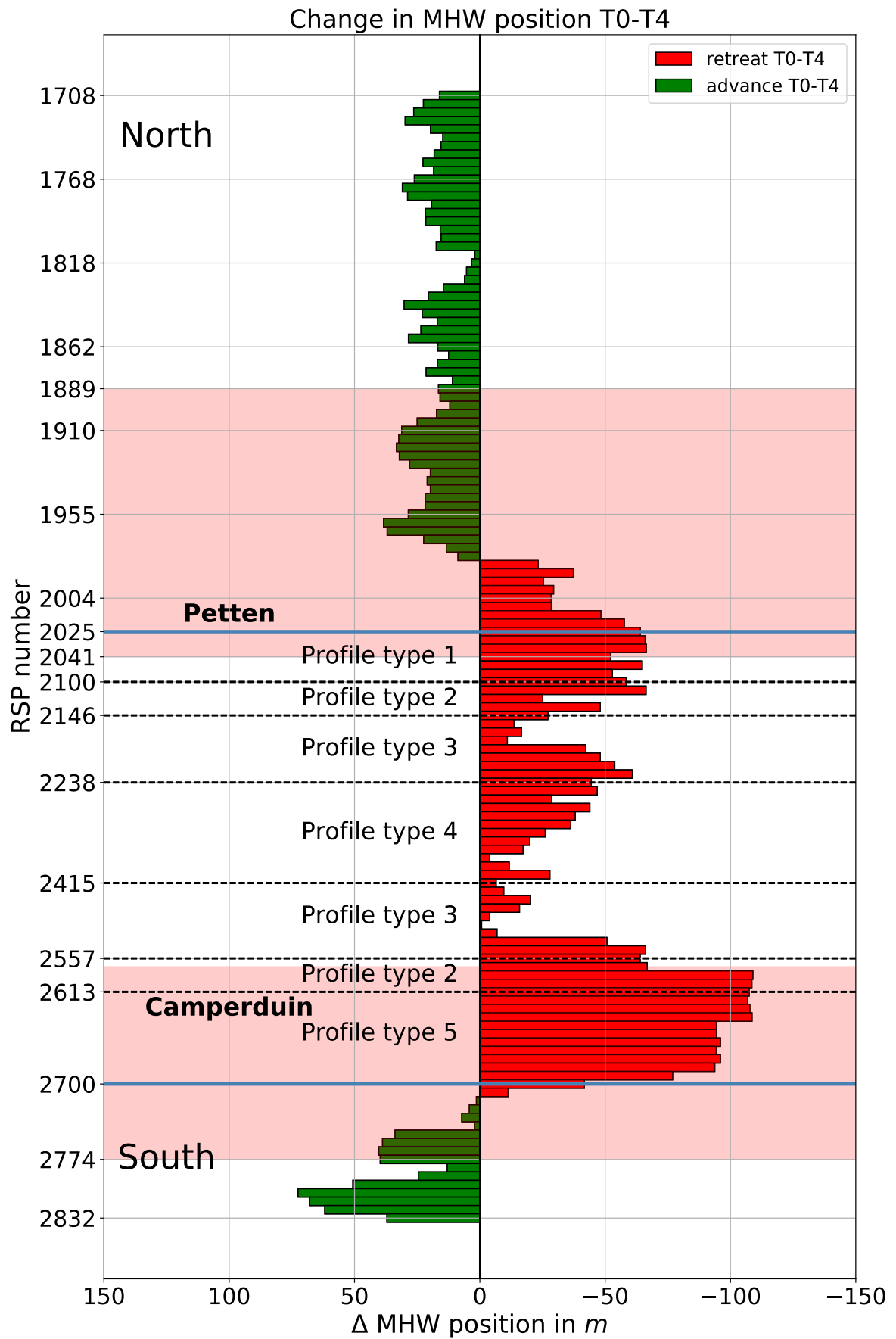


Figure H.17: Cumulative change of the MHW - position between T0-T4. The blue line indicates the boundaries of the new HD-system and the red coloured areas are the northern and southern shoulder.

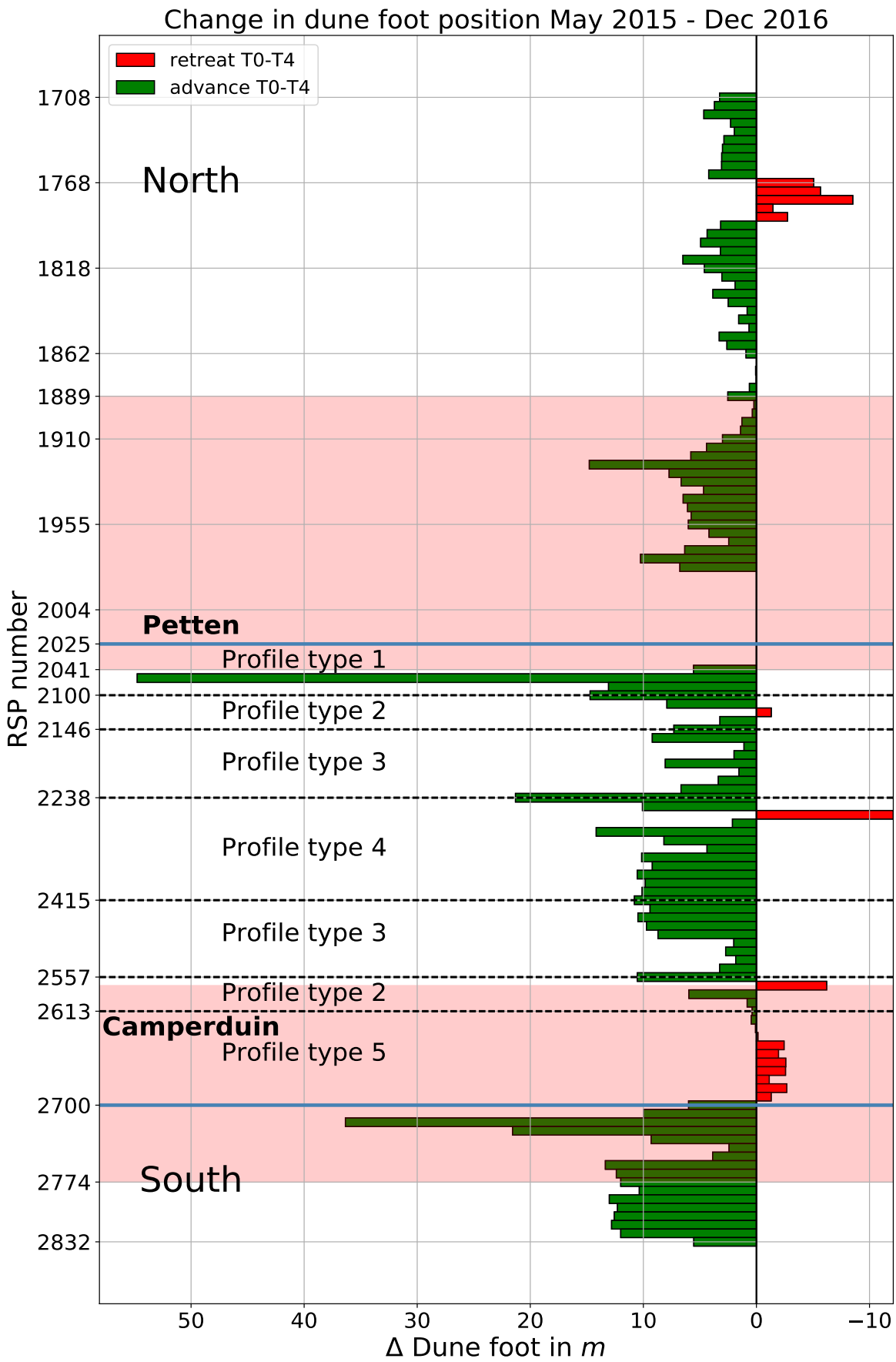


Figure H.18: Cumulative change of the dune foot position between T0-T4. In green positive values and in red negative values. The blue line indicates the boundaries of the new HD-system.

H.4.2. Correlations

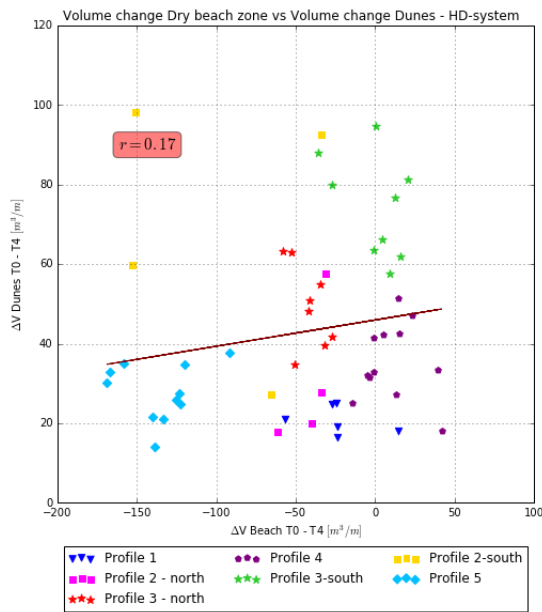


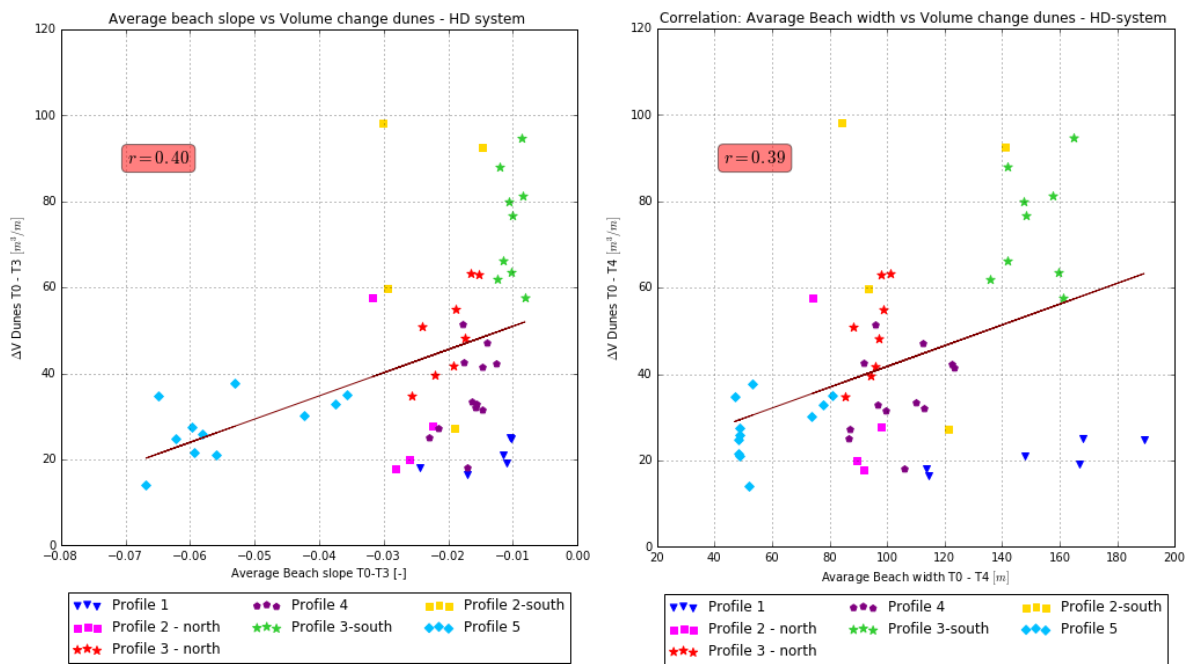
Figure H.19: Correlation between volume change of the dry beach zone (y-axis) versus dunes (x-axis) for the new dunes of the HD system. Profile type 1-5 are indicated by different colors and markers.

H.5. Results per profile type

Volume changes

Figure H.21a shows the relation between the measured volume changes of the dry beach zone for the period May 2015 - December 2016. The largest decrease in volume change is derived along dune profile 2 (South) and dune profile 5 where large spatial variations in volume change are pronounced for dune profile 2. For the Northern part of the HD system, along dune profile 1, 2 and 4 also a decrease in beach volume is found. The beaches along dune profile 3 (South) and dune profile 4 show on average an increase in beach volume.

Figure H.21b shows the relation between the measured volume changes of the dunes for the period May 2015 - December 2016. The largest dune growth rates are derived for profile 2 (South) and profile 3 (South). Also in the Northern part of the system, dune profile 3 show larger dune growth rates than the adjacent dune profiles 2 and 3. The spatial variations in dune growth are most pronounced along dune profile 2 (South).



(a) Mean beach slope

(b) Mean Beach width

Figure H.20: Correlation between mean beach slope or beach width of the dry beach zone (y-axis) against the volume change of the Dunes (x-axis) for the new dunes of the HD system in the period T0-T4 . Profile type 1-5 are indicated by different colors and markers.

Beach Slope

Figure H.22a shows the relation between the measured slope of the dry beach zone for the period May 2015 - December 2016. The figure shows that steeper slope were found in the Southern part of the project domain along dune profile 2 (Suuth) and 5. For these profiles also the largest alongshore spreading in beach slope is measured. For dune profile 1, 2 (North), 3, 4 and 3 (South) the beach slope stays rather constant, this is strongly pronounced along dune profile 3 (South).

Beach Width

Figure H.22a shows the relation between the measured width of the dry beach zone for the period May 2015 - December 2016. The figure shows that the smallest beaches are found along dune profile 5. The beaches are significantly wider at both ends of the HD system along dune profile 1 and along dune profile 3 (South). Spatial variation is largely pronounced along dune profile 1 while spatial variation is small for the adjacent beaches of dune profile 2 (North) and dune profile 3 (North).

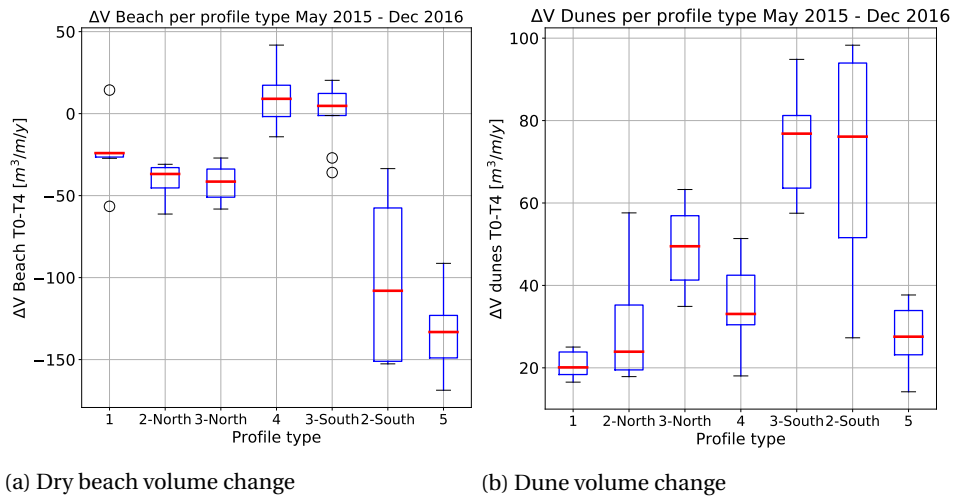


Figure H.21: Volume change of dry beach and dunes per profile

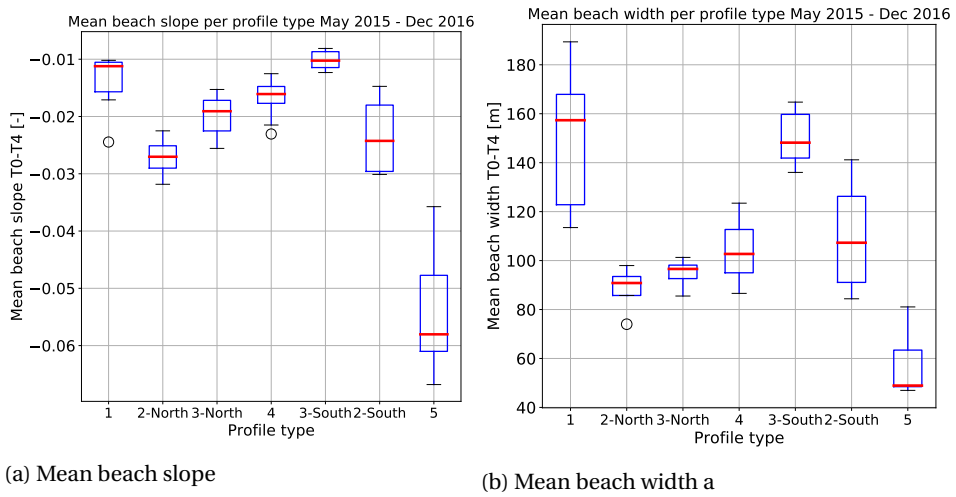


Figure H.22: Mean beach slope or beach width in the period T0-T4 for each dune profile.



Erosion and Sedimentation Plots

I.1. Full Domain

Bed level change: May 2015 - Dec 2015 (T0-T1)

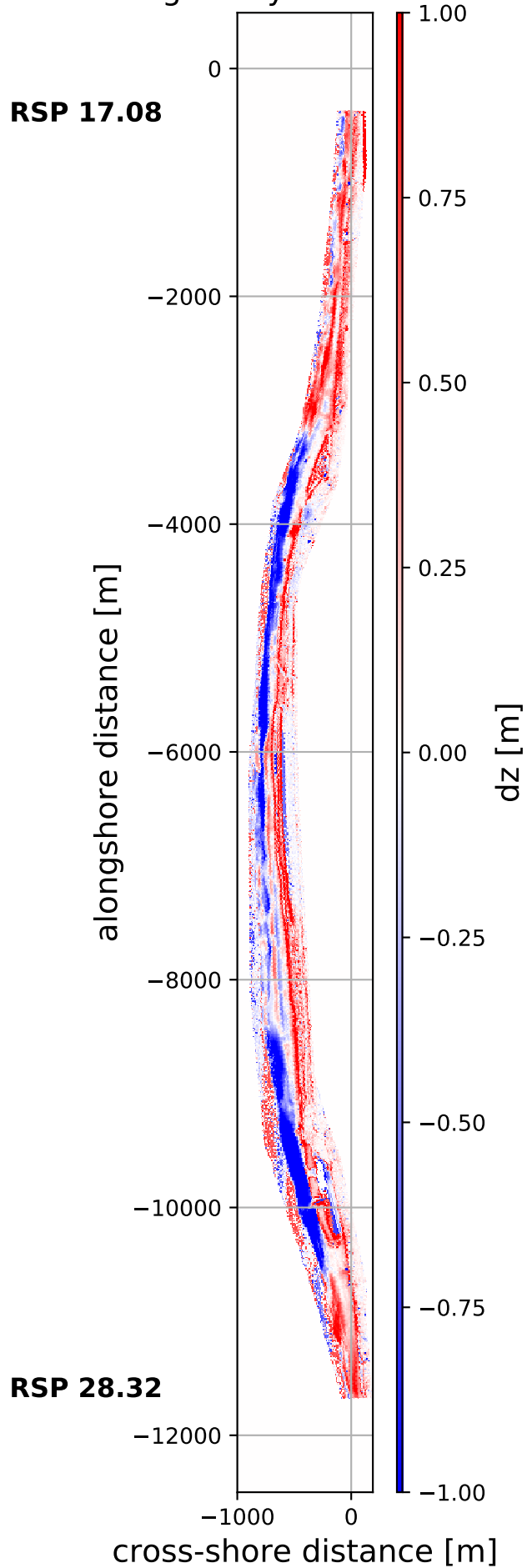


Figure I.1: Measured sedimentation (red) and erosion (blue) along the project domain between RSP 17.08 and RSP 28.32 in the period May 2015 - December 2015 (T0-T1). Note that the figure has the same orientation as the Dutch coastline in which North is at the upper part of the figure and South is at the lower part of the figure.

Bed level change: May 2015 - Dec 2016 (T0-T4)

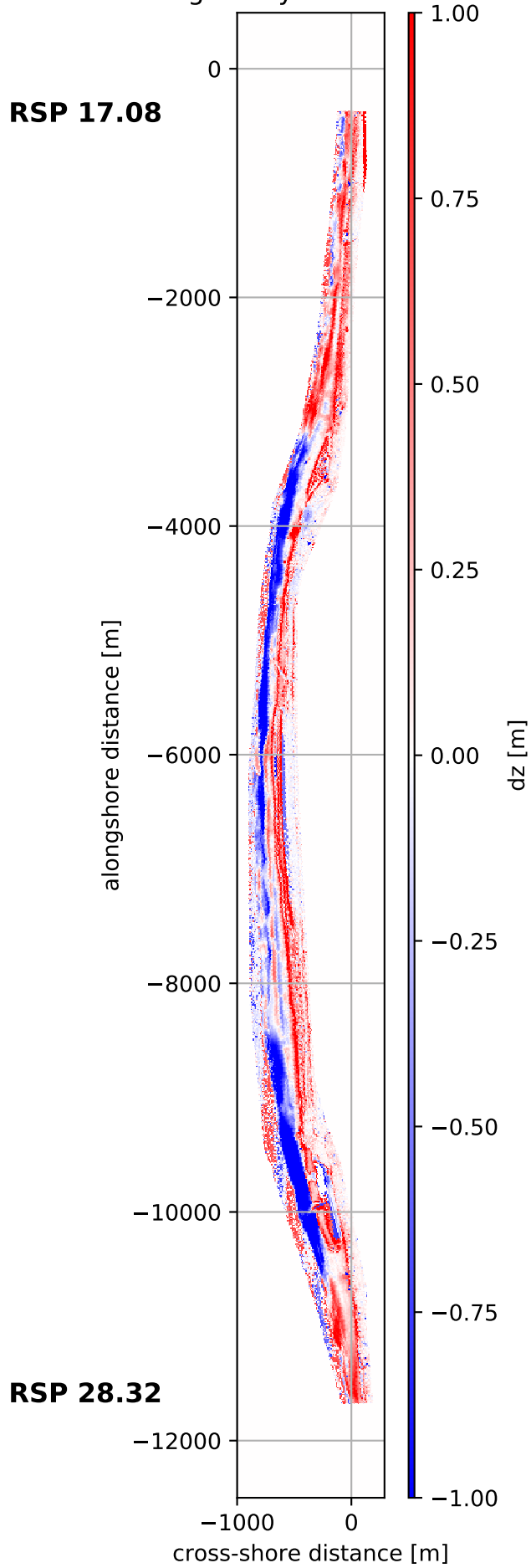


Figure I.2: Measured sedimentation (red) and erosion (blue) along the project domain between RSP 17.08 and RSP 28.32 in the period May 2015 - December 2016 (T0-T4). Note that the figure has the same orientation as the Dutch coastline in which North is at the upper part of the figure and South is at the lower part of the figure.

Bed level change: Dec 2015 - March 2016 (T1-T2)

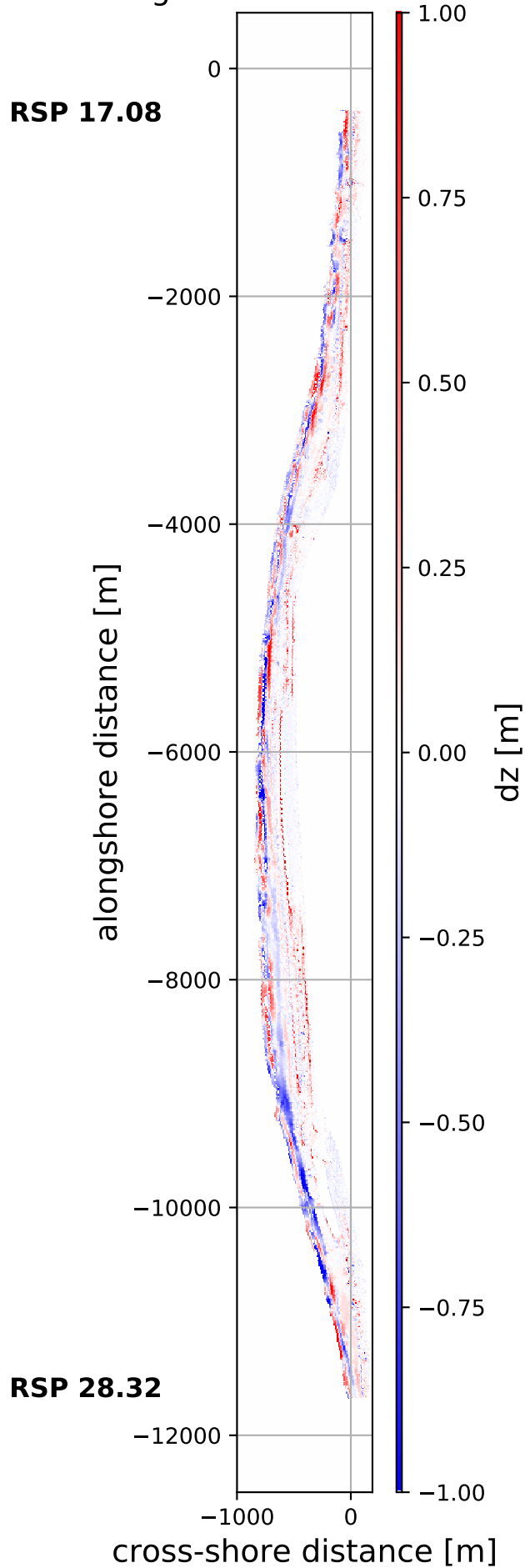


Figure I.3: Measured sedimentation (red) and erosion (blue) along the project domain between RSP 17.08 and RSP 28.32 in the period December 2015 - March 2016 (T1-T2). Note that the figure has the same orientation as the Dutch coastline in which North is at the upper part of the figure and South is at the lower part of the figure.

Bed level change: March 2016 - Sept 2016 (T2-T3)

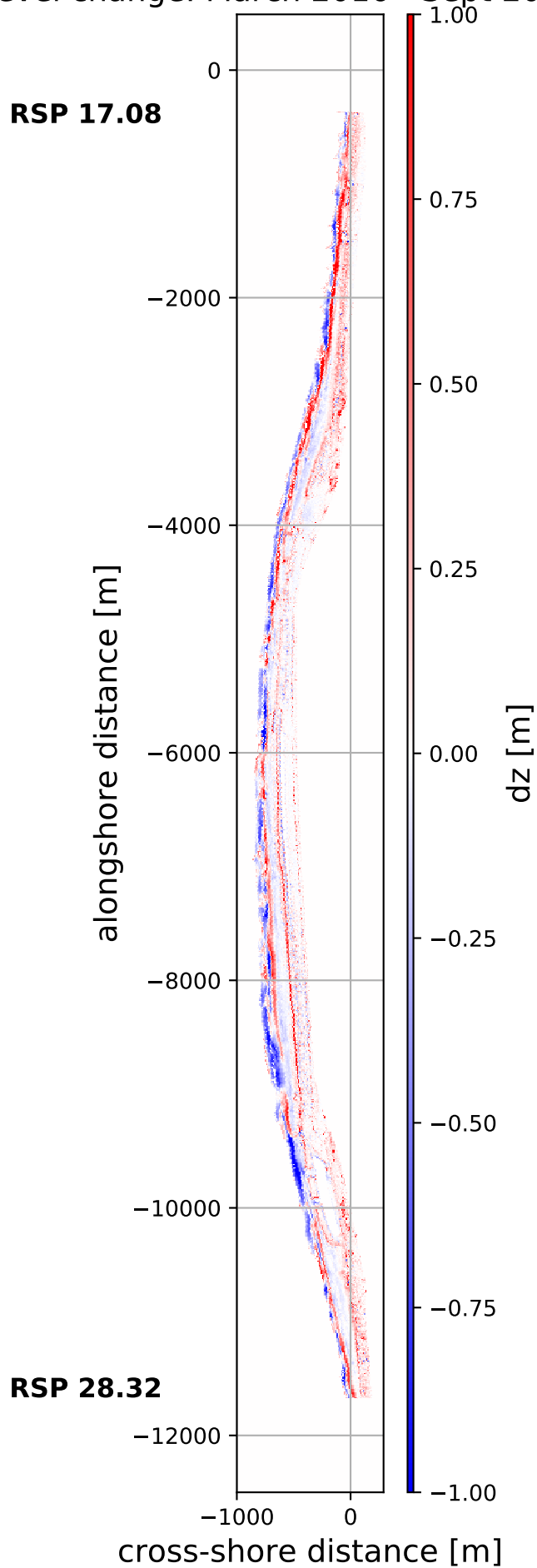


Figure I.4: Measured sedimentation (red) and erosion (blue) along the project domain between RSP 17.08 and RSP 28.32 in the period March 2016 - September 2016 (T2-T3). Note that the figure has the same orientation as the Dutch coastline in which North is at the upper part of the figure and South is at the lower part of the figure.

Bed level change: Sept 2016 - Dec 2016 (T3-T4)

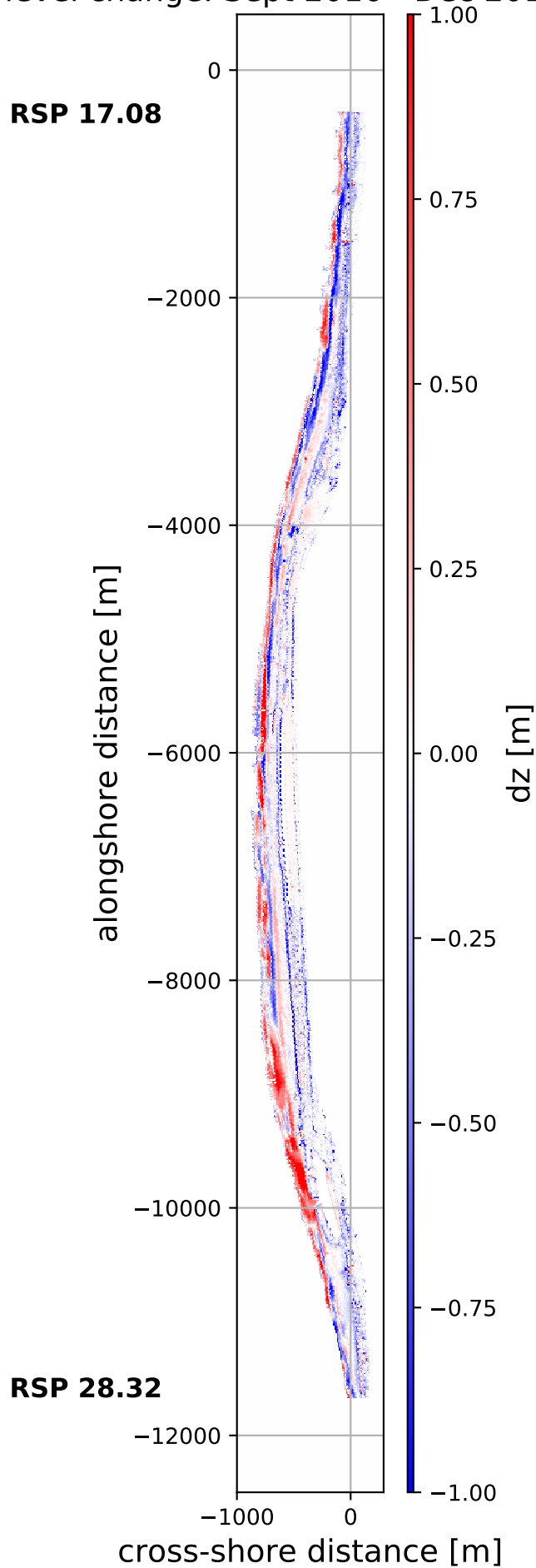


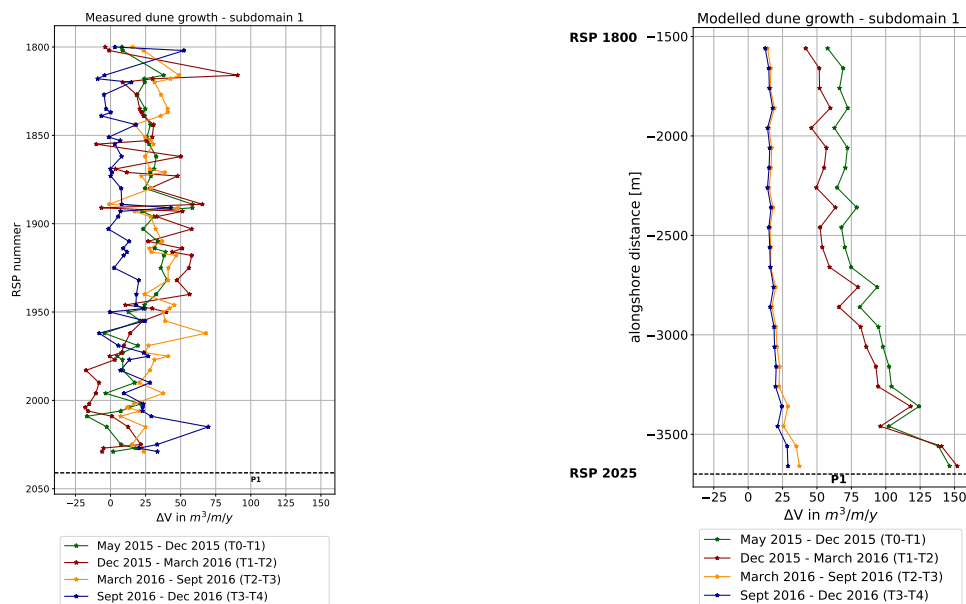
Figure I.5: Measured sedimentation (red) and erosion (blue) along the project domain between RSP 17.08 and RSP 28.32 in the period September 2016 - December 2016 (T3-T4). Note that the figure has the same orientation as the Dutch coastline in which North is at the upper part of the figure and South is at the lower part of the figure.

Additional Results - AeoliS Model

J.1. Periodic Dune Volume Changes

Subdomain 1 with median grain size $D_{50} = 304 \mu\text{m}$

Figure J.1 shows the periodically dune volume changes of the measurements and the model in the period May 2015 -December 2016. The observed and model results show temporal and spatial variations in dune volumes. In the measurements dune growth is largely pronounced between May 2015 - December 2015 and March 2016 - September 2016. The results show that the model significantly overestimates the dune growth in the first two periods, between Dec 2015 - March 2016, whereas the model underestimates for the third period, between March 2016 - September 2016 and correctly predicts for the last period between September 2016 - December 2016, although the spatial variations are rather predicted to be constant.



(a) Periodically measured dune growth rates in T0-T4.

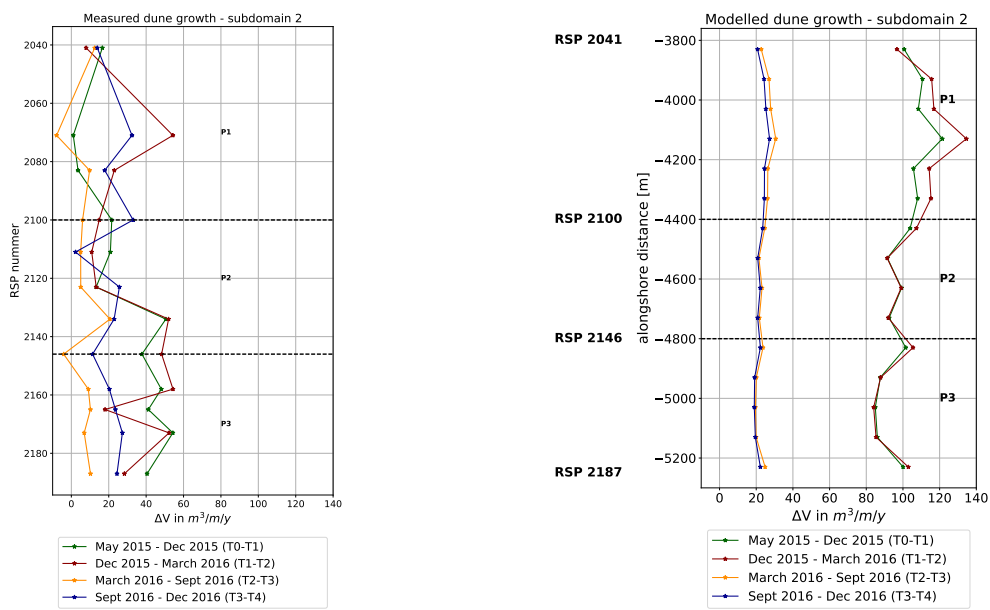
(b) Periodically modelled dune growth rates in T0-T4.

Figure J.1: Periodically measured and modelled dune growth rates between May 2015 - Dec 2016 of subdomain 1 along the northern shoulder of the HD system. The dashed horizontal black lines indicates the locations of the five different profile types P1 - P5. Note: the vertical labels differs. Therefore, reference locations in RSP coordinates are given at the left side of the y-axis in the model results (right figure).

Subdomain 2 with median grain size $D_{50} = 321 \mu\text{m}$

Figure J.2 shows the periodically dune volume changes of the measurements and the model in the period May 2015 - December 2016. The observed results show spatial and temporal variations in dune volumes. In the

measurements dune growth is largely pronounced in the first two periods, between May 2015 - December 2015 and December - March 2016 in the Southern area of the sub domain and in the second and fourth period in the Northern area of the domain. The model results show some spatial variations alongshore and show that the model overestimates the dune growth in the first two periods, in particular in the area between just Northwards and Southwards of RSP 2100. Dune growth for profile type 1, indicated by RSP coordinates 2041 and 2100, is larger in the second period, between December 2015 - March 2016, than in the first period, between May 2015 - December 2016 after construction. The model correctly predicts for the last two periods between March 2016 - December 2016, although the spatial variations are rather predicted to be constant alongshore.



(a) Periodically measured dune growth rates in T0-T4.

(b) Periodically modelled dune growth rates in T0-T4.

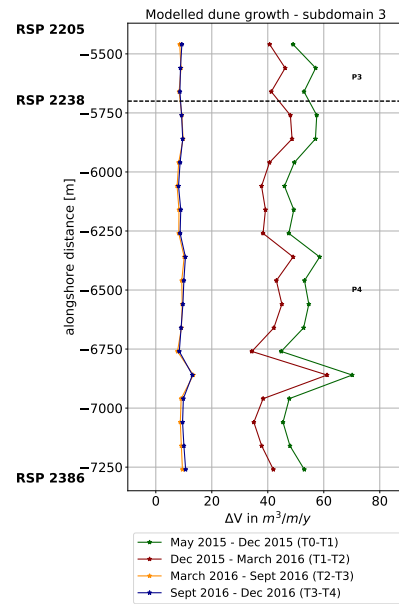
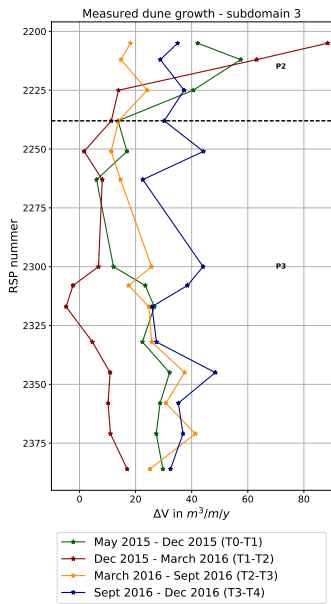
Figure J.2: Periodically measured and modelled dune growth rates between May 2015 - Dec 2016 of subdomain 2 along the northern area of the HD system. The dashed horizontal black lines indicates the locations of the five different profile types P1 - P5. Note: the vertical labels differs. Therefore, reference locations in RSP coordinates are given at the left side of the y-axis in the model results (right figure).

Subdomain 3 with median grain size $D_{50} = 341 \mu\text{m}$

Figure J.3 shows the periodically dune volume changes of the measurements and the model in the period May 2015 - December 2016. The observed results show spatial and temporal variations in dune volumes. In the measurements dune growth is largely pronounced in the first period for the northern area, indicated by the dashed black line, and also Southwards of RSP 2300. Furthermore, in the third and fourth period, between March 2016 - December 2016 large dune growth is measured alongshore. The large dune growth in the North is the effect of a relative large dune growth of $20 \text{ m}^3/\text{m}$ in a short amount of time (84 days). The model results show some spatial variations alongshore and show that the model overestimates the dune growth in the first period mainly in the area Northwards of RSP 2238. The dune growth in the second period between Dec 2015 - March 2016 is strongly overestimated by the model whereas the model underestimates the last two periods between March 2016 - December 2016.

Subdomain 4 with median grain size $D_{50} = 224 \mu\text{m}$

Figure ?? shows the periodically dune volume changes of the measurements and the model in the period May 2015 - December 2016. The observed results show spatial and temporal variations in dune volumes. In the measurements dune growth is largely pronounced in the first two periods, between May 2015 - December 2015 and December - March 2016. Dune growth is relative constant alongshore for the fourth period between September 2016 - December 2016. The results show that the model significantly overestimates the dune growth in the first two periods, between Dec 2015 - March 2016, whereas the model correctly predicts for the

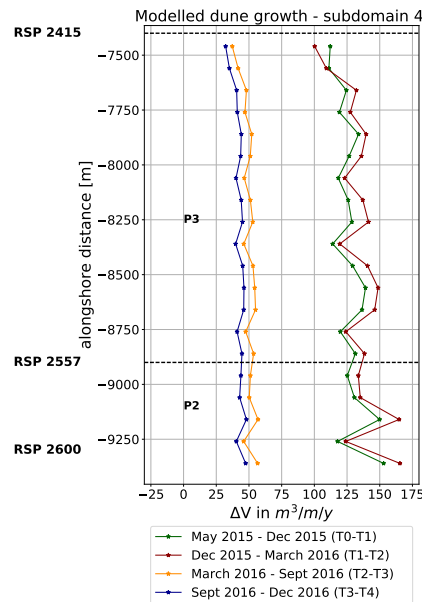
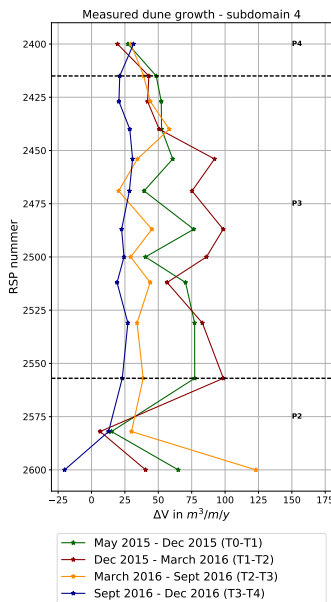


(a) Periodically measured dune growth rates in T0-T4.

(b) Periodically modelled dune growth rates in T0-T4.

Figure J.3: Periodically measured and modelled dune growth rates between May 2015 - Dec 2016 of subdomain 3 along the middle area of the HD system. The dashed horizontal black lines indicates the locations of the five different profile types P1 - P5. Note: the vertical labels differs. Therefore, reference locations in RSP coordinates are given at the left side of the y-axis in the model results (right figure).

third period, between March 2016 - September 2016 and overestimates again for the fourth period, between September 2016 - December 2016.



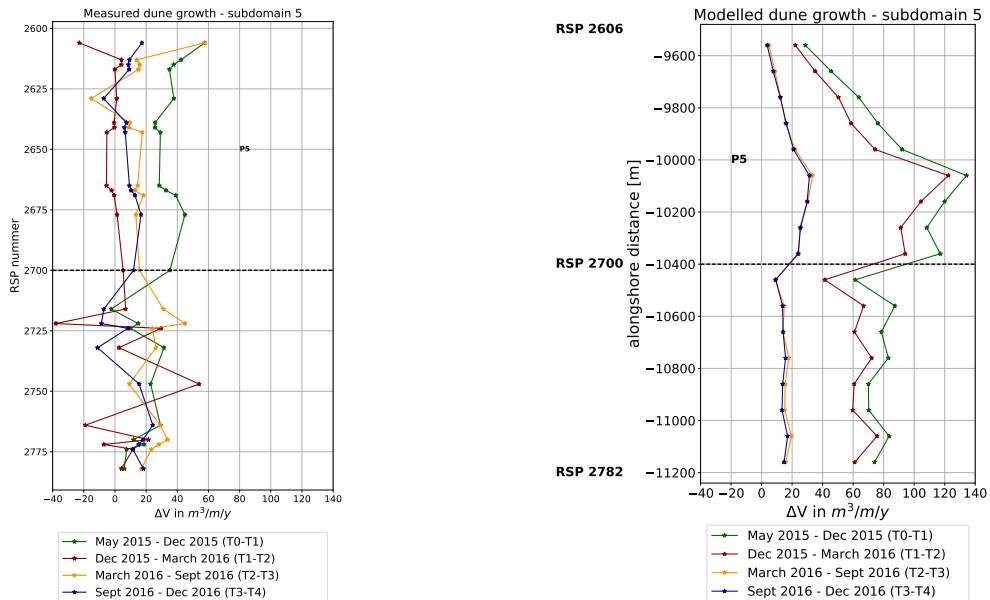
(a) Periodically measured dune growth rates in T0-T4.

(b) Periodically modelled dune growth rates in T0-T4.

Figure J.4: Periodically measured and modelled dune growth rates between May 2015 - Dec 2016 of subdomain 4 along the southern area of the HD system. The dashed horizontal black lines indicates the locations of the five different profile types P1 - P5. Note: the vertical labels differs. Therefore, reference locations in RSP coordinates are given at the left side of the y-axis in the model results (right figure).

Subdomain 5 with median grain size $D_{50} = 278 \mu\text{m}$

Figure J.5 shows the periodically dune volume changes of the measurements and the model in the period May 2015 - December 2016. The observed results show spatial and temporal variations in dune volumes. In the measurements dune growth is largely pronounced in the first period, between May 2015 - December 2015, and in the third period, between March 2016 - September 2016. The results show that the model significantly overestimates the dune growth in the first two periods, between December 2015 - March 2016, in particular along the northern area the overestimation is strongly for the second period between December 2015 - March 2016. The model correctly predicts for the last two periods, between March 2016 - December 2016.



(a) Periodically measured dune growth rates in T0-T4.

(b) Periodically modelled dune growth rates in T0-T4.

Figure J.5: Periodically measured and modelled dune growth rates between May 2015 - Dec 2016 of subdomain 5 along the southern shoulder of the HD system. The dashed horizontal black lines indicates the locations of the five different profile types P1 - P5. Note: the vertical labels differs. Therefore, reference locations in RSP coordinates are given at the left side of the y-axis in the model results (right figure).